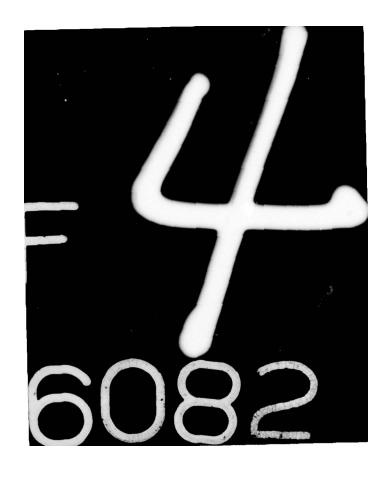
ARMY MATERIALS AND MECHANICS RESEARCH CENTER WATERTO--ETC F/G 11/9 PROCEEDINGS OF THE TTCP-3 CRITICAL REVIEW: TECHNIQUES FOR THE C--ETC(U) AD-A036 082 JAN 77 AMMRC-MS-77-2 UNCLASSIFIED NL 1 OF 4 1





METON I DOCU	MENTATION PAGE	READ INSTRUCTIONS BEFORE COMPLETING FORM
. REPORT NUMBER	2. GOVT	ACCESSION NO. 3. RECIPIENT'S CATALOG NUMBER
AMMRG- MS-77-2		
TITLE (and Subside)		TYPE OF REPORT & PERIOD COVE
PROCEEDINGS OF THE TT	CP-3 CRITICAL REV	(IEW;) (9))
TECHNIQUES FOR THE CH	ARACTERIZATION OF	Final Report,
POLYMERIC MATERIALS.	INCIO ME CITO M	THY
. AUTHOR() Materials and	Mechanics Resear	Ch . CONTRACT OR GRANT NUMBER(s)
Center, 6-8 J	uly 76 at Waterton	wn, Mass
nated to place at		1 03/3/3P
PERFORMING ORGANIZATION NA	AF AND ADDRESS	10. PROGRAM ELEMENT, PROJECT, TA
Army Materials and Med		AREA & WORK UNIT NUMBERS
Watertown, Massachuset		
DRXMR-R		
1. CONTROLLING OFFICE NAME AN	D ADDRESS	REPORT DATE
U. S. Army Materiel I		Padiness Jan 77
Command, Alexandria,	Virginia 22333	389
14. MONITORING AGENCY NAME & A	DDRESS(if different from Cont	rolling Office) 15. SECURITY CLASS. (of this report)
		lholossi fi od
		Unclassified 15a. DECLASSIFICATION/DOWNGRADIN SCHEDULE
		SCHEDULE
Approved for public re		
Approved for public re	elease; distributio	
17. DISTRIBUTION STATEMENT (of fl	elease; distributio	
	elease; distributio	
17. DISTRIBUTION STATEMENT (of fl	elease; distributio), Il dillorent from Report)
17. DISTRIBUTION STATEMENT (of fl	elease; distributio), Il dillorent from Report)
17. DISTRIBUTION STATEMENT (el 11	elease; distribution of the state of the sta	FEB 28 1977
17. DISTRIBUTION STATEMENT (of fi	elease; distributions abstract entered in Block 20	FEB 28 1977
17. DISTRIBUTION STATEMENT (of fi	elease; distribution of the state of the sta	FEB 28 1977
17. DISTRIBUTION STATEMENT (of the statement of the state	please; distribution of the state of the sta	FEB 28 1977 by block number) operties
19. KEY WORDS (Continue on reverse of Spectroscopy Chemical analysis Thermal analysis	elease; distribution of the state of the sta	FEB 28 1977 by block number) operties
17. DISTRIBUTION STATEMENT (of the statement of the state	please; distribution of the state of the sta	FEB 28 1977 by block number) operties erials
19. KEY WORDS (Continue on reverse of Chemical analysis Chromatography	please; distribution of the state of the sta	FEB 28 1977 by block number) operties erials
19. KEY WORDS (Continue on reverse of Chemical analysis Chromatography	please; distribution of the state of the sta	FEB 28 1977 by block number) operties erials y block number)
19. KEY WORDS (Continue on reverse of Chemical analysis Chromatography	please; distribution of the state of the sta	FEB 28 1977 by block number) operties erials y block number)

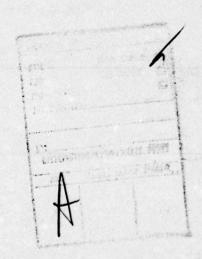
ECURITY CLASSIFICATION OF THIS PAGE(Then Date Entered)

Block No. 20

ABSTRACT

Proceedings of the "TTCP-3 Critical Review; Techniques for the Characterization of Polymeric Materials" sponsored by The Technical Co-operation Program Sub Group P Technical Panel 3 (Organic Materials) (TTCP-3); held at the Army Materials and Mechanics Research Center, Watertown, Massachusetts, 6-8 July 1976.

The objective of this Review is to evaluate the potential of new and/or improved techniques and combinations thereof in the prediction of field life of polymeric and composite materials in military hardware.



CONTENTS

and the second s	Page
Opening Remarks - Dr. G. R. Thomas, AMMRC	. 1
Materials Advisory Board Report on Characterization - F. W. Billmeyer, Rensselaer Polytechnic Institute, Troy, New York	. 3
First Annual Chemical Characterization and Analysis Conference - February 24 and 25, 1976 - C. A. May, Lockheed Missiles and Space Company	. 5
Report on Air Force Sponsored Meeting, March 1976 - D. Ulrich, AFSOR	. 7
SESSION I: SPECTROSCOPIC METHODS	. 9
Chairman: W. W. Wright Royal Aircraft Establishment, United Kingdom	
Modern Vibrational Spectroscopic Techniques for the Characterization of Polymers - P. C. Painter and J. L. Koenig, Case Western Reserve University	. 11
Characterisation of Styrene-Butadiene Copolymers - A. V. Cunliffe and R. J. Pace, Explosives Research and Development Establishment, Waltham Abbey, Essex, England	. 25
The Uses of Infrared Spectroscopy for the Characterization of Polymeric Materials - D. M. Wiles, National Research Council of Canada	. 35
Fourier Transform Infrared Spectroscopy as a Method for Studying Weathering of Glass-Fiber Epoxy Composites - J. F. Sprouse, AMMRC	. 43
Neutron Radiographic Techniques for Inspection of Polymeric Materials - D. H. Petersen and W. E. Dance, Vought Corp. Advanced Technology Center, Incorporated	. 55
The Application of ESCA to Studies of Structure Bonding and Reactivity	la fregula
of Polymers - D. T. Clark, University of Durham	. 67
Carbon-13 Fourier Transform NMR Techniques in Polymer Characterization - Dr. W. B. Moniz, Naval Research Laboratory	. 99
Stress Mass Spectrometry of Polymeric and Composite Materials - C. J. Wolf and M. A. Grayson, McDonnell Douglas Research Laboratories	. 117
Application of Chemiluminescence to the Characterization of Polymeric Materials - R. A. Nathan, G. D. Mendenhall, and J. A. Hassell, Battelle Columbus Laboratories	. 123
The Early Stages of Actinic Deterioration - D. M. Wiles, National Research Council of Canada	
RESEATCH COUNCIL OF CANADA	143

	Page
SESSION II: SEPARATION TECHNIQUES	147
Chairman: C. Bersch Naval Air Systems Command, U.S. Navy	
Review of Separation Techniques for Polymers - G. L. Hagnauer, AMMRC	149
High Performance Liquid Chromatography - G. Fallick and J. Cazes, Waters Associates, Incorporated	159
Analysis of Polymer Materials by Liquid Chromatography and Infrared Spectroscopy - S. C. Pattacini and J. J. Stoveken, Perkin-Elmer Corporation	177
Effect of Ester Impurities in PMR-Polyimide Resin - R. W. Lauver, NASA Lewis Research Center	183
Thin Layer Chromatography - C. A. May, Lockheed Missiles and Space Company	195
Use of Separation Methods for Quality Assurance of Polymeric Materials - C. D'Oyly-Watkins, MQAD, Woolwich, England	197
SESSION III: THERMAL AND THERMAL MECHANICAL METHOD	209
Chairman: H. Schwartz Air Force Materials Laboratory, USAF	
Applications of Combined Pyrolysis-Gas Chromatography-Mass Spectrometry to the Analysis and Evaluation of Polymeric Materials - C. Merritt, Jr.,	
U.S. Army Natick R&D Command	211
Applications of Thermal Methods of Analysis - J. M. Barton, W. A. Lee, and W. W. Wright, RAE, Farnborough, England	223
Differential Scanning Calorimetry Applications in the Thermal, Kinetic, and Rheological Characterization of Thermosetting Systems -	
M. R. Kamal, McGill University, Canada	237
Characterization of Thermosetting Epoxy Systems by Torsional Braid Analysis - J. K. Gillham, Princeton University	251
Polymer Characterization Using Differential Scanning Calorimetry - W. D. Bascom and P. Peyser, Naval Research Laboratory	259

	Page
SESSION IV: DIELECTRIC ANALYSIS	267
Chairman: L. Krichew National Defence, Canada	
Dielectric and Calorimetric Monitoring of the Resin Matrix During the Cure of Composite Structures - C. A. May, Lockheed Missiles and Space Company	269
ETMA: Electrical, Thermal and Mechanical Analyses of Polymers: Theory and Uses - S. Yalof, Tetrahedron Associates, Incorporated	271
Thermal Analysis of PMR-Polyimides by Dielectrometry - R. E. Gluyas, NASA Lewis Research Center	277
SESSION V: MOISTURE CHARACTERIZATION	297
Chairman: L. Krichew National Defence, Canada	
The Surface Composition and Energetics of Graphite Reinforcing Fibers - L. T. Drzal, University of Dayton Research Institute	299
Transport Behavior of Water in Polymeric Materials - J. L. Illinger and N. S. Schneider, AMMRC	301
SESSION VI: APPLICATIONS	317
Chairman: D. Pinkerton Materials Research Laboratories, Australia	
Novel Techniques for Measuring Field Service Deterioration of Composite Materials - R. E. Sacher, AMMRC	319
Application of the Dielectric Analysis to Polymeric Materials Control - D. H. Kim, The Boeing Commercial Airplane Company	329
Dynamic Mechanical Properties in Fiber Reinforced Epoxy Resin Based Networks - J. G. Williams, Materials Research Laboratories, Maribyrnong, Victoria 3032, Australia	343
Electron Spin Resonance Studies of the Degradation of Polymeric Materials - D. K. C. Hodgeman, Materials Research Laboratories, Maribyrnong, Victoria 3032, Australia	353
Polymer Characterisation by Pyrolysis Gas Chromatography - J. R. Brown and D. J. Hall, Materials Research Laboratories, Maribyrnong, Victoria 3032, Australia	365
Vapour Pressure Osmometry - Its Limitations as a Method for Molecular Weight Determinations - C. E. M. Morris, Materials Research Laboratories,	
Maribyrnong, Victoria 3032, Australia	373
Closing Remarks - Dr. G. R. Thomas, AMMRC	381

OPENING REMARKS

Dr. George R. Thomas

Army Materials and Mechanics Research Center Watertown, Massachusetts 02172

Last August I addressed the membership of the TTCP and the attendees of a Critical Review of Deterioration of Organic Materials in Service Environments in Melbourne, Australia as their keynote speaker. In that address I reviewed the situation with respect to Environmental Deterioration of Organic Materials for Military Applications as I saw it.

In essence I felt the situation with respect to Environmental Deterioration could best be described as chaotic. Materials did not always perform in a similar manner at similar sites. The scatter in data was so great that a trend noted in statistically reduced data was highly suspect and not interpretable with respect to why it occurred and what to do about it. Indeed, the literature was a massive compilation of confusion.

We here at the Army Materials and Mechanics Research Center had just completed a two-year study on deterioration of a "well characterized" material. Our objective in that study was to develop a methodology whereby we could predict the use life - up to twenty years in one year. This was a pretty ambitious undertaking since it took more than five years to determine whether or not a material would last for five years. I reviewed the results of that study in that keynote address. Some of the conclusions I presented were as follows: First in our program we characterized some 17 different exposure sites located in Germany, the USA, the Panama Canal Zone, Puerto Rico, and Australia. While there were differences with respect to temperature, relative humidity, and ultraviolet radiation, the differences between similar sites was not sufficient to account for major differences in the rate of deterioration.

We raised some question as to the validity of interpretation of such test methods as short beam shear, tensile, flexural strength. There was nothing in the environment or the test methods which would account for the scatter in data that we had obtained intra and inter test sites. The only conclusion I could draw from our study was that the samples we exposed were not identical but this contradicted our own finding that the manufacturer's material met "specification" which consisted of values for tensile fatigue and short beam shear strengths.

We examined the manufacturing methods at the work site and our suspicions were confirmed. From a strictly chemical point of view the allowable deviations in procedure were sufficient to account for considerable differences in a product which met specifications. These, as it turned out, were rather minimal. Indeed, it was difficult not to meet specification values.

Fortunately we had initiated exploratory studies for alternative methods of characterization - alternative for tensile, fatigue, and short beam shear. I described these methods and some of the results which we had obtained. We found interesting results using ESCA, AUGER, stress mass spectrometry, infrared spectometry with attenuated total reflectance and Fourier transform techniques, laser pyrolysis and thermal pyrolysis coupled with gas chromatography and mass spectrometry, torsional braid and torsional pendulum analysis, moisture transport analysis. It would have been a fitting conclusion to that address had I been able to show that indeed we could control and predict the performance properties of the composite by varying the processing conditions in a manner definable by the methods I described, but we were not at that point last August. Indeed, we won't be at that point this August. Discovering new characterization techniques was a relatively easy accomplishment but understanding their significance is going to take a little more time.

At the conclusion of that review, my brethren in TTCP were sufficiently convinced that it was necessary to continue to search for new techniques and to apply known but seldom used techniques to want to hold a Critical Review of Deterioration of Organic Materials in conjunction with this year's meeting and that in a "nutshell" is why we are here today.

Without further ado, I for one would like to get on with the substance of this meeting. But not before I thank the speakers, the members of the TTCP, my co-workers on the organizing committee - Mr. Bersch, U.S. Navy; Mr. Schwartz, USAF; the Conference Planning Director, Dr. Sacher, and the Conference Coordinator, Miss Sterling, for their respective efforts in making this meeting possible.

MATERIALS ADVISORY BOARD REPORT ON CHARACTERIZATION

F. W. Billmeyer

Rensselaer Polytechnic Institute,

Troy, New York

FIRST ANNUAL CHEMICAL CHARACTERIZATION AND ANALYSIS CONFERENCE

February 24 and 25, 1976

C. A. May

Lockheed Missiles & Space Company

Sunnyvale, California

As the use of polymeric materials in aerospace applications continues to grow so does their use in man rated vehicles. Accordingly, the safety of such devices becomes increasingly critical. Most of these materials are proprietary combinations of at least two, and generally more, ingredients. The inherent danger thus exists that formulative changes, either inadvertently or by design, have been made which can alter the performance characteristics of a product. In order to have complete confidence in fabrications involving polymeric materials it is important that the user know he is receiving a chemically identical product that has been properly processed with each lot of material.

In order to establish reliable physiochemical quality assurance procedures the chemical nature of the product must be understood. Unfortunately, much of this data is not available. This need has been recognized and a number of aerospace laboratories are now using the tools of the polymer chemist to better identify and control the materials they use. Most of the current efforts involve studies on adhesives and fiber reinforced prepregs containing epoxy matrices. It was the purpose of this meeting to discuss the current state-of-the-art at the bench level on the chemical characterization of thermoset resins.

Attendance at the meeting was by invitation only. Efforts were made to keep the group small. Only twenty people were in attendance. The organizations represented were: Air Force Materials Laboratory, Army Materials and Mechanics Research Center, Boeing Airplane Company, Lockheed Missiles & Space Company, McDonnell Aircraft, NASA-Ames Research Center, Naval Research Laboratory, Newey & Busso Associates, Rockwell Science Center, Tetrahedron Associates and Waters Associates. All of the personnel involved have had bench experience in the application of physiochemical techniques to aerospace materials.

The format was to have open discussion with all attendees participating. The objectives were to develop an exchange of laboratory techniques and point out problem areas deserving future effort. The meeting consisted of four sessions each of 1/2 day duration. The general topics discussed were dielectric analysis and relaxation phenomena, thermomechanical techniques, spectroscopy and chromatography. Each session had a moderator who possessed expertise in one of the aforementioned fields. It was the responsibility of the moderator to get the discussion rolling. For these efforts we are particularly indebted to Stanley Yalof of Tetrahedron in the dielectric area, David H. Kaelble of Rockwell Science Center on thermomechanical methods, Chester F. Poranski of the Naval Research Laboratory who lead the spectroscopy section and gave a fine dissertation on C13 NMR and Gary Fallick of Waters Associates for heading up the chromatography session. During each session there was lively discussion which appeared to grow as the meeting proceeded. As a practical finale, a progress report was given on how the methods discussed are being used to analyze epoxy formulations and develop physiochemical quality assurance procedures.

Considering that this was a first of its kind get together, the meeting was highly successful. During the early stages there was some reluctance on the part of some of the attendees to enter in the discussion. As the meeting gained momentum, however, everyone got into the act. In fact, the major complaint was that there was insufficient time to cover everything of interest. Following the meeting many very constructive comments were received along with suggestions for future gatherings. There appears to be a definite need for this type of seminar, with some minor changes, the general format appears excellent, and there is little doubt that everyone in attendance looks forward to future conferences.

REPORT ON AIR FORCE SPONSORED MEETING, March 1976

D. Ulrich AFSOR

SESSION I. SPECTROSCOPIC METHODS

Chairman: W. W. Wright
Royal Aircraft Establishment, United Kingdom

MODERN VIBRATIONAL SPECTROSCOPIC TECHNIQUES FOR THE CHARACTERIZATION OF POLYMERS P. C. Painter and J. L. Koenig, Case Western Reserve University

CHARACTERISATION OF STYRENE-BUTADIENE COPOLYMERS

A. V. Cunliffe and R. J. Pace, Expolsives Research and Development Establishment,
Waltham Abbey, Essex, England

THE USES OF INFRARED SPECTROSCOPY FOR THE CHARACTERIZATION OF POLYMERIC MATERIALS D. M. Wiles, National Research Council of Canada

FOURIER TRANSFORM INFRARED SPECTROSCOPY AS A METHOD FOR STUDYING WEATHERING OF GLASS-FIBER EPOXY COMPOSITES
J. F. Sprouse, AMMRC

NEUTRON RADIOGRAPHIC TECHNIQUES FOR INSPECTION OF POLYMERIC MATERIALS D. H. Petersen and W. E. Dance, Vought Corp. Advanced Technology Center, Inc.

THE APPLICATION OF ESCA TO STUDIES OF STRUCTURE BONDING AND REACTIVITY OF POLYMERS D. T. Clark, University of Durham

CARBON-13 FOURIER TRANSFORM NMR TECHNIQUES IN POLYMER CHARACTERIZATION Dr. W. B. Moniz, Naval Research Laboratory

STRESS MASS SPECTROMETRY OF POLYMERIC AND COMPOSITE MATERIALS C. J. Wolf and M. A. Grayson, McDonnell Douglas Research Laboratories

APPLICATION OF CHEMILUMINESCENCE TO THE CHARACTERIZATION OF POLYMERIC MATERIALS R. A. Nathan, G. D. Mendenhall, and J. A. Hassell, Battelle Columbus Laboratories

THE EARLY STAGES OF ACTINIC DETERIORATION
D. M. Wiles, National Research Council of Canada

MODERN VIBRATIONAL SPECTROSCOPIC TECHNIQUES FOR THE CHARACTERIZATION OF POLYMERS

P. C. Painter and J. L. Koenig

Department of Macromolecular Science Case Western Reserve University

Raman scattering originates in the variation of molecular polarizability with molecular vibration. In contrast, the infrared spectrum originates in changes of dipole moment with molecular vibration. For a molecule such as benzene with a high degree of symmetry, vibrations active in the Raman effect are absent in the infrared and vice-versa. Consequently, both the infrared and Raman spectrum are necessary for a vibrational analysis of the molecule.

Few polymer molecules have such a high degree of symmetry even when the chain is in the preferred conformation. However, even though the normal modes of vibration are then theoretically active in both the Raman and infrared, the fundamentally different origin of the two effects often results in lines appearing with strong intensity in the Raman spectrum being weak or absent in the infrared. This is illustrated in Figure 1 for trans-1, 4-polychloroprene;

$$CI$$

$$(CH_2 - C = CH - CH_2^2)_n$$

Vibrational spectroscopy has been widely used to study the structure, intermolecular interactions, chemical reactions and degradation of polymers in addition to being a prime means of identification, since the spectrum of a polymer is as characteristic as a fingerprint.

Trans-1,4-polychloroprene is a useful model system with which to illustrate the sensitivity of this technique. When this polymer is prepared at 40°C the chain contains a considerable number of "defect" units, such as cis; 1, 2; 3, 4 as well as head-to-head and inverted units. The structural isomers are shown in Figure 2. This polymer has a low degree of crystallinity and is widely used as an elastomeric material. However, as the temperature of polymerization is reduced the number of defects decreases and a polymer prepared at -20°C is a brittle highly crystalline material. These changes are reflected in the Raman spectrum shown in Figure 3, which compares the spectra of samples polymerized at -20, 0, +20, +40°C respectively. The spectrum of the highly crystalline (-20°C) material contains sharp well-defined lines characteristic of a polymer chain in the preferred conformation. In the spectra of samples polymerized at higher temperatures these lines broaden considerably and weak amorphous modes near 1218 cm⁻¹ and 1075 cm⁻¹ appear. Similar changes appear in the infrared spectrum. This figure illustrates the sensitivity of the technique yet also some of its limitations. Subtle effects such as local conformational changes or, for example, the initial stages of oxidative attack certainly contribute to the spectrum but the characteristic bands and lines that contain the relevant information are lost in those of the unaffected polymer chain. The advent of computerized systems has solved many of the problems associated with conventional spectroscopy.

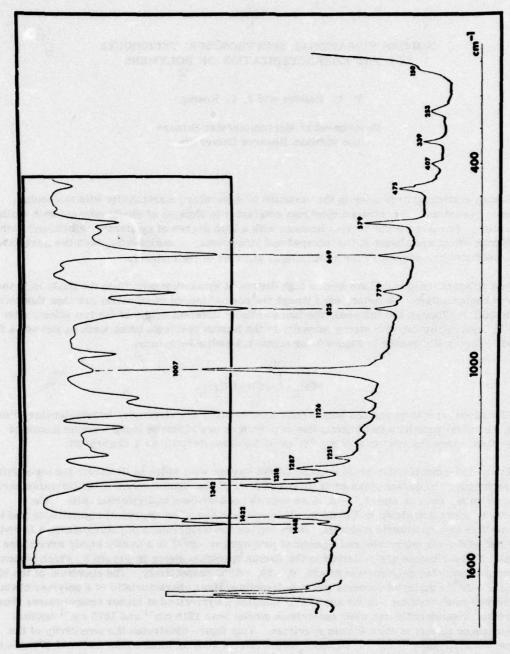


Figure 1: Raman spectrum of trans-1, 4-polychloroprene [polymerized at -20°C]. Insert: infrared spectrum of the same sample.

Figure 2. Structural isomers of polychloroprene.

- I. trans-1, 4-polychloroprene
- II. cis-1,4-polychloroprene
- III. unit arising from 1,2 polymerization IV. unit arising from 3,4 polymerization.

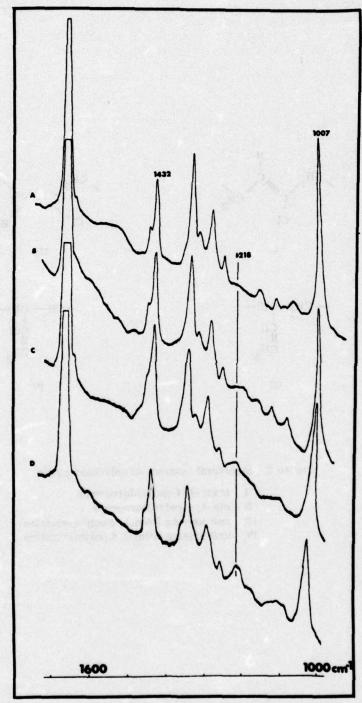


Figure 3: Raman spectra of trans-1, 4-polychloroprene samples polymerized at (A) -20°C, (B) 0°C, (C) +20°C, and (D) +40°C.

Most of the results published to date concern computerized infrared systems, particularly FT-IR, and we will concentrate on these applications since they demonstrate how many spectroscopic problems can be solved. Computerized Raman systems have only recently been introduced and we expect the publication of equivalent results obtained on these systems in the near future.

First let us consider the separation of the spectral contributions of a heterophase system, the amorphous and crystalline bands of trans-1,4-polychloroprene. We have been able to obtain the "purified" spectrum of the preferred conformation of a predominantly trans-1,4-polychloroprene (trans-CD) polymer from the semicrystalline polymer. The infrared spectrum, designated 1, of this sample, was obtained at room temperature on a Digilab FTS-14 Fourier transform spectro-photometer. The sample was then heated to 80°C for 15 min. in the spectrophotometer and another infrared spectrum, designated 2, was obtained under the same conditions. These two samples should differ only in the degree of crystallinity attained (barring the possibility of slight oxidative degradation which would be readily observable in the carbonyl region of the spectrum if present in significant concentration). Finally, the sample was allowed to cool to room temperature and another spectrum was recorded and stored after 120 min.

An absorbance subtraction routine was employed to obtain the crystalline vibrational spectrum of trans-CD. In Figure 4 the absorbance spectra 1 and 2 are shown together with the difference spectrum 3 obtained by subtraction of the less crystalline spectrum 2 from the more crystalline spectrum 1. The subtraction was performed on the basis of elimination of the amorphous component of the semicrystalline trans-CD spectrum with the resultant difference spectrum 3 representing the spectrum of crystalline trans-CD. The absorbance procedure employed will be illustrated mathematically.

For spectrum 1 the following equation can be written at each frequency

$$A_{T_1} = A_{A_1} + A_{C_1} + A_{M_1}$$
 (1)

where A_{T_1} is the total absorbance of all components in sample 1; A_{A_1} is the absorbance of amorphous trans-CD component in sample 1; A_{C_1} is the absorbance of crystalline trans-CD component in sample 1; and A_{M_1} is the absorbance of other components in sample 1, such as 1, 2 and 2,4 placements. Similarly, it can be written for spectrum 2

$$A_{T_2} = A_{A_2} + A_{C_2} + A_{M_2}$$
 (2)

It is desired to subtract A_{T_2} from A_{T_1} as follows

$$A_{S} = A_{T_1} - kA_{T_2}$$
 (3)

where A_S is the absorbance due to the subtracted spectrum and k is an adjustable scaling parameter. Substitution of Eqs. (1) and (2) in Eq. (3) gives

$$A_{S} = (A_{A_{1}} + A_{C_{1}} + A_{M_{1}}) - k(A_{A_{2}} + A_{C_{2}} + A_{M_{2}})$$
(4)

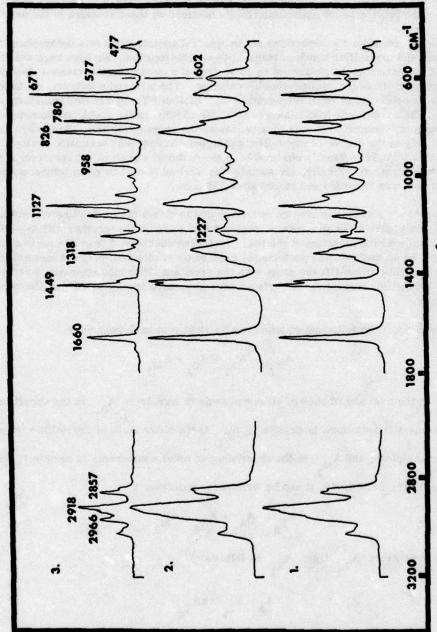


Figure 4: Infrared spectra of trans-1,4-polychloroprene (-20°C polymer). 1, absorbance spectrum at room temperature; 2, absorbance spectrum at 80°C; 3, absorbance spectrum of crystalline vibrational bands of trans-1,4-polychloroprene (spectrum 1 - spectrum 2).

Rearrangement of Eq. (3) gives

$$A_{S} = (A_{A_{1}} - kA_{A_{2}}) + (A_{C_{1}} - kA_{C_{2}}) + (A_{M_{1}} - kA_{M_{2}})$$
 (5)

In this procedure it is desired to obtain the spectrum of crystalline trans-CD by elimination of the contribution of the amorphous trans-CD to the subtracted absorbance spectrum, A_S . In other words, the criterion for subtraction of A_{T_2} from A_{T_1} used was

$$A_{A_1}^{-k}A_{A_2}^{A} = 0 ag{6}$$

where

$$k_A = A_1 / A_2 \tag{7}$$

The criterion employed for elimination of the amorphous component was the disappearance of bands at 602 and 1227 cm⁻¹. Earlier work has shown that the broad 502 cm⁻¹ band is insensitive to crystallization. More recently, the amorphous band at 1227 cm⁻¹ has been used in the determination of crystallinity in polychloroprenes; the results of this study agree with independent dilatometric results. Application of the subtraction criterion, shown in Eqs. (6) and (7), can be applied to the total absorbance subtraction in Eq. (5):

$$A_{S} = (A_{C_{1}}^{-k} A_{C_{2}}^{A}) + (A_{M_{1}}^{-k} A_{M_{2}}^{A})$$
 (8)

According to Eq. (8), this subtracted spectrum now contains the spectrum of the crystalline trans-CD plus the spectrum of the other structural modifications: cis-1, 4; 1, 2 and 3, 4 placements. Since the latter modifications are only present in relatively small concentrations, they will not make a major contribution to the subtracted spectrum.

In the actual subtraction employed, there is the implicit assumption that the infrared spectrum of the amorphous component in the heated sample is not significantly different from that of the sample at room temperature. A difference spectrum was also obtained from two room temperature spectra taken at different times of crystallization and thus at different degrees of crystallinity. This difference spectrum of the crystalline trans-CD component was essentially identical to that shown earlier in Figure 4. The similarity between the two difference spectra indicates that the effect of the temperature range used in this study on the infrared spectrum of the amorphous component is minimal.

The difference spectrum which results from the subtraction of the spectrum recorded at 80°C from the spectrum recorded after the sample has been allowed to cool to room temperature and recrystallize showed no significant frequency shifts from spectrum 3. In conclusion, this type of procedure represents an excellent method to study vibrational spectra of semicrystalline polymers.

When polymers polymerized at different temperatures are compared in the above manner, the difference spectra show a shift in the crystalline frequencies as indicated in Table I. Such changes could result from the inclusion of structural defects in the crystalline domain. The presence of such defects would contribute to the vibrational spectrum of the crystalline regions. The increase of structural defects as a function of polymerization temperature, with the resultant inclusion of a larger concentration of defects, could manifest itself in vibrational changes in the

Table I

Crystalline vibrational frequencies of trans-1, 4-polychloroprene as a function of polymerization temperature

-1

Crystalline vibrational fre for trans-1,4-polychloropr at the following te		polymerized	Change in frequency
-20°C	0°c	40°C	from the -20°C to + 40°C polymer (cm ⁻¹)
1660	1660	1660	0
1449	1448	1447	-2
1318	1316	1313	-5
1250	1252	1254	none ade character at 4 contrat
1167	1167	1167	t sampagan af skap it o bid Leavin
1127	1127	1127	mestic calculations of the second
1083	1083	1083	and its not the state of the control of the
1007	1005	1004	-3
958	954	953	-5
826	826	826	Ō
780	779	778	-2
671	671	671	lan dule (de) jet at par <mark>o</mark> nnosi
577	576	576	that in make second after a deman

crystalline spectrum. The removal of interfering absorbance due to solvents is an important application. A classical limitation of infrared analysis has been the study of aqueous solutions due to strong, broad infrared absorbance of water. With FT-IR, if the aqueous solutions are examined such that total absorbance does not occur, the water spectrum can be subtracted. For biological systems where water is the only interesting solvent, this improvement can be utilized and demonstrated for protein solutions. The aqueous solution infrared spectrum of hemoglobin obtained by FT-IR is shown in Figure 5 (spectrum 2). No useful detail can be observed until the water spectrum (spectrum 1) is subtracted to yield spectrum 3 where the classical amide I and II modes at 1657 and 1547 cm are observed. A comparison of the infrared absorbance spectrum of hemoglobin as a cast film (less water) is shown in Figure 6. The secondary structure of protein can be determined using conformationally sensitive frequencies.

Finally, we will illustrate the application of computer enhanced vibrational spectroscopy to the separation of reacted and unreacted species. The useful life of many polymeric systems is limited by their susceptibility to oxidation degradation. Rubbers are particularly vulnerable to oxidation, and as a consequence considerable research has been carried out in an effort to determine the mechanism of this oxidative chemical reaction. Infrared has been used to study this chemical process but has been limited because the reaction must proceed to a substantial degree before detectable absorbances appear. With the difference spectra technique, considerable improvement results. In Figure 7, the infrared absorbance spectra of a sample of unoxidized polybutadiene and a sample held in air at 30°C for 6 hr. Using the band at 740 cm⁻¹ as the basis for subtraction, the scale expanded (25 X) difference spectrum is also shown. The decrease in the band at 3007 cm⁻¹ is associated with the cis to trans isomerism, which is also reflected by the increase in the band at 975 cm⁻¹ assignable to the trans portion of the molecule. The band at 1090 cm⁻¹ is probably associated with an oxidation product containing a C - O band, but the specific nature of the functionality has not been determined at this time. The changes occuring as the time of reaction proceeds to 235 and 640 hr. are shown in the difference spectra of Figure 8. The appearance of bands due to hydroxyl (3300 cm⁻¹ carbonyl (1770, 1720, and 1700 cm⁻¹) are now obviously reflecting the formation of these oxidation products.

ACKNOWLEDGMENT

The authors gratefully acknowledge the financial support received from the Army Research Office-Durham under grant No. DAAG29-76G-0104.

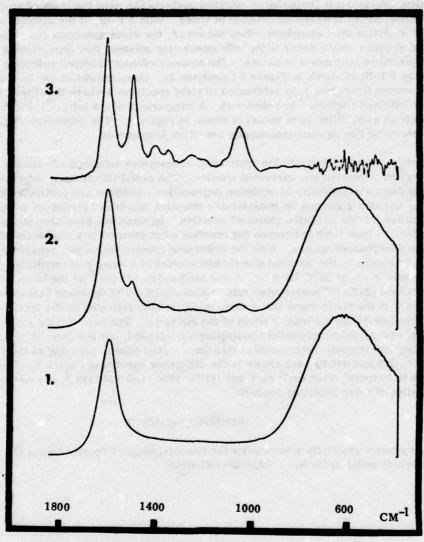


Figure 5: Aqueous solution infrared spectrum of hemoglobin obtained with Fourier transform spectrophotometer.

1, absorbance spectrum of H₂O; 2, absorbance spectrum of aqueous hemoglobin solution; 3, absorbance spectrum of hemoglobin in aqueous phase (spectrum 2 - spectrum 1).

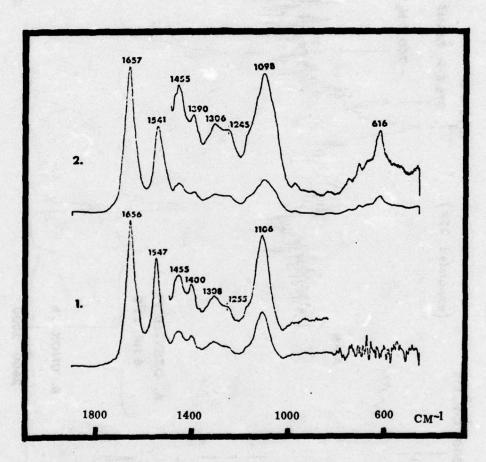


Figure 6: Infrared absorbance spectra of hemoglobin. 1, aqueous solution (pH = 4,8).

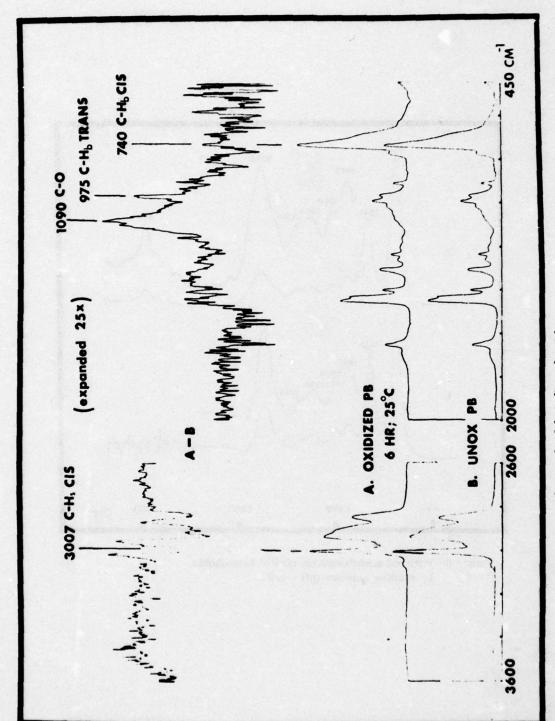


Figure 7: Oxidation of polybutadiene for 6 hr.

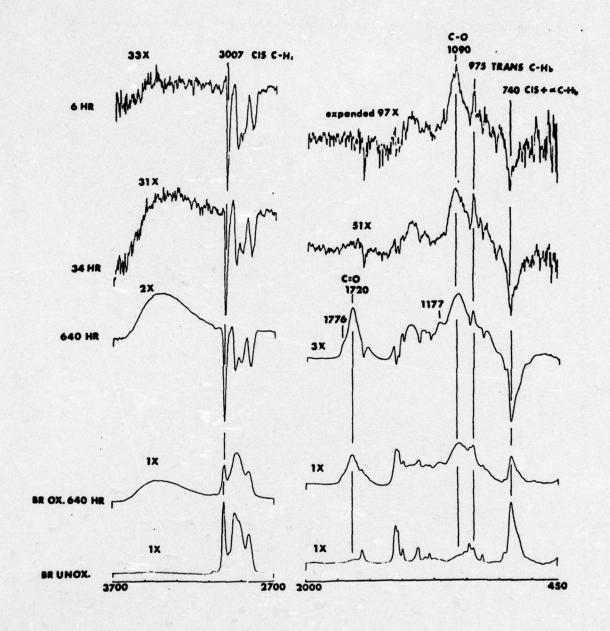


Figure 8: Difference spectra for oxidation of polybutadiene for 6, 34, and 640 hr. at 25°C.

CHARACTERISATION OF STYRENE-BUTADIENE COPOLYMERS

A. V. Cunliffe and R. J. Pace

Explosives Research and Development Establishment, Waltham Abbey, Essex, England

INTRODUCTION

I work in a small group which uses various instrumental methods to characterise polymeric materials according to molecular weight and chemical composition. To illustrate the techniques which we employ, I wish to describe some work on the characterisation of styrene-butadiene latexes. These are materials of high styrene content (approximately 85% by weight) which were produced on a pilot plant scale at ERDE by an emulsion process, and we were involved in drawing up a specification. We were mainly concerned with the properties of the copolymer itself, although parameters associated with the latex, such as solid content and particle size, were measured by other workers. Standard techniques of infra-red spectroscopy, I h nmr spectroscopy, viscosity measurement, etc, were employed, but the two newer methods which I wish to consider in more detail are the applications of TC nmr to the composition of the copolymers and the measurement of gel content using a method based on gel permeation chromatography (GPC). A feature of the preparation was that the polymerisation was taken to much higher conversion than normal for an emulsion polymerisation, and this led to substantial crosslinking towards the end of the reaction.

CHEMICAL COMPOSITION OF COPOLYMERS

The course of the reaction was monitored by the solid content and viscosity of the latex. The residual styrene monomer was measured by gas liquid chromatography on the methanol soluble fraction. The routine method of measuring the chemical composition of the copolymer is by infra-red spectroscopy. Various methods can be used to prepare samples as film, such as applying the latex directly to a silver chloride plate, or by precipitating the polymer, dissolving it in a suitable solvent (chloroform) and then casting a film (1). All methods seemed to give very similar results. The method was calibrated by comparing the spectra with a standard literature spectrum which was taken to be 85% styrene and 15% butadiene, so that it is not an absolute method (1). Moreover, the measurement actually compared the trans 1,4 butadiene content with that of styrene, so that in order to measure the total butadiene to styrene ratio it is necessary to assume that the butadiene microstructure does not vary between different samples. This appeared to be the case in our samples.

As a check on the infra-red method, we also measured the composition by ¹H nmr, which should be an absolute method. However, there are also difficulties with this approach. A major problem in attempting to measure ¹H nmr on any material containing appreciable quantities of diene units is the presence of gel. Crosslinked material gives rise to very broad proton NMR signals, which are usually not visible in a normal high resolution spectrum, so that the spectrum shows only peaks due to soluble material (1). This may not reflect the overall composition of the copolymer. In this

particular case, however, the composition determined by nmr agreed well with that from IR. Secondly, we found that the method of preparation of the sample for nmr was important. It was necessary to precipitate the latex to isolate the copolymer, and two methods were employed. A standard method is to precipitate the latex using aluminium sulphate. However, we found that with this method the nmr spectra showed evidence of interference from materials other than copolymer, presumably due to incomplete removal of soap used in the emulsion process. For the purposes of the analysis, the nmr spectrum of the copolymer may be divided into three areas, corresponding to aromatic, olefinic and aliphatic hydrogens. If we attempted to measure the composition from the ratio of aromatic to the total hydrogens, this gave an unexpectedly low value for the styrene content. However, by assuming a value for the 1,2 content of the copolymer, it is possible to measure the composition from the ratio of the aromatic to olefinic areas. (If x is the fraction of 1,2 units, then the olefinic region corresponds to 2 + x protons.) This is very similar to the infra-red method, and gave very similar results. It was clear that the discrepancy between the two 'H nmr results arose because there was extra aliphatic absorption, presumably due to the presence of soap and perhaps due to incomplete removal of water. (The aliphatic to olefinic butadiene ratio was greater than could possibly arise even if the material was entirely 1,4 linked.)

In order to remove these difficulties it was necessary to take care to obtain pure copolymer samples. This could be achieved by precipitating the material from methanol, carefully washing with methanol, followed by redissolving in THF or benzene and reprecipitating with methanol several times. Following this procedure, it is possible to obtain accurate values for both the styrene to butadiene ratio and the 1,2 butadiene to 1,4 butadiene (cis + trans) ratio in the copolymer.

More detailed information about copolymer structure can be obtained from ¹³C nmr spectroscopy. The technique also has the advantage that the signals also include contributions from the gel fraction so that the results should reflect the total composition rather than that of the sol fraction. The peak assignment and general approach follow the work of Katritzky and Weiss (2,3). The ¹³C nmr spectrum is sensitive to diad sequences, and the presence of styrene, and 1,2(vinyl),cis 1,4 and trans 1,4 butadiene units gave rise to 16 diads (Fig 1). Katritzky and Weiss (2,3)

	Styrene	cis	trans	vinyl
s	SS	Sc	St	Sv
c	cS	cc	ct	cv
t	tS	te	tt	tv
v	vS	vc	vt	vv

Figure 1

The 16 diads from the four individual repeat units in styrene-butadiene copolymers.

assign 26 peaks in the 13 C nmr spectrum of styrene-butadiene copolymers, and it is thus possible to obtain values for the concentration of all 16 diads, plus extra relationships which give a check on the method.

The concentrations of the 16 diad peaks give, first of all, the relative amounts of styrene, and 1,2,1,4 cis and 1,4 trans butadiene units. That is, the measurement

gives the average styrene content and a complete measure of the average microstructure of the butadiene units. This is frequently very useful in identifying different types of SBR, since the microstructure is characteristic of the method of preparation. Thus it should be possible, for example, to distinguish between emulsion and anionically prepared styrene butadiene copolymers on the basis of the butadiene microstructure. Moreover, the variation in microstructure should be reflected in the properties of the materials.

Table I shows results on the butadiene microstructure for different types of copolymer. The low vinyl solution samples are prepared by an anionic process using

TABLE I

Microstructure of Different Types of Styrene-butadiene Copolymers (2,3)

Sample Type	Sample	% Styrene	trans	cis	vinyl
Solution: Low vinyl	1	6	58	37	5
	2	9	56	39	5
	3	15	63	30	7
	4	26	60	30	10
Solution: High vinyl	5 6	19 3 6	53 54	24 24	55 55
Emulsion	7	12	79	7	14
	8	68	75	9	15
	9	73	80	7	12

alkyl lithium initiators in a hydrocarbon solvent, and it is clear that all the samples show similar microstructure, and can easily be distinguished from high vinyl solution polymers, and the emulsion polymers which show a characteristically low cis content.

In addition to the average amounts of the various structures, the diad concentration also gives an indication of the grouping of the monomer units within the chain. Thus if we compare the relative amounts of SS diads with other styrene containing diads (Sc, St etc), this gives an indication of the tendency of the styrene to link with itself; that is, to occur in blocks. This may be expressed as the average block length $n_{\rm S}$ given by:

$$n_{S} = 0.5 \left[\left(1 + \frac{SS}{Sc + St + Sv} \right) + \left(1 + \frac{SS}{cS + tS + vS} \right) \right]$$

where SS is the concentration of styrene-styrene diads etc. The tendency is most marked in the case of styrene butadiene block copolymers, where the average block

length is very high, since the styrene is present almost entirely in blocks (sample 2, table II). In this case, of course, practically all the styrene is present in SS

TABLE II Styrene-styrene Diad Distribution SS and Average Styrene Block Lengths $n_{\rm S}$ for Styrene-butadiene Copolymers (2,3)

Sample Type	Sample	Styrene	Styrene Diads SS OBS %	SS Random %	n _s
Solution: Low vinyl	1	6	1.5	0.4	1.3
	2	9	9.0	0.8	> 100
	3	15	12.5	2.3	5.9
	4	26	15.2	6.6	7.5
Solution: High vinyl	5	19 36	9.4 17.4	3.6 12.6	2.0
Emulsion	7	12	3.0	1.4	1.4
	8	68	53.2	46.2	4.0
	9	73	56.4	53.3	4.6

diads and the styrene-butadiene diad peaks are too small to observe. However, results for a variety of other styrene-butadiene copolymers indicate that there is a similar tendency for the styrene to form blocks in all cases. This is apparent from consideration of the diad populations in table II, where the observed values are compared with those expected for a completely random copolymer. It is clear that the observed diad population is always greater than the random one, indicating a tendency for the styrene units to be grouped together. This is most marked for low vinyl solution polymerised SBRs, prepared anionically, and has been observed previously (4,5). For the high styrene emulsion system, the effect is less marked, the distribution of styrene diads approaching the random value, and this is in accord with the reactivity ratios for the system.

In a similar way, investigation of other diads gives an indication of the tendency of other units eg cc or Sv units, to group together. Although the effects are less marked than for the styrene case, the populations differ appreciably from the random value in a number of cases.

We see that the ¹³C nmr spectra of styrene butadiene copolymers can give a fairly detailed description of their structure. It is possible to measure the styrene content, determine completely the butadiene microstructure, and give some indication of the way in which the units are grouped together. Of course, diad populations only give an indication of order over short range, and in this respect studies with higher resolution at higher fields may give more detailed information, for instance about triad or tetrad sequences.

MOLECULAR WEIGHT AND GEL CONTENT

The second fundamental property of the copolymer which we attempted to specify was the molecular weight distribution.

The simplest way to obtain a semi-quantitative assessment of molecular weight distribution was by GPC. Although there are difficulties in obtaining absolute molecular weights from GPC, the technique rapidly gives values which are internally consistent, and which should provide a method for monitoring changes in molecular weight parameters between different samples.

When we tried to run GPC curves for the styrene-butadiene systems, we ran into experimental difficulties which highlighted appreciable variation between different samples. In order to protect the styragel columns which we were using, it is necessary to filter the solutions (of the polymer in THF) through fine filters, to remove insoluble material. We found that some of the samples were extremely difficult to filter, and these samples also tended to cause increased pressure in the GPC system, indicating blocking of the columns by the copolymer. It was clear that the samples contained varying amounts of gel, and this prompted us to look more closely at the gel content of the materials. The GPC measurements gave insight into the nature of the gel present, and we found it desirable to develop a new method of measuring gel content based on this technique, which circumvents some of the problems with classical methods of measuring gel content.

When we attempted to run chromatographs on the copolymers we found basically three types of sample. Occasionally, we found samples in which all the material dissolved in THF, the solutions filtered easily, and we had no trouble with the chromatograph.

A larger proportion of the samples were only partially soluble, but the insoluble gel particles were relatively large. These could easily be filtered off, and the resulting solutions again behaved satisfactorily on the chromatograph. However it was the third type of behaviour which caused greater problems. The samples appeared to dissolve, but the solutions were hazy and it was clear that there were small gel particles dispersed throughout the solution. They were very difficult to filter, readily blocking the filters. Moreover, the filtered solution was still not completely clear, and when applied to the GPC columns it caused increased pressure and poor baseline stability in the system. They gave a characteristic chromatograph which indicated the presence of gelled material which was, however, too small to be removed by the smallest filter. Typical chromatographs are shown in figure 2. The totally soluble materials, either with or without filterable gel removed gave a broad distribution, often with indications of shoulders on the main peak. The materials containing microgel appear to contain a sharp peak at very high molecular weight. However, this material is not being separated by the columns. Above a certain molecular weight for a given set of columns all material is excluded and appears as an excluded peak corresponding to material passing through the system in the shortest possible time. The relative sharpness of the peak arises because all polymer above a critical molecular weight has the same retention time. With the column set used for the styrene-butadiene latex, the excluded material corresponded to material with an effective molecular weight greater than several million.

It is clear that, even in the materials with appreciable microgel, the soluble fraction gives a relatively straightforward chromatograph. The area of the soluble fraction, which can be readily measured, gives an accurage measure of the sol content in the materials. We therefore devised a method of estimating the sol/gel properties of the materials based on the measurement of sol content from GPC. The following procedure was adopted.

A known weight of the copolymer, obtained by precipitating the latex in methanol, is shaken in tetrahydrofuran (THF) for 3 days. A known weight of narrow distribution

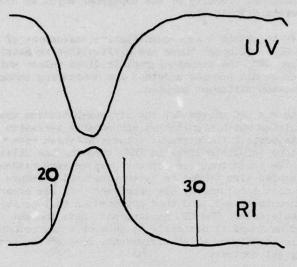


Figure 2(a)

GPC trace for a styrene-butadiene copolymer free from microgel

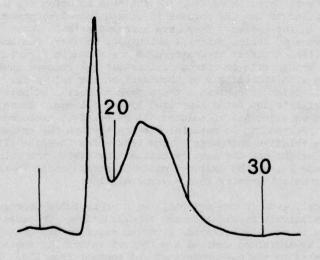


Figure 2(b)

GPC trace for a styrene-butadiene copolymer containing microgel

2,000 MW polystyrene is added. The solution is then filtered through a 0.9 micron asbestos filter. The soluble fraction is then run on the GPC. Typical GPC traces are shown for materials with (fig 3(b)) and without (fig 3(a)) microgel. The material with microgel gives three peaks, which correspond, in order of increasing molecular weight to 2,000 MW polystyrene A, soluble copolymer B, and excluded microgel C. By calibration with a totally soluble styrene-butadiene copolymer of similar composition to the ones being investigated, it is possible to measure both the amount of soluble material and the microgel. The difference between the sum of these quantities and the initial quantity of the material gives the amount of gel which has been removed. The GPC trace also gives the molecular weight distribution of the sol.

The main advantage of the method is that the amount of soluble material is accurately measured, and does not depend on a separation process such as filtration or centrifuging. The separation into microgel and macrogel is another useful property of the system, although the exact distribution will depend on the size of filter used and the filtration procedure adopted.

The type of behaviour obtained is illustrated by an experiment in which the variation in gel content with time was followed for an emulsion SBR polymerisation. We were particularly interested in the results at high conversion, since these corresponded to the conditions used in the particular preparations in which we were interested. Table III shows the sol, microgel and macrogel contents for a typical

TABLE III

Variation of Gel Content with Conversion for 85:15 Styrene-butadiene Emulsion Polymerisation

Reaction Time (hours)	Conversion %	Sol %	Microgel %	Macrogel %
10	80	98	2	0
10.5	86	95	5	0
11	89	66	3	31
11.5	96	58	0.5	41.5
12	99	58	0	42
14	99	56	0	44

run. It is clear that a negligible amount of gelation occurs up to about 80% conversion in the relatively high styrene materials. Initially, above about 80% conversion, gel is produced mainly as microgel. However, at higher conversion, appreciable amounts of gel are produced as macrogel, which can be removed by filtration, and the amount of microgel becomes small.

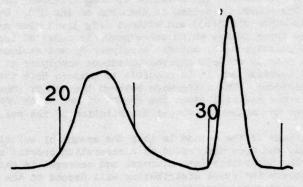


Figure 3(a)

GPC trace for a styrene-butadiene copolymer free from microgel, with 2000 MW polystyrene internal marker

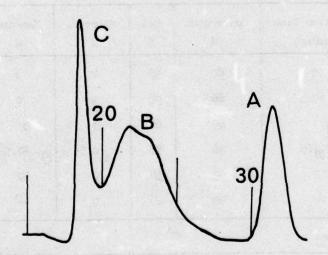


Figure 3(b)

GPC trace for a styrene-butadiene copolymer containing microgel.

A: 2000 MW polystyrene. B: soluble copolymer. C: microgel

The above method is carried out on copolymer which has been precipitated from methanol to give a solid polymer. We believe that it gives an accurate estimate of the sol content, and hence the total gel content, but that the distribution between microgel and macrogel may be dependent on the precipitation process and the existence of the material as a solid. We have therefore also applied the internal marker technique to a procedure devised by Gaylor et al (6) which is applied directly to the latex. In this method, the acqueous latex is dissolved in THF by dropwise addition with stirring, to give a concentration of about 0.5%. The solution is then filtered, and chromatographed on a set of columns which separate the water peak, the 2,000 MW polystyrene marker, and the sol and gel fractions of the copolymer. By comparison with the determinations on the precipitated copolymer, we hope to investigate in more detail the nature of the gel particles.

The main disadvantage of the methods arose from problems associated with blocking of the GPC columns with gel particles. This was particularly serious and expensive with the styragel columns. However, Gaylor et al (6) showed that relatively inefficient, low resolution porous glass columns were sufficient for the separation of sol and gel, and these are much cheaper and easier to repack. We have used porous silica columns which have similar advantages.

REFERENCES

- J. Haslam, H. A. Willis and D. C. M. Squirrell, "Identification and Analysis of Plastics", 2nd Edition, Iliffe Books (1972).
- A. R. Katritzky and D. E. Weiss, "Carbon-13 Nuclear Magnetic Resonance Spectroscopy of Polymers, Part IV", J. Chem. Soc., Perkin II, 21 (1975).
- A. R. Katritzky and D. E. Weiss, "Carbon-13 Nuclear Magnetic Resonance Spectroscopy of Polymers, Part V", J. Chem. Soc., Perkin II, 27 (1975).
- 4. A. A. Korotkov and N. N. Shesnokova, Rubber Chem. Tech., 33, 623 (1960).
- 5. A. F. Johnson and D. J. Worsfold, Makromol. Chem., 85, 273 (1965).
- 6. V. F. Gaylor, H. L. James and J. P. Herdering, "Chromatographic Techniques for Rapid Measurement of Gel in Elastomers", J. Poly. Science, 13, 1575 (1975).

THE USES OF INFRARED SPECTROSCOPY FOR THE CHARACTERIZATION OF POLYMERIC MATERIALS

D. M. Wiles

Chemistry Division
National Research Council of Canada
Ottawa, Ontario, KIA OR9, Canada

TECHNIQUES

Infrared (IR) spectroscopy has been used to characterize and analyze materials for most of this century; it is especially useful for organic materials. Absorptions from an incident polychromatic IR beam occur at frequencies corresponding to vibrations and rotations of groups which undergo changes in dipole moment. It is this specificity which partially compensates for the inherent lack of sensitivity in IR spectroscopy and accounts for the widespread use of the method. Like all other types of chemical spectroscopy (e.g. NMR, ESR, ESCA) IR spectroscopy is less suited to polymeric materials than it is to low molecular weight organic compounds. Nevertheless, polymer chemists have employed IR techniques for many decades and fiber scientists have used them increasingly as the science and technology of textile products becomes rapidly more complex.

Transmission Spectroscopy

Most commercial spectrometers are designed for the direct measurement of transmission IR spectra - recordings of those IR wavelengths which are absorbed by the sample as the incident beam is transmitted through it. The most common form for a sample, whether or not it contains (or consists entirely of) macromolecules, is a disc or pellet of KBr into which a small quantity of the specimen has been mixed before pressing. The problems of grinding up and dispersing "rubbery" plastics with KBr can frequently be alleviated by performing these operations at liquid nitrogen temperature where most polymers are reasonably brittle.

There are many instances, however, where plastics and fibers should be characterized in their original form and non-destructive sample preparation techniques are called for. There are many examples in the scientific literature illustrating the use of thin films as IR samples. These could be commercial, chill-cast films of thermoplastics, or hot-pressed or solution-cast films made in the laboratory from resin. IR spectra of individual fibers (e.g., 30 µm monofilaments) have been measured with an IR microscope by Grass et al (1), and orientation measurements have been made on a single-thickness coil of monofilament (2).

More recently, a very simple device has been described (3) with which the IR absorption spectrum of a short length of any fiber can be obtained. Figure 1 shows the spectrum obtained in this way for a 6 denier monofilament of polycaprolactam.

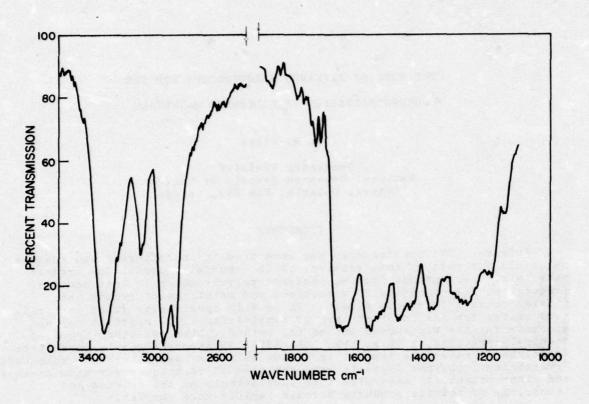


Figure 1. Infrared absorption spectrum of a six denier monofilament of nylon 6, recorded at 30 cm⁻¹/min.

Internal Reflection Spectroscopy

Many polymeric samples (e.g., fibers, fabrics, films) are too opaque to allow direct measurement of their IR absorption spectra by transmission spectroscopy. Sometimes, in addition, the IR spectrum of the surface zone of a sample (transparent or opaque) is required. In both these situations, the appropriate technique is internal reflection spectroscopy, IRS (variously referred to as ATR, FATR, MATR). In the IRS method, the sample is placed in good contact with an inorganic reflection element (e.g., germanium) and the IR beam is reflected from the reflection element—sample interface. The reflected beam penetrates into a thin surface layer of the sample and will be attenuated by any IR absorbing groups in that layer. In other words, a surface spectrum will be produced. Wilks (4) has recently reviewed the techniques and limitations of IRS; the relevant mathematical theory has been developed by Harrick (5).

IRS spectra are usually directly comparable to transmission IR spectra notwithstanding the slight distortions of absorption bands as a function of wavelength and refractive index which accompany surface spectral measurements. The IR intensity transmitted by an IRS mirror/reflection element assembly varies greatly with the f number of the spectrometer beam. Spectrometers with low f numbers (e.g., for most Perkin-Elmer models,

 $f \sim 4.5$) give low transmission unless special IRS mirror assemblies are used. On the other hand, low divergence spectrometers (e.g., for most Beckman models, $f \sim 10$) give significantly higher transmission values.

By recording IRS spectra at different angles of incidence and on reflection elements having different refractive indices, spectra corresponding to different depths of penetration into a sample may be recorded (6,7). Quantitative comparison of these spectra requires careful control of experimental conditions as well as the use of an internal standard absorption band. With such control, however, one can construct a concentration/depth profile to show (Figure 2) the distribution of photo-oxidation products in polypropylene film.

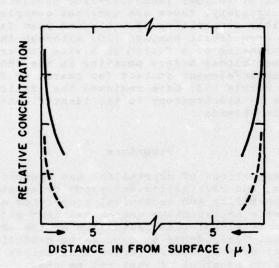


Figure 2. The concentration profile of photo-oxidation products in the cross-section of an unstabilized polypropylene film, after 40 hr irradiation ----, after 70 hr irradiation — . Measurements made by internal reflection spectroscopy.

APPLICATIONS

A great deal of information can be derived from the IR spectra of macromolecules. There are many reports of the identification of films, fibers, fiber blends, copolymers, coatings and other finishes. Chemical modifications, degradation, pyrolysis and combustion are also amenable to examination by IR spectroscopy. In addition, however, morphological phenomena can also be identified in some cases; crystallinity, chain folding, stereoregularity and orientation may all cause significant, detectable alterations in IR absorption bands.

Identification

The methodology and interpretation are sufficiently well-known that IR spectroscopy is considered a standard method for fiber identification. For such purposes, it is essential to use standard spectra and correlation charts in order to relate unknown spectra to known, characteristic absorptions. The text by Henniker (8) describes the principles and practices of the IR spectroscopy of polymers; the Hummel collection (9) of spectra of polymeric materials is particularly valuable. In Canada, the National Research Council offers a Search Program for Infrared Spectra (SPIR) whereby the NRC computer will indicate which among 142,000 standard spectra most closely match the spectrum of an unknown.

Whereas the bulk of polymer identification problems can be solved by transmission IR spectroscopy, there are numerous examples of the use of IRS as well. The fiber composition of a blended yarn fabric can be identified directly from fabric samples (10) although there are difficulties. Pre-pressing of a fabric in a vice for several hours between polished steel blocks before mounting in the IRS holder can sometimes improve sample/element contact for coarse or fluffy fabrics. Finally, McCall and Morris (11) have reviewed the applications of IRS as well as transmission IR spectroscopy to the identification of cotton and cotton-synthetic fiber blends.

Structure

The relative proportions of crystalline and amorphous phases, the size of crystallites, and crystallite-amorphous orientation determine the aesthetics, dye permeability and mechanical properties of fibers and plastics. Consequently an extensive search has been made for IR bands indicative of groups in either the crystalline or the amorphous phases in order to study their dependence on processing conditions, as well as their ultimate effect on properties. Space limitations preclude anything other than reference to examples of what can be done.

Bahl and co-workers (12) described the assignment of structure bands in polyethylene terephthalate; Edelmann and Wyden (13) have used IRS to measure PET amorphous (1370 cm⁻¹) and crystalline (1343 cm⁻¹) content. From both IR and X-ray data, Sibilia et al (14) concluded that the tensile strength of PET fibers is dependent on amorphous orientation, rather than crystallinity, fold content or the lateral ordering of crystallinity. IR spectra of many of the crystalline forms of cellulose have been reviewed by Liang (15).

In the investigation of the stereoregularity of polypropylene, IR spectroscopy has proven to be particularly informative. The ratio of absorptions at 997 cm⁻¹/974 cm⁻¹ can be used as a measure of helical content (16) since all three tactic forms of polypropylene absorb at 974 cm⁻¹. It should be noted, however, that IR measurements cannot distinguish between the isotacticity and crystallinity of this polymer.

Chemical and Photochemical Changes

It has been known for many years that modifications to plastics and fibers, as a result of chemical reactions, are frequently readily detectable by IR spectroscopy. This is particularly true of cellulose fibers, especially cotton; O'Connor has summarized this work admirably (17,18) including the use of the IRS technique. The appearance and disappearance of specific absorption bands in the spectra of nylon 6 were used by Fukuhara et al (19) to elucidate the chemical changes resulting from steam and dry heat treatments.

Since so many chemical and structural changes occur predominantly on or near film and fiber surfaces, IRS measurements are particularly relevant to their investigation. Carlsson and Wiles (6) described in detail the use of the IRS method for the quantitative comparison of polypropylene film surfaces which had been exposed to various electric discharge treatments.

Virtually all polymers, including those used in fiber form, suffer delaterious effects on exposure to near ultraviolet radiation in air. Although the rates of photodegradation vary enormously depending on the type of polymer, chain scission, loss of physical properties and chemical changes detectable by IR spectroscopy are commonly involved. IR measurements played a key role in the identification of the photo-oxidation products of branched polyethylene (20), PET and PET/cotton blend fabrics (21), nylon 66 and Nomex (22) to mention a few examples.

The IRS technique has been invaluable in the study of the thermal and photo-oxidative degradation of rubbers, plastics and fibers. Chan and Hawkins (23) first demonstrated the use of IRS to give advanced warning of weathering deterioration of plastics, using a band ratioing technique to allow for variable contact and sampled area. Since then Carlsson and Wiles (7), Carlsson et al (24,25) and Blais et al (26,27) have shown that many fiber-forming polymers undergo preferential surface photodegradation. Day and Wiles (28) were able to demonstrate that carboxylic acid end groups are a primary photochemical product arising from a chain scission process which occurs predominantly on and near the surface facing the source of UV light. Subsequently Blais et al (26) showed the connection between photochemical and mechanical surface changes, using IRS measurements to monitor the former.

REFERENCES

- F. Grass, H. Siesler, and H. Krassig, Melliand Textilber. Int. 52, 1001-1005 (1971).
- G. A. Tirpak and J. P. Sibilia, J. Appl. Polym. Sci. <u>17</u>, 643-648 (1973).
- 3. D. J. Carlsson, F. R. S. Clark, and D. M. Wiles, Text. Res. J. 46, 318-321 (1976).
- 4. P. A. Wilks, Amer. Laboratory 4, 42-55 (1972).
- N. J. Harrick, "Internal Reflection Spectroscopy," Interscience Publishers, Inc., New York (1967).

- 6. D. J. Carlsson and D. M. Wiles, Can. J. Chem. 48, 2397-2406 (1970).
- 7. D. J. Carlsson and D. M. Wiles, Macromolecules 4, 174-179 (1971).
- 8. C. J. Henniker, "Infra-red Spectrometry of Industrial Polymers," Academic Press, New York (1967).
- D. O. Hummel, "Infra-red Analysis of Polymers, Resins and Additives: an Atlas." Vol. I, "Plastics, Elastomers, Fibers & Resins." Pt. 1, Text; Pt. 2, Spectra, Tables, Index. Wiley-Interscience, New York (1969).
- D. J. Carlsson, T. Suprunchuk, and D. M. Wiles, Can. Text. J. <u>87</u> (11) 73-84 (1970).
- E. R. McCall and N.M. Morris, Develop. Appl. Spectrosc. <u>7B</u>, 228-251 (1968).
- S. K. Bahl, D. D. Cornell, F. J. Boerio, and G. E. McGraw, J. Polym. Sci., Polym. Lett. Ed., <u>12</u>, 13-19 (1974).
- 13. K. Edelmann and H. Wyden, Kant. Gummi, Kunstst. 25, 353-357 (1972).
- 14. J. P. Sibilia, P. J. Harget, and G. A. Tirpak, Amer. Chem. Soc. 167th meeting (Los Angeles). Polymer Preprints <u>15</u>, (1) 660-665 (1974).
- C. Y. Liang, in "Instrumental Analysis of Cotton Cellulose and Modified Cotton Cellulose" (R. T. O'Connor, ed.) Chapter 2, pp. 59-61, Marcel Dekker, New York, 1972.
- 16. R. H. Hughes, J. Appl. Polym. Sci. 13, 417-425 (1969).
- R. T. O'Connor, in "Cellulose and Cellulose Derivatives," Part IV (N. M. Bikales and L. Segal, eds.) Chap. 13, Part A3, pp. 51-87 (1971).
- R. T. O'Connor, in "Instrumental Analysis of Cotton Cellulose and Modified Cotton Cellulose," (R. T. O'Connor, ed.) Chapter 8, pp. 401-462 (1972).
- S. Fukuhara, Y. Suzuki, S. Omote, and T. Komatsubara, Nippon Gomu Kyokaishi 44, 611-615 (1971) [through Chemical Abstracts 75, 141485 (1971)].
- 20. J. F. Heacock, J. Appl. Polym. Sci. 7, 2319-2322 (1963).
- M. S. Kulinga, L. P. Kolov, and A. F. Tumanova, Technol. Text. Ind. U.S.S.R. 6, 87-89 (1970).
- 22. G. Hargreaves and J. H. Bowen, Text. Res. J. 43, 568-576 (1973).
- 23. M. G. Chan and W. L. Hawkins, Amer. Chem. Soc. 156th Meeting (Atlantic City) Polymer Preprints 9, (2), 1638-1643 (1968).

- D. J. Carlsson, R. D. Parnell, and D. M. Wiles, J. Polym. Sci., Polym. Lett. Ed. <u>11</u>, 149-153 (1973).
- D. J. Carlsson, L. H. Gan, R. D. Parnell, and D. M. Wiles, J. Polym. Sci., Polym. Lett. Ed. <u>11</u> 683-688 (1973).
- 26. P. Blais, M. Day, and D. M. Wiles, J. Appl. Polym. Sci. 17, 1895-1907 (1973).
- 27. F. Blais, D. J. Carlsson, R. D. Parnell, and D. M. Wiles, Can. Text. J. 90 (7) 93-96 (1973).
- 28. M. Day and D. M. Wiles, J. Appl. Polym. Sci. <u>16</u>, 175-189; 191-202; 203-215 (1972).

FOURIER TRANSFORM INFRARED SPECTROSCOPY AS A METHOD FOR STUDYING WEATHERING OF GLASS-FIBER EPOXY COMPOSITES

James F. Sprouse

Organic Materials Laboratory
Army Materials and Mechanics Research Center
Watertown, Massachusetts 02172

INTRODUCTION

The incorporation of an interferometer and a digital computer into an infrared spectrometer has been a significant technological advancement for infrared spectrometers. High resolution spectra can now be measured in very short times for materials that in the past have required tedious sample preparation. Also, internal reflection spectroscopy (IRS) is now becoming an everyday tool in the laboratory instead of an occasionally used instrument accessory.

Fourier transform infrared spectrometers offer several advantages over conventional instruments although the final result on either instrument is still an infrared finger-print. Probably the greatest advantage realized from FTS-IR is the improvement in energy throughput for a sample. FTS instruments require no energy-wasting slits to isolate individual frequency elements and the optics are quite large compared to conventional instruments. All frequencies of light are incident to the sample throughout the spectrum scan in a FTS-IR and the resulting output signal is intensity as a function of time (an interferogram). The final intensity-frequency information is obtained by completing a Fourier transformation of the interferogram by use of a digital computer.

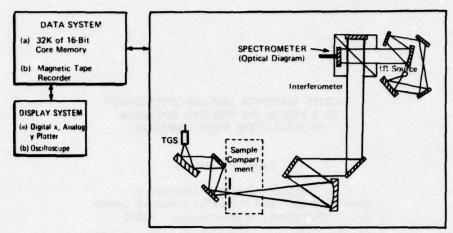
FTS-IR generally provides an infrared spectrum in much less time than a conventional instrument with equivalent signal-to-noise ratio, or in the same amount of time with better signal-to-noise ratio. The \sqrt{M} improvement to signal-to-noise ratio is realized in FTS-IR where M is the number of resolution elements scanned.

Another significant advancement FTS-IR has brought to the field of infrared spectroscopy is the interfacing of a digital computer to the IR spectrometer. Since the interferogram requires signal averaging and a transformation, a digital computer is required for achieving usable results. This automatically provides the capability for data processing such as scale expansion, spectral comparisons and absorbance spectra arithmetic for chemical separations without wet chemistry.

The FTS-IR is ideally suited for internal reflection spectroscopy. As with conventional instruments, IRS provides a nondestructive IR method for surface analysis of materials not easily placed into solution, such as epoxy thermosets. The high energy throughput and signal averaging advantages of FTS-IR have made internal reflection spectroscopy a valuable tool for organic materials characterization.

EXPERIMENTAL AND RESULTS

Fourier transform infrared spectroscopy is being used at AMMRC to characterize cure and post cure of epoxy resins and to study weathering properties of composites made from these resins.



STORED-RATIO INTERFEROMETRIC IR SPECTROMETER
FIGURE 1

Studies have been completed on a stored-ratio interferometric instrument (Digilab Model FTS-10M) as shown in Figure 1. The instrument operates in the middle IR from 3800 to 450 cm $^{-1}$. It has a resolution capability of 2 cm $^{-1}$ but most spectra are measured at resolution 4 cm $^{-1}$ where approximately 1.2 seconds are required for one scan of the operating IR region.

As may be seen in Figure I, AMMRC's instrument has an all-core computer system consisting of 32K of 16-bit memory. A seven-inch, nine-track magnetic tape recorder complements the all-core memory in the computer. Both oscillographic and recorder outputs are available for spectra display.

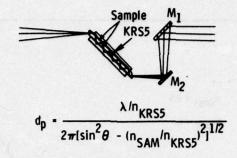
During characterization of cure and post cure of epoxy resins, and weathering studies of composite materials, both absorbance and reflectance spectra have been measured. Cure and post cure were studied by absorbance spectra of epoxy resin thin films on potassium chloride windows. After a thin film of the resin was spread on the windows, and absorbance spectra measured from 3800 to 450 cm⁻¹, the plates were placed in a forced air oven at 163°C and cured for 45 minutes. Absorbance spectra were again measured, and then at 1-hour post cure intervals. Post cure was completed at 177°C. The salt plate method is a very simple technique for studying the epoxy resins. Spectra were measured at resolution 4 cm⁻¹ and 64 signal averages.

Weathering studies using internal reflection spectroscopy (IRS) were completed on a 7-ply glass fiber epoxy composite (Scotchply 1009-26). Figure 2 shows the experimental arrangement for the IRS studies (1). The IRS attachment (Harrick Model TPMRA-P) used a KRS5 reflection element (50 x 20 x 2 mm; $n_{KRS5} = 2.5$) with an angle of incidence equal to 45°. The refractive index for cured 1009 resin is approximately 1.5 (2).

As may be seen in Figure 2, the KRS5 crystal is sandwiched between two samples of the composite (45 x 20 mm). Then the samples are pressed against the crystal by applying a torque of 80 inch-ounces. Spectra were measured at resolution 4 cm $^{-1}$ and 2500 signal averages. Reflectance spectra of the composite are presented as the logarithm of the ratio of the sample emission spectra to the KRS5 emission spectra.

^{1.} Harrick, N. J., "Internal Reflection Spectroscopy," Interscience Publishers, New York (1976), p. 30 185.

^{2.} Lee, H., and Neville, K., "Handbook of Epoxy Resins," McGraw-Hill Book Company, New York (1967), p. 4-29.



 d_p = depth of penetration into sample $(n_{KRS5} > n_{SAM})$

 λ = wavelength of radiation in μ m

n_{KRS5} = refractive index of KRS5

n_{SAM} = refractive index of sample

 θ = angle of incidence of radiation

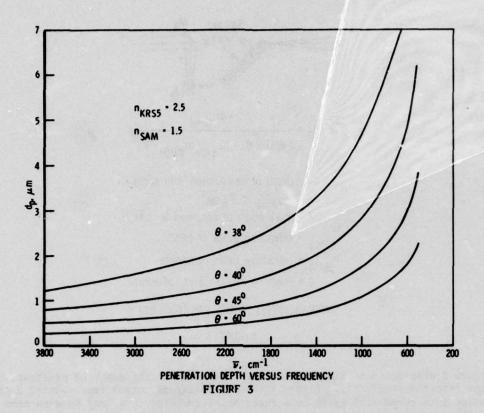
INTERNAL REFLECTANCE SPECTROSCOPY

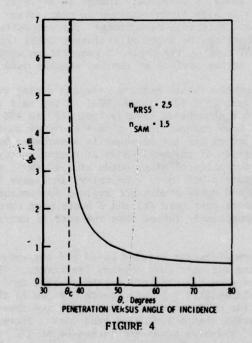
FIGURE 2

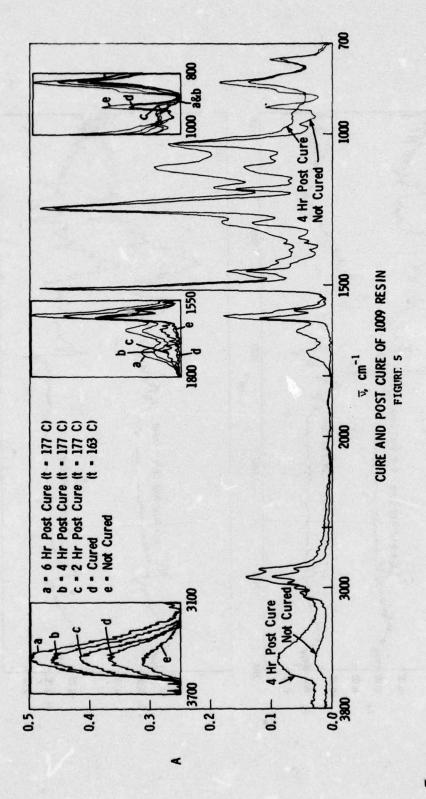
Figure 2 also presents the equation for approximating the depth of penetration of radiation into the sample (1). Figure 3 shows a family of curves representing depth of penetration into cured 1009 resin as a function of frequency. As may be seen from the figure, the more energetic the radiation, the greater the depth of penetration. Also, as may be seen from Figures 3 and 4, a very small change in angle of incidence around the critical angle, θ , results in significant changes in penetration depth. This provides for surface layer or gel coat thickness measurements for composites, when the coatings are 3 or 4 microns thick, by changing the angle of incidence until the substrate spectra (filler glass) is just resolved. Of course, the depth of penetration would only be an approximation of the average thickness over the surface of the two samples used for the IRS measurements.

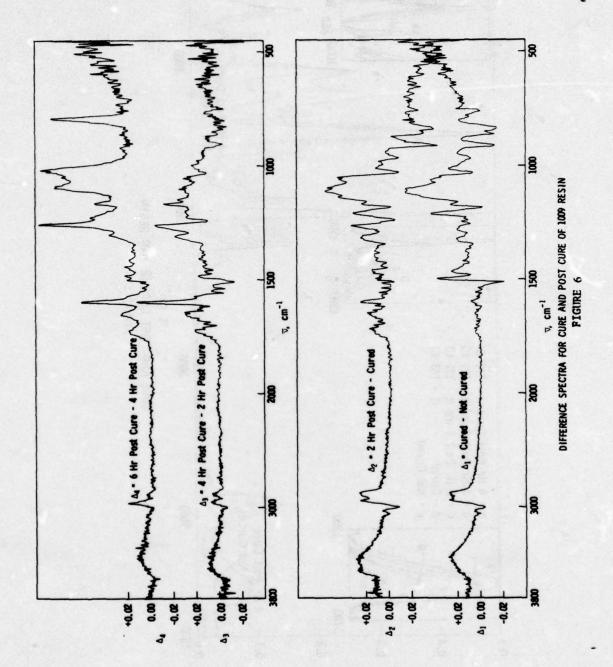
Figure 5 shows infrared absorbance spectra measured during cure and post cure of 1009 resin (2 parts DEN 438; 1 part EPON 828; 3% BF₃:MEA) by the salt plate method described earlier in the text. The two absorbance spectra from 3800 to 450 cm⁻¹ show the 1009 resin before cure and after 0.75 hour cure at 163°C plus 4 hours of post cure at 177°C. The major differences in the spectra are the increase in absorbance by hydroxyls at approximately 3500 cm⁻¹; the formation of carbonyl bands at approximately 1730 and 1650 cm⁻¹ (oxidation products); the formation of ether bonds at 1110 cm⁻¹; and the loss of epoxy ring absorbance at approximately 915 cm⁻¹. The inlays in Figure 5 show scale expansions for the hydroxyl, carbonyl and epoxy absorbance regions for noncured resin (e), cured (d), 2 hours post cure (c), 4 hours post cure (b) and 6 hours post cure (a). The oxidation bands at 1730 and 1650 are not appreciably formed when the cure is carried out in vacuum or in nitrogen atmosphere.

Figure 6 shows difference spectra between cured and not-cured resin, and between the successive steps of the cure and post cure thermal treatments. The difference spectra were obtained by normalizing the aromatic absorption band at 1510 cm⁻¹ for all spectra to that of the uncured resin. This compensates for path length changes in the resin films resulting from resin shrinkage. In the difference spectra, a positive change in absorbance indicates bond formation, and a negative change indicates bond loss. Increases in absorbance at 3500 cm⁻¹ show formation of hydroxyl bonds and increases at 1730 and 1650 cm⁻¹ show the formation of aliphatic and aromatic carbonyl groups, respectively. The absorbance at 915 cm⁻¹









shows the epoxy ring opening (negative change) during cure and post cure. The usefulness of difference spectra can easily be seen for Δ_3 where loss of the epoxy ring is easily detected between 2 and 4 hours post cure but this change was not apparent from the absorbance spectra in Figure 5, even after scale expansion. It should be noted that the ordinate in Figure 6 is easily interpreted to 0.002 absorbance units while the ordinate in Figure 5 is typically useful to only 0.01 absorbance units. Figure 7 shows graphically the changes that occur during the cure and post cure of the 1009 resin. These data were extracted directly from the difference spectra and normalized to the 915 cm⁻¹ absorbance of the uncured resin. As can be seen from the graph, approximately 65% of the epoxy is still unreacted at the end of the 163° C cure cycle. Only after 4.75 hours of post cure has the resin approached complete reaction. Minimum detectable amount of the epoxy has not been established to date, but it is expected to be approximately 0.01% by weight.

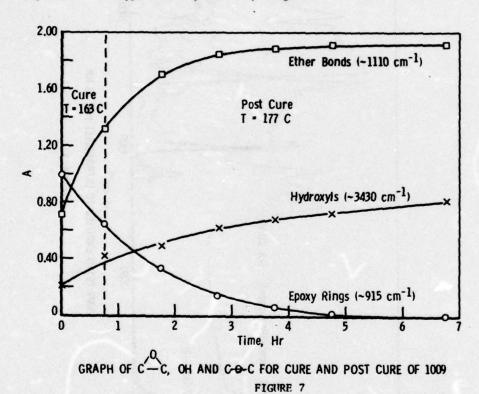
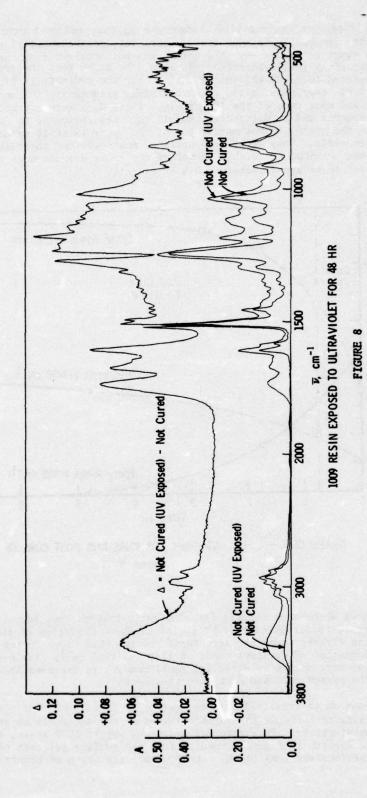
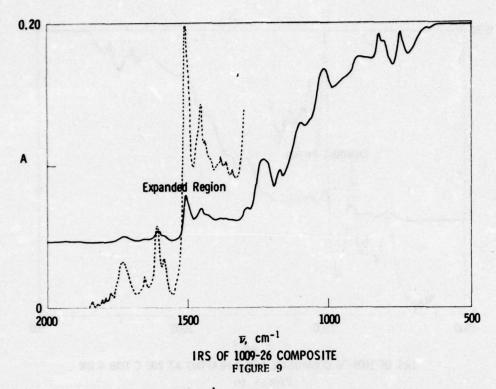


Figure 8 shows absorbance spectra for 1009 resin that has not been cured, before and after it was exposed to ultraviolet light to induce photo-oxidation of the resin. The difference spectra clearly shows the structural changes that occur during the UV exposure, especially the formation of carbonyl bands at 1730 and 1650 cm⁻¹. The use of difference spectra has proven very useful in detecting small changes in infrared absorbance characteristics of the 1009 system cure and post cure treatments.

Figure 9 shows an internal reflectance spectra of a new sample of 1009-26 composite. The spectra is characteristic of the surface layers of the materials as it is received from the commercial manufacturer. This material is 26% by weight 1009 resin, and 74% Owen Corning 801 E-glass. The spectra in Figure 9 results from the surface gel coat of resin which is approximately 5 micrometers (µm) thick. At 2000 cm⁻¹ the depth of penetration of light



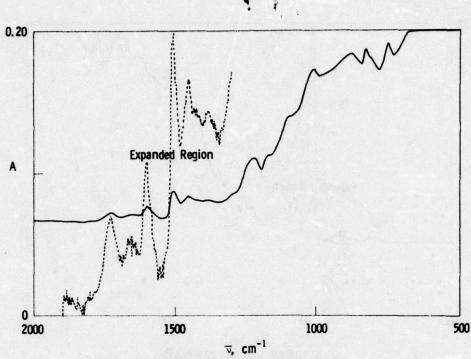


is approximately 0.8 µm and at 600 cm⁻¹ the depth of penetration is approximately 3 micrometers. The changing baseline reflects the increase in penetration depth as a function of decreasing frequency. The absorbance bands are well resolved and may be compared with the absorbance spectra for a thin film of the same resin system in Figure 5. Absorbance bands above 2000 cm⁻¹ are generally not resolved using IRS on the thermoset. The scale expansion between 1800 and 1300 cm⁻¹ shows the carbonyl bands at 17 0 and 1650 cm⁻¹ in much greater detail. Also, the aromatic bands at 1610 and 1510 cm⁻¹ are easily identified in addition to the other bands at 1240 and 1110 cm⁻¹.

IRS resolves nearly all the absorbance bands below $2000~\rm{cm^{-1}}$ that are resolved by transmittance measurements. It also provides the advantage of being able to measure spectra of the cured resin after it has been fabricated into a composite.

Figure 10 shows thermal oxidation of the sample in Figure 9. The sample of 1009-26 composite was heated inside a forced air oven at 200°C for 4 hours, then the infrared surface spectra measured by IRS. Thermal oxidation is seen as evidenced by the increase in absorbance of the aliphatic carbonyl band at 1730 cm⁻¹. The expanded areas of Figures 9 and 10 are normalized so the 1510 cm⁻¹ bands are of equal intensity. Therefore, the 1730 cm⁻¹ bands can be compared directly for a measure of oxidation. Also, difference spectra can be used for IRS equally well as for absorbance spectra.

IRS was used to characterize weathering of the 1009-26 composite. Samples of the 1009-26 were exposed at the Desert Test Center, Yuma, Arizona, and at the Tropic Test Center, Panama Canal Zone. The samples were returned to the laboratory at 6-month exposure intervals for analyses. Both test sites were characterized by bright sunshine and high surface temperatures.



IRS OF 1009-26 COMPOSITE AFTER HEATING AT 200 C FOR 4 HR
FIGURE 10

Figure 11 shows the results of IRS measurements on the above samples. The abscissa is graphed in total langleys of solar radiation (λ = 0.85 to 3.5 microns) measured at the sites. Curve "a" in Figure 11 shows a transmittance spectra (IRS) of an unexposed sample of 1009-27, curves "b" and "c" show the sample after 6 and 12 months exposure at Yuma. As fiber blooming occurs on the surface of the composite, the infrared spectra proceeds from that of the resin to that of E-glass (borosilicate) where only the broad inorganic stretching bands for Si-0 and B-0 are resolved. The absorbance at 1400 cm⁻¹ for the B-0 band can be used as a measure for quantifying fiber blooming. The solid curve in Figure 11 shows absorbance at 1400 cm⁻¹ for the samples exposed at Yuma. New E-glass produces an absorbance at 1400 cm⁻¹ of 0.048 when measured by IRS using the same parameters as for the Yuma samples. A sample exposed at Panama for 6 months produced absorbance at 1400 cm⁻¹, nearly equal to the E-glass, therefore showing nearly complete loss of surface resin.

Figure 12 shows a more detailed analyses of a 1009-26 sample exposed at the same Panama site for 24 months. An IRS spectra of the top surface showed the presence of a small amount of resin as evidenced by the scale expansion of the 2000 to 1300 cm⁻¹ region in the upper left corner of Figure 12. The aromatic band at 1510 cm⁻¹ is clearly present indicating that resin is still on the surface layer, although the visual appearance of the surface only shows bloomed glass. If the glass is carefully removed from the top surface, then a scale expansion of the 2000 to 1300 cm⁻¹ region shows the resin is similar to that of oxidized resin (Figure 10). Spectra of the bottom surface shows a loss of resolution for the 1510 cm⁻¹ aromatic band, and the spectra shows extensive fiber blooming with some resin still present. The bottom surface is not as badly fiber bloomed as the top surface of the 6-month exposure.

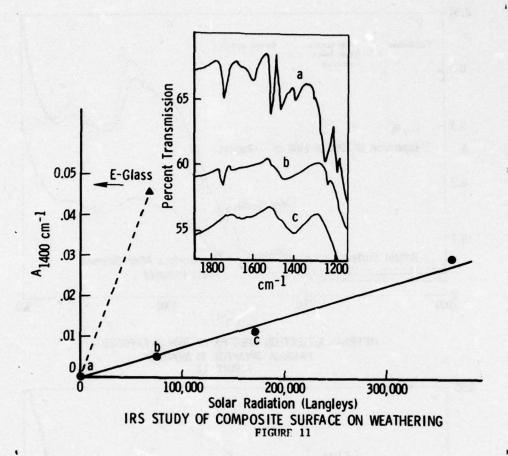
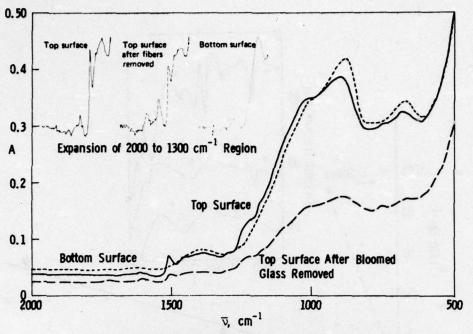


Figure 13 demonstrates the usefulness of difference spectra when used with IRS. The dashed curve again is the reflectance spectra for the composite sample (glass removed) exposed at Panama for 24 months. The top spectra is that of E-glass. When the E-glass spectra is subtracted from the top surface spectra (glass removed), the resulting spectra is an enhancement of the 1009 resin without the E-glass. This technique allows the oxidation of the resin to be studied without the strongly absorbing inorganic bands of the E-glass masking the resin spectrum. This technique has proven very useful for characterizing environmental deterioration processess of the resin.

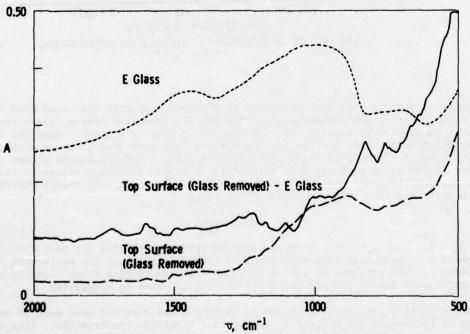
CONCLUSION

FTS-IR has proven to be a very powerful analytical technique for both characterizing epoxy resin cure processes and, when combined with IRS, studying the weathering of epoxy thermosets. It has provided us with a technique for quantifying fiber blooming and it should prove very useful for measuring gel coat thicknesses on composites.

Future applications for FTS-IR are to carry out the cure and post cure of epoxy resins directly in the sample compartment of the Fourier transform spectrometer. This allows infrared spectra to be measured at approximately 1-second intervals for kinetic characterization. Our laboratory has applied FTS-IR to only a limited number of applications to date, but it already has proven a valuable asset for characterizing polymeric materials and deterioration of those materials.



INTERNAL REFLECTION SPECTRA OF 1009-26 EXPOSED AT PANAMA OPEN FOR 24 MONTHS FIGURE 12



DIFFERENCE SPECTRA OF PAN 24 MONTH TOP SURFACE FIGURE 13

NEUTRON RADIOGRAPHIC TECHNIQUES FOR INSPECTION OF POLYMERIC MATERIALS

D. H. Petersen and W. E. Dance

VOUGHT CORPORATION ADVANCED TECHNOLOGY CENTER, INC. P. O. BOX 6144, DALLAS, TEXAS 75222

SUMMARY

Neutron radiography was used for the nondestructive inspection and evaluation of the polymeric phases in complex structures. Data are presented demonstrating the sensitivity of neutron radiographic procedures for detection of bondline voids/defects and the capability of the technique to predict bondline strength for assessing structural service-ability. Also discussed is the application of neutron radiography to the inspection of honeycomb and composite aerospace structures.

INTRODUCTION

Advanced composite and adhesively bonded structures are attractive for the fabrication of advanced DoD systems because of such advantages as: (1) design flexibility; (2) weight savings; and (3) cost reduction. Perhaps the greatest of their virtues is their effectiveness in cost-conscious practical designs utilizing metal/nonmetal material combinations. The increasing use of polymeric materials in both primary and secondary structures is accompanied by the requirement of adequate methods for inspection and structural certification. One must be able to nondestructively assess both the mechanical properties and the nature of the cured chemical state. This paper addresses the problem of nondestructive testing and evaluation (NDT&E) of polymeric phases in advanced structural designs and describes several applications of neutron radiography for verification of structural integrity.

A major problem in the fabrication of structures containing organic phases is the all-too-frequent occurrence of voids and/or porosity. This may be due to poor fabrication procedures or may be symptomatic of subtle chemical problems related to molecular weight distribution, impurities, microgel properties, or state of aging and advancement of the initial prepreg (or adhesive) system. Localized defects such as these are often too small to be identified by more conventional X-ray or acoustic-based NDT&E procedures and yet may be large enough to cause premature component failure. Neutron radiography enjoys the unique capacity to selectively image hydrogenous materials such as the matrix phase in graphite/epoxy composites and the adhesive bondline in bonded structures. This paper presents the results of Vought Corporation Advanced Technology Center (ATC) research on the application of neutron radiography for selectively imaging the polymeric phase of advanced aerospace structures.

TECHNICAL DISCUSSION

State of the Art

Neutron radiography and X-ray radiography techniques are quite similar in principle, but the characteristics of the radiation and source of the measured signals differ vastly. X-rays are attenuated by interaction with the atomic electrons. Greater numbers of orbital electrons in the higher atomic number elements cause increased absorption in these elements. Typically, although not exact in the scientific sense, the degree of X-ray attenuation is equated to specific gravity. Adhesives and composites which are composed of low atomic number elements (low density) will attenuate X-rays less than metals such as aluminum, and very much less than materials such as steel. On the other hand, thermal neutrons are attenuated by nuclear interactions. Hydrogen and gadolinium have the capacity to attenuate neutrons several orders of magnitude more effectively than most other elements. This is illustrated by Figure 1 which shows the actual dependence of the mass absorption coefficient on atomic number comparing the coefficients for X-rays and thermal neutrons. The hydrogen content of organic materials such as epoxy adhesives typically ranges from 8 to 12%. It is readily evident then that organic adhesive bondlines as thin as a few thousandths of an inch can be neutron radiographically imaged even when sandwiched between inch-thick aluminum adherends. Titanium and ferrous adherends, which have higher neutron absorption cross sections than aluminum, also are relatively transparent to thermal neutrons. X-ray procedures generally cannot resolve or differentiate the adhesive bondline once the adherend thickness reaches a few tenths of an inch. Additionally, the neutron radiographic technique is not troubled by discontinuities such as occur at bondline overlap edges as are acoustic and ultrasonic techniques. This is particularly important because of the nature of the stress distribution along the edges of bonded joints. The edges should be the area of most effective inspection. Neutron radiography procedures uniquely fill certain NDT&E technology gaps such as these for which the more conventional approaches are not well suited.

Figure 2 describes the typical steps followed in the radiographic inspection of a structure. In this study fast neutrons generated by bombarding a beryllium target with deuterons, or from a californium-252 isotope source are moderated to thermal energies in order to maximize the neutron absorption contribution from hydrogen. Typical moderators are water, polyethylene, or paraffin materials. The neutron beam is then collimated to achieve spatial resolution, and the ratio of the neutron flux to gamma ray background is maximized for good neutron image contrast. The structural element being inspected is inserted in the neutron beam between the source and the imaging assembly. Since photographic films are not exposed directly by neutrons, a radiation converter is required. Once the film is exposed by the products of the reaction between the converter and the neutron beam, it can be developed using standard X-ray film handling procedures.

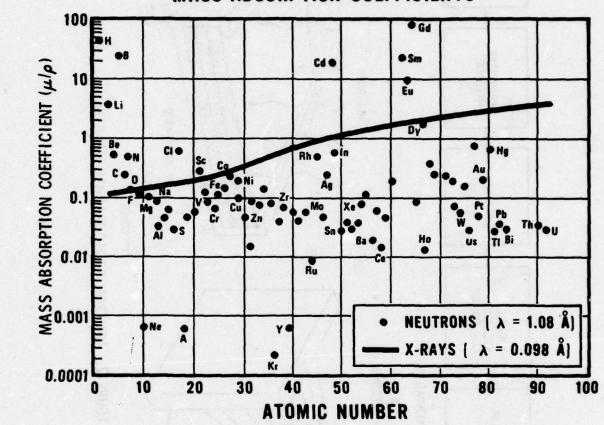
The interpretation of neutron radiographs uses essentially the same skills as are required for X-ray radiography. The essential difference between neutron and X-ray radiographic interpretative processes lies in the difference in the elemental species which are imaged.

Experimental

For the most part, the structures inspected and described here simulated actual production units. The makeup of each will be discussed in conjunction with the individual radiograph interpretations which follow. Californium-252 and a Van de Graaff accelerator were used alternately as neutron sources.

The californium-252 based neutron radiography inspection experiments were performed using a 2.8-milligram source on loan from the Louisiana State University Californium-252 Demonstration Center in conjunction with the U.S. Energy Research and Development

FIGURE 1. COMPARISON OF NEUTRON AND X-RAY MASS ABSORPTION COEFFICIENTS *



†J. Thewlis, Brit. J. Appl. Phys. 7, 345 (1956)

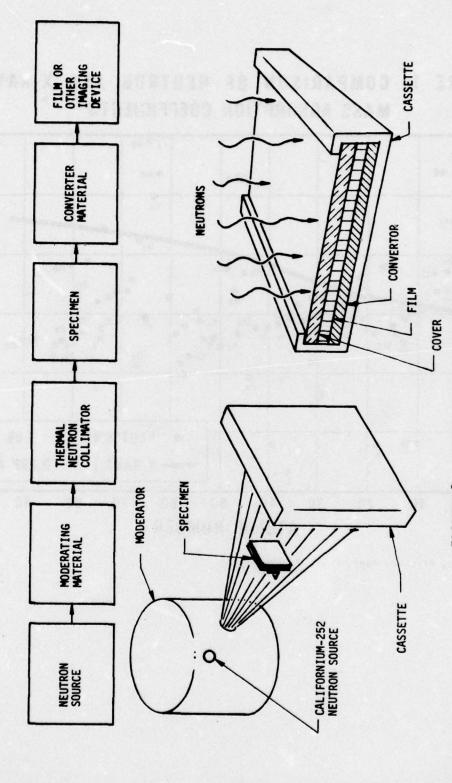


FIGURE 2. NEUTRON RADIOGRAPHIC IMAGING

Administration Californium-252 Evaluation Program. The neutron radiography procedures employed are schematically detailed in Figure 2. The thermal neutron flux was approximately 10^4 neutrons/cm²-sec. Industrial X-ray film, Types SR-54 and AA, were used. A 0.001 inch thick vapor-deposited gadolinium metal film was used as a converter; an L/D ratio of 18 was typical.

Certain of the experiments were conducted using the ATC 3.0 MeV Van de Graaff accelerator. A thermal neutron flux of approximately $10^6/\mathrm{cm}^2$ -sec at the specimen was obtained by moderating the fast neutrons from the $^9\mathrm{Be}(\mathrm{d},\mathrm{n})^{10}\mathrm{B}$ reaction. Eastman Kodak SR-54 (single emulsion) film was used with a neutron beam collimation ratio range of L/D = 18 to 50. The neutron converter used in this study was an 0.001" gadolinium metal foil.

The neutron radiographs were prepared and reprinted without employing any photographic enhancement techniques. (It should be remembered that considerable contrast and resolution are lost when preparing the photographic reproductions recorded in this paper and hence the reader's visual interpretation is more difficult than it would be with the original negatives.)

Adhesive Bondline Flaw Detection and Strength Prediction

Neutron radiography is capable of distinguishing between materials with different neutron mass absorption coefficients. For a bondline of uniform thickness, variations in the radiograph film contrast indicate variations in hydrogen content uniformity. Such variations could be the result of adhesive voids or inclusions. Conversely, contrast variations in void free bondlines could indicate that in fact uniform bondline thickness had not been achieved. Voids may be fissures or bubbles extending from adherend to adherend or they may be localized within a portion of the glue line causing a gross unbond at one adherend surface. Inclusions usually will have absorption coefficients less than that of the adhesive. Low coefficients will cause the inclusion to appear as a void; inclusions which have high absorption coefficients are readily recognized as such.

An enlarged radiograph of a defective adhesive bondline is shown in Figure 3. This figure is a magnified image of a nominal 1.0" x 0.5" adhesive overlap. The dark areas at the overlap edges are due to filleting of the adhesive. The light spots are voids, and as can be seen, voids as small as 0.010" are resolved. Figure 3 shows an extreme case of void content. Obviously, this bondline is atypical of bonding overall. However, defects such as this are all too common on a localized basis in laminate structures. The bondline shown in Figure 3 resulted from inadequate bleed of trapped air and/or volatiles during bondline cure. Ordinarily one does not encounter this severe a case of gross void content except in small islands within a large bondline. However, extensive porosity or small voids do occur.

When one encounters localized voids or general porosity in an adhesively bonded structure, the real world question becomes - will the bondline have sufficient strength to survive the anticipated dynamic load environment? This determination involves many factors which will not be addressed here including the effect of defect size and shape on fracture toughness and durability, the mode of loading, stress distribution, load sequence, and the effect of environment on the adhesive properties. If one assumes that the static shear strength is an adequate criterion for serviceability, neutron radiography offers considerable potential for NDT&E of adhesively laminated structures. Assuming that the tensile shear strength of an adhesive bondline is approximately proportional to the bonded area, it should be possible to rapidly estimate the ultimate failure load of the adhesive bondline by measurement of the void fraction. This was done for the specimens of the type shown in Figure 3 and the results are listed in Table I.

A meticulous quantitative analysis of the bondline void fraction of the specimen shown in Figure 3, specimen No. 1 of Table I, was conducted. The void area fraction in this bondline was determined graphically to be 43% (0.261 in² bonded area). Minimum void size included in this analysis was approximately 0.015". If the value of 43% is used to



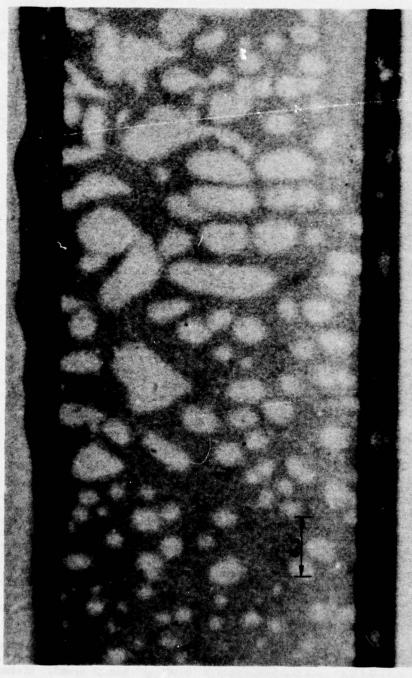


FIG.3 ENLARGED NEUTRON RADIOGRAPH OF AN ADHESIVE BONDLINE SHOWING AN EXTREME CASE OF HIGH VOID CONTENT.

TABLE 1. PREDICTED VS. ACTUAL SHEAR FAILURE LOADS OF FLAWED BONDLINES.

Error		10 0.7	100 4	50 3	210 10	10 0.	8 3	8 8
Actual	Failure Loads (lbs)	1500	1590	1590	2070	1350	2640	2650
Predicted	Failure Load (lbs)	1490	1530	1540	1860	1340	2550	2580
Estimated	Bonded Area (in ²)	0.261	0.267	0.270	0.326	0.235	0.446	0.451
Specimen	No.	-	2	3	4	2	9	7

predict the failure load for this specimen, based on the mean ultimate shear load of the control specimens which had little or no voids, a value of 1490 lbs. is obtained which is very close to the observed value of 1500 lbs. Errors in predictions are given in pounds and percent of actual failure load. The reference shear strengths were taken as the mean shear strengths of control specimens having estimated void areas of 1% or less.

Figure 4 illustrates the application of this technique for prediction of lap shear failure loads by neutron radiography using two specimens, one with no voids and one with approximately 50% bondline void area. The figure shows the correlation between the void area as imaged in the neutron radiographs before test, and the respective ultimate shear loads. Based on the 2860 pound ultimate shear failure load observed for the control, one would predict that at 50% bondline void content the flawed specimen should fail at about 1430 pounds. The observed failure load was 1350 pounds which is within 6% of the prediction. This is certainly well within the typical scatter of lap joint shear strength test measurements. On more critical inspection using graphical techniques, this specimen, No. 5 of Table II, was found to have 0.235 in² bonded area which calls for a prediction of 1340 pounds ultimate shear load. Obviously, visual inspection is convenient, simple and adequate, but when more accurate bondline strength prediction is desired, quantitative techniques are preferable.

Detection of Bondline Defects in Honeycomb Structures

A typical aerospace structure generally includes some use of honeycomb materials. The problem of defects can be severe, and usually several NDT&E techniques are employed in order to verify the structural integrity. Ultrasonic C-scan procedures are perhaps most commonly employed for inspection. However, too often these results are inadequate; frequently they are accompanied by destructive testing to identify the nature of the detected anomalies. An example of the benefits of neutron radiography of such a panel are demonstrated in the following discussion.

A set of thermal radiator panels containing built-in bondline defects was radiographed. Figure 5 shows the C-scan of the panel indicating three areas of defects. The neutron radiograph, Figure 6, shows not only the presence of the structural discontinuities but defines their nature. The uppermost discontinuity detected ultrasonically is actually an active thermal control aluminum tube fabricated into the structure. The center defect is an adhesive unbond in which the adhesive was present but was prevented from filleting to the honeycomb by insertion of a plastic film between the adhesive and the honeycomb during layup. This condition is representative of failure to remove the peel-ply during fabrication. The honeycomb-shaped image in the radiograph is actually the image of the adhesive. The aluminum does not show, as it is essentially transparent. The smeared effect in the center defect zone is due to the absence of adhesive wetting and the lack of accumulation at the honeycomb walls because the adhesive was squeezed away from the honeycomb core ends. In the original radiograph there was actually a transparent zone at the honeycomb edges due to adhesive squeeze-out. This image contrast was lost during photographic reproduction to positive prints.

The lower defect zone is due to an absence of adhesive on the upper surface (closest to the film cassette). There is no filleting at the front surface. The slightly defocused honeycomb image is actually the adhesive filleting at the rear skin.

Clearly, the neutron radiography NDT&E technique provides an in-depth inspection technique for such honeycomb structures. It can function alone as the sole method for inspection or it may be used to complement other techniques.

Defect Detection in Polymer Matrix Composite Structures

In Figure 7 are shown radiographs of sections of two graphite/epoxy composites, one sound and the other riddled with voids. The voids resulted from the combined effect of

NEUTRON RADIOGRAPH BEFORE TEST

Void Area = 0%

PHOTOGRAPH AFTER TEST



Failure Shear Load = 2860 lbs Stress = 5720 psi



Void Area = 50%



Failure Shear Load = 1350 lbs Stress = 2700 psi

FIG. 4. ADHESIVE JOINT FAILURE PREDICTED BY NEUTRON RADIOGRAPHY.

Specimen (A)

Specimen (B)

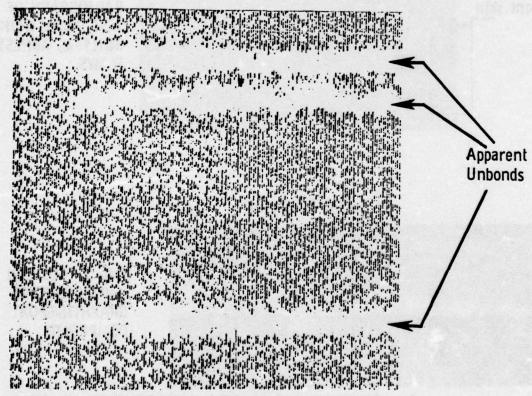
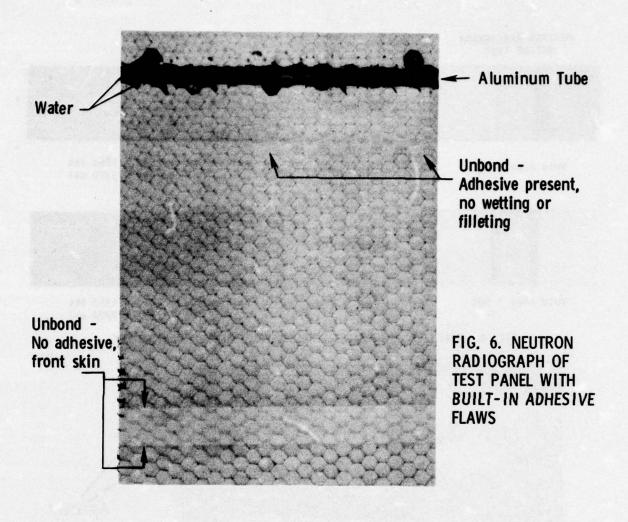


FIG. 5. ULTRASONIC C-SCAN OF EPOXY-BONDED ALUMINUM HONEYCOMB PANEL



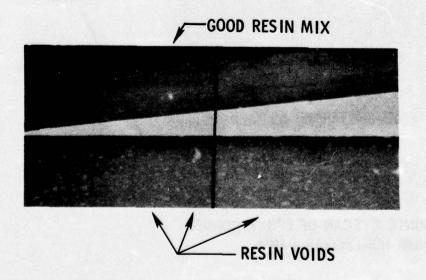


FIG. 7. NEUTRON RADIOGRAPH OF GRAPHITE/EPOXY COMPOSITE

(1) inadequate removal of volatiles during the vacuum processing step and (2) delay of compaction until well after the polymeric matrix had reached the gel point. Such processing is obviously artificial and the resultant voids are larger than those usually occurring in graphite/epoxy composites. Usually the voids are small and are referred to as porosity. By using the approach demonstrated in Figure 3, one can magnify the image and resolve localized voids as small as 0.01 inches.

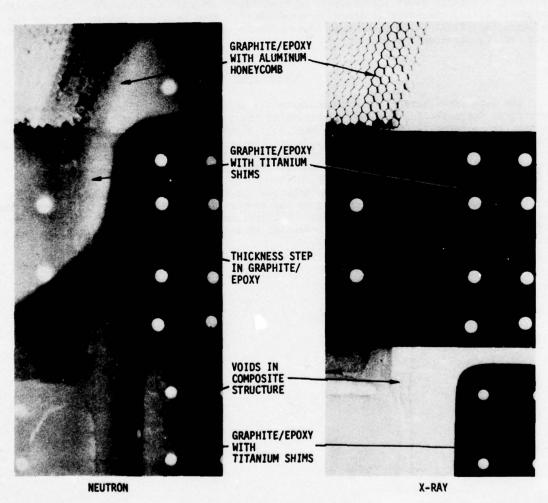
Real world aircraft structures using graphite/epoxy composites are rarely simple flat plate monolithic materials. Figure 8 describes a "composite skin structure" one typically encounters. Features to be noted include: (1) the metal shim at the fastener points; (2) the honeycomb stiffener; and (3) the secondary bonding. The comparison of the neutron radiograph with the X-ray radiograph demonstrates the power of neutron radiography for inspection of these advanced aerospace structures. The results of ultrasonic or acoustic methods are usually muddled by the complexity of the structure and are inadequate in themselves. They must be supplemented by other methods. On the other hand, neutron radiography clearly shows the presence of bondline voids and composite skin to honeycomb unbonds. Again, considerable image contrast is lost when printing photographs from the radiographs. Still it is clear that neutron radiography uniquely images the defects in this complex structural element.

CONCLUSIONS

The data shown here clearly demonstrate the unique benefits of neutron radiography techniques for assessing the serviceability of the polymeric phase of complex structures. Neutron radiography techniques can be used to inspect many types of configurations for which conventional procedures are unsuitable. Neutron radiography procedures are adaptable to production as well as field NDT&E requirements and provide a unique data source for assessment of the serviceability of advanced designs utilizing organic materials.

Neutron radiography is not a new technique but it is only recently that its applicability to advanced materials structures has been reviewed in depth. It is expected that once refinements in inspection techniques and instrumentation and improvements in cost effectiveness are attained, the full potential of this method can be exploited for polymeric materials structures.

FIG.8 NEUTRON AND X-RAY INSPECTION OF A GRAPHITE/EPOXY COMPOSITE STRUCTURE CONTAINING METAL COMPONENTS



THE APPLICATION OF ESCA TO STUDIES OF STRUCTURE BONDING AND REACTIVITY OF POLYMERS

D.T. Clark

University of Durham

1. Introduction

Since solids communicate with the rest of the universe by way of their surfaces, it is a truism that structure and bonding (in the chemical sense) of the surface of solids is of fundamental importance in any detailed discussion at the molecular level of many important phenomena. Despite the obvious importance of the nature of the surface and immediate subsurface of polymeric coatings for example, there are few techniques currently available for routinely delineating the aspects of structure and bonding which are of crucial importance in determining many of the physical, chemical, mechanical and electrical properties. This is more particularly the case when the horizon is broadened to encompass not only 'academic' studies under relatively idealized conditions but real situations corresponding to polymeric coatings in their working environment. For example, it may be important to study various properties as a function of ageing or weathering or surface modification in general (e.g. CASING prior to adhesive bonding). Techniques capable of handling such widely differing situations non-destructively (as far as the samples are concerned) have until the advent of ESCA been conspicuous by their absence.

Over the past six years or so we have been applying the relatively newly developed technique of Electron Spectroscopy for Chemical Applications (ESCA) to studies of structure and bonding across a broad front encompassing organic, inorganic and polymeric systems. These studies together with complementary theoretical analysis have demonstrated that ESCA is an extremely powerful tool for investigations of structure and bonding with an information content per spectrum unsurpassed by any other spectroscopic technique. This distinctive attribute confers upon ESCA wide ranging applicability and versatility in respect of studies on polymeric systems and it is the purpose of the

lecture to enlarge upon this theme.

It will become apparent that there are areas of study in which the required information can only at present by derived from ESCA studies, while in others the technique nicely complements the more established spectroscopic tools. In general, however, ESCA provides data at a much coarser level than most other spectroscopic tools and information pertaining for example to conformational effects may only be inferred rather indirectly. In many areas of application ESCA does not compare favourably in terms of resolution, sensitivity etc. with more established spectroscopic tools. The fact remains, however, that this is more than compensated by the great range of information available from a single ESCA experiment such that in the future one can envisage that ESCA will be the technique of choice for any initial investigation of a polymer sample. The ability to provide information straightforwardly on uncharacterized samples is unique to ESCA and gives the technique great potential (already exploited in some areas) for tackling not only academic problems but those of an applied 'trouble-shooting' nature.

The application of ESCA to structure and bonding in polymers has largely been pioneered at Durham, however the field is already so large that it is only possible in the time available to give a brief outline of the sorts of application which can be made.

(For background reading extensive reviews covering much of the published material are available 1-7). In presenting this lecture therefore, I have had two primary objectives in mind. Firstly to delineate the areas of applicability of the technique and hence give the uninitiated some idea of the sort of problems to which ESCA might readily be applied. Secondly to indicate some of the 'growth areas' over the next few years. Since ESCA may still be relatively unfamiliar to many of you a brief introduction to the technique is given in section (2) and further details are available in refs.

2. The ESCA Experiment

ESCA involves the measurement of binding energies of electrons ejected by interactions of a molecule with a monoenergetic beam of soft X-rays. For a variety of reasons the most commonly employed X-ray sources are AlKa_{1,2} and MgKa_{1,2} with corresponding photon energies of 1486.6 eV and 1253.7 eV respectively. In principle all electrons, from the core to the valence levels can be studied in this respect the technique differs from u.v. photoelectron spectroscopy (UPS) in which only the lower energy valence levels can be studied. The basic processes involved in ESCA are shown in Fig. 1.

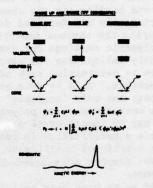


Fig. 1.
Schematic illustrating photoionization, shake up and shake off processes

With the conventionally employed X-ray photon sources cross sections for core levels for most elements of the periodic table are within two orders of magnitude of that for the C₁ levels and the technique thus has a convenient sensitivity range for all elements. The cross sections for photoionization of core levels is generally considerably higher than for valence levels and this taken in conjunction with the fact that core orbitals are essentially localized on atoms, and therefore have binding energies characteristic of a given element means that in ESCA the predominant emphasis is on the study of core levels. Although core electrons do not take part in bonding they monitor closely valence electron distributions and it is this particular feature which endows the technique with such wide ranging capabilities.

The removal of a core electron (which is almost completely shielding as far as the valence electrons are concerned) is accompanied by substantial reorganization of the valence electrons in response to the effective increase in nuclear charge. This perturbation gives rise to a finite probability for photoionization to be accompanied by simultaneous excitation of a valence electron from an occupied to an unoccupied level (shake up) or ionization of a valence electron (shake off). These processes giving rise to satellites to the low kinetic energy side of the main photoionization peak, follow monopole selection rules and their measurable parameters (intensities and separation with respect to the direct photoionization peaks) enormously broadens the scope of the technique as will become apparent in the ensuing discussion.

De-excitation of the hole state can occur via both fluorescence and Auger processes, for elements of low atomic number the latter being the more probable. The lifetimes of the core hole states are typically in the range $10^{-13} - 10^{-15}$ sec. emphasizing the extremely short time scales involved in ESCA compared with most other spectroscopic techniques.

The basic experimental set up for ESCA is shown in Fig. 2, and is largely self explanatory.

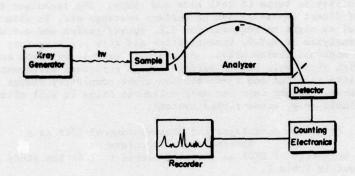


Fig. 2
Schematic of basic experimental set up for ESCA

The most flexible of the commercially available designs employ double focussing electrostatic analyzers with retarding lens systems. This allows ready access to the sample for in situ preparation or modification and also allows angular studies to be made straightforwardly. Two alternatives to this arrangement with its relatively high constructional costs have been marketed commercially; the cylindrical mirror analyzer (Physical Electronics) and a novel design marketed by DuPont based on a low pass mirror, quadrupole lens and high pass filter. In addition to making routine angular dependent studies difficult such designs also make logical upgrading difficult. The philosophy of 'bolt on' modification and upgrading has much to commend itself particularly in inflationary periods and there is commercial as well as scientific logic in instrumental designs which anticipate developments over a decade or so. The two most important instrumental developments which are already available are X-ray monochromatization and position sensitive detectors. The former (Hewlett Packard, Dispersion Compensation, A.E.I. Slit Filtering) based on dispersion of AlKa1,2 radiation from spherically bent quartz discs improves signal/noise signal/background (by removing the bremmstrahlung) and resolution whilst the latter increases the rate of data acquisition over that available from a single channeltron such that real time investigations by ESCA become feasible.

To maintain the integrity of the sample during the time taken for measurement and to obviate scattering of electrons entering the analyzer samples are maintained in the spectrometer source at pressures of 10⁻⁷ torr or better. The relatively low sticking coefficient for most small molecules comprising the extraneous atmosphere in the spectrometer means that the vacuum requirements are somewhat less stringent than in the study of e.g. evaporated metal films where pressures in the range 10⁻¹⁰ torr would typically be required. Conventional cold trapped diffusion pumps backed by two stage rotary pumps are therefore normally employed and the vacuum requirements are such that it is feasible to use pre-pumped insertion locks. Samples may thus be introduced from atmosphere into the spectrometer and be ready for investigation at the requisite operating pressure in a matter of minutes. Samples may conveniently be studied as films or powders mounted on a sample probe which may be taken into the spectrometer from atmosphere via insertion locks and valves. Provision is usually made to enable samples to be heated or cooled in situ and ancillary equipment may be mounted directly onto the source of the spectrometer for in situ preparation or pre-treatment (e.g. argon ion

bombardment, plasma synthesis, electron bombardment, u.v. irradiation, chemical treatment etc.). Addition of a quadrupole mass spectrometer facilitates many sample treatment studies and allows close control to be kept of the extraneous atmosphere in the sample region.

Powders may be studied by mounting on double sided Scotch tape, films may be studied directly as such or films may be produced by solvent casting, dip coating, spin casting or by hot pressing etc. The method of presentation of samples for analysis allows considerable flexibility in terms of both size and shape. The technique therefore provides a means of direct investigation of surface coatings etc. in situ without the necessity of removal as might be required for I.R. investigation and definitely would be required for microanalysis or N.M.R. investigation and this obviates many ambiguities and problems which might otherwise arise. As a simple example we might consider a block copolymer which might well have a surface domain structure different from the bulk. Taking the sample into solution and re-deposition might completely change both the bulk and surface structures. In any case for many polymeric films it will often be the case that they are insoluble (e.g. cross-linked system).

3. Principle Advantages and Disadvantages of ESCA as a Spectroscopic Technique

The principle advantage of ESCA as a spectroscopic tool in the study of polymeric materials are set out in Table 1.

Table 1

Principle Advantage of ESCA in Studying Polymeric Materials

- (1) Technique essentially non-destructive.
- (2) High sensitivity and modest sample requirement.
- (3) Materials may be studied in situ in their working environments with a minimum of preparation.
- (4) Large number of information levels available from a single experiment.
- (5) For solids unique capability of differentiating surface from sub-surface and bulk phenomena. Analytical depth profiling possible.
- (6) Information levels such that 'ab initio' investigations are feasible.
- (7) Data often complimentary to that obtained by other techniques. Unique capabilities central to the development of a number of important fields.
- (8) Theoretical basis well understood, results of considerable interest to theoreticians and may be quantified.

The typical X-ray fluxes employed in commercially available spectrometers are such that there are relatively few systems for which appreciable radiation damage occurs during the time taken to record a spectrum. Polythiocarbonyl fluoride depolymerizes rather rapidly whilst polyvinylidene fluoride slowly eliminates HF and cross-links. By contrast the dose rates involved in conventional Auger spectroscopy (employing an electron beam for excitation) are several orders of magnitude larger so that radiation damage poses severe problems. The surface chemistry of polymers may therefore only be conveniently studied by ESCA and Auger spectroscopy is not a viable alternative. This contrasts with the situation for inorganic systems. The sample requirements are modest and the surface sensitivity of the technique is such that the technique samples the outermost 100 Å or so of sample and depending on spectrometer design to 0.2 sq. cms. in area.

Although as will become apparent if we consider any one level of information available from ESCA and compare this with that available from the most competitive of the other available spectroscopic technique; for the particular case in question, it is invariably the case that ESCA compares relatively unfavourably. The most distinctive feature of ESCA as a spectroscopic tool however which sets it apart from any other is the large range of available information levels and these are shown in Table 2. For a fuller description see refs.

Table 2

Hierarchy of Information Levels Available in ESCA

- (1) Absolute binding energies relative peak intensities, shifts in binding energies. Element mapping for solids, analytical depth profiling, identification of structural features etc. Short range effects directly longer range indirectly.
- (2) Shake up shake off satellites. Monopole excited states; energy separation with respect to direct photoionization peaks and relative intensities of components of 'singlet and triplet' origin. Short and longer range effects directly (Analogue of U.V.).
- (3) Multiplet effects. For paramagnetic systems, spin state, distribution of unpaired electrons (Analogue of E.S.R.).
- (4) Valence energy levels, longer range effects directly.
- (5) Angular dependent studies. For solids with fixed arrangement of analyzer and X-ray source, varying take off angle between sample and analyzer provides means of differentiating surface from sub-surface and bulk effects. Variable angle between analyzer and X-ray source angular dependence of cross sections, asymmetry parameter β, symmetries of levels.

It is the composite nature of these information levels which endows ESCA with such wide ranging capabilities and has seen the technique emerge as one of the most powerful shots in the chemist's locker. The way in which these information levels may be exploited will become apparent from the discussion given below.

In studying solids the short mean free paths of electrons and their strong dependence on kinetic energy (some of the older data is reproduced in Fig. 3) provides a means of differentiating surface from subsurface and bulk phenomena and hence analytical depth profiling, by studying core levels with different escape depth dependencies.

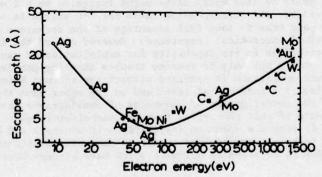


Fig. 3. Escape depth dependence on kinetic energy for electrons.

Such studies can be considerably broadened in scope if coupled with angular dependent studies. The information levels available from ESCA studies are such that samples may be studied for which there is a minimum of prior information and in this respect ESCA is again different in character than most other forms of spectroscopy. Having elaborated the advantages we may briefly consider the disadvantages which are surprisingly few. In terms of cost standard ESCA instrumentation falls in the same league as continuous wave NMR although 'state of the art' instrumentation come somewhat closer to the cost of Fourier transform MMR spectrometers. In setting up a routine ESCA facility therefore the overall costs are comparable to that for Fourier Transform I.R., Laser, Raman and Mass Spectrometries. The vacuum system associated with ESCA instrumentation means that routine sample handling requires provision of vacuum interlocks and also implies that it is not possible to switch the spectrometer on to routinely investigate a sample. In this respect the technique is comparable with mass spectrometry however it does not suffer from the same background problems. A similar criticism may of course be levelled at NMR where the stability of the field is such that there is usually a considerable time lag involved between switching the instrument on and recording a spectrum. Whilst the technique has superior depth resolution (in the range < 100 Å) to any other, the spatial resolution is poor and typically an area ~ 0.25 cm. is sampled. As a corollary of this of course we may note that unless the outermost ~ 100 Å or so of a thin organic or polymeric film of the sample is representative of the bulk then it is not possible to say anything about the bulk structure by means of ESCA without sectioning the sample.

With conventional unmonochromatized X-ray sources, and slitted designs two features are of importance in studying thick samples. The first is sample charging arising from a distribution of positive charge over the sample surface under the conditions of X-ray bombardment. The second is that the polychromatic nature of the X-ray source (characteristic lines superimposed on bremmstrahlung) leads to a relatively poor signal/ background ratio for the technique. Sample charging for insulating films usually amounts to no more than a few eV shift in the kinetic energy scale and may readily be corrected for by standard techniques and we shall briefly address ourselves to these in a subsequent section. The advent of efficient monochromatization schemes and multiple collector assemblies considerably alleviates the signal/background and signal/noise ratios however sample charging can be much more severe a problem for thick insulating film and needs careful consideration. Since the composite linewidths for C1 levels for organic and polymeric materials studied by means of unmonochromatized X-rays are largely dominated by the inherent width of the X-ray source there is a considerable overall improvement in linewidths on going to instrumentation employing monochromatization schemes. It is still the case however that the overall shift to linewidth ratio for C₁ levels as a function of electronic environment are poor compared with say ¹³C NMR. A particularly interesting case is that for C_{1s} levels appropriate to hydrocarbons in which carbon is formally in sp³, sp² and sp hybridization whilst for the core levels the shift to line width ratio might typically be $^{\circ}$ 1 with an efficient monochromatization scheme, the corresponding ratio for 13 C shifts is $^{\circ}$ 10³.

Finally we may note that to take full advantage of the technique often requires a relatively high level of theoretical competence. However one of the interesting features about the technique is its capability for exploitation at many levels. Thus the technique lends itself not only to routine trouble shooting problems where often only a straightforward comparison is required without any attempt being made to understand the problem at a fundamental level and on the other hand the technique provides a powerful tool for the investigation of phenomena of considerable interest to a chemical physicist. We may note in this connection that the technique is quite competitive in terms of time taken to record a spectrum (typically ~ 10 minutes) and with developments already in hand the technique should lend itself to real time applications. The areas of application of ESCA in relation to polymers which have already been delineated are

shown in Table 3.

Table 3

ESCA Applied to Polymers

A. Aspects of Structure and Bonding (Static Studies)

- (i) Gross chemical compositions
 - (a) elemental compositions,
 - (b) % incorporation of comonomers in copolymers,
 - (c) polymeric films produced at surfaces.
- (ii) Gross structural information
 e.g. for copolymers, block, alternating or random nature.
 Domain structure in block copolymers.
- (iii) Finer details of structure
 - (a) structural isomerisms,
 - (b) experimental charge distributions in polymers.
- (iv) Valence bands of polymers.
- (v) Identification of polymers, structural elucidation.
- (vi) Monopole excited states.

B. Aspects of Structure and Bonding (Dynamic Studies)

- (i) Surface treatments e.g. CASING, plasma modification.
- (ii) Thermal and photochemical degradation.
- (iii) Polymeric films produced at surfaces by chemical reaction e.g. fluorination (including the use of ESCA for depth profiling and quantitative measurement of film thickness).
- (iv) Chemical degradation of polymers, e.g. oxidation, nitration etc.

C. Electrical Properties

- (i) Mean free paths of electrons as a function of kinetic energy.
- (ii) Photoconductivity of polymers.
- (iii) Statics and dynamics of sample charging.
- (iv) Triboelectric phenomena.

For samples studied as solids three situations may clearly be distinguished. In the first the sample is in electrical contact with the spectrometer. This is usually the case for films deposited in situ on a conducting substrate in the spectrometer source. Since the mean free path for the incident X-ray beam is very large it is possible depending on the conditions for films of the order of 1000 Å to have sufficient charge carriers to remain in electrical contact with the spectrometer. This can most readily be shown to be the case by applying a bias voltage to the sample probe. If the sample is in electrical contact the apparent shift in energy scale will exactly follow the

applied bias. By shifting the position of the true zero of the kinetic energy scale it is possible to study the secondary electron distribution and this provides a direct energy reference. If the sample has been deposited on a substrate such as gold it is possible to measure the core levels of the sample whilst monitoring the Au_{4f} core level and this

provides a very convenient means of energy referencing.

The second situation which arises is for thick insulating samples. Thus it is often convenient to study samples mounted on double sided Scotch tape either as powders or as discrete films. In this circumstance there is only a fortuitous possibility that the sample will be in electrical contact with the spectrometer and in general it will be floating at some potential due to surface charging and indeed this charging process may be time dependent. If care is taken in the measurements the charge built up on a sample and its time dependence may be used to investigate electrical and chemical characteristics of samples and an example of this is given in a subsequent section. The most reliable method of energy referencing is to follow the slow build up of hydrocarbon contamination at the surface. With a base pressure of $\sim 10^{-8}$ torr the partial pressure of extraneous hydrocarbon material is such that taken in conjunction with the low sticking coefficient for most organic and polymeric systems it normally takes several hours before any signal arising from hydrocarbon (binding energy 285 eV*) is apparent. It is of course possible to deliberately leak in straight chain hydrocarbon material to follow the build up at the surface. Such material almost always goes down in uniform coverage and at submonolayer coverage acquires the same surface potential as the sample. This is not necessarily the situation with regard to metals deposited on the surface since there is a marked tendency to island and as such differential charging may occur. In addition since gold is normally evaporated from a filament the possibility of surface damage, reaction or evaporation of substrate during deposition cannot be discounted. The use of the so-called 'gold decoration' technique is therefore not recommended for organic and polymeric materials. Since the factors which determine both absolute and relative binding energies of core levels may be shown to be very short range in nature it is often possible to study smaller molecules which contain the appropriate structural features as thin films in electrical contact with the spectrometer which may be straightforwardly referenced. Comparison may then be drawn between this model and the insulating sample in question and thus allow direct correction for sample charging. A further possibility which has received considerable attention of recent years is the use of electron 'flood guns'; the prime motivation being the very large sample charging for thick insulating samples in spectrometers employing monochromatic X-ray sources. The removal of bremmstrahlung as a source of secondaries can lead to shifts in the kinetic energy scale in the hundred eV range and can be compensated by flooding the sample with low energy electrons. Samples can become negatively charged however and the method needs great care to achieve an accuracy comparable with that for the other methods. An alternative source of low energy electrons is to illuminate the sample region with U.V. radiation from a low pressure low power mercury lamp via a quartz viewing port in the source region of the spectrometer. Sufficient secondaries are generated from photoemission from the metal surfaces that sample charging is reduced to a low level.

The third situation which can arise is for thick films > 1 micron which have been built up by deposition on a conducting substrate. Such films behave as 'leaky' capacitors in that they exhibit rather striking time dependent charging and discharging characteristics and follow an applied bias potential in a particular manner. Since the dynamic equilibrium which is established under X-ray irradiation invariably produces an overall positive charge on the sample the application of a positive bias voltage causes a smaller shift in the kinetic energy scale than the applied voltage whereas a negative

^{*}This must of course be independently established for a given spectrometer. It almost certainly arises from long chain hydrocarbon material.

bias voltage produces a larger shift in kinetic energy scale than the applied voltage. From a study of these effects and from the secondary electron distribution the energy referencing may readily be established. The investigation of such effects as a function of film thickness in the range 1 - 100 micron provides an interesting insight into the electrical characteristics of polymer samples.

The energy reference in each case for the measurements described above is the fermi level and although the exact location of this level in relation to the valence and conduction bonds is generally unknown for polymers, as we have noted under the conditions of X-ray irradiation it is possible for an 'insulator' to be in electrical contact with the spectrometer i.e. their fermi levels are the same. Despite the difficulties associated with defining an analytical expression for the fermi level of an insulator, the use of the fermi level as energy reference is operationally convenient. If the work function of the insulator is known we may calculate the binding energy with respect to the vacuum level.

5. Mean Free Paths of Electrons as a Function of Kinetic Energy in Organic and Polymeric Materials

Undoubtedly the most important area of application of ESCA to organic and polymeric materials is in the study of solids where the surface sensitivity and the capability of differentiating surface from subsurface phenomena places the technique in a class of its own. Both these features are a consequence of the extremely short mean free paths (escape depths) of electrons in solids. Thus in general the ESCA spectrum of a given core level consists of well resolved peaks corresponding to electrons escaping without undergoing energy losses, superimposed on a background tailing to lower kinetic energy arising from inelastically scattered electrons, as is evident from the wide scan spectra shown in Fig. 4. (These also show how the direct photoionization and Auger peaks may readily be distinguished on changing the photon energy since the kinetic energy for the latter are independent of how the initial core hole is created).

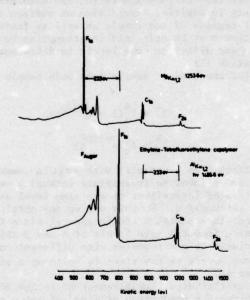


Fig. 4.
Wide scan ESCA spectra for an ethylene-tetrafluoroethylene copolymer obtained
Using MgKa_{1.2} and AlKa_{1.2} Photon Sources.

For the commonly used X-ray sources the mean free path of the photons is typically $\sim 10^4$ Å which is many orders of magnitude larger than the typical mean free paths of photoemitted electrons so that in the applications which are outlined below we may assume that the X-ray beam is essentially unattenuated over the range of surface thickness from which the photoelectrons emerge. The intensity of electrons of a given energy observed in a homogeneous material may be expressed as

$$dI = FaNke^{-x/\Omega}dx$$

where F is the X-ray flux, α is the cross section for photoionization in a given shell of a given atom for a given X-ray energy, N is the number of atoms in a given volume element, k is a spectrometer factor for the fraction of electrons that will be detected and depends on geometric factors and on counting efficiency, Ω is the electron mean free path and depends on the KE of the electron and the nature of the material must travel through.

The two situations of common occurrence are for a bulk homogeneous material for which the intensity of the elastic peak is given as in equation (1), and for an overlayer of thickness d for which expressions (2) and (3) are obtained.

For bulk homogeneous material A of thickness essentially infinite compared with the typical electron mean free paths the intensity of the elastic peak I_{α} is:-

$$I_{\alpha}^{A} = F_{\alpha}N_{A}k\Omega_{A}$$
 ... (1)

It should be noted that this expression refers essentially to a given angle (ϕ) between the X-ray source and the analyzer (this is fixed in most commercially available spectrometers), and a fixed take off angle (θ) for the electrons with respect to the sample. Since different core levels from different samples may well show different angular dependencies (with respect to θ and ϕ) for the absolute intensities according to (1), and since absolute intensities depend also on surface roughness and the atom density in the outermost regions of the sample as well as factors peculiar to a given spectrometer, great caution must be exercised in attempting to use ratios of absolute intensities for the same and different core levels in different samples as a means of establishing Ω from equation (1).

For an overlayer (thickness d) of sample A on bulk sample B the corresponding expressions are:-

$$I^{A} = I_{\alpha}^{A} (1 - e^{-d/\Omega}A) \qquad \dots (2)$$

$$V^{B} = I_{\alpha}^{B} (e^{-d/\Omega}A) \qquad \dots (3)$$

It is clear that the difficulties associated with angular dependent, instrument factors, and atom densities of A and B involved in absolute intensity measurements can be obviated by studying ratios of intensities of the same level as a function of angle for overlayers of different thickness d. In this way we may obtain directly escape depths for photoemitted electrons in material A and in general since the kinetic energy will be different for photoemission from the core levels of A and B this will yield two values $\Omega_{\mathbf{A}}$ and $\Omega_{\mathbf{A}}^{\prime}$. If the experiment is now repeated with different core levels of sample A and with a different X-ray source we may start to build up a picture of escape depths as a function of kinetic energy.

It is clear therefore that direct measurement of escape depths in organic and polymeric materials requires the production of films of known thickness as overlayers on a given substrate and the measurement of relative intensities of a given core level as a function of angle (0). Such studies are by no means trivial experimentally however we have recently completed a detailed investigation using as prototype models various paralene polymers produced by in situ polymerization of p xylylenes produced in a pyrolysis tube from paracyclophane precursors. Both the parent and substituted derivatives have been studied to give a range of core levels spanning different escape depths and allowing comparisons to be drawn for different polymer samples. In each case film thicknesses have been measured directly by means of a quartz deposition monitor and

careful angular dependent studies have confirmed that the polymer films are produced uniformly and evenly in these experiments. The mean free paths obtained directly in these measurements for the parent systems are ~ 12 Å, 20 Å and 26 Å for kinetic energies of ~ 970 eV, ~ 1200 eV and ~ 1400 eV respectively (Fig. 5). It is interesting to note that the escape depths evaluated for the polymer overlayer from the attenuation of the gold substrate signal using a MgKa_{1,2} photon source is identical to that determined from the increase in intensity of the C_{18} levels studied with an AlKa_{1,2} source since the kinetic energies of the photoemitted electrons are virtually the same in the two cases. It is worthwhile emphasizing at this stage that sampling depth and escape depth should not be confused. For escape depths of 12, 20 and 26 Å roughly 95% of the signal intensity of the elastic peaks derive from the topmost 36, 60 and 78 Å of sample in each case. It is important therefore to keep this distinction in mind.

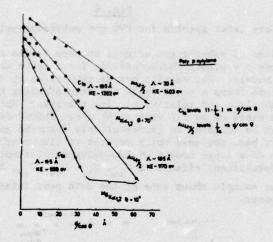


Fig. 5
Mean free paths measured as a function of kinetic energy in paralene films of known thickness.

6. Information Derived from Absolute and Relative Binding Energies and Relative Peak Intensities

Having presented the salient background information we now proceed briefly to a consideration of a representative cross section of the types of information available on polymeric materials studied by means of ESCA. The first levels of information available derive from the measurement of absolute and relative binding energies and relative peak intensities. The distinctive nature of core levels means that identification of elements is straightforward (cf. Fig. 4). With appropriate calibration, the relative intensities and shifts in binding energy for components of a given core level may be used to identify structural features and repeat units. Fig.6 for example shows high resolution ESCA spectra for two polymer samples and from the absolute and relative binding energies and relative peak intensities these may be identified as PVC and polyisopropyl acrylate.

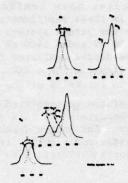


Fig. 6

Core level spectra for PVC and polyisopropyl acrylates

Previous studies of substituent effects on core levels in simple monomeric systems has shown that these are highly characteristic for a given substituent and follow simple additivity models. The results may be quantified by detailed non-empirical calculations and this forms a sound basis for understanding the electronic factors determining both absolute and relative binding energies. This has enabled computationally inexpensive models based on an all valence electron CNDO/2 SCF MO formalism to be developed which can be extended to quantitatively describe polymers. A large amount of data has previously been reviewed which relates to fluorocarbon based polymers. However a systematic study of a large number of homopolymers of simple vinyl monomers provides a compilation of substituent effects on C_{1s} , N_{1s} , O_{1s} , F_{1s} , Si_{2p} , P_{2p} , S_{2p} and Cl_{2p} levels. Fig. 7 for example shows some of the data pertaining to substituent effects on C_{1s} levels in polymers.

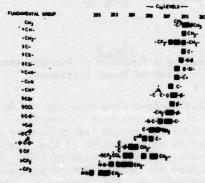


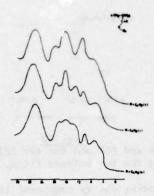
Fig. 7

Correlation diagram for C_{1s} levels in polymeric system as a function of electronic environment. (The horizontal scale for each block is taken to indicate the range of binding energies found for a given structural type.)

The characteristic nature of many substituent effects can now be used as a fingerprint much in the same manner as one might use infrared or NMR data.

It is sometimes the case that isomeric species have core level spectra which are virtually identical. Although the spectra may therefore be used to identify the gross structure they may not allow a distinction to be drawn between isomeric species. As a simple example we might consider the isomeric polybutyl acrylates. The 0_{18} and 0_{18} core

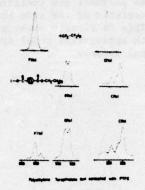
level spectra for samples of these polymers are indistinguishable. By contrast the valence levels are highly characteristic of the side chain structure since this forms an appreciable part of the whole. This is clearly apparent from the valence levels shown in Fig. 9 moreover comparison with appropriate model systems allows an unambiguous assignment of particular structural isomers.



Valence level spectra of isomeric polybutyl acrylates excited by MgKa_{1,2} radiation

The detection and semi-quantitative estimation of surface contamination of polymers is of importance in a number of fields. We have previously shown that ESCA has a unique capability for the detection of the initial stages of oxidation of polymers initiated at the surface and of adsorbed water and hydrocarbon contaminants. One area where knowledge of the precise nature of the surface is of critical importance is in delineating models for the interpretation of data relating to triboelectric phenomena. Contacting polymer films from opposite ends of the so-called triboelectric series results in charge transfer such that there is a considerable build up of static charge on each component of the contacting pair. Such charge transfer could conceivably occur via electron transfer from the material of low to that of higher work function thus equalizing the fermi levels or alternatively by mass transfer (transfer of ions) between the two components of the contacting pair. Even more likely is that both processes are of importance however the two possible mechanisms are not entirely separable since the propensity for adsorption of ions at the surface of a given polymer will undoubtedly be a subtle function of its electronic structure as will the work function. It is known that triboelectro-phenomena in general are explicable in terms of a charge density of the order of 1 in 104 of surface sites which is probably an order of magnitude lower than can currently be detected by ESCA. Nonetheless is is of interest to see if in contacting polymer samples there is mass transfer or not between the components. If mass transfer is observed it certainly does not resolve the problem of how charging occurs but it certainly allows one to say that mass transfer cannot be ruled out as a possible mechanism.

We have therefore studied the surfaces of a variety of polymer films both before and after contacting events. The great advantage of such an investigation by means of ESCA is the ability to look at both halves of a contacting pair. As one example Fig.10 shows the core level spectra for PTFE, and PET films, which are highly characteristic for each polymer. In addition there is also shown the core level spectra for the polyethylene terephthalate component after lightly contacting the PTFE film. Since the polymers are from the opposite ends of the triboelectric series the films show a strong tendency to adhere to one another, even on a light contact.



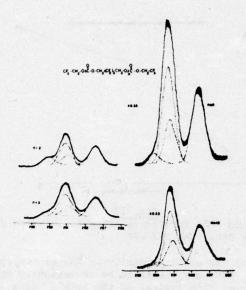
Core level spectra for PTFE and PET and for the PET component after lightly contacting the two polymer films.

The observation of the high binding energy component in the $\rm C_{18}$ spectrum and the observation of the $\rm F_{18}$ levels shows that some PTFE transfers to the PET surface. It may be estimated that this represents fractional monolayer coverage. Of particular interest is the fact that in the $\rm F_{18}$ peak in addition to the major high binding energy component associated with covalent $\rm CF_{2}$ linkages there is a lower binding energy peak attributable to fluoride ion thus providing evidence for bond cleavage accompanying the mass transfer. Examination of the other half of the component namely PTFE shows the presence of PET as evidenced by the characteristic $\rm O_{18}$ and $\rm C_{18}$ levels. These simple experiments illustrate the utility of ESCA in this area.

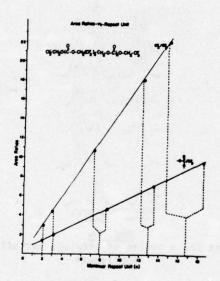
It is often the case that particular structural features may be characteristic of the end groups of a given polymer system. The direct detection of such end groups by means of their characteristic binding energies provides a convenient means of establishing DP's in relatively low molecular weight material. A particularly favourable situation arises for systems for which the terminal groups involve CF3 residues. If due care is taken to ensure that ESCA statistically samples the repeat unit (by for example considering the relative intensities of differing levels of the same element with differing escape depth dependencies) then the comparison of area ratios for chemically shifted components of a given core level may be used to straightforwardly estimate DP's. For example in a series of fluorocarbonate polymers of the general formulae shown in Fig. 11 may readily be shown that the carbon 1s levels appropriate to carbonate

-O-C-O and $\overline{\text{CF}}_2$ environments occur at approximately the same binding energy. The C_{1s} levels for the series of low molecular weight materials shown in Fig. 11 fall into three distinct regions and with appropriate calibration of linewidths and lineshapes for individual components from the study of model compounds the lineshape and analysis produces the component analysis indicated by the dotted curves. From the relative areas of the CF_3 carbons to the $\overline{\text{CF}}_2$ and carbonate carbon peaks DP's may be elaborated as indicated in Fig. 12. The two methods of elaborating DP's give slightly different results which may indicate specific orientation effects, however the two are within $\sim 10\text{Z}$ and show an excellent correlation with DP's determined by vapour pressure osmometry and thus is shown in Fig. 13. By contrast DP's determined by ^{19}F NMR do not agree with those determined by these two techniques although the reason for this discrepancy is not clear.

Although there are well developed techniques for studying chemical compositions and features of structure and bonding pertaining to the bulk of polymer samples, until the advent of ESCA, information with regard to surface compositions could only be inferred rather indirectly by for example surface free energy measurements. Since any solid



C_{1s} core level spectra for a series of fluorocarbonate polymers



DP's for fluorocarbonate polymers obtained from CF₃/CF₂ and CF₃/-O-C-O core level intensities

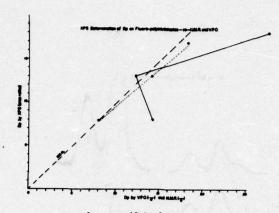
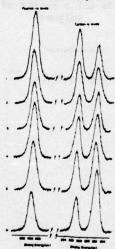


Fig. 13

Correlation between DP's for fluorocarbonate polymers determined by ESCA, NMR and VPO

communicates with the rest of the world primarily by way of its surfaces such information is important in many areas. ESCA may therefore be conveniently employed to answer the question 'is the surface composition typical of the bulk'. As a simple example Fig.14 shows the core level spectra for a series of ethylene-tetrafluoroethylene copolymers



Core level spectra for a series of ethylene tetrafluoroethylene copolymers

The higher binding energy component of the C_{1s} levels arise from <u>CF</u>₂ groups whilst the binding energy component is appropriate to CH₂ components. The shifts in binding the two component peaks also establishes that the copolymers are largely that the copolymers are largely work in ESCA applied to polymers involved imple fluorocarbon monomers and this has allowed the becaround of information on absolute and relative binding tructural feature and on the relative intensities of core imple homopolymers the compositions of the copolymers independent means.

that the materials are copolymers of ethylene and tetrafluoroethylene which are largely alternating in character and that the outermost surface sampled by ESCA is identical in composition to the bulk. This is shown in Table 4 where a comparison is drawn with compositions determined by standard microanalysis (carbon by combustion, fluorine by potassium fusion). ESCA is highly competitive as a routine means of establishing compositions for fluoropolymers in particular, in terms of accuracy, non-destructive nature and speed.

<u>Table 4</u>
Analysis of ethylene/tetrafluoroethylene comonomer incorporations

Sample	Composn. monomer mixture mol % Coff	Copolymer composition (mol % C ₂ F ₄)				
		Predicted from monomer reactivity ratios	Calc. from C analysis	Calc. from F analysis	Calc. from area ratio Cls peak: Fls peak	Calc. from Cls (CH2 peak): Cls (CF2 peak)
1	94	63	61	61	63	62
2	80	53	52	54	52	52
3	65.5	50	49	48	47	46
4	64	50	47	45	44	45
5	35	45	41	40	42	40
6	15	36	-	-	32	31

The application of ESCA to the elaboration of copolymer compositions is well established in the case of fluorocarbon based systems for which the span in shift range for the Cls levels is particularly favourable consequent upon the large electronic effect of replacing hydrogen by fluorine. With appropriate calibrations however this type of analysis can be extended to systems for which the shift range is somewhat less favourable. For example we have made extensive studies of polyalkyl acrylates and metacrylates.

The core level spectra for a series of polyalkylacrylates are shown in Fig. 15.

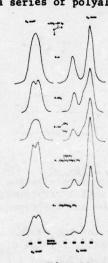


Fig. 15
Core level spectra for a series of polyalkylacrylates

The 0_{18} levels show a doublet structure (somewhat obscured in the case of polyacrylic acid because of hydrogen bonding effects); the binding energies for the two components being characteristic for an ester group (cf. polyethylene terephthalate). The C_{18} levels in each case show a high binding energy component attributable to $-\underline{C}_{0}$ type environments shifted \sim 4 eV from the main peak which in each case arises from CH_3 , $\underline{\text{CH}}_2$ and $\underline{\text{CH}}$ type environments from the backbone carbons and carbons of the alkyl group not attached to oxygen. In going from polyacrylic acid to the polymethylacrylate a shoulder to the high binding energy side of the low binding energy component develops, shifted by \sim 1.6 eV and attributable to the carbon attached to the ester oxygen. This shoulder gradually decreases in relative intensity with respect to the main peak as the chain length of the alkyl group increases. The assignment of core levels is readily confirmed by reference to simple model compounds for which detailed theoretical analyses have been performed.

In previous studies on polymeric systems we have shown that the substantial differences in escape depth dependence for deep lying valence levels which are core like in character (viz. F_{2s}) with respect to tightly bound core levels (e.g. F_{1s}) may usefully be employed for analytical depth profiling. A study of the valence levels for simple model compounds reveals that in esters the 0_{2s} levels are well separated from the remainder of the valence band and are essentially core like in nature. The approximate kinetic energies pertaining to photoemitted electrons from 0_{1s} and 0_{2s} levels using a MgKa $_{1,2}$ photon source are ~ 720 eV and ~ 1227 eV respectively and from a consideration of the generalized curve of escape depth versus kinetic energy these should correspond to significant differences in electron mean free paths. By studying a series of simple oxygen containing organic molecules as condensed films such that ESCA statistically samples the molecules it can be shown that with the particular experimental arrangement peculiar to our spectrometer the apparent 0_{1s} to 0_{2s} area ratio is 11 ± 1 . By measuring the area ratios of the 0_{1s} to C_{1s} peaks versus the stoichiometric ratios for these molecules it is also possible to derive the instrumentally dependent apparent sensitivity ratios for oxygen with respect to carbon for unit stoichiometry. Typical data are shown in Fig. 16.

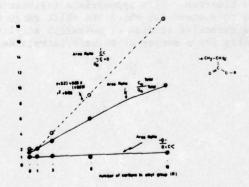
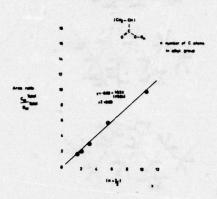


Fig. 16
Plot of area ratios for the core levels versus number of carbons on the alkyl group of a series of polyalkyl acrylates. (These have been corrected for differences in cross section and instrumental sensitivity (see text)).

For polyacrylic acid the measured areas for the various structural features for the $^{0}_{1s}$ levels and $^{0}_{1s}$ levels and the overall ratios for the $^{0}_{1s}$ to $^{0}_{1s}$ levels (corrected for differing sensitivity factors) are 1.0, 2.0 and 1.6 respectively, in excellent agreement with the theoretical values of 1.0, 2.0 and 1.5 based on a statistical sampling of the polymer repeat unit. The area ratios for the individual components for the $^{0}_{1s}$ levels show an excellent correlation with the number of carbon atoms in the alkyl

groups.* (Slope; Experimental 0.99, Theoretical 1.0). By contrast the plot of Total $^{\rm C}_{1s}/^{\rm O}_{1s}$ area ratios (corrected) against the chain length for the alkyl group fall on a smooth curve, however replotting the data in a different form, as shown in Fig. 17 reveals the underlying linear correlation with the appropriately derived theoretical parameter.



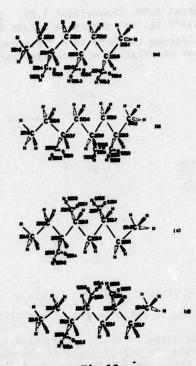
Plot of area ratios for the C_{1s} and O_{1s} levels of a series of polyalkyl acrylates as a function of chain length of the alkyl group.

Within experimental limits the slope is unity as required by theory if the ESCA experiment statistically samples the repeat units of the polymers. In sum total therefore the ESCA data shows that for these systems the outermost few tens of Angstroms of the samples are representative of the bulk and that compositions, integrity of the immediate surface, and homogeneties may routinely be established. The analysis also strongly suggests that there are no specific orientation effects of side chain alkyl groups at the surface.

The theoretical models previously developed to quantitatively describe absolute and relative core binding energies for fluoropolymers based on the charge potential model may readily be extended to the polyalkyl acrylates once appropriate values for the charge potential parameters k and E° are established for each core level. This is readily accomplished by studying model compounds and absolute binding energies for model polymer systems may then be directly committed since the factors which determine these have been shown to be short range in nature. This is shown in Fig. 18.

Whilst for the polymer samples discussed above, structure and bonding in the outermost few tens of Angstroms sampled by ESCA corresponds to that in the bulk this is not always the case. For example Fig. 19 shows the ESCA spectra for a further series of polyalkyl acrylates.

*It is convenient in this correlation to plot the area ratios for the two best resolved peaks, namely the carbonyl carbon which although of low relative intensity for the longer chain systems nonetheless is well removed from the main component arising from the backbone and carbons not directly attached to oxygen. This obviates any error due to deconvoluting the signal arising from the other carbons directly attached to oxygen (viz. of the ester group) since for the long chain systems it is obviously preferable to have a small error in a large rather than a small quantity. Since the area ratio does not therefore include the carbons of the ester group which are directly bonded to oxygen this leads to an obvious break in the curve for polyacrylic acid.



Conformational models of polyacrylic acid with calculated binding energies from the charge potential model shown for (a) HT-HT 'isotactic' model, (b) HT-HT 'syndotactic' model, (c) HH-HT 'isotactic' model and (d) HR-HT 'syndotactic' model.



Spectra for 0_{1s} and C_{1s} core levels for a $\frac{\text{Fig.19}}{\text{series}}$ of surface oxidized polyalkyl acrylates.

A distinctive feature clearly evident in all of the spectra is the obvious inequality in intensity of the two component peaks of the 0_1 levels. A similar analysis to that presented in a previous section provides the following information. Fig. 20 for example shows a plot of the ratio of intensities for the individual components of the 0_1 levels and also the total $0_{1s}/0_{2s}$ ratios.



(a) Plot of the intensity ratios for the individual components of the 0_{1s} levels and also the 0_{1s}/0_{2s} ratios for a series of polyalkyl acrylates.

(b) Plot of the C_{1s} and O_{1s} area ratios versus the number of carbons in the alkyl groups.

For comparison purposes the dotted lines indicate the correlations expected for samples which on the ESCA depth profiling scale correspond to a statistical sampling of the appropriate repeat unit in the polymer. It is clear that there are considerable deviations from such correlations in a direction which overall suggests that the samples are oxidized. If we consider the polydecyl acrylate for example, the 01s/02s ratio is significantly higher than for the reference compounds suggesting that since the mean free path for the 01 levels is considerably shorter than for the 02 level that the oxidation is largely confined to the surface. The absolute binding energies in each case for the 01s component levels which have apparently increased in intensity corresponds to C=0 structural features, as is apparent from a comparison with data for the model systems. It is interesting to note that high resolution infrared studies revealed no major distinction of the type clearly evident from the ESCA spectra and the carbonyl region for all of the samples showed only a single peak in the range 1734 + 6 cm-1 consistent with -C structural features. This is readily understandable since the infrared data pertains essentially to the bulk. Further evidence for the oxidized nature of the poly-n-decyl acrylate surface is provided by the greatly increased wettability with respect to water compared with polyisopropyl acrylate as a representative example of the unoxidized samples. This was immediately apparent from the relative contact angles assessed from the photographs for the two samples. A comparison was also made with poly-2-ethylhexyl and polyoctadecyl acrylates the latter having a contact angle closely similar to that of polyisopropyl acrylate whilst the former showed a wettability intermediate between that of polyisopropyl acrylate and poly-n-decyl acrylate. It is interesting to note that although the data for the poly-2-ethylhexyl acrylate generally fits well into the overall analysis previously presented as is evident from Figs. 15-17, a close inspection of the relative intensities of the component peaks of the Ols levels reveals some evidence for a small extent of oxidation Fig. 16.

If the surface oxidation inferred from the inequality of the component peaks of the O₁ levels is attributable to surface carbonyl features then this should also be manifest in the carbon 1s levels. It should, however, be emphasized that since the escape depth dependence for photoemitted electrons in the energy range considered is such that the mean free path increases with increasing kinetic energy then any surface feature will be relatively more prominent for the more tightly bound O₁ levels than for

the C_{1s} levels. A detailed examination of the C_{1s} spectra for the series of surface oxidized samples (Fig. 19) shows that the overall line profiles can only be quantitatively fitted with the addition of a small peak in the C_{1s} spectrum appropriate to isolated carbonyl features as might arise from oxidation.

7. Analytical Depth Profiling by Means of ESCA Whilst it is clear that ESCA nicely complements many of the more familiar spectroscopic tools the technique comes into its own in the study of surfaces and the differentiation with respect to subsurface and bulk. The capability of elaborating features of structure and bonding in inhomogeneous samples on the tens of angstroms scale is unique to ESCA. In this section we briefly consider the experiments which provide a means of analytical depth profiling. We have previously, noted that the great surface sensitivity of ESCA in the study of solids is associated with the extremely short mean free path for electrons and the strong dependence on kinetic energy. There are two broad categories of experiments which may be carried out, although inevitably in any definitive study the two are inextricably linked. The first category of experiment is to sample levels of the same or different elements having different escape depth dependencies. If we consider a fluorocarbon based material for example photoemission from the F1s, C1s and F2s levels with MgKa1,2 radiation corresponds to electrons with the kinetic energies of ~ 560 eV, 960 eV and 1220 eV respectively. This wide span in kinetic energies is reflected in the substantial differences in escape depth and hence sampling depth. Inhomogeneities in the surface and sub-surface compositions of a sample will therefore be reflected in differing intensity ratios for these levels compared with those for a homogeneous material. The first application of this approach was in the study of the initial stages of the surface fluorination of polyethylene. By studying simple homopolymers such as polyvinylfluoride, polyvinylene fluoride, polyvinylidene fluoride, polyvinylene fluoride, polytrifluoroethylene and PTFE in which ESCA statistically samples the repeat unit, intensity ratios for the F F_{1s}/C_{1s} and F_{2s}/C_{1s} levels may be established. Since the fluorination reaction is initiated at the surface and is diffusion controlled we may anticipate that the fluorine content will be higher at the surface. Since a greater proportion of the overall signal intensity for the elastic peaks derives from the outermost surface the shorter the mean free path, a heterogeneous sample with progressively lower fluorine content into the bulk will have larger F_{1s}/F_{2s} and F_{1s}/C_{1s} intensity ratios than for a homogeneous sample whilst the F_{2s}/C_{1s} ratio will be smaller. This is in fact the case and a careful analysis of the data pertaining to the surface fluorination of polyethylene allows one to follow the changes in composition of the first monolayer as a function of time.

The converse of this situation arises for the surface modification of fluoropolymers by interaction with inert gas plasmas. The surface modification of polymers for improvement of adhesive bonding, and altering surface properties in general in that concomitant modification of bulk properties is an active area of research in both industrial and academic laboratories and has been accomplished by a variety of means ranging from Corona discharge treatment, direct chemical modification and by interaction

with plasmas excited in inert gases either capacitively or inductively.

It is possible using ESCA to perform kinetic studies of surface modifications and to elaborate the relative importance of direct and radiative energy transfer processes, and the technique has provided new insights into the initial stages of the process. For example Fig. 21 shows the core level spectra for an ethylene-tetrafluoroethylene copolymer treated at low power in a pulsed inductively coupled RF plasma excited in argon. It is clear that as a function of time the F_{1s} levels decrease in intensity, the high binding energy component of the C_{1s} levels attributable to CF₂ structural features decrease in intensity and a peak appears and increases in intensity corresponding in binding energy to CF structural features. Finally the integrated intensity of the total C_{1s} levels increases as a function of time. These observations are readily interpretable in terms of a surface modification process involving cross linking. The fact that the process is initiated at the surface is readily shown by monitoring the charge in F_{1s}/F_{2s} intensity ratios as shown in Fig. 22. In this case since the fluorine content decreases as a function of reaction time the F_{1s}/F_{2s} ratio also decreases as a function of time.

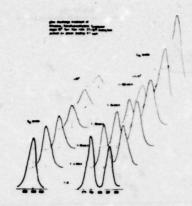
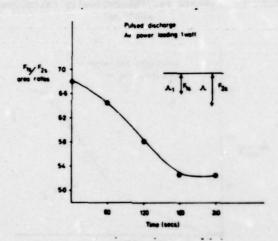


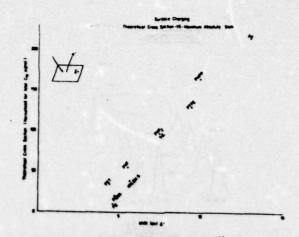
Fig. 21
Core level spectra for argon plasma treated ethylene-tetrafluoroethylene copolymer



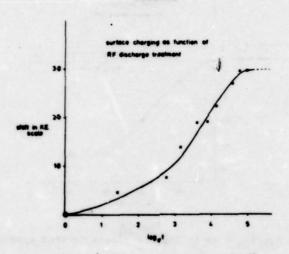
F_{1s}/F_{2s} area ratios for plasma treated samples

As an interesting side light we might also mention that changes in surface compositions may also be monitored by studying the shift in kinetic energy scale resulting from sample charging. Thus under a given set of experimental conditions it may readily be shown that surface charging for insulating samples or for conductors mounted insulated from the spectrometer is a strong function of the total cross section for photoionization and this is shown for a series of polymers and for gold in Fig. 23. Fig. 24 shows a plot of sample charging as a function of reaction time for the ethylene tetrafluoroethylene copolymer. The initial shift in kinetic energy scale is very close to that for polyvinylidene fluoride which is as one might have expected since the copolymer is largely alternating and has a closely similar stoichiometry. The surface charging however decreases for the surface modified samples to a value somewhat similar to polyethylene thus indicating without reference to the detailed structure of the core level spectra themselves the decreased fluorine content of the surface.

There are other examples of the use of core levels of differing escape dependence for extracting information on inhomogeneities of composition in the surface and subsurface of solids. For example for oxygen the 0_{2s} levels are sufficiently core like and distinctive to form a useful comparison with 0_{1s} levels for analytical depth profiling in oxygen containing systems, as we have previously noted.



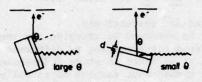
Sample charging; shift in KE scale vs. theoretically calculated total cross section



Pig. 24
Surface charging as a function of RF discharge treatment

We turn now to angular dependent studies. As a preface to a discussion in relation to solids it is worthwhile briefly considering the more general possibilities. The cross section for photoionization from a given level is strongly dependent on the photon energy and exhibits angular dependence expressed in terms of the asymmetry parameter \(\beta \). Angular resolved and photon energy dependent studies have been carried out on gas phase systems with particular reference to valence levels and the requisite instrumentation involves the variation in angle between photon source and electron analyzer. This tends to be a specialized area and the equivalent experiment for solids has extra complications which make it non-trivial in nature. For most commercially produced spectrometers the angle between photon source and analyzer is fixed so that the angular dependent studies referred to in the literature for solids are different in type for those described for gases since they do not directly involve investigations of the asymmetry parameter \(\beta \). The basic philosophy behind angular dependent studies for solids is to vary the take off angle between the sample surface and the electron analyzer. Since electron mean free paths are so short it is clear that a grazing exit angle for the photoemitted electrons will enhance surface features compared with a take off angle

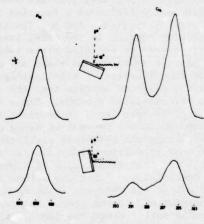
normal to the surface. Angular dependent studies of a single core level can in principle therefore give rise to information concerning inhomogeneities in the surface and subsurface regions of a sample. If core levels are available with different escape depth dependencies then we can combine angular dependent studies with experiments along the lines of those previously described to provide a very complete picture of structure and bonding as a function of depth into the sample. The rationale behind such experiments is illustrated in Fig. 25.



Fixed angle θ between analyzer and photon source. Variable take off angle θ enhances surface features at large θ (eg. for overlayer Id.)

Angular dependent studies for solids in which the variable is take off angle θ with respect to the surface

As an example of such angular dependent studies we may briefly consider the ethylene-tetrafluoroethylene copolymer system surface modified by interaction with argon plasmas. If we consider the untreated sample angular studies of the C_{1s} levels shows that the relative intensities of the component peaks arising from $-CF_2-CF_2$ and $-CH_2-CH_2$ structural units are independent of the take off angle θ as would be expected for a homogeneous sample. It should be emphasized however that the absolute intensities for the C_{1s} levels are strongly dependent on take off angle. By contrast for the treated samples, angular studies readily reveal the inhomogeneous nature of the surface regions from investigations of the C_{1s} levels alone. Fig. 26 for example shows the C_{1s} levels for a treated sample measured at angles θ of 18° and 80° respectively with respect to the normal to the sample surface.



Ethylane - Tetrafluoroathylane capalyme RF Argan plasma 0-2 watt 25 secs 100 ju

Angular dependence of core level spectra for glow discharge treated sample of ethylene-tetrafluoroethylene copolymer

The differences are quite striking. The decrease in fluorine content in the surface regions is revealed by the large relative decrease in intensity of the component arising from <u>CF</u>₂ structural features and concomitant increase in the lower binding energy components associated with <u>CF</u> and <u>C-C-C</u>. The calculated relative intensities for the components of the C_{1s} levels are:-

(CF₂: \underline{CF} : \underline{C} 1: 0.23: 1.86) and (CF₂: \underline{CF} : \underline{C} 1: 0.88: 3.1)

for take off angles of 18° and 80° respectively.

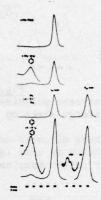
Further information may be obtained by studying the angular dependence of the intensity ratios for different core levels corresponding to different escape depth dependencies. In doing this however care must be taken to study independently the angular dependence of these core levels for the homogeneous samples to establish a reference. Also shown in Fig. 26 are the F_1 levels for the discharge treated sample and since the mean free path of the photoemitted electrons is now considerably less than for the C_1 levels the lowered fluorine content of the surface region is manifest in a marked decrease in the relative intensities of the F_1 levels with respect to that from the C_1 levels appropriate to carbons having no fluorines directly attached from 1.94 at 18° to 1.03 at 80° . The angular dependence of core level spectra can thus add considerably to our overall picture and such studies will become increasingly important.

8. Shake up Phenomena in Polymers

The removal of a core electron (which is almost completely screening as far as the valence electrons are concerned) is accompanied by reorganization of the valence electrons in response to the effective increase in nuclear charge. This perturbation gives rise to a finite probability for photoionization to be accompanied by simultaneous excitation of a valence electron from an occupied to an unoccupied level (shake up) or ionization of a valence electron (shake off). These processes giving rise to satellites to the low kinetic energy side of the main photoionization peak, follow monopole selection rules and considerably extend the scope of ESCA as a technique as will become apparent. The relationship between direct photoionization, shake up and shake off are shown schematically in Fig. 1. Before considering shake up phenomena in general it is worthwhile considering briefly some theoretical aspects of the processes involved. We have previously emphasized that the binding energy is characteristic of a given core level and varies within narrow limits (chemical shifts). Relaxation energies (associated with contraction of the valence electron cloud consequent upon core ionization) are also characteristic of a given core level and also vary within narrow limits as a function of the bonding environment of the atom on which the core level is located. For C₁ levels for neutral systems for example, binding energies measured with respect to the fermi level as energy reference fall in the range 285 - 295 eV whilst relaxation energies might typically fall in the range 12 + 2 eV. The direct relationship between shake up and shake off processes and relaxation energies may be readily understood from theoretical relationships first established by Manne and Aberg. They showed that the weighted average over the direct photoionization and shake up energy appropriate to the unrelaxed systems. Since relaxation energies fall within such a narrow range for a given core level it is clear that shake up and shake off are perfectly general phenomena which are present in every system, the feature which changes from one system to another being the weighting coefficients (probabilities) for each transition. It is clear that transition probabilities for high energy shake off processes should be relatively small and that transitions of highest probability should fall reasonably close to the centroid. In principle relaxation energies should be available from experiment provided all of the relevant shake up and shake off processes can be estimated in terms of energies and intensities. In practice this is not a feasible proposition particularly for solids since the overall situation is considerably complicated by the presence of the general inelastic tail (arising from photoemission from a given core level followed by energy loss by a variety of scattering processes) which provides a broad energy distribution usually peaking for organic systems ∿ 20 eV below the direct photoionization peaks. This generally obscures any underlying high energy shake

up or shake off processes such that it is only for systems exhibiting relatively high intensity low energy shake up peaks that information derived from this source can conveniently be exploited. Fortunately such a situation generally obtains for polymer systems which contain either unsaturated backbones or pendant groups since low energy $\pi \to \pi^*$ shake up transitions are available.

As a typical example Fig. 27 shows the C₁ spectra for typical saturated polymers polyethylene (high density) and polydimethylsiloxane, and polystyrene and polydiphenylsiloxane which represent prototype systems with saturated backbones and unsaturated pendant groups.

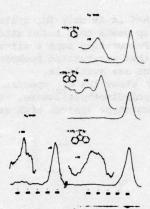


Core level spectra of polyethylene, polystyrene, polydimethylsiloxane and polydiphenylsiloxane showing shake up structure

For the latter, well developed shake up structures are apparent which clearly distinguishes them from the saturated systems although the differences in lineshape and linewidths for the main photoionization peaks are closely similar. (For the siloxanes of course, the relative intensities of the C_{1s} with respect to the 0_{1s} and Si_{2p} levels may be used to effect a ready distinction between the two siloxanes). It will become apparent that the transitions giving rise to the satellite structures in PS and PDPS are due to $\pi \rightarrow \pi^*$ transitions as might indeed be inferred from the much smaller shake up peak associated with the Si_{2p} levels and the lack of any low energy shake up structure accompanying levels for PDPS. To elucidate the nature of these shake transitions as a preliminary to utilizing such data for structural studies, we have made a systematic study of para substituted polystyrenes the objective being to study the transition energies and peak intensities as a function of the electronic demand of the substituents in the classic mould of physical organic chemistry. To complement the experimental studies, theoretical computations of shake up probabilities have been made within the sudden approximation employing the equivalent cores concept and a semi empirical all valence electron SCF MO formalism. Within this framework the calculation of shake up probabilities involves summation over weighted overlap terms involving the occupied and virtual orbitals involved in the transitions.

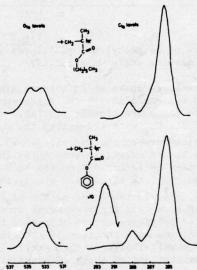
These investigations allow a ready interpretation of the low energy satellite structure as arising from $\pi + \pi^*$ shake up transitions involving the two highest occupied and lowest unoccupied orbitals of the pendant phenyl groups.

Low energy shake up satellites may be used to remove ambiguities in the interpretation of the primary sources of ESCA namely absolute and relative binding energies and relative peak intensities and are highly characteristic of the unsaturated system from which they derive. Fig. 28 for example shows the core level spectra for polystyrene, polyvinylnaphthalene and polyvinylcarbazole.



Core level spectra for polystyrene polyvinylnaphthalene and polyvinylcarbazole showing low energy shake up structures

Clearly the distinctive nature of shake up satellites can add a new dimension to ESCA data for systems in which the shifts in core levels are negligible. As one example Fig. 29 shows the $^{\rm C}_{1\rm S}$ and $^{\rm O}_{1\rm S}$ levels for poly-n-hexylmethacrylate and polyphenylmethacrylate



Core level spectra for poly-n-hexylmethacrylate and polyphenylmethacrylate showing the shake up structure for the latter

The core level spectra are essentially the same, however the distinctive nature of the shake up structure for the unsaturated pendant group allows a ready distinction to be made. Another example is provided by the study of surface domain structure in block copolymers of polydimethylsiloxane and polystyrene since the low energy shake up structure is specific for the latter. We complete this section by considering how ESCA may be used to elaborate details of copolymer compositions and provide information on surface morphology in systems for which the primary sources of information are of themselves insufficient and for which the extra dimension is provided by observation of shake up satellites. As particular examples we consider alkane-styrene copolymers of general formula

It should be evident from the previous discussion that characteristic low energy shake up structure accompanying direct photoionization of the C_{18} levels should be specifically associated with the styrene component. Fig.30 shows the measured C_{18} levels and shake up satellites for the series of alkane-styrene copolymers and it is evident by visual inspection that the relative intensities of the shake up satellites with respect to the main photoionization peaks decrease with increasing chain length of the alkane component.

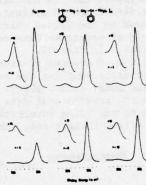
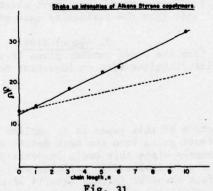


Fig. 30

C1s levels for a series of alkane-styrene copolymers showing shake up structure

A clear trend exists between shake up intensity and the chain length of the alkane component and the structure of the shake up satellites and the energy separations remain essentially constant. This becomes clearer from a graphical representation of the data as shown in Fig. 31. Also shown is the correlation expected on the basis that the repeat units of the polymers are statistically sampled (dotted line). It is clear that copolymer compositions may be established from the measurement of shake up intensities and the least square plot of the intensity ratio of the direct photoionization peak to shake up satellites versus n (the chain length of the alkane component) gives a correlation coefficient of 0.997 the slope being 1.91 and intercept 12.91.

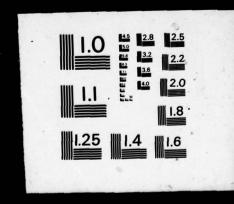


Plot of ratio of area ratios for direct photoionization peak and low energy shake up satellite for a series of alkane styrene copolymers as a function of chain length n of the alkane component.

The calculated slope assuming statistical sampling of the repeat unit is 0.90. The fact that an additive model applies to the experimental data but with a much larger dependence of intensity on n than predicted theoretically would strongly suggest that there are specific orientation effects of the polymer chains in the surface regions sampled by ESCA. An alternative possibility is that the samples are contaminated with hydrocarbon.

ARMY MATERIALS AND MECHANICS RESEARCH CENTER WATERTO--ETC F/G 11/9 PROCEEDINGS OF THE TTCP-3 CRITICAL REVIEW: TECHNIQUES FOR THE C--ETC(U) AD-A036 082 JAN 77 AMMRC-MS-77-2 NL UNCLASSIFIED 20F 4

2 OF 7 ADA036082



Such contamination would contribute to the C_{1s} peak at 285 eV but not to the low energy satellite structure. Even if the extent of contamination were such as to produce the linear correlation found experimentally (which is most unlikely on the basis of the method of preparation) on the basis of the likely escape depth dependence on kinetic energy for C_{1s} levels employing MgKa_{1,2} radiation such an explanation is untenable. What is clearly required is a model in which the repeat unit is not statistically sampled in such a sense that the phenyl groups are discriminated against. As n becomes large we might reasonably expect a structure based on the folded chain structure of polyethylene. With this in mind and with the aid of models we have considered possible structures which would lead to the results illustrated in Fig. 32.

Two such models which exhibit an increased gradient with respect to that expected if the data correspond to statistically sampling the repeat unit are shown in Fig. 32 for the particular case of n = 3. The model with a phenyl group specifically oriented at the surface come remarkably close to the experimental data and it may fairly be claimed that for this system in addition to providing information on composition; shake up satellites also provide an interesting insight into the possible surface morphology.

Folded chain medals (e.g. n=3)

Possible structures for alkane styrene copolymers which would lead to non-statistical sampling of the repeat unit (for the particular case of n = 3).

9. Conclusion.

It should be evident from the brief outline given in the previous section that ESCA is an exciting and versatile technique with an important role to play in the characterization

of polymers.

Since the prime objective of this paper is to outline the sorts of problems which ESCA can be applied to without going into too much detail no attempt has been made to provide an extensive list of references since this would inevitably be almost exclusively to our own work. The references are to review type articles written by the author over the past five years which in fact provides further details of some of the work described here. All of the work described originates from research programmes in my own laboratory at Durham and further information is available if required. The published work is largely in J. Polymer Science (Polymer Chem. Ed.), Trans. Faraday Soc. Disc. Faraday Soc., J. Chem. Soc. etc. A considerable portion of the material is as yet unpublished or is in the course of preparation.

REFERENCES

- D.T. Clark 'Chemical Applications of ESCA' in Electron Spectroscopy, Ed. W. Dekeyser, D. Reidel Publishing Co., Dordrecht, Holland (1973). (NATO Summer School Lectures, Ghent, September 1972).
- D.T. Clark, plenary lectures ACS Symposium 'Advances in Polymer Friction and Wear', Los Angeles, March 1974, Ed. L.H. Lee, 5A, Plenum Press, New York, 1975.

250

- 3. D.T. Clark and W.J. Feast, J. Macromol. Sci. Reviews in Macromol. Chem., C12, 191 (1975).
- D.T. Clark 'Structure and Bonding in Polymers as Revealed by ESCA' in 'Electronic Structure of Polymers and Molecular Crystals', Ed. J. Ladik and J.M. Andre, Plenum Press, New York, 1975. (NATO Summer School Lectures, Namur, September 1974).
- D.T. Clark in 'Structural Studies of Macromolecules by Spectroscopic Methods', Chapter 9, Ed. K. Ivin, J. Wiley and Sons, London (1976).
- D.T. Clark 'Some Chemical Applications of ESCA' in 'Molecular Spectroscopy', Ed. A.R. West, Heydon and Sons (London) 1976.
- D.T. Clark, plenary lecture ACS Symposium 'Advances in Characterization of Polymer and Metal Surfaces', New York, April 1976, Ed. L.H. Lee, Academic Press, New York, 1976.

CARBON-13 FOURIER TRANSFORM NMR TECHNIQUES IN POLYMER CHARACTERIZATION

Dr. W.B. Moniz

Chemistry Division, Naval Research Laboratory

Washington, D.C. 20375

INTRODUCTION

Nuclear magnetic resonance (NMR) spectroscopy provides a means for chemical characterization of complex molecular systems with the following advantages, among others. First, it is structure specific. That is, not only can functional groups be identified, but detailed molecular constitution may be deduced. Second, because of the narrow widths of NMR lines, components in a mixture can often be identified and quantified without the requirement for physical separation procedures. 3) The significant presence of molecules contain ng hydrogen, carbon, boron, fluorine, or phosphorus can readily be determined. While Nt² is not as sensitive a procedure as, for example, chromatography or infrared spectroscopy, the attributes listed above will be shown to recommend it for many areas of polymer characterization. The focal point of this paper is the application of carbon-13 (and to a lesser extent, proton) NMR in the characterization of thermosetting polymers at the pre-polymer stage, during cure, and after cure. The applications of proton and carbon-13 NMR in the characterization of thermosetting polymers at the discussed here.

CARBON-13 NMR AND THE FOURIER TRANSFORM METHOD

The carbon-13 NMR sensitivity to chemical structure (the so-called chemical shift) is some twenty-five times that of proton NMR. Thus, while proton NMR has become a major tool for the determination of organic molecular structure, the potential of carbon-13 is even greater. The NMR signal from the carbon-13 nucleus is inherently weak as a consequence of its small magnetic moment. Further, the natural abundance of carbon-13 is only 1.1%. The use of pulsed Fourier transform (FT) NMR, coherent signal averaging, and elimination of the multiplet structure due to proton-carbon coupling permit carbon-13 signal enhancement of several thousand. Thus, the spectrum of a complex molecule containing carbon-13 in natural abundance can be obtained in a few minutes. The advent of low cost minicomputers to perform the Fourier transform and commercial pulsed NMR spectrometers, permit the taking of carbon-13 FT spectra on a routine, semi-automated basis.

SPECTRUM CALIBRATION

The location of a signal in the NMR spectrum is indicative of the chemical environment of the particular carbon atom. The locations are expressed in parts per million (ppm) of the applied magnetic field with respect to the signal of the reference standard, tetramethylsilane, which is assigned a chemical shift of zero ppm. All spectra are displayed with the magnetic field increasing to the right, with the zero ppm mark near the right end.

LANC-NOT FILMED

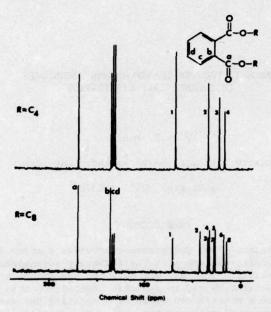


Figure 1. Carbon-13 spectra of di-n-butyl phthalate (top) and di(2-ethylhexyl) phthalate (bottom).

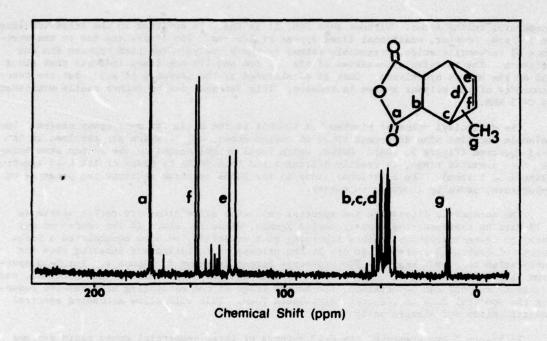
APPLICATIONS

Prepolymers

The resolving power and structure specificity of carbon-13 FT NMR is exemplified in the spectra of di-n-butyl phthalate (DBP) and di(2-ethylhexyl) phthalate (DDP) shown in Figure 1. DBP and DOP find use as non-reactive diluents in some epoxy resins. The structures of their alkyl R groups are as follows.

In the C-13 spectra of Figure 1 a distinct signal is observed for each chemically different carbon atom in the two molecules. It is to be noted that carbon atoms which are equivalent due to symmetry give rise to only one signal. Thus, the corresponding numbered carbon atoms in the R groups are alike in pairs, as are the carbonyl groups, and the aromatic carbons symmetrically disposed around the ring from the side chains. The carbon-13 spectrum of the DBP thus shows only the signals due to eight chemically different carbon atoms, as expected. In the C-13 spectrum of DOP, all eight R-group carbons are individually resolved, indicating the precision with which structure specific assignments may be unambiguously made in many C-13 spectra.

The C-13 spectrum of a more complex molecular system is shown in the upper part of Figure 2. Nadic methyl anhydride (NMA) is the trade name for a curing agent consisting of the isomeric mixture of the maleic anhydride adducts of methylcyclopentadiene. The structures are shown in the figure. The methyl group may be located at any of several positions. The C-13 spectrum consists of the superposition of the resonance lines of all the isomers and is complex. Nonetheless, the lines cluster according to functional groupings, and are assigned as shown. The lines at 171 ppm (a) are attributed to anhydride carbonyl carbon atoms. The bottom portion of Figure 2 shows the C-13 spectrum of a



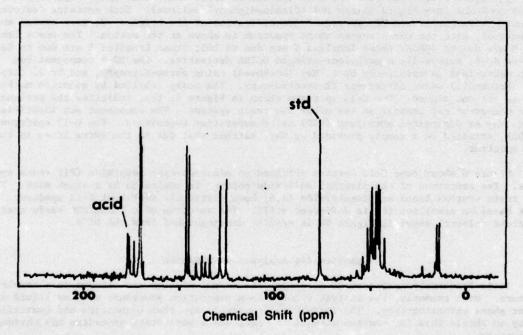


Figure 2. Carbon-13 NMR spectra of Nadic methyl anyhydride (NMA) (top), and NMA in which approximately 25% of the anyhydride has hydrolyzed to acid (bottom).

commercial curing agent. Without question, it is NMA. In addition to the anhydride lines at 171 ppm, however, additional lines appear at 178 ppm. The latter are due to the presence of carboxylic acids, presumably formed by the hydrolysis reaction between NMA and moisture. The relative intensities of the 171 ppm and 178 ppm lines indicate that about 25% of the NMA is hydrolyzed. Cure is accelerated by the presence of acid, but the functionality of the polymer system is reduced. This variable can be rather easily monitored by C-13 NMR.

The diglycidyl ether of bisphenol A (DGEBA) is the basis for many epoxy resins. The molecule contains nine different types of carbon atoms, all of which are resolved in the C-13 spectrum (Figure 3, top). DGEBF, which lacks methyl groups on the carbon atom bridging the aromatic rings, is readily distinguished from DGEBA by means of its C-13 spectrum (Figure 3, bottom). The additional lines in the DGEBF spectrum indicate the presence of impurities, probably isomeric in nature.

The scientific literature and spectral reference collections are rather sparse in C-13 data on thermosetting resins, curing agents, diluents, etc. In the course of our chemical characterization efforts involving such materials, we have accumulated a large number of carbon-13 spectra. We are in the process of collating and indexing them for publication as an NRL Report. The prototype format is shown in Figure 4. The C-13 spectrum is presented along with the structure, line assignments, source of the material, etc. Providing support can be obtained, the second stage of the cataloging will involve reducing the spectral data to computer retrievable form. This will allow automated spectral identification and mixture analysis.

In Figure 5 are presented the C-13 spectra of three commercial epoxy resin systems based on TGMDA (see Figure 4) and DDS (diaminodiphenyl sulfone). Each contains features allowing straightforward "fingerprint" identification of its origin. We have worked most extensively with the resin system whose spectrum is shown at the bottom. The peaks labelled M are due to TGMDA; those labelled S are due to DDS; those labelled I are due to Celanese SU-8, supposedly a methylene-bridged DGEBA derivative. The SU-8 component has been determined independently by C. May (Lockheed) using chromatography, and by J. Carpenter (McDonnell) using difference IR spectroscopy. The peaks labelled by question marks are as yet unassigned. The C-13 spectrum shown in Figure 5, top, indicates the presence of a component not present in the other two resin systems. The component was identified by C. May as diglycidyl phthalate (DGP) using separation techniques. The C-13 spectrum of DGP, obtained on a sample provided by May, matches that due to the extra lines in the top spectrum.

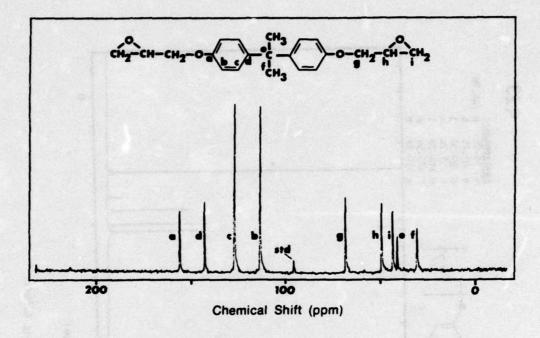
Figure 6 shows some C-13 spectra obtained on addition-type polyimide (PI) resin systems. The resonance of the dimethyl sulfoxide solvent is indicated by a slash mark. The two resin systems based on bismaleimide (A,B) have distinctly different C-13 spectra; that based on acetylene (C) is different still. The spectrum of a TGMDA/DDS resin system (acetone solvent) shown in Figure 6D is readily distinguished from the PI's.

Quantitative Analysis of Mixtures

It is frequently necessary to determine the amount of each constituent in a complex mixture. Most commonly, the analyst resorts to a separation procedure such as liquid or vapor phase chromatography. The individual components are then identified and quantified. A way to obtain this information without the need for a separation procedure has obvious advantages.

The example given here of quantitative analysis by C-13 NMR is particularly impressive, because the mixture to be analyzed consists of isomers of high boiling compounds whose separation by chromatographic procedures is rather difficult.

The sample is a commercial lot of polyphenyl ether, consisting mostly of the (meta,



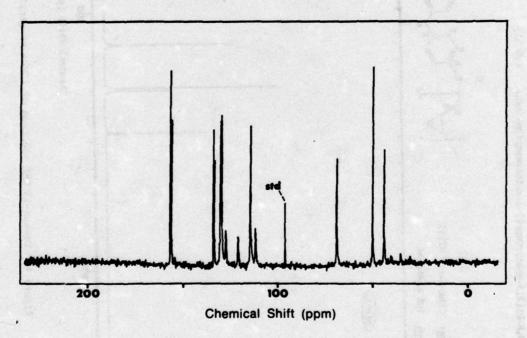


Figure 3. Carbon-13 NMR spectra of DGEBA (top) and DGEBF (bottom).

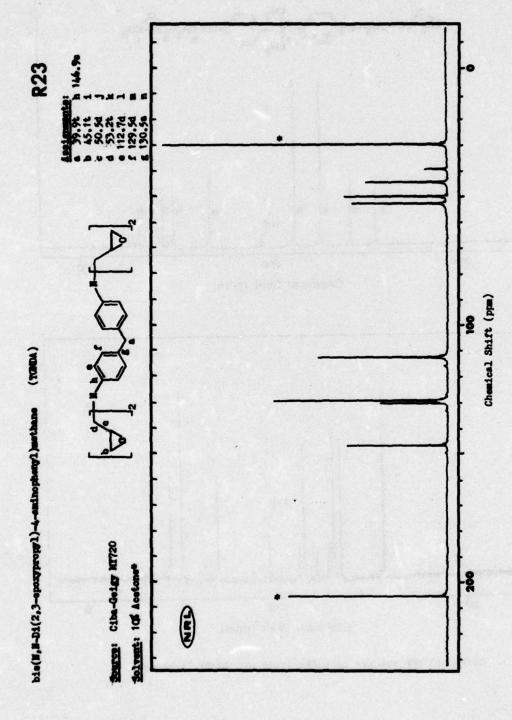
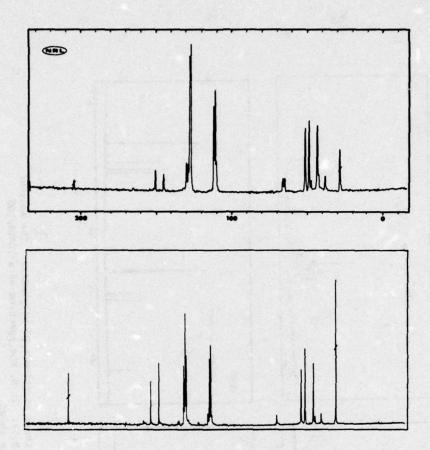


Figure 4. Carbon-13 NMR spectrum of TGMDA in catalog format.



(3)

TGMDA/DDS BASED EPOXY RESIN SYSTEMS

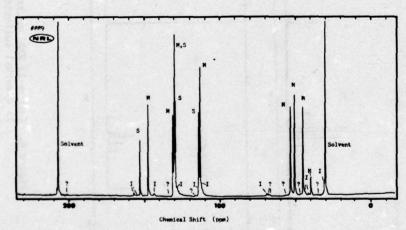


Figure 5. Carbon-13 NMR spectra of three commercially available resin systems based on TGMDA/DDS. The solvent is acetone.

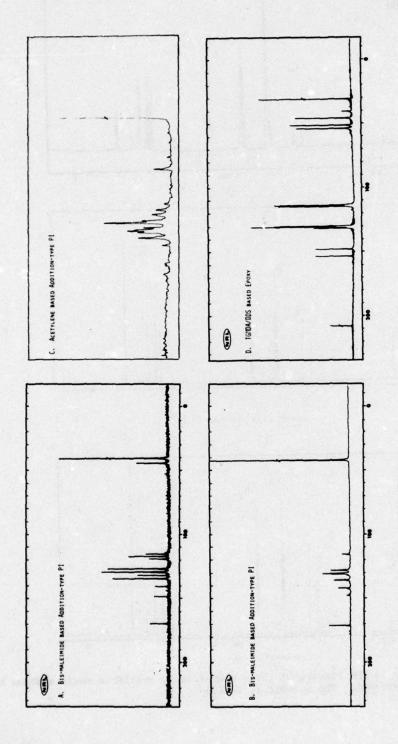


Figure 6. Carbon-13 NMR spectra of three addition-type polyimides. The solvent is dimethyl sulfoxide (A,B,C). In D, the spectrum of a TGMDA/DDS resin system in acetone is shown.

(2)

meta) isomer of C6H5-0-(C6H40-)2C6H5:

Small amounts of the (meta, para), and the (meta, ortho) isomers are also present:

The C-13 NMR spectrum of the mixture is shown in Figure 7. Whereas individual carbon atom resonances are assignable in the C-13 spectrum, only more general assignments of protons ortho, meta, or para to the oxygen functions are possible in the proton spectrum, and no signals unique to particular isomers are identifiable. The pairs of peaks of the C-13 spectrum labelled m,m; m,p; and m,o are attributed to the corresponding isomers. Straightforward measurement of the peak areas yields a sample composition of 77 percent (m,m) isomer, 16 percent (m,p) isomer, and 7 percent (m,o) isomer.

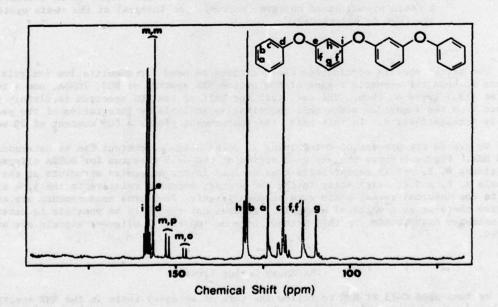


Figure 7. Carbon-13 NMR spectrum of a mixture of polyphenyl ethers.

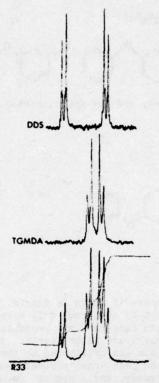


Figure 8. Proton NMR spectra of the aromatic region of DDS (top), TGMDA (middle), and a resin system based on them (bottom). An integral of the resin system spectrum is superposed.

The proton spectra of mixtures can sometimes be used for quantitative analysis. Figure 8 shows the aromatic region of the proton NMR spectra of DDS, TGMDA, and a resin system (R33) based on them. The fact that one half of the DDS spectrum is cleanly resolved from the remainder means that quantitative analysis by integration of the peak areas is straightforward. In this case, the measurement yields a DDS content of 20 weight%.

We are in the process of determining if DGEBA oligomer content can be determined by C-13 NMR. Figure 9 shows the exp nded region of the C-13 spectrum for DGEBA oligomers containing 0, 2, and 15 repeat units n as defined in the molecular structure at the top. Signals a, b, and c, originating in the end groups, decrease relative to the j, k signals due to the internal repeat units as n becomes larger. Peak area measurements are expected to give the average n value of a sample. It does not appear to be possible to determine the oligomer distribution by this method, because individual oligomer signals are not resolved.

The Epoxy Curing Process

We have used C-13 FT NMR to follow the cure of an epoxy resin in the NMR spectrometer. DGEBA was polymerized with piperidine (5 parts per hundred parts resin) at 90°C (Figure 10). Figure 10(a) is the C-13 spectrum of DGEBA measured at 90°C, with the C-13 resonances of the reactive epoxide group indicated. In Figure 10(b), the lines due to the three types of carbon atoms in piperidine are indicated. After approximately 30 minutes

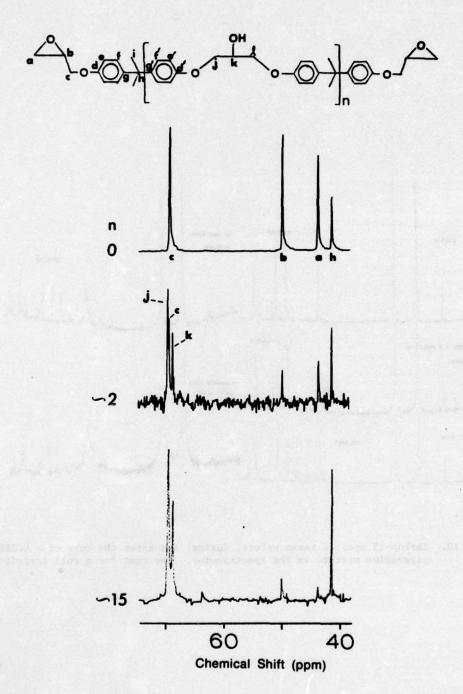


Figure 9. Carbon-13 NMR spectra of the 40-70 ppm region of DGEBA oligomers containing the indicated number of repeat units, n.

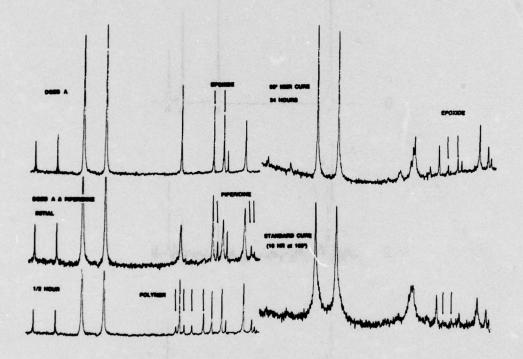


Figure 10. Carbon-13 spectra taken before, during, and after the cure of a DGERA/ piperidine mixture in the spectrometer. See text for a full description.

at 90°C (Figure 10(c)), new lines due to polymer formation have appeared. These grow with further curing, while the lines associated with the epoxide group and piperidine decrease in size.

Both spectra on the right in Figure 10 were measured at 180°C. At lower temperatures (below the glass transition), the cured polymers are too rigid to give narrow lines. (This phenomenon is discussed in the following section on limitations of NMR.) The C-13 NMR spectrum of the sample cured for 24 hours at 90°C is shown in Figure 10(d). Residual lines from the epoxide group show that the cure is incomplete. Figure 10(e) shows the spectrum of a DGEBA/piperidine sample which has undergone a standard cure (16 hours at 120°C). The residual epoxide group lines are substantially smaller than those in the 24 hour 90° cure. The broader lines also indicate that the sample cured at 120° is more rigid than the sample cured at 90°.

LIMITATIONS OF NMR

Sensitivity

As was mentioned in the introduction, NMR can not be classed as a sensitive tool. Pulsed Fourier transform NMR and coherent signal averaging have improved matters by several orders of magnitude. However, utilizing such techniques, even proton NMR barely approaches the sensitivity of IR spectroscopy. On the other hand, when sample size is not the limitation, NMR spectra yield unique, structure specific information, For C-13 NMR, sample sizes are typically 1-2 g. However, usable C-13 spectra can frequently be obtained from 10 mg samples and usable proton spectra from 10 mg samples for molecular weights below about 300. For higher molecular weight, the sensitivities are lowered because of the multiplicity of lines and line broadening due to restricted motion (as with the epoxy curing sequence).

Quantitative Accuracy

Noise is usually the limiting factor in obtaining accurate peak area measurements for quantitative work. One can usually obtain accurate results for constituents present at the 5% or greater level. Peak overlap will increase this limit. If signals are strong and well resolved, the one percent accuracy of integrating devices may be approached. Because of complicating factors in the C-13 FT NMR having to do with the Fourier method, proton decoupling, and nuclear relaxation effects, quantitative C-13 experiments must be very carefully designed. By and large, proton NMR quantitative measurements do not suffer these drawbacks.

Physical State of the Sample

In the discussion of the epoxy curing sequence, it was pointed out that the NMR lines broaden as the rigidity of the sample increases. This is a limitation of NMR. Unless a substance is liquid, or can be melted, or its molecular motion increased by dissolving it in a solvent, the NMR lines are broadened beyond detectability. In liquids, the large dipole-dipole interactions between nuclear spins are averaged to zero by rapid molecular tumbling. In solids, this cancellation does not occur, and the resulting line widths are thousands of times those of the liquids. In the field of thermosetting polymers, then, the forms of NMR so far discussed are limited to the prepolymer stages. As illustrated in the case of DGEBA/piperidine during the early curing stages, useful spectra can sometimes be obtained from gels. Solvent swelling and heating above the glass transition temperature can also produce sufficient motion to yield useful spectra.

The possibility of obtaining useful C-13 NMR signals from rigid thermosetting polymers is not hopeless, however. The field of solid state NMR has been completely revolutionized

by the recent discovery of proton-enhanced NMR (2). With this technique, it is now possible to observe, in the C-13 resonances of organic solids, line widths approaching those measured in liquids. Moreover, the weak signals from the rare C-13 spins are greatly amplified by transfer of polarization from the abundant proton spins. Proton-enhanced C-13 NMR and a method for obtaining resolved proton NMR spectra of solids are discussed in the following sections.

HIGH RESOLUTION NMR OF SOLIDS

Proton-enhanced Carbon-13 NMR

The details of the proton-enhanced C-13 experiment will not be described in detail. The effect of the experiment is to eliminate the large dipolar fields in the solid by ingenious manipulation of the nuclear spin systems (2). The final step towards high resolution is to remove broadening effects which have a spacial origin by rapid specimen rotation at the so-called "magic angle" in the magnetic field. Rotational speeds upwards of 100,000 rpm are required.

Cured Epoxies

Samples were prepared from DGEBA (Dow DER 332) cured with piperidine containing CTBN, meta-phenylene diamine (MPDA), hexahydrophthalic anyhydride (HHPA), and Nadic methyl anhydride (NMA).

Figure 11 shows proton-enhanced carbon-13 spectra of the epoxies without magic angle spinning. Aside from being able to distinguish the various cures, one is not able to say much about the spectra (3).

The spectra of Figure 12 were obtained with the addition of magic angle spinning at 2kHz (120,000 rpm). As a frame of reference, the high resolution spectra of the uncured mixtures dissolved in acetone are superposed. The signals from acetone are indicated by slash marks. The arrow at ca. 70 ppm indicates the signals attributed to a new species formed in the curing process. The vertically expanded region of Figure 12 shows the advancement of curing even in the acetone solvent. Peak f of the epoxide group is not detected in the solids, suggesting that most epoxide groups have reacted. More detailed comments on these spectra are given elsewhere (4).

Prognosis for Solid State NMR

The spectra of the cured epoxies shown in Figure 12 clearly demonstrate that the benefits of high resolution C-13 NMR can be achieved with thermosetting polymers. Hence, structure determinations, the degree of cure, the presence of additives, etc., are all within grasp for intractable polymers.

Schaefer and Stejskal (5) at Monsanto have recently demonstrated that certain nuclear relaxation times from the proton-enhanced carbon-13 spectra of polymer samples spinning at the magic angle correlate strongly with the notched Izod impact strength. Presumably, the motions responsible for the nuclear relaxation are related to those involved in impact energy dissipation. These findings are worthy of intensive investigation.

Information of a useful nature can also be obtained from proton line-narrowing experiments in solids utilizing multiple-pulse techniques (6). Lind at McDonnell-Douglas (7) has used the method to study random alternating block copolymers of dimethylsiloxane and bisphenol-A carbonate. Peak areas and nuclear relaxation behavior of the methyl and aromatic protons were used to characterize the molecular motion and domain structure in terms of block lengths.

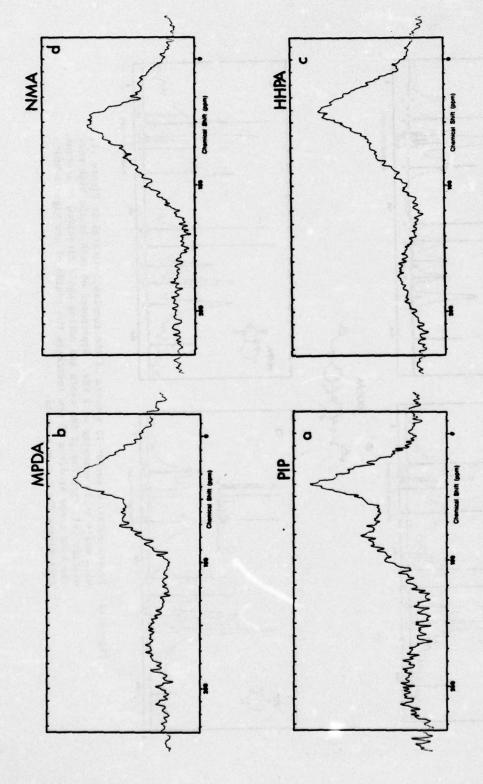
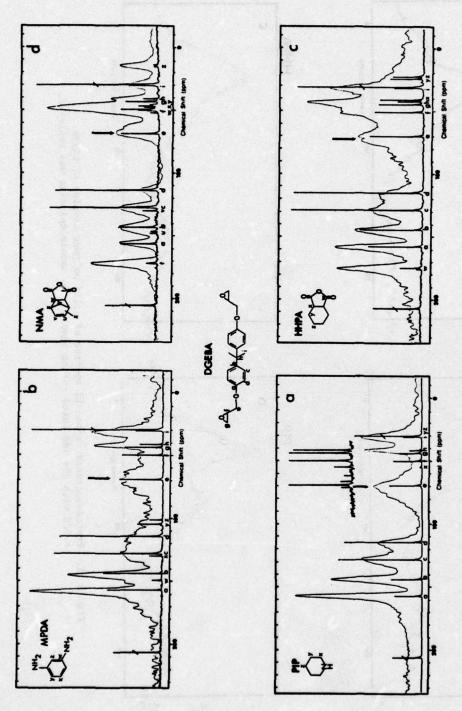


Figure 11. Proton-enhanced carbon-13 spectra of solid polymer samples of DGEBA curred with the indicated curing agents. No sample spinning was employed.



Proton-enhanced carbon-13 spectra of the samples indicated in Figure 11, with magic angle spinning at 2 kHz. Superposed on each is the high resolution C-13 spectrum of the resin and curing agent dissolved in acetone. The bold arrow at circa 70 ppm indicates the region of new signals which form during the curing process. Figure 12.

12

High resolution methods in solid state NMR appear to be ready for full exploitation in the chemical and structural characterization of polymers. At present, they are techniques for the research environment rather than production. Nonetheless, their unique powers need to be recognized and applied, for information of a very practical nature often is obtained.

ACKNOWLEDGEMENTS

The work involving pre-polymers was carried out in collaboration with Drs. C. Poranski and S. Sojka. J. Kopfle and D. Birkle obtained most of the spectra shown.

Drs. A. Garroway and H. Resing are collaborators in the proton-enhanced carbon-13 work, which is supported in part by the Naval Air Systems Command.

I acknowledge with thanks the frequent exchanges of information with C. May of Lockheed and J. Carpenter of McDonnell-Douglas, and their donation of samples.

REFERENCES

- 1. F.A. Bovey, "High Resolution NMR of Macromolecules," Academic Press, N.Y. (1972).
- A. Pines, M.G. Gibby, and J.S. Waugh, "Proton-Enhanced NMR of Dilute Spins in Solids," J. Chem. Phys. 59, 569 (1973).
- H.A. Resing and W.B. Moniz, "A First Step Toward High Resolution Carbon-13 NMR Spectroscopy of Intractable Polymers; Epoxies," Macromolecules, 8, 560 (1975).
- A.N. Garroway, W.B. Moniz, and H.A. Resing, "Carbon-13 NMR in Cured Epoxies: Benefits
 of Magic Angle Rotation," preprint for the Symposium on Characterization of Coatings
 and Polymers, ACS Centennial Meeting, San Francisco, Aug. 1976.
- 5. J. Schaefer and E.O. Stejskal, Monsanto Co., St. Louis, Private Communication.
- J.S. Waugh, L.M. Huber, and U. Haeberlen, "Approach to High Resolution NMR in Solids," Phys. Rev. Lett. 20, 180 (1968).
- A.C. Lind and D.P. Ames, "Multiple-Pulse Reduction of Proton Dipolar Broadening in Solid Copolymers," J. Polym. Sci., B, <u>12</u>, 339 (1974).

STRESS MASS SPECTROMETRY OF POLYMERIC AND COMPOSITE MATERIALS*

Clarence J. Wolf and Michael A. Grayson

McDonnell Douglas Research Laboratories McDonnell Douglas Corporation St. Louis, Missouri 63166

The stress-induced fracture of polymeric materials is preceded by a sequence of complex, partially understood events occurring on both the molecular and macroscopic levels. These events range from flow of ordered regions to rupture of primary chemical bonds in the polymer chain. In recent years, stress-induced bond rupture in polymers has received increased attention; the importance of bond cleavage in the overall sequence of events preceding failure, however, is still uncertain (1-4). Stress mass spectrometry is a new, unique application of mass spectrometry to study the mechanical degradation of polymers and characterize the residual volatiles indigenous to the material (5). Materials are subjected to a stress, either mechanical or thermal, and the resultant products are analyzed mass spectrometrically. In addition, the entire experiment, including application of stress, is performed directly in the ion source housing of the mass spectrometer.

Both applications of stress-MS are described. In one case, the mechanical degradation products of nylon-66 were determined, and in a separate study, the unreacted volatile compounds trapped within an epoxy composite were identified. In all cases, it is important to differentiate between products which are indigenous and those which are mechanical degradation products.

EXPERIMENTAL

A time-of-flight mass spectrometer (TOFMS) (Bendix model 12-107) was used for the analysis and detection of volatile compounds released during mechanical loading of the polymer specimens. The samples were stressed using apparati constructed on the ion source flanges of the TOFMS ion source housing (see Fig. 1). A schematic of the system used either to fracture the sample or apply tension to a dogbone-shaped specimen is shown in Fig. 1a. The tensile apparatus with sliding weight and weight

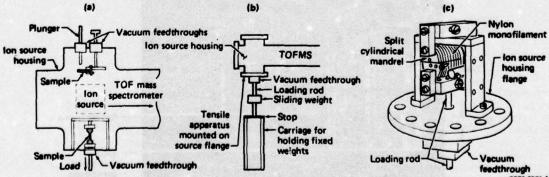


Fig. 1 Ion source flange modifications for stress mass spectrometry studies: a) system used for stress and fracture of solids, b) diagram indicating method of applying stress, and c) system used to stress and fracture filaments

^{*}This research was conducted under the McDonnell Douglas Independent Research and Development Program.

carriage is depicted in Fig. 1b. The system for applying tension to monofilaments, e.g., nylon, is shown in Fig. 1c. The system used to abrade or saw solid materials, such as composites, is shown in Fig. 2.

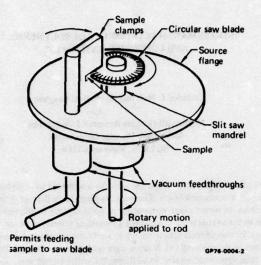


Fig. 2 Diagram of abrasion apparatus for stress mass spectrometry

Data from these experiments are acquired by either continuous ion monitoring or oscilloscope photography of z-axis modulated mass spectral displays. For the former case, a four-channel monitor (Bendix model MA-006) modified for extended mass range was used. In the latter case, the Rapid Events Mass Spectral Data Acquisition (REMSDA) system was used (6). The REMSDA system permits acquisition of data during the brief time prior to, during, and immediately following the sample fracture. With this system, z-axis modulated mass spectra (6) can be displayed on the oscilloscope screen for 1.6 ms to 3.2 s with timing intervals from 0.2 ms to 205 ms. A photograph of the REMSDA output is shown in Fig. 3. The mass-to-charge ratio is along the x-axis, elapsed time is along the y-axis, and the intensity of the peak is determined by the brightness of the line (z-axis).

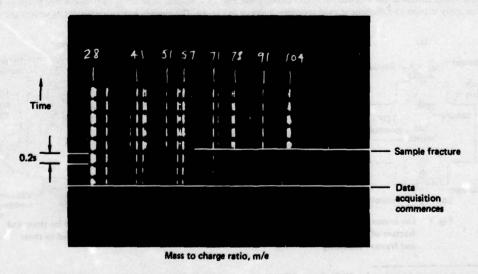


Fig. 3 Rapid Events Mass Spectra Data Acquisition (REMSDA) display from the fracture of polystyrene

The volatile organic compounds indigenous to the matrix of the polymer are characterized by vaporization gas chromatography/ mass spectrometry (VGC/MS) (7). This technique permits efficient sampling of indigenous volatiles by using the column as a trap. After the sampling is complete, conventional GC/MS procedures are used to identify the indigenous volatiles using a mass spectrometer (AEI MS-30 single beam) interfaced to the gas chromatograph with a silver frit molecular effusion separator (8).

RESULTS

Mechanical Degradation of Nylon

Nylon 66 (DuPont), free of additives, was studied in the form of a drawn monofilament 0.2 mm in diameter. VCG/MS characterization of the monofilament revealed the indigenous volatiles shown in Fig. 4. In subsequent heating intervals,

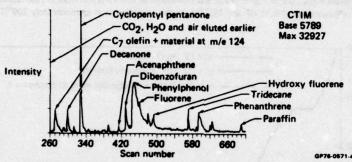


Fig. 4 Chromatogram of a VPGC/MS analysis of the volatiles released from nylon 66 (heated for 15 min at 210°C)

only a small amount of phenyl phenol was present. These compounds are typical of surface finishes and die lubricants used in the manufacture of nylon 66 monofilament. In addition, cylic hexamethylene adipamide was released when the nylon was heated in the solids probe of the mass spectrometer.

The samples were loaded in tension to fracture. During loading of the nylon 66 monofilament, no volatile material was detected, even though sample extension was typically 10%. At sample fracture, mechanical degradation products were detected only when one or more of the fracture surfaces was frayed or "fibrillated" (see Fig. 5b). No products were detected when the sample fractured cleanly (see Fig. 5a).

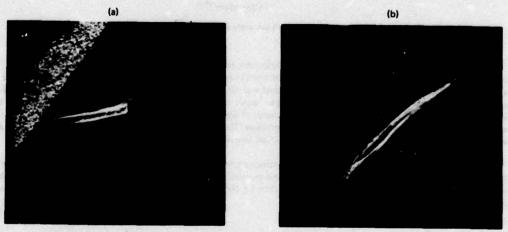


Fig. 5 Photographs of the nylon 66 monofilament following fracture in the mass spectrometer:
a) clean fracture, b) fibrillated or frayed fracture

Low ionization potential mass spectrometry was used to identify many of the products. Ammonia and ethylene were positively identified; ethane, formaldehyde, butenol, and butenal were tentatively identified. These compounds are different from the indigenous volatiles found in the characterization study and hence are assumed to be products of mechanical degradation. The significance of the release of products only upon fibrillation of the fracture surface is not yet certain.

Volatiles Released from an Epoxy Composite

An epoxy fiberglass composite was abraded with the saw apparatus shown in Fig. 2. The epoxy was a mixture of novolac and diglycidyl ether of bisphenol-A (DGEBA) with boron trifluoridemonoethylamine complex curing agent.

When the composite was heated in the solids probe of the MS-30, i.e., EGA/MS, a number of compounds were evolved, three of which were monitored by use of the characteristic ions H_2O , HF, and DGEBA monomer. The evolution of these three products as a function of temperature is shown in Fig. 6. Water was monitored at m/e 17 rather than 18; the amount decreases as a function of temperature. The concentration of both HF and DGEBA reaches a maximum at approximately $200^{\circ}C$, above the T_g of the composite.

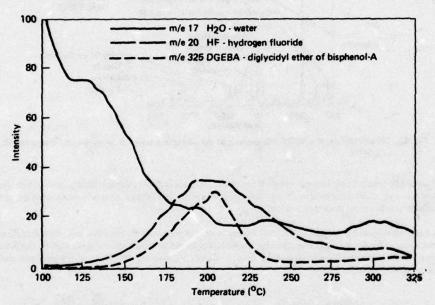


Fig. 6 Volatiles evolved during evolved gas analysis mass spectrometry (EGA/MS) study of an epoxy composite

Water released from the composite was measured during abrasion by continuous ion monitoring. The water released during three operations of the sawing procedure was measured: 1) when the saw was rotated without a sample, 2) when the composite was cut, and 3) when the aluminum sample clamp was cut. The results of this study, together with the ion signal from the injection of a known amount of water $(4 \times 10^{-9} \text{ g/s})$ are shown in Fig. 7. Note that the water released druing abrasion is on the order of $4.5 \times 10^{-9} \text{ g/s}$, and corresponds to several percent of water in the composite. The jagged peaks are a result of the manual rotation of the saw, a somewhat discontinuous operation. The amount of H_2O released from sawing the aluminum sample clamp is approximately two orders of magnitude less than that observed from the composite.

In addition to water, we observed that toluene was released upon abrasion of the composite. The TOF was calibrated for toluene by injecting a known quantity $(3.2 \times 10^{-9} \text{ g/s})$ and monitoring the m/e 92 peak. The results are shown in Fig. 8 where the amount of toluene released corresponds to approximately $3 \times 10^{-10} \text{ g/s}$. Note that toluene is evolved only when the composite is cut.

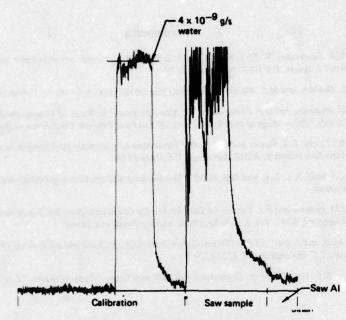


Fig. 7 Water evolved from an epoxy composite during mechanical abrasion

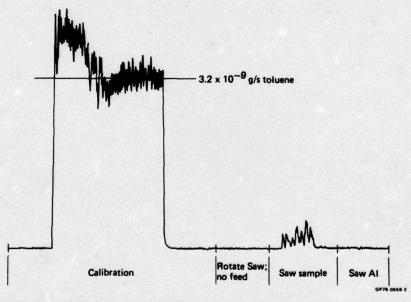


Fig. 8 Determination of toluene evolved from an epoxy composite during mechanical abrasion

CONCLUSIONS

Our studies indicate that stress mass spectrometry is a useful technique for studying stress-induced chemical reactions in polymeric systems. However, it is imperative that the indigenous volatile compounds in the polymer matrix be characterized before the results are interpreted. In addition, controlled abrasion can be utilized for qualitative and quantitative analysis of volatile compounds, such as solvent or unreacted monomer, trapped within the matrix of a polymer or composite.

REFERENCES

- S.N. Zhurkov, V.A. Zakrevskyi, V. Ye Korsukov, and V.S. Kuksenko, "Mechanism of Submicrocrack Generation in Stressed Polymers," J. Polym. Sci. (A-2) 10, 1509 (1972).
- 2. B.A. Lloyd, K.L. DeVries, and M.L. Williams, "Fracture Behavior of Nylon 6 Fibers," J. Polym. Sci. (A-2) 10, 1415 (1972).
- V.R. Regel', T.M. Muninov, and O.F. Pozdnyakov, "A Mass Spectrometric Study of Volatile Products Evolving in Degradation of Solids," Proceedings of the Physical Basis of Yield and Fracture Conference, Oxford, 1966, pp 194-199.
- M.A. Grayson, R.L. Levy, D.L. Fanter and C.J. Wolf, "Stress Mass Spectrometry of Polymeric Materials," 24th Annual Conference on Mass Spectrometry, ASMS, San Diego, CA, (May 1976).
- M.A. Grayson, C.J. Wolf, R.L. Levy and D.B. Miller, "The Mechanical Degradation of Polystyrene," J. Polym. Sci. (Phys.), August 1976 (in press).
- M.A. Grayson, J.M. Putnam and F.J. Yaeger, "A Data System for Continuous-Scan MS Experiments Based upon the Use of a Time-Sharing Computer Utility," Int. J. Mass Spectrom. and Ion Physics (in press).
- 7. R.L. Levy, C.J. Wolf, and J. Oro', "A Gas Chromatographic Method for Characterization of the Organic Content Present in an Inorganic Matrix," J. Chromatog. Sci. 8, 524 (1970)
- 8. M.A. Grayson and R.L. Levy, "A Micro Separator for GC/MS with Open Tubular Columns," J. of Chromatog. Sci. 9, 687 (1971).

APPLICATION OF CHEMILUMINESCENCE TO THE CHARACTERIZATION OF POLYMERIC MATERIALS

Richard A. Nathan, G. David Mendenhall, and John A. Hassell

BATTELLE Columbus Laboratories Columbus, Ohio

Many aspects of chemiluminescence are not well understood. When those that are familiar with chemiluminescence think of the phenomenon, their thoughts turn initially to fireflies, luminescent bacteria, or aquatic life, or high efficiency light sources such as the Cyalume light stick manufactured by American Cyanamid. Both bioluminescence systems and cool lights were designed either by nature or by man for high efficiency. In contrast to this, Battelle researchers have been utilizing the natural chemiluminescence that is emitted from organic materials as an analytical tool. Frequently the efficiencies of these processes are on the order of 10^{-8} or less.

Because this is generally a new concept to most of you I will spend most of the time today on the following points:

- What is chemiluminescence?
- · How is it formed?
- · How is it measured?
- What are the measurements like?
- What is it good for?

Origins of Chemiluminescence

Chemiluminescence is really quite a common phenomenon. However, even organic chemists are frequently not familiar with the breadth of reactions that emit chemiluminescence spontaneously. These include:

- Oxidation reactions organic and inorganic
- Hydration of inorganic compounds
- Inorganic acid-base reactions
- Grignard reactions
- Inorganic vapor phase reactions
- Bioluminescence
- Anodic oxidations in electrolytic cells
- Thermal decompositions

In fact there are really only two requirements for the chemiluminescent process. The first is that the reaction itself must accumulate sufficient energy to raise one of the reaction components to an excited electronic or vibrational state. The only other requirement is that at least one material present be able to emit light even if it is an extremely inefficient process.

Currently it is thought that the light is emitted from a termination step in which two alkyl peroxy radicals combine to produce a carbonyl-containing compound, usually a ketone, an alcohol and oxygen. Some small fraction of the ketone is found in an excited state, and when this relaxes to its electronic ground state, light is emitted. Figure 1 shows a typical oxidation scheme for cis-polyisoprene and is exemplary of the oxidation processes of polymers.

ghi

CH₃

$$C = CH$$

$$CH_2 \rightarrow CH_2 \rightarrow R + 0_2 \rightarrow Products$$

Initiation:
$$ROOH \rightarrow ROO + OH \rightarrow ROO +$$

FIGURE 1. AUTOXIDATION OF cis-POLYISOPRENE

Instrumentation

Currently there is no suitable commercial instrumentation for measuring ultra-weak chemiluminescence for analytical purposes. Hence, in the ten years we have been carrying out such research at Battelle we have found it necessary to construct our own equipment. Figure 2 is an artist's rendition of one of our current high sensitivity instruments, clearly showing its working parts. It essentially consists of three concentric boxes. The inner-most box serves as an oven. Just outside of it is another box which serves to shield the rest of the apparatus from the oven's heat. The outer-most box is simply a container to make the entire instrument light tight. This photon counting instrument is equipped with a filter wheel which contains up to 20 Corning glass filters and allows us to measure the spectral distribution of the chemiluminescence emission.

Chemiluminescence instrumentation need not be this complicated. Figure 3 shows a simpler apparatus which consists only of a light-tight box containing a hot plate, a photomultiplier, and associated electronics.

Benefit of Chemiluminescence

The benefit of chemiluminescence as an analytical tool is based almost entirely upon the extreme sensitivities that are achieveable by this technique. For example, emission rates of 10 photons/sec are easily detected from a sample. This corresponds to 3.2×10^6 photons/yr or 5.2×10^{-16} moles of photons (Einsteins) per year. Assuming an efficiency of 10^{-8} , decomposition rates of 5.2×10^{-8} moles/yr are detectable. Using various analytical tricks in favorable cases, one can achieve efficiencies of 10^{-3} which allows the measurement of decomposition rates on the order of 5×10^{-14} moles/yr. Such sensitivities are orders or magnitude greater than sensitivities available from most other analytical techniques, and it is this sensitivity that makes chemiluminescence such a powerful tool. It permits us to measure slow degradation reactions nondestructively under actual use conditions and in most cases precludes the need for any accelerated aging procedures. When dealing with sensitivities such as this, we can look at the degradation processes from materials normally thought to be inert under conditions of interest. For example, plastic desk tops, clothes, food, and other normally inert organic materials can be studied conveniently by this technique.

Figure 4 shows an idealized chemiluminescence curve. The intensity of chemiluminescence is plotted vs. time at constant temperature. The luminescence gradually increases to a maximum value which corresponds to the autocatalytic buildup of initiating species. If little hydrocarbon is consumed by the time this maximum value, termed Imax, is achieved, the emission intensity will remain constant. The time required to reach one half of this maximum intensity is referred to as $t_{1/2}$ and is a measure of the induction period.

Frequently, conditions allow us to measure oxidation rates directly. As the curve shows, once the oxygen is turned off to the sample, the chemiluminescence intensity rises. The reason for this is that as the oxygen is depleted in the sample the oxidation rate continues almost unchanged as oxidation rates are typically not particularly dependent on oxygen concentration above 100 torr partial pressure or so. However, the quenching of the excited states which give rise to luminescence is sensitive to oxygen concentration, and hence, as the oxygen concentration decreases, the quenching decreases and the luminescence intensity increases. The oxidation rate stays constant, only the luminescence intensity increases. Once the oxygen is fully depleted, the curve decreases rapidly. The time between when the oxygen is turned off and the oxygen is depleted is termed t_f. If you know the oxygen concentration under saturated conditions (at the time at which the oxygen is turned off), you have a direct measure of the time required to use up that much oxygen, and hence, the oxidation rate at that temperature can be calculated directly.

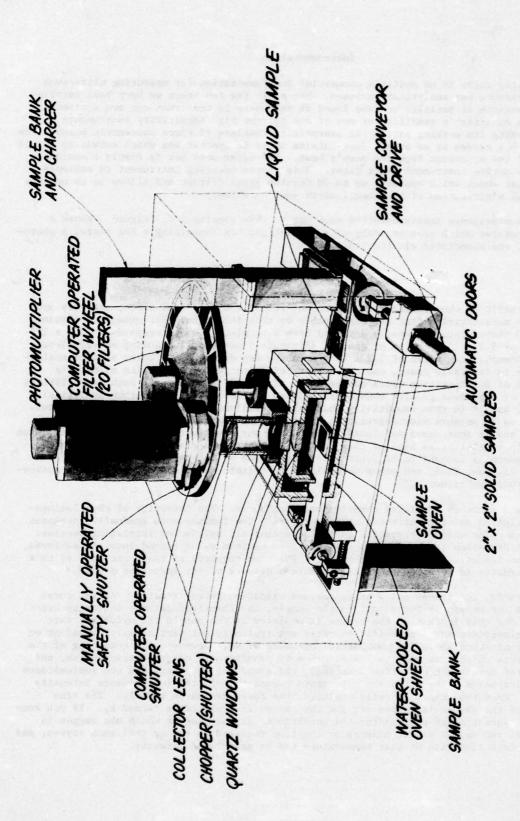


FIGURE 2. PHOTON COUNTING INSTRUMENTATION FOR CHEMILUMINESCENCE STUDIES

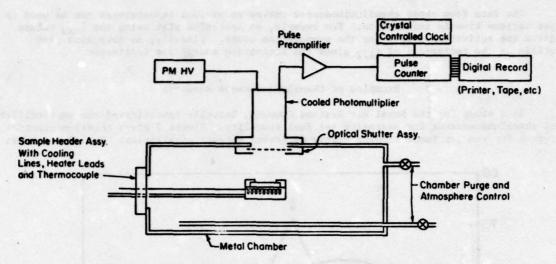


FIGURE 3. CHEMILUMINESCENCE APPARATUS FOR SOLID SAMPLES

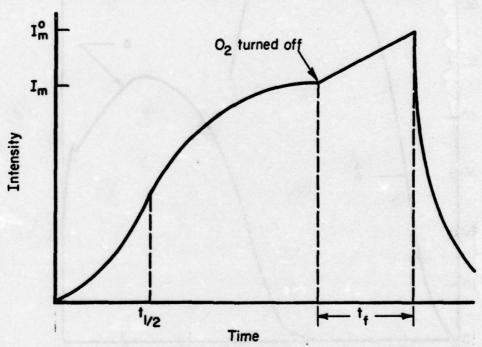


FIGURE 4. TYPICAL INTENSITY-VERSUS-TIME CURVE FOR AUTOXIDATION OF HYDROCARBONS

The sample is heated to a convenient test temperature at time = zero.

t1/2-induction period-direct measure of stability useful for detecting traces of oxidation catalysts.

tf-time required to consume oxygen dissolved in sample-direct measure of oxidation rate.

The data from these chemiluminescence curves at various temperatures can be used to get various kinetic information. For example, an Arrhenius plot using the I_{max} values gives the activation energy for the propogation steps. Simarily, an Arrhenius plot utilizing the reciprocal of $t_{1/2}$ gives the activation energy for initiation.

Examples of Chemiluminescence Research

In a study for the Naval Air Systems Command, Battelle investigated the applicability of chemiluminescence for assessing jet fuel stability. Figure 5 gives chemiluminescence curves for two jet fuels showing vastly different thermal stabilities. Fuel B was known

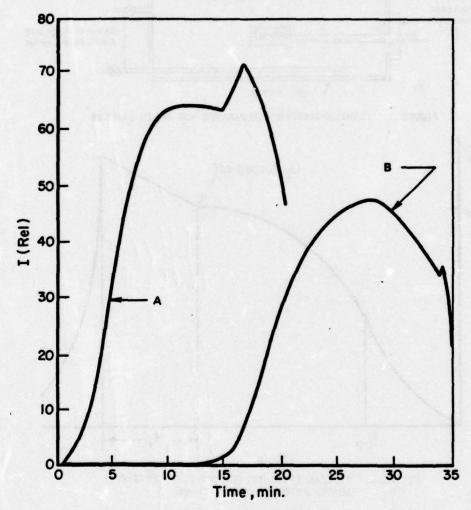


FIGURE 5. CHEMILUMINESCENCE FROM OXIDATION OF JET FUELS INTENSITY VERSUS TIME (T = 175 C)

A - jet fuel with poor thermal stability; B - jet fuel with good thermal stability to have good thermal stability in aircraft. Notice that it has a relatively long induction period and low maximum intensity. Fuel A, on the other hand, known to have poor thermal stability has a short induction period and a relatively high maximum intensity. This indicates that the chemiluminescence technique can be useful as a black box analytical method for the evaluation of thermal stabilities of various organic materials.

Early stages of the jet fuel program involved the use of model hydrocarbons. Figure 6 shows an Arrhenius plot for 1-tridecene in which an unusual phenomenon is shown. The Arrhenius plot clearly shows that 2 mechanisms were occurring depending upon the temperature

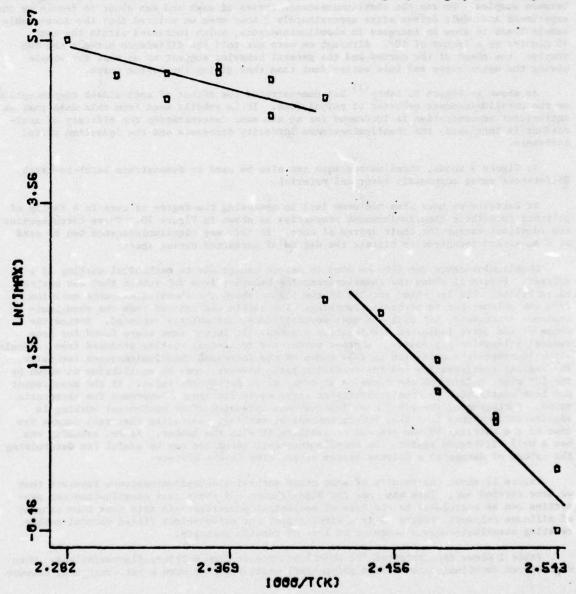


FIGURE 6. ARRHENIUS PLOT OF 1-TRIDECENE OXIDATION WITH 10⁻³M DIPHENYLANTHRACENE RELATING I TO TEMPERATURE

range of oxidation. Such behavior is unusual and is currently unexplained, but it can be used emperically to show that chemiluminescence can be used to validate or invalidate accelerated procedures and confirms the danger involved in assessing a material's stability under accelerated conditions—it is always possible that in going from use conditions to the accelerated conditions a mechanism change occurs which invalidates any extrapolations based on the accelerated conditions.

Figure 7 shows chemiluminescence curves from two samples of polyethylene sent to us by a company who was dubious about the ability of chemiluminescence to detect small differences between samples. We ran the chemiluminescence curves of each and was about to terminate the experiment and admit defeat after approximately 1 hour when we noticed that the less-stable sample began to show an increase in chemiluminescence, which increased within the next 45 minutes by a factor of 10^3 . Although we were not told the difference between the two samples, the shape of the curves and the general behavior suggest to us that the sample giving the upper curve had less antioxidant than that giving the bottom curve.

As shown in Figure 8, Ashby (1) has demonstrated the effect of antioxidant concentration on the chemiluminescent behavior of polyolefins. It is readily seen from this data that as antioxidant concentration is increased (or at the same concentration the efficacy of antioxidant is increased) the chemiluminescence intensity decreases and the induction period increases.

As Figure 9 shows, chemiluminescence can also be used to demonstrate batch-to-batch differences among supposedly identical material.

At Battelle we have also had some luck in assessing the degree of cure in a family of polymers from their chemiluminescent properties as shown in Figure 10. These three epoxies are identical except for their degree of cure. In this way chemiluminescence can be used as a sensitive technique to titrate the degree of unreacted curing agent.

Chemiluminescence can also be used to detect damage due to mechanical working of a polymer. Figure 11 shows the chemiluminescence behavior from SBR rubber that was carbon-black filled. The left-hand portion of the figure shows the chemiluminescence emission from the polymer before mechanical working. The sample was removed from the chemiluminescence instrument, hit with a hammer several times, and quickly replaced. Notice the shape of the curve indicates a relaxation process. It is the same shape found for free radical relaxation processes. In other words, the mechanical working produced free radicals, which increased the oxidation rate as shown by the increased chemiluminescence intensity. The radical concentration and the oxidation rate, however, come to equilibrium as shown by the far right portion of the curve as it comes to an asymptotic value. If the measurement had been continued, the chemiluminescence curve would continue to approach the asymptotic value. Furthermore, the final chemiluminescence intensity after mechanical working is significantly higher than that before mechanical working, indicating that real damage was done to the material by the process of striking it with the hammer. Hence, assuming one has a well calibrated system, the chemiluminescence technique may be useful for determining the extent of damage to a polymer system at any time in its history.

Figure 12 shows the results of some other mechanical-chemiluminescence research that we have carried out. This was done for NASA-Johnson and shows that chemiluminescent properties can be correlated to the loss of mechanical properties—in this case loss tangent of silicone polymers. Figure 13 is a similar plot for carbon-black filled natural rubber, relating chemiluminescence behavior to loss of tensile strength.

Table 1 shows data obtained for chemiluminescence from polytetrafluoroethylene. When we observed chemiluminescence from polytetrafluoroethylene we were a bit concerned, because

⁽¹⁾ G. Ashby, J. Poly. Sci., 50, 99 (1961).

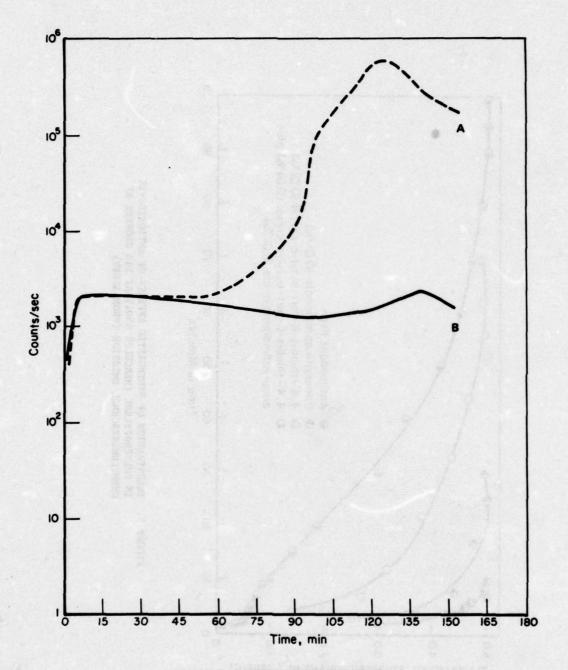
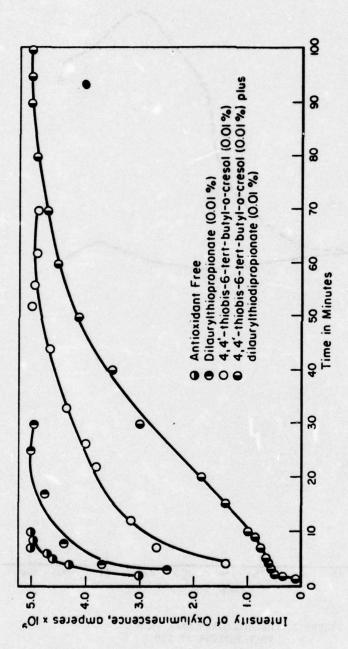


FIGURE 7. CHEMILUMINESCENCE FROM POLYETHYLENE AT 150 C



PIGURE 8. ILLUSTRATION OF SYNERGISTIC EFFECTS OF ANTIOXIDANTS IN POLYPROPYLENE (HERCULES 6501) AT 143 DEGREES BY CHEMILUMINESCENCE EMISSION (FROM ASHBY)

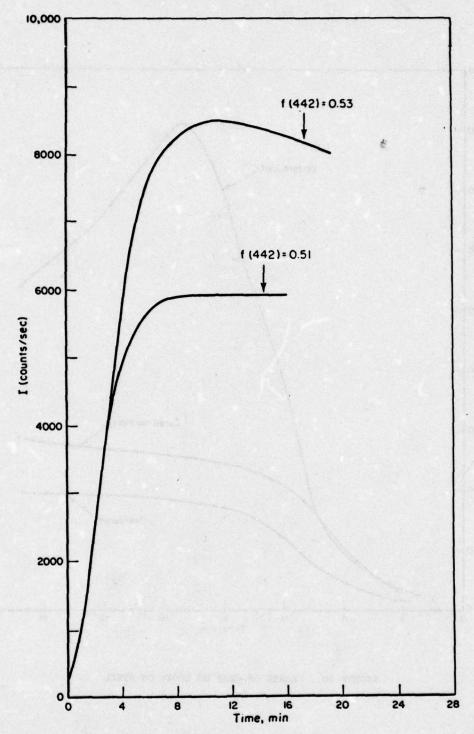


FIGURE 9. DEMONSTRATION OF BATCH-TO-BATCH DIFFERENCES WITH CHEMILUMINESCENCE

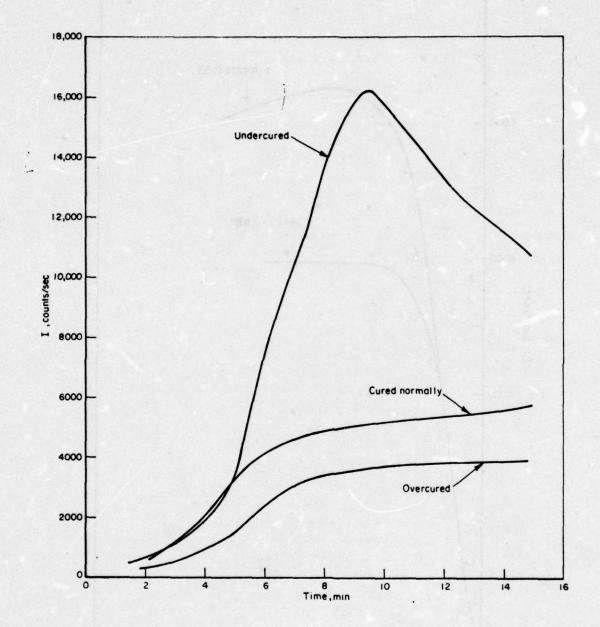


FIGURE 10. DEGREE OF CURE OF EPOXY ON STEEL

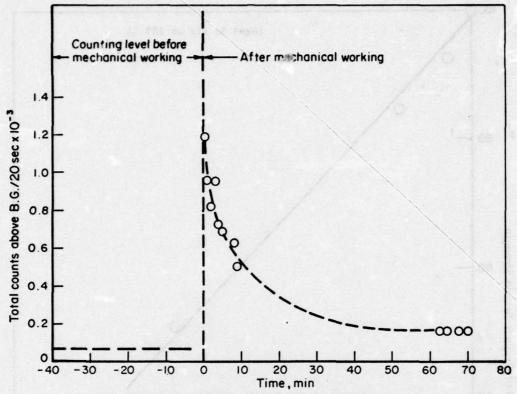


FIGURE 11. EFFECT OF MECHANICAL WORKING ON CHEMILUMINESCENCE PROPERTIES

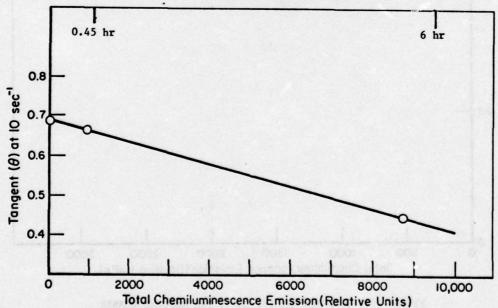


FIGURE 12. CORRELATION BETWEEN TOTAL CHEMILUMINESCENCE EMISSION AND LOSS TANGENT FOR GE W-96 SILICONE

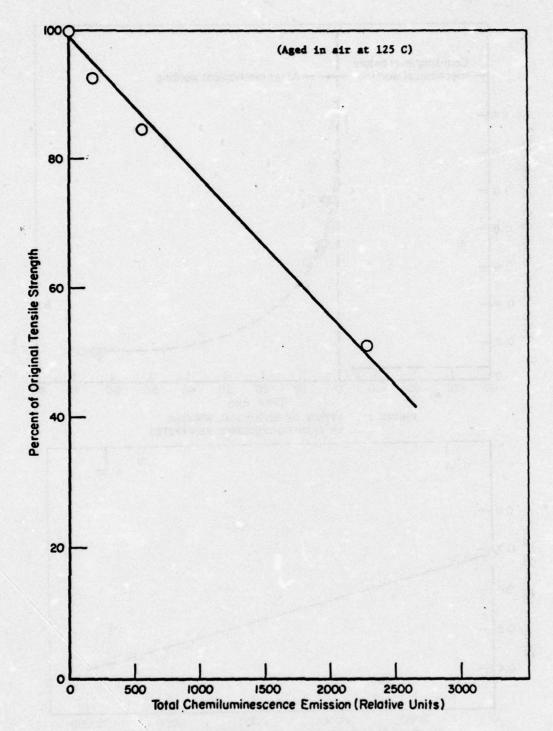


FIGURE 13. PROPORTIONALITY CURVE FOR NATURAL RUBBER

TABLE 1. CHEMILUMINESCENCE OF POLYTETRAFLUOROETHYLENE (HALON) MEASURED IN OXYGEN AT 80 C (176 F)

Sample	Time (min)(a)	Counts/sec(b)			
Halon G-10					
1. As received	7.5. 40	54 (max) 48			
2. Same	7.5	49 (max)			
3. Extracted 24 hours	60 110	21 (max) 11 11			
4. Extracted 48 hours	5 40	14			
Halon G-80					
5. As received	8 100 17 hours	173 (max) 68 38			
6. Same	12.5 125	150 (max) 45			
7. Surface abraded	8	46 (max)			

⁽a) Samples aged in chemiluminescence apparatus.

the conventional theories to explain the chemiluminescence emission did not seem to hold. Oxidation of polytetrafluoroethylene is extremely slow at the temperatures of the experiment, although reactions of non fluorinated-end groups might occur. We found, however, that repeated extraction of the polymer removed the chemiluminescence which indicated to us that the luminescence was primarily if not totally the result of impurities in the polymer. (2) Analysis of the data indicated to us that the impurity was present in less than 0.5 percent.

Table 2 shows some chemiluminescent values for a urethane polymer aged 2 weeks at 95% RH and 85 C. It indicates a nice correlation between hardness values and the chemiluminescence intensity. However, at this point in this program with the Naval Air Systems Command to determine the mechanism of moisture-induced reversion of epoxy and urethane potting compounds such data is misleading. Table 3 indicates that for the same material no correlation exists between the hardness values and the chemiluminescence maxima, but one can correlate the chemiluminescence values with weight gain. Obviously, the suitability of chemiluminescence for the problem of moisture-induced reversion is not clear cut.

⁽b) Unfiltered emission detected.

⁽²⁾ G. D. Mendenhall, R. A. Nathan, and J. A. Hassell, J. Poly. Sci., in press.

TABLE 2. HEXCEL URALITE 3113 EXPOSED 2 WEEKS AT 95% RH and 85 C

Hardness (Shore A)	Chemiluminescence Maximum	
59	612	
47	231	
38	137	

TABLE 3. HEXCEL URALITE 3113 EXPOSED TO 95 PERCENT RH AND 85 C

Time (hrs)	Hardness (Shore A)	Wt Gain (%)	Chemiluminescence Maximum
19.5	53	1.9	361
67.5	51	2.4	260
187.5	41	1.2	1033

Table 4 shows that chemiluminescence is very sensitive to the aging conditions of the various epoxy materials. Notice that the greatest decrease in chemiluminescence intensity is due to temperature and not to relative humidity, indicating that the process leading to chemiluminescence might not be significant to the moisture-induced reversion.

TABLE 4. CHEMILUMINESCENCE VALUES (COUNTS/SQ CM)
FOR EPOXY POLYMERS SUBJECTED TO VARIOUS
CONDITIONS FOR 2 WEEKS

	SCTH 280			
Conditions	Low Cure	Medium Cure	High Cure	EPOX
23 C, O percent RH	53	134	57	53
23 C, 95 percent RH	41	138	50	50
85 C, O percent RH	28	31	30	34
85 C, 95 percent RH	14	24	26	35

At Battelle we have been looking at materials other than polymer's. For example, Figure 14 shows an Arrhenius plot from the chemiluminescence of a cold cereal. The company indicated to us that after extended aging tests the lab cereal had been shown to be less stable than the plant cereal even though the formulations were identical. Chemiluminescence analysis, carried out in less than 4 hours, clearly supported this finding. At each temperature the chemiluminescence intensity from the lab cereal was significantly greater than the chemiluminescence obtained from the plant cereal. In addition, we found that the Arrhenius plots became nonlinear above approximately 45 C. This was consistent with the company's knowledge that accelerated aging tests carried out above about 45 C gave erroneous results.

Table 5 shows chemiluminescence from shrimp and tuna fish samples obtained from the Food and Drug Administration. These measurements were carried out with samples at dry ice temperatures, and hence, for the shrimp little selectivity was found; probably simply because the reactions were extremely slow at these temperatures. The tuna fish samples, however, were more straight forward. Whether or not the samples were packed in oil or water, we found that the good tuna samples gave chemiluminescence behavior 75 and 95 counts/sec after 5 minutes, while those determined to be decomposed generally gave counts above 100. We hope to pursue this and to develop techniques for the rapid assessment of tuna quality using this technique.

Table 6 shows some data from the chemiluminescence evaluation of soybean protein. The protein was stored at 50 for up to 50 days. Not only did the absolute intensity increase by about 40 percent over that period, but on measuring the spectral distribution of the emission we found that there was a significant shift to shorter wavelength. Frequently such spectral shifts can be used to determine details of the mechanism of the degradation process.

Application

In summary chemiluminescence can be applied to materials in four ways:

- Service life prediction
- Materials evaluation
- Understand degradation mechanism
- Assess remedial action.

We feel chemiluminescence is an extremely powerful technique for studying degradation processes, although a great deal of caution must be used in its application. The chemiluminescence process is the result of at least four consecutive reactions, each of which can be affected by the nature of the material. The nature of the substrate and the reactions involved are rather complex, and the correlations between chemiluminescence and changes of interest are frequently empirical. Because chemiluminescence tells you that something is happening early in the process, it is quite useful. But it does not provide knowledge of what is happening: it does not provide structural information. Hence, at Battelle we are frequently using chemiluminescence in conjunction with spectral techniques such as infrared and nuclear magnetic resonance to provide both kinetic and mechanistic information about degradation processess.

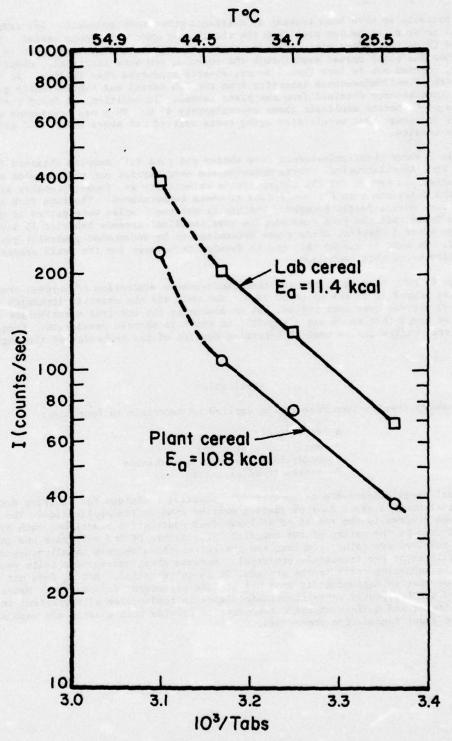


FIGURE 14. CHEMILUMINESCENCE FROM COLD CEREAL

TABLE 5. CHEMILUMINESCENCE FROM FDA TUNA-FISH AND SHRIMP SAMPLES

Sample	Quality	Maximum Counts/Sec	Average Counts/Sec After 5 Min
Shrimp 1	Good	30	12
Shrimp 2	Bad	37	15
Shrimp 3	Worst	37	17
Tuna A (oil packed)	Good	225	75
Tuna A (oil packed)	Decomposed	370	155
Tuna B (oil packed)	Good	133	95
Tuna B (oil packed)	Decomposed	473	415
Tuna B (water packed)	Good	137	75
Tuna B (water packed)	Decomposed	133	110

TABLE 6. EXAMINATION OF SOYBEAN PROTEIN(a)

Aging Time at 5 C, days	Cutoff Filter(b),	Counts/Gram-Sec	F(λ)(c)
0	None	299	1.0
	442	292	0.98
	490	143	0.48
	526	76	0.25
	592	4	0.01
50	None	359	1.0
	442	308	0.86
	490	150	0.42
	540	50	0.14

(a) Measured at 25 C in an oxygen atmosphere,
(b) Filter has OD >0.50 at wavelengths shorter than λnm.
(c) Fraction of unfiltered counting rate.

THE EARLY STAGES OF ACTINIC DETERIORATION

D. M. Wiles

Chemistry Division
National Research Council of Canada
Ottawa, Ontario K1A OR9, Canada

INTRODUCTION

The deleterious effects of sunlight on a wide variety of materials are well known and are the cause of considerable concern since these effects frequently cause failure of these materials during use. This situation is a particular problem when the materials are comprised of organic polymers - plastics, fibers, rubbers, protective coatings, composites, etc. The reason is that macromolecules derive their uniquely useful properties from their very high molecular weights. The breaking of one bond (or sometimes even less) per polymer molecule can have a disastrous effect on the physical properties of polymeric materials. Since there is ample energy in the ultraviolet (UV) part of terrestrial sunlight (especially in the "sunburn" region, ~290 to 315 µm) to break most chemical bonds, a very common manifestation of actinic deterioration in polymers is backbone bond scission and a dramatic loss of physical properties, e.g., embrittlement.

The use of long-term outdoor exposures of materials to establish serviceability is not particularly satisfactory, for a number of reasons: it takes too long; sunlight is not reproducible, hourly, daily, weekly, monthly or geographically; although the major effect of the weathering of polymers is photo-degradation, there are other, non-actinic effects as well, e.g., precipitation, heat, light-dark cycling, etc., which complicate the situation. Notwithstanding the apparent paradox of trying to duplicate sunlight (which is not constant), numerous researchers have found it convenient to use artificial (laboratory) light sources, for the elucidation of actinic deterioration, where these light sources are designed to correspond as closely as possible to terrestrial sunlight. Work at the National Research Council (1,2) and in many other laboratories has indicated that the use of arc lamps instead of the sun involves a number of difficulties. When the radiation from a xenon arc or a carbon arc, for example, is filtered so as to approximate closely terrestrial sunlight, the acceleration factor (hours of machine exposure compared to days of outdoor exposure) is not particularly high. In other words, the greatest saving in time by using a laboratory light source instead of the sun to determine the resistance of a material to UV degradation derives primarily from the 24 hours per day exposure that is possible with the former.

In this context, therefore, it is important to be able to detect the earliest possible stages of actinic deterioration in materials whether they are being exposed to real or to artificial sunlight. Only in this way can the useful outdoor service life of these materials be evaluated with anything like the required rapidity.

CHEMICAL TECHNIQUES

The investigation of actinic deterioration, in common with virtually all other types of materials research, involves analytical chemistry. One must know the chemical characteristics of the materials involved, and one must be able to detect changes in these characteristics which are directly related to the useful properties (e.g., physical, mechanical, electrical) of the materials. Especially in the case of organic molecules, chemical spectroscopy of all kinds is useful. Nuclear magnetic resonance, electron spin resonance, electronic absorption and infrared (IR) absorption spectroscopy have all been used, frequently in combination, to determine photochemical changes in materials. ESCA and Fourier Transform IR spectroscopy are both highly promising techniques although the equipment is expensive and not immediately applicable to polymeric systems. Perhaps the best single technique is IR spectroscopy and certainly the appropriate spectrophotometers are ubiquitous.

One of the key features in the photochemistry of macromolecules is that specific chromophores (groups, complexes, impurities, etc.) must be present in order for specific wavelengths in the incident radiation to be absorbed. The fact that light must be absorbed before a photochemical reaction can occur is an obvious but fundamental law of photochemistry. By knowing which groups absorb light energy and become electronically excited it is possible to identify which are the primary products in actinic deterioration. This leads to the establishment of the primary bond-breaking reactions and hopefully the connection between these and the loss of useful physical properties.

Inherently absorbing polymers such as poly (ethylene terephthalate) [PET], polycarbonates, etc. absorb enormous quantities of energy from sunlight. Absorption is confined to a thin surface layer (often (lum in thickness); the surface layer facing the light source effectively absorbs all of the damaging radiation and so protects the remainder of the polymer. Nevertheless, such polymers which have moderate to high crystallinity can fail mechanically when only the front surface layer is extensively photodegraded.

Let us consider the actinic deterioration of PET, as an example of an inherently absorbing polymer. The three primary products of PET photo-oxidation are CO, CO₂ and carboxylic acid end groups (3) and they are formed as a result of absorption by (electronic oxidation of) the ester carbonyl chromophore in each repeating unit of the polymer chains. These products can only be formed in bond-breaking reactions but the formation of only one of these - the COOH end groups - can be readily monitored. Since most of the actinic damage occurs in the "front" surface, internal reflection spectroscopy (surface IR) can be used to detect the onset of acid group formation. Since this has been shown (4) to correlate directly with mechanical failure, IRS allows for the early detection of relevant actinic deterioration and thereby minimizes the exposure time required to estimate the service life outdoors of PET materials.

The situation is somewhat more complicated in the case of polymers which have no inherent absorption at wavelengths $\rangle 290~\mu m$. They should be indefinitely resistant to sunlight and yet very few are, owing to the presence in them of UV absorbing impurities or substituents introduced during synthesis, processing or even storage. Common impurities include hydroperoxide, peroxide or carbonyl groups, catalyst residues, conjugated unsaturation, etc. The dominant chromophoric impurity in a "non-absorbing" polymer appears to depend on the complete history of the plastic or fiber sample. In the case of polypropylene, the relative importance of potential photo-initiation sources may be ranked (5) as follows:

OOH >Ti catalyst residues >C = 0

Thus, although both carbonyl groups and ketone groups dominate the actinic deterioration of polypropylene once it is well underway, the early stages are best identified by looking for the first sign of hydroperoxide group formation. Fortunately, IR spectroscopy can be used to detect this chromophore at levels below $10^{-3}\mathrm{M}$.

The photo-oxidation of polyolefins is primarily a surface phenomenon so that the IRS technique is particularly applicable. Crystalline polyolefins (polypropylene and high density polyethylene) suffer a drastic loss of physical properties when their surfaces have undergone actinic deterioration because they have medium to high crystallinity. This is not true of low density polyethylene, although its photochemistry is virtually the same, because it has low to negligible crystallinity.

OTHER TECHNIQUES

In any analytical problems, it is always preferable to utilize more than one technique for the detection of property changes. Notwithstanding the value of IR spectroscopy in identifying the early stages of actinic deterioration, therefore, other complementary techniques should be used whenever this is feasible. Since the value of materials in service rarely depends directly on their chemical characteristics, it is mandatory to use physical, mechanical, electrical, etc. property measurements as well as chemical determinations to identify the onset of deterioration.

It is common practice to monitor the tensile properties of polymeric materials as a function of the time of exposure to UV radiation. While it is difficult to make such measurements with accuracy, and although tensile property values depend in a very complex way on molecular morphology, nevertheless these measurements can be highly informative in the case of semicrystalline plastics and fibers, for two reasons. There is a connection between the surface photo-oxidation of polypropylene and PET, for example, and their tensile properties; the % elongation at break is sensitive to surface chemical changes even though the load-at-break is not. In fact, it has been shown for polypropylene (6) and for PET (7) that a fall-off in % elongation is detectable at least as soon as (if not before) changes in IR absorption in the early stages of UV degradation.

It does not appear that all polymers exhibit tensile property dependencies on photo-oxidation which are suitable for identifying the early stages of actinic deterioration. Conventional polystyrene, for example, is not considered to be a crystalline polymer and it does not behave physically like polypropylene or PET when its surface is degraded. Another technique, involving dielectric property measurements, has however been shown (8) to relate to the photo- and photo-oxidative degradation of polystyrene. There is no doubt that both the dielectric constants and the dissipation factors (tan &) of polystyrenes of different molecular weights increase with exposure of these polymers to UV light in air. Undoubtedly these effects will derive from the introduction of polar groups and polarizable entities into the non-polar plastic during actinic deterioration. More basic research on this dielectric technique would be required in order to establish to which other thermoplastics it is applicable.

Numerous other laboratory methods have been (or can be) used to monitor sensitively chemical, physical and other property changes in materials exposed to sunlight. It is well known that the discoloration of poly (phenylene oxide) and Nomex on exposure to UV light can be determined accurately and can be related to the extent of irradiation. Chemiluminescence and thermal susceptibility measurements are also relevant to some systems.

An understanding of the photochemistry of each macromolecular system is necessary for the prediction of its outdoor service life or for the implimentation of an appropriate stabilization package to prolong its use. This is not sufficient, however, and methodologies such as the ones described above are needed as well in order to meet the realities of modern materials research.

REFERENCES

- 1. A. S. Tweedie, M. T. Mitton and P. Z. Sturgeon, Text. Chem. Color. 3, 27-40 (1971).
- 2. J. D. Cooney and D. M. Wiles, Text. Res. J. 46, 342-346 (1976).
- 3. M. Day and D. M. Wiles, J. Appl. Polym. Sci. 16, 175-189; 191-202; 203-215 (1972).
- 4. P. Blais, M. Day and D. M. Wiles, J. Appl. Polym. Sci. 17, 1895-1907 (1973).
- D. J. Carlsson and D. M. Wiles, J. Macromol. Sci. Rev. Macromol. Chem. C14, 65-106 (1976).
- P. Blais, D. J. Carlsson and D. M. Wiles, J. Polym. Sci. A-1, 10, 1077-1092 (1972).
- 7. M. Day and D. M. Wiles, Can. Text. J. 89(6) 69-73 (1972).
- R. Greenwood and N. Weir, Amer. Chem. Soc. (Philadelphia, 1975) Coatings and Plastics Preprints 35, 184-189 (1975).

SESSION II: SEPARATION TECHNIQUES

Chairman: C. Bersch Naval Air Systems Command, U.S. Navy

REVIEW OF SEPARATION TECHNIQUES FOR POLYMERS G. I Magnauer, AMMRC

ERFORMANCE LIQUID CHROMATOGRAPHY
G. Fallick and J. Cazes, Waters Associates, Inc.

ANALYSIS OF POLYMER MATERIALS BY LIQUID CHROMATOGRAPHY AND INFRARED SPECTROSCOPY S. C. Pattacini and J. J. Stoveken, Perkin-Elmer Corp.

EFFECT OF ESTER IMPURITIES IN PMR-POLYIMIDE RESIN R. W. Lauver, NASA Lewis Research Center

THIN LAYER CHROMATOGRAPHY
C. A. May, Lockheed Missiles and Space Co.

USE OF SEPARATION METHODS FOR QUALITY ASSURANCE OF POLYMERIC MATERIALS C. D'Oyly-Watkins, MQAD, Woolwich, England

REVIEW OF SEPARATION TECHNIQUES FOR POLYMERS

Gary L. Hagnauer

Organic Materials Laboratory
Army Materials and Mechanics Research Center
Watertown, Massachusetts 02172

Materials which incorporate polymers generally are quite complex in their composition. In research and development, processing, quality control or quality assurance, it is often necessary to use or develop techniques for polymer separation to facilitate--

(i) separation from substances that are not high polymers (monomers, stabilizers,

plasticizers, fillers, etc.)

(ii) separation of soluble polymer from insoluble polymer (fluoropolymers, crosslinked polymers, microgel)

(iii) separation of chemically heterogeneous polymers (polymer blends, copolymers, polymeric impurities)

(iv) separation of structurally heterogeneous polymers (linear, branched, crosslinked, rings, stereo-isomers)

(v) separation of structurally homogeneous polymers fractionation.

Oftentimes low molecular weight components may be separated by evaporation, sublimation or solvent extraction techniques. If the polymer is soluble, extraction may be used or solids may be removed by filtration, centrifugation or sedimentation. Precipitation, crystallization and selective adsorption techniques may also be used. Insoluble polymers may be isolated by flotation, by phase changes with temperature, or by chemically modifying the polymer or other solids.

When confronted with the problem of separation, it is advisable first to use some qualitative or diagnostic method to determine the number of components and, if possible, to identify the components without actually isolating them. Depending on the system and degree of complexity, a host of spectroscopic, chromatographic and thermal analysis techniques are available. For quantitative analysis, more detailed knowledge of the system and some degree of prior separation is usually required. In preparative analysis the polymer is separated in such a way that reasonable amounts are available for characterization or special studies. Finally, macroscale separations may be required, for example, to remove contaminants, monomer or low molecular weight ends in manufacturing or to isolate polymer from waste materials for recycling.

Ultimately the technique or combination of techniques selected for separation depends on the nature of the polymer as well as the required extent of separation. Recent developments in thermal (mass) chromatography^{1,2} show promise for the separation and identification of the more volatile, low molecular weight components of polymer materials. Gel filtration, microfiltration and ultrafiltration techniques are being developed which show promise for the large-scale separation and concentration of polymers in solution.^{3,4} Thin layer chromatography (TLC) is a promising analytical technique for rapid separation of chemically and structurally heterogeneous polymers.⁵⁻⁷ Perhaps the most versatile, new technique for polymer separation is high performance liquid chromatography (HPLC). Recent technological advances in liquid chromatography to improve reliability, reduce operating time, enhance separating efficiency and increase sensitivity make HPLC an attractive analytical

and preparative technique. 8,9 The liquid-solid (adsorption) and liquid-liquid (partition) affinity modes separate molecules according to their chemical differences and are useful therefore for separating chemically heterogeneous and tactic polymers. The liquid or size exclusion (gel permeation chromatography GPC) mode separates molecules according to their size in solution and is excellent for separating the high molecular weight components from a mixture. For GPC the columns are packed with a porous substrate (crosslinked polystyrene or porous glass beads) selected not to adsorb the sample and with a pore size distribution to cover the size range of molecules to be separated. To isolate polymer from smaller sized molecules the column may be packed with substrate having an average pore diameter of about 10Å. In this case smaller molecules enter pores in the packing and therefore take a longer time to elute from the column(s) compared to polymer molecules which are excluded completely by their size from penetrating the packing. This separation technique is illustrated in Figure 1 for the separation of the polymer component (viscosity extender) present in a commercial hydraulic fluid. 10 The separation is quantitative and may be run on a preparative scale for polymer identification and characterization.

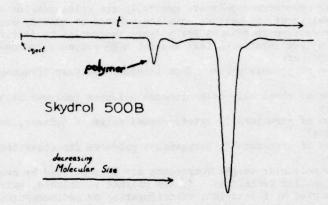


Fig. 1. Chromatogram of Skydrol 500B hydraulic fluid

In the strict sense, polymers are not chemically pure substances. They are molecular mixtures, generally consisting of long-chain, homologous molecules of various molecular weights, and are characterized by "average" molecular weights and the distribution of their molecular weights. Experimental techniques, such as end-group analysis, osmometry, light-scattering, ultracentrifugation and viscometry, measure different molecular weight averages which are important in polymer chemistry and can be related to certain polymer properties. For example, the number average molecular weight, $M_{\rm n}$ is defined

$$\bar{M}_{n} = \sum_{i} (n_{i}M_{i}) \sum_{i} n_{i} = \sum_{i} w_{i} / \sum_{i} (w_{i}/n_{i})$$
(1)

the weight-average molecular weight, $\bar{\mathbf{M}}_{\mathbf{W}}$, is

$$\bar{M}_{w} = \sum_{i} (w_{i}M_{i}) / \sum_{i} w_{i} = \sum_{i} (n_{i}M_{i}^{2}) / \sum_{i} (n_{i}M_{i})$$
 (2)

the z-average molecular weight, \bar{M}_z , is

$$\tilde{M}_{z} = \sum_{i} (z_{i}M_{i}) / \sum_{i} z_{i} = \sum_{i} (w_{i}M_{i}^{2}) / \sum_{i} (w_{i}M_{i})$$

$$= \sum_{i} (n_{i}M_{i}^{3}) / \sum_{i} (n_{i}M_{i}^{2})$$
(3)

and the viscosity-average molecular weight, $\bar{M}_{_{\boldsymbol{V}}}$, is

$$\bar{M}_{V} = \begin{bmatrix} \Sigma & (w_{i}M_{i}^{a})/\Sigma & w_{i} \end{bmatrix}^{1/a} = \begin{bmatrix} \Sigma (n_{i}M_{i}^{1+a})/\Sigma & (n_{i}M_{i}) \end{bmatrix}^{1/a}$$
(4)

where M_i is the molecular weight of polymer species \underline{i} , n_i and w_i are the number and mass of molecules of species \underline{i} , $z_i = w_i M_i$, and \underline{a} is the molecular weight exponent in the intrinsic viscosity [n] relation

$$[\eta] = KM^{a}$$
 (5)

The majority of technologically important polymers have relatively broad and unsymmetrical molecular weight distributions as shown in Figure 2.

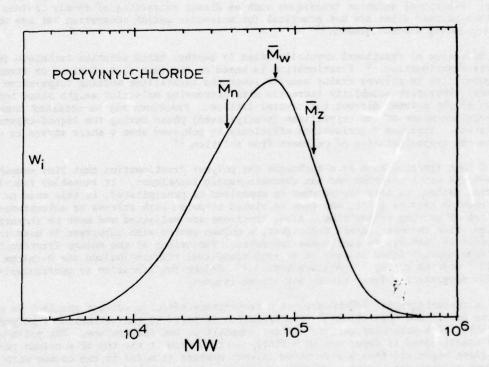


Fig. 2. Molecular weight distribution of polyvinylchloride, weight fraction W₁ versus molecular weight ($\bar{M}_n = 3.7 \times 10^4$, $\bar{M}_w = 7.5 \times 10^4$, $\bar{M}_z = 1.2 \times 10^5$).

As mentioned previously, some polymers are also polydisperse with respect to molecular structure (e.g., branching in low density polyethylene and tacticity in isotactic polypropylene) and chemical composition (e.g., monomer distribution in copolymers and segment size and distribution in block and graft copolymers).

FRACTIONATION

A number of different techniques both analytical and preparative have been developed to separate polymers on the basis of molecular weight. Polymer fractionation experiments usually are performed either to analyze the molecular weight distribution of a polymer or to prepare narrow distribution fractions for special property studies. No technique can assure complete separation of the polymer sample into monodisperse fractions. Rather, the purpose of fractionation is to narrow the molecular weight distribution and provide a wide range of molecular weight fractions.

Batch solution and chromatographic techniques are most widely used for polymer fractionation. 11-13 Batch solution methods include fractional precipitation and fractional solution which depend on the fact that solubility decreases with increasing molecular weight for polymers of the same composition. Separation is achieved by partitioning polymer molecules in two immiscible phases. In fractional precipitation the fractions are removed from the polymer-rich precipitated phase; while in fractional solution fractions are removed from the polymer-lean solution phase. In fractional precipitation the solvent power of the system is decreased stepwise by (i) addition of nonsolvent, (ii) elimination of solvent by evaporation, or (iii) lowering the solution temperature. In fractional solution a concentrated polymer solution phase (coacervate) formed by addition of nonsolvent is selectively extracted with a series of eluents of increasing solvent power and the polymer fractions are obtained from the dilute solution phase. Fractional solution techniques such as direct extraction of finely divided polymer and thin polymer films are not practical for molecular weight separation but are useful for separating stereo-isomers. 14

Selective or fractional crystallization is another batch solution technique for polymer fractionation. Fractionation is based on the fact that chemical or structural irregularities in polymer chains usually lower the crystalline melting temperature of the polymer. Therefore solubility increases with decreasing molecular weight since terminal groups of the polymer disrupt the crystal lattice. Fractions may be obtained from either the solution phase or the crystalline (precipitated) phase during the liquid-crystal phase separation. Improved fractionation efficiency is achieved when a shear stress is used to induce the crystallization of polymers from solution. 16

Column fractionation is a technique for polymer fractionation that lies somewhere between the batch solution and the chromatographic techniques. It resembles fractional solution methods in that the polymer is deposited or precipitated, in this case on a substrate of sand or glass, and then is eluted stepwise with solvent or solvent-nonsolvent mixtures of varying composition. Also, fractions are collected and must be characterized. However, like chromatographic techniques, a column packed with substrate is used and the technique is amenable to continuous operation. Variations of the column fractionation technique using a fixed solvent or solvent-nonsolvent mixture include the θ -column method 17 and the rising temperature method. Column fractionation is particularly useful for separating polymer blends and stereo-isomers.

In chromatographic fractionations a temperature and/or a solvent gradient is generally used to facilitate separation. 19 Fractionation is based on the variation of polymer solubility with molecular weight, solvent composition and temperature. The polymer sample to be fractionated is deposited in a finely divided form at the top of a column packed with glass beads and then a solvent-nonsolvent mixture is added to the column with a gradient of improving solvent quality as the experiment proceeds. Low molecular weight polymer is first to elute followed by higher molecular weight species. Experimental modifications include placing polymer-coated beads at the bottom of the column and reversing eluent flow, different designs for mixing devices to provide a solvent gradient, maintaining a temperature gradient between the top and bottom of the column, and fraction collecting devices. This technique is referred to as precipitation chromatography or the Baker-Williams method and may be scaled-up for preparatory fractionation.

In both analytical and preparative applications the aforementioned solubility techniques are being supplanted by liquid exclusion chromatography (GPC). 13,20,21 Also GPC is replacing standard techniques for molecular weight analysis, such as viscometry and osmometry. If properly interpreted, more reliable and precise results are obtainable by GPC in a shorter period of time than by other methods of determining molecular weight and molecular weight distribution.

Liquid-liquid, liquid-solid and thin layer chromatographic techniques were already mentioned for the separation of chemically and structurally heterogeneous polymers. Recently TLC has been successfully applied in determining the molecular weight distributions of polymers. By eluting samples with mixed solvents, good separation can be achieved over a limited molecular weight range. A precipitation mechanism is postulated to be the prime source of polymer fractionation in TLC.

Other methods which have been used to fractionate polymers and to evaluate their molecular weight distributions include zone-refining, 23 thermal diffusion, 24,25 isothermal diffusion, 26 foaming, 27 turbidimetric titration, 28,29 sedimentation velocity, 30-32 equilibrium sedimentation, 30-32 density gradient sedimentation, 31-32 electrospray mass spectroscopy, 33 laser light scattering, 34 rheology, 35 electron microscopy, 36,37 and ultrafiltration through membranes of different pore sizes. 38

GEL PERMEATION CHROMATOGRAPHY

Recent work in the Army's polyphosphazene R&D program demonstrates the versatility of GPC as a technique for polymer separation and characterization. The polymer exclusion mode is used to determine percent-polymerization at different reactions times t for the polydichlorophosphazene polymerization reaction (Figure 3) while changes in molecular weight distribution (Figure 4) are determined by analytical GPC.³⁹ In the synthesis of poly[bis(m-chlorophenoxy)phosphazene], analytical GPC is used to determine the product's molecular weight distribution (Figure 5a) and preparative GPC is used to fractionate the polymer (Figure 5b and 5c) for further characterization and property studies.⁴⁰ By combining GPC with light scattering and viscosity analysis more detailed information is obtained concerning polymer chain structure and polymer interactions. GPC is also used to investigate polymer chain degradation (Figure 6).⁴¹

Properly applied, GPC (liquid exclusion chromatography) is a powerful technique for polymer separation and characterization. Universal calibration, corrections for axial dispersion and on-line data handling techniques improve the accuracy of GPC. The technique is adaptable to automation and computer control, and recent advances in instrumentation (recycle, high pressure systems, pulseless flow, etc.) and column packings have resulted in smaller sample size, faster analysis and improved resolution. Differential refractometers and UV-visible monitors are most widely used in GPC to measure the relative amount of sample in the column effluent. However, many, perhaps more specialized, devices may be utilized as detectors not only for monitoring concentration but also for on-line characterization, e.g., variable wavelength UV-visible (Schoeffel Instrument Corp.) and infrared (Wilks Scientific) monitors, an intrinsic viscosity detector (Applied Research Lab.) and a laser low-angle light scattering molecular weight detector (Chromatix).

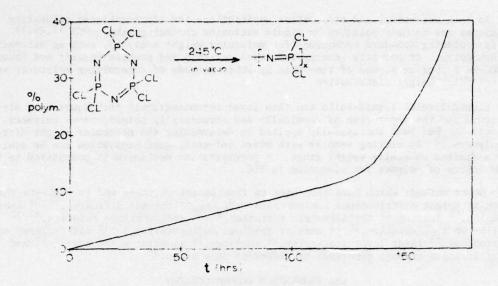


Fig. 3. Percent-polymerization versus polymerization time \underline{t} for the thermal bulk polymerization of polydichlorophosphazene.

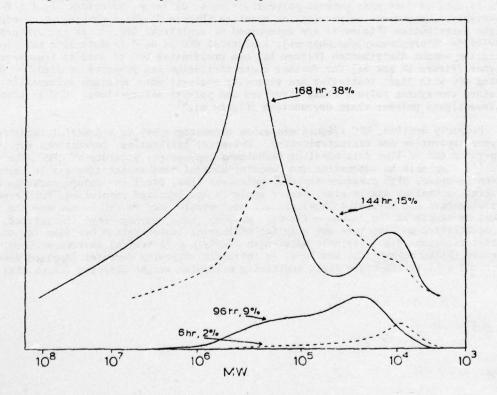


Fig. 4. Change in the molecular weight distribution with polymerization time and percent-polymerization for reaction shown in Figure 3.

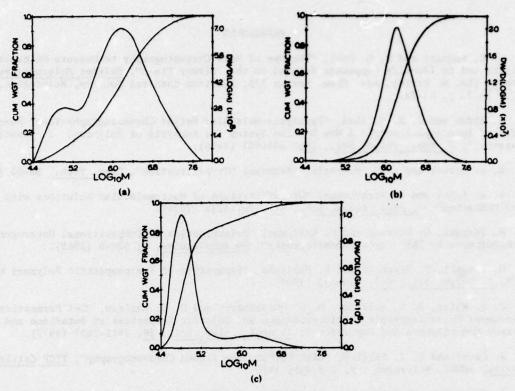


Fig. 5. Molecular weight distributions of unfractionated (a) and fractionated (b) and (c) poly[bis(m-chlorophenoxy)phosphazene].

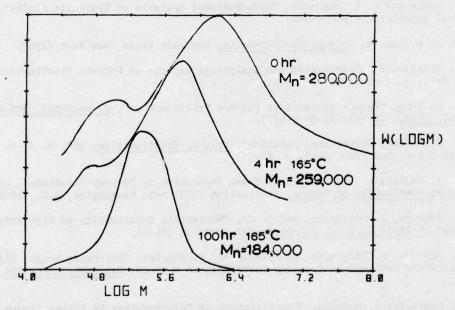


Fig. 6. Change in the molecular weight distribution of poly[bis(m-chlorophenoxy)phosphazene] upon heat-aging at 165°C in air.

REFERENCES

- 1. C. E. Bennett and D. G. Paul, "The Use of Mass Chromatography to Measure Molecular Weights and to Identify Compounds Related to the Polymer Field", Polymer Molecular Weight Methods (Ed. M. Ezrin), Adv. Chem. Series 125, American Chemical Society, Washington, D.C., 1973, p. 63-72.
- 2. E. Kiran and J. K. Gillham, "Pyrolysis-Molecular Weight Chromatography-Vapor-Phase Infrared Spectrophotometry: A New On-Line System for Analysis of Polymers. I. Instrumentation", J. Appl. Polym. Sci., 20, 931-947 (1976).
- 3. M. C. Porter and A. S. Michaels, "Membrane Ultrafiltration", Chem. Tech., 56-63 (1971).
- 4. R. W. Baker and H. Strathmann, "Ultrafiltration of Macromolecular Solutions with High-Flux Membranes", J. Appl. Polym. Sci., 14, 1197-1214 (1970).
- 5. H. Inagaki, H. Matsuda and F. Kamiyama, "Determination of Compositional Heterogeneity in Copolymers by Thin Layer Chromatography", Macromolecules, 1, 520-6 (1968).
- 6. H. Inagaki, T. Miyamoto and F. Kamiyama, "Separation of Stereospecific Polymers by TLC", J. Polym. Sci., B-7, 329-333 (1969).
- 7. J. L. White, D. G. Salladay, D. O. Quisenberry and D. L. Maclean, "Gel Permeation and Thin-Layer Chromatographic Characterization and Solution Properties of Butadiene and Styrene Homopolymers and Copolymers", J. Appl. Polym. Sci., 16, 2811-2827 (1972).
- 8. J. Cazes and G. J. Fallick, "High Performance Liquid Chromatography", TTCP Critical Review, AMMRC, Watertown, MA, 6-8 July 1976.
- 9. J. Stovenken, "Applications of Liquid Chromatography", TTCP Critical Review, AMMRC, Watertown, MA, 6-8 July 1976.
- 10. J. House and G. L. Hagnauer, "Compositional Analysis of Hydraulic Fluids", AMMRC Technical Report to be published.
- 11. M. J. R. Cantow, Polymer Fractionation, Academic Press, New York (1967).
- 12. R. Konigsveld, "Preparative and Analytical Aspects of Polymer Fractionation", Adv. Polym. Sci., 7, 1-69 (1970).
- 13. L. H. Tung, "Recent Advances in Polymer Fractionation", J. Macromol. Sci-Revs. Macromol. Chem., C6 (1), 51-84 (1971).
- 14. J. H. Elliot, "Fractional Solution", Polymer Fractionation, (Ed. M. J. R. Cantow), Academic Press, New York, 1967, p. 67-93.
- 15. A. J. Pennings, "Liquid-Crystal Phase Separation in Polymer Solutions", Characterization of Macromolecular Structure, Publication 1573, NAS, Washington, D.C., 1968, p. 214-244.
- 16. K. Yamaura, S. Matsuzawa, and Y. Go, "Mechanical Denaturation of High Folymers in Solution", Kolloid-Z. u. Z. Polymere, 240, 820-826 (1970).
- 17. H. Matsuda, M. Takeshima, S. Shimizu and S. Kuroiwa, 'Molecular Weight Distribution of Polystyrene Obtained by θ -column Fractionation Method', Makromol. Chem, 134, 309-311 (1970).
- 18. T. Ogawa and S. Hoshino, "Fractionation of Polypropylene by Rising Temperature Method", J. Appl. Polym. Sci., 17, 2235-2244 (1973).

- 19. R. S. Porter and J. F. Johnson, "Chromatographic Fractionation", Polymer Fractionation (Ed. M.J.R. Cantow), Academic Press, New York, 1967, p. 95-121.
- 20. K. H. Altgelt and J. C. Moore, "Gel Permeation Chromatography", Polymer Fractionation (Ed. M.J.R. Cantow), Academic Press, New York, 1967, p. 123-179.
- 21. A. C. Ouano, E. M. Barrall III, J. F. Johnson, "Gel Permeation Chromatography", Polymer Molecular Weights Part II (Ed. P. E. Slade., Jr.), Marcel Dekker, New York, 1975, p. 287-378.
- 22. E. P. Otocka, 'Thin-Layer Methods for Determining Molecular Weight Distribution', Molecular Weight Methods (Ed. M. Ezrin), Adv. Chem. Series 125, American Chemical Society, Washington, D. C. (1973) p. 55-62.
- 23. J. D. Loconti and J. W. Cahill, "Zone-Refining Fractionation of Polymers", <u>J. Polym. Sci.</u>, <u>A-1</u>, 3163-73 (1963).
- 24. D. L. Taylor, "An Evaluation of Column Thermal Diffusion as a Means of Polymer Characterization", J. Polym. Sci., A-2, 611-625 (1964).
- 25. A. H. Emery, Jr., "Thermal Diffusion", Polymer Fractionation (Ed. M.J.R. Cantow), Academic Press, New York, 1967, p. 181-90.
- 26. W. Burchard and H. J. Cantow, "Isothermal Diffusion", Polymer Fractionation (Ed. M.J.R. Cantow), Academic Press, New York 1967, p. 285-306.
- 27. K. Imai and M. Matsumoto, "Stereoregularity-Fractionation of Poly(vinyl alcohol) by Foaming", Bull. Chem. Soc. Japan, 36, 455-8 (1963).
- 28. H. Giesekus, 'Turbidimetric Titration', Polymer Fractionation (Ed. M.J.R. Cantow), Academic Press, New York, 1967, p. 191-249.
- 29. J. R. Urwin, "Molecular Weight Distributions by Turbidimetric Titration", <u>Light Scattering From Polymer Solutions</u> (Ed. M.B. Huglin), Academic Press, New York, 1972, p. 789-824.
- 30. J. W. Williams, Ultracentrifugation of Macromolecules, Academic Press, New York (1972).
- 31. H. W. McCormick, "Sedimentation", Polymer Fractionation (Ed. M.J.R. Cantow), Academic Press, New York, 1967, p. 251-84.
- 32. Th. G. Scholte, "Sedimentation Techniques", Polymer Molecular Weights Part II (Ed. P. E. Slade, Jr.) Marcel Dekker, New York, 1975, p. 501-89.
- 33. M. Dole, H. L. Cox, Jr. and J. Gieniec, "Electrospray Mass Spectroscopy", Polymer Molecular Weight Methods (Ed. M. Ezrin), Adv. Chem. Series 125, American Chemical Society, Washington, D.C., 1973, p. 73
- 34. B. Chu, Laser Light Scattering, Academic Press, New York, 1974, p. 228-36.
- 35. J. Schurz, "Rheological Methods", Polymer Fractionation (Ed. M.J.R. Cantow), Academic Press, New York, 1967, p. 317-39.
- 36. D. V. Quayle, "Molecular Weight Determinations of Polymers by Electron Microscopy", Brit. Polym. J., 1, 15-23 (1969).
- 37. W. K. R. Barnikol and G. V. Schulz, "Determining the Molecular Weight Distribution of Noncrystalline Polymers with Electron Microscopy", Makromol. Chem., 145, 299-308 (1971).

- 38. M. Hoffmann and M. Unbehend, 'New Fields of Application for Osmometry", Makromol. Chem., 88, 256-71 (1965).
- 39. G. L. Hagnauer, unpublished results.
- 40. G. L. Hagnauer, and B. R. LaLiberte, "Molecular Weight Distribution of Poly[bis(m-chlorophenoxy)phosphazene]", J. Polym. Sci., Phys., 14, 367-71 (1976).
- 41. G. L. Hagnauer and B. R. LaLiberte, "Poly[bis(m-chlorophenoxy)phosphazene]. Macromolecular Characterization and Degradation Studies", J. Appl. Polym. Sci., to be published in 1976.

HIGH PERFORMANCE LIQUID CHROMATOGRAPHY

Gary Fallick & Jack Cazes

Waters Associates, Inc. Milford, MA 01757

During the past decade, with gas chromatography established as a basic analytical technique, high speed liquid chromatography has begun to grow at a much more rapid rate. The reason for this is evident in Figure 2769, in which the useful ranges of molecular weights for gas and liquid chromatography are indicated. Gel Permeation chromatography, or size separation, is split out as a separate liquid chromatographic technique because of its much wider molecular weight range of utility. Overall, all modes of liquid chromatography offer a much greater range of applicability in terms of resolvable compounds than does gas chromatography. Furthermore, since GPC separations are based on differences in size of the molecule, a much wider molecular weight range can be dealt with than with the other modes of liquid chromatography which rely on chemical differences among the species being separated. Hence GPC is of particular interest to the polymer chemist and engineer. In Figure 2166, the various modes of liquid chromatography are summarized. This paper will include examples of GPC and some of the other modes of LC as applied to characterizing polymer additives and oligomers as well as the high polymer.

The scope of gel permeation chromatography is indicated in Figure 3403. The polymeric component in a complex mixture can be separated from some of the other lower molecular weight species, and these low MW additives further resolved from each other if they differ in size. Within the polymer itself, such as the polymer gum base in chewing gum, the various molecular sizes in the gun base can be separated and displayed as a continuous distribution by the GPC technique. Consequently, GPC is a method for approximating the average molecular weight of a polymer and also indicating its molecular weight distribution. This is significant since both of these factors effect the properties of the material. Among the properties which are influenced by molecular weight and/or molecular weight distribution are those listed in Figure 2308.

The significance of the molecular weight distribution is indicated by the curves in Figure 3107. It is a comparison of melt index versus tensile strength for three polymer samples which differ in molecular weight distribution, but have the same average molecular weight value. For the same melt index, the polymer with the broadest molecular weight distribution has the lowest tensile strength. This is explained by the higher fraction of very low molecular weight species which would be present in the broad distribution polymer. The low MW fraction would tend to weaken the material in tension. Alternatively, for a given tensile strength, the compound with the narrow molecular weight distribution has the highest melt index. In this case, there must be a higher proportion of high molecular weight material in the broad molecular weight sample in order to offset the weaker low molecular weight fraction and bring the tensile strength up. This higher molecular weight material will tend to thicken the resin melt viscosity and give it a lower melt index. Therefore, the narrow molecular weight distribution polymer will exhibit a higher melt index.

A more precise study of the influence of molecular weight distribution on rheological or mechanical properties is found in Figures 3135, 3134 and 3136. Many times attempts to predict polymer properties such as tensile strength from melt or solution viscosities are not successful. Solution and hot melt viscosities were plotted versus molecular weight and in each case it was found that there were two discrete curves produced, one in which the polymers had a rather narrow molecular weight distribution, dispersity about two, and the other where the materials had a much broader molecular weight distribution, with dispersities ranging from three to five. Dispersity is the ratio of weight average to number average molecular weight. In this case, tensile strength could not be correlated with either solution or melt viscosi y, because of the variation in molecular weight distribution between samples. If however, the peak molecular weight value is compared to tensile strength, a single correlation is established, indicating that the peak or average molecular weight value was a more reliable indicator of polymer properties, since the dispersity effect was eliminated. This demonstrates how the basic chromatogram can contribute to an effective interpretation of polymer properties better than some average value which can be influenced by MWD.

It is now appropriate to consider some actual examples of using the gel permeation chromatogram to understand various polymer related problems. These problems include defective powder coatings, selection of appropriate adhesives, fabricating a composite, evaluating the cause of an injection molding problem, and quality control of a lamination production.

One of the growing areas of surface finishing, is powder coatings, the solventless application of a polymer matrix coating to various objects. The mechanism involves fluidizing a powder, impinging it on a heated surface, where it melts and flows out to form the desired finish. A powder coating manufacturer experienced the problem of orange peel, or shark skin, an irregular rough surface instead of the desired high gloss surface. Only certain lots of the powder coating caused orange peel. Careful examination and testing of all the components in the powder coating failed to reveal the cause of this variation. Examination of the materials by gel permeation chromatography reveals, in Figure 3408, a significant difference between a satisfactory high surface gloss batch and a batch which exhibited orange peel. The orange peel coating tended to have polymer of higher molecular weight. The higher molecular weight material will tend to have higher melt viscosity. During the period in which this sample was heated and allowed to flow, before going into the cooling stage, the higher melt viscosity probably prevented complete flow out and surface leveling. Therefore, upon cooling the surface remained irregular, whereas the lower molecular weight material provided the desirable glossy surface.

In the production of wood composites such as plywood or particle board, phenolic and urea formaldehyde resins are used. The selection of these resins is critical to insure a high quality board at an economical price. In Figure 3444, an alternate source of phenolformaldehyde resin was compared to the standard glue in use. The alternate glue was less expensive, however, it lacked the level of high molecular weight material necessary to provide a strongly bonded product. This could also result in a lower viscosity. The fraction in the very left of the alternate resin chromatogram, the very high molecular weight material, was found to be a tackifier added to compensate for the lower viscosity. The alternate glue had to be cooked further with additional formaldehyde to bring it into the range where it would bond with sufficient strength and durability. A different problem in the same industry is indicated in Figure 3449. In this case, the urea formaldehyde resin which was used to produce particle board was found to vary in its curing characteristics from one batch to the next. Some bad batches remained tacky. The molecular weight distributions of these two resins, one with a good cure, the other with a bad cure, were quite similar as indicated by the lower trace, that of the refractive index monitor. However, there were some very distinct differences when this molecular weight distribution was also monitored with an ultra-violet monitor which selectively responds to the reactive end groups. It is apparent that the batch of resin which cured satisfactorily has a higher level of functionality and therefore has greater cure capability. This accounts for the satisfactory cure observed with this batch of material.

One of the largest engineering foam parts to date is a single shot of injection molded polycarbonate containing 3% glass nucleating agent. It weighs over 80 lbs. The manufacturer was experiencing severe problems in which some batches of molding compound failed to give parts with satisfactory surface uniformity and finishing qualities. Since all other machine and operator variables had been ruled out as the source of the problem, the molecular weight distribution of the polymer was suspected as a possible cause. Molecular weight distributions were measured for a number of batches. As indicated in Figure 3417 the profiles of the polymer were virtually identical. Subsequent calculation of the weight and number average molecular weights from these chromatograms showed again that the three batches of resins were extremely similar. It was unlikely that any small difference could be the cause of the poor surface finish in some batches. At this point, it was decided to examine the low molecular weight range of the material, since the foaming characteristics and the surface finish could certainly be dependent upon the additives present in this molding compound. As indicated in Figure 3418, there were some pronounced differences in the quantities of the various additives. Since the ratio of two or more additives can be a critical factor due the synergistic effect of additive combinations, the variation in additives which was determined suggests that the observed material variation was due to the shifting ratios of the additives in the formulation.

Another approach to evaluating polymer additives is indicated in Figure 3211. A Soxhlet extract of some polyethylene additives was evaluated. Identities of the specific peaks were assigned by running standards of materials known to be used as conventional polyolefin additives. It is clear that a small amount of the low molecular weight fraction of polymer was also extracted. The extraction was performed with cyclohexane. Apparently the extract was not taken completely to dryness before rediluting and injecting the sample into the liquid chromatograph, as indicated by the appearance of the cyclohexane peak at the very low end of the molecular weight range.

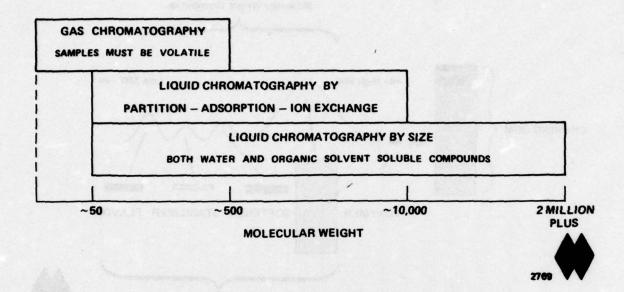
The IBM Corporation is a very large producer and user of printed circuit boards. In their printed circuit board manufacturing operation, they experienced considerable variations in board cure time and warpage which were ultimately traced to lot to lot variation in epoxy resins. It was possible to compensate for some of this variation by changing the cure cycle and temperature. However, it was most desirable to keep this process constant in order to maintain economical production rates. Within limits, some variation could be tolerated and compensated for by changing the amount of hardener used to cure the epoxy. Traditional methods of measuring epoxy resin reactivity such as epoxide or hydroxyl equivalents were not sufficiently sensitive. Using GPC enabled IBM to detect the extent of variation in the medium and high molecular weight range. For example, Resin A in Figure 3453 has much more area in the high molecular weight range and therefore, less hardener needs to be used. GPC also enabled IBM to determine the acceptable limit of the high and medium molecular weight range, beyond which the resin had to be rejected since it was outside the allowable range in which the curing agent could compensate. Once the resin had been approved, the appropriate level of hardener could be added to the resin according to extensive curing studies. In this case, dicyandiamide, as indicated in Figure 3409, was the hardener used. GPC is then used as a production control device to insure that dicyandiamide had been added and in the correct amount. This latter documentation is based on the height of the "dicy" peak.

More than one mode of liquid chromatography has been used to characterize epoxy resins. Figure 2638 shows a typical GPC chromatogram of Epon 828, a widely used liquid epoxy. It shows a characteristic profile without showing a great deal of detail. If desirable, it is appropriate to separate the Epon 828 components by an LC mode based on chemical differences rather than size. The oligomers are resolved clearly, as shown in Figure 2465. Similarly, in Figure 2454, a higher viscosity epoxy resin, Epon 1004 is separated by the chemical differences rather than size. Once again, much more detail is provided about the relative levels of each oligomer. The same technique can be used, Figure 2457, to look at some of the other impurities which are sometimes produced during the synthesis of the epoxy resin. These various impurities can also be separated, as can the basic starting material, Bisphenol A.

The foregoing examples depict a range of capabilities for separating polymers and additives. Often a higher level of resolution is necessary to establish or verify the purity of a specific component. Typical cases are materials such as liquid crystals which are most efficient in their highly purified form. One way of enhancing the ultimate level of separation in the test for purity is to increase the length of the column in the liquid chromatograph, where the separation actually takes place. Another technique, termed "recycle" accomplishes the same thing without the need to actually use additional lengths of column. Recycle effectively multiplies the column length without actually using more lengths of column. The way recycle is done is indicated in Figure 2295. The flow from the last detector in the liquid chromatograph is passed back into the pumping system and through entire system once again until complete resolution is obtained. An example of recycle is the purification of two, three-Dimethylnaphthalene shown in Figure 2727. After the first pass the material was not completely resolved, but it was clear that there were some minor components present, one partially resolved and the other probably present as suggested by the non-Gaussian shape of the main peak in the chromatogram. Additional passes through the system permitted the complete separation of impurities from the compound of interest by the fourth pass.

The gel permeation chromatogram can be used in a variety of ways to provide better insight into polymer related performance of the product. In addition, there are often various approaches to the same problem. Typical situations include the option of extracting an additive versus looking at it directly in the matrix, or separating oligomers, such as epoxy, by either size or chemical differences. While much of the discussions have referred to molecular weight distribution, the separation is actually based on size rather than true molecular weight. If it is desired to establish an absolute molecular weight a calibration procedure must be used. One other aspect is that the polymer must be in solution to be chromatographed. Therefore, this method is not applicable to fully cured resins unless the problem originates with residual extractable materials in the cured composite. Nonetheless, by working within this context all modes of liquid chromatography have proven to be extraordinarily versatile methods for both fundamental and applied polymer studies.

COMPARISON OF CHROMATOGRAPHY BY MW



MODES OF HIGH PRESSURE LIQUID CHROMATOGRAPHY

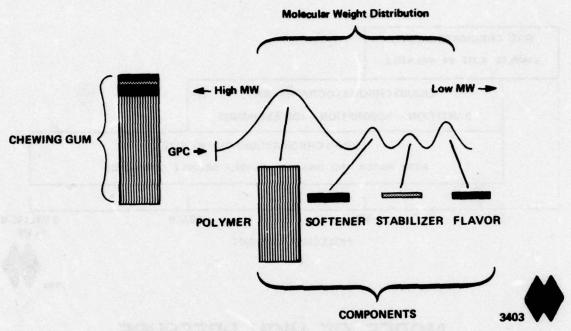
- LIQUID / SOLID ADSORPTION
- LIQUID / LIQUID PARTITION
- EXCLUSION SIZE
- ION EXCHANGE
- BONDED PHASES

PIC™ - PAIRED-ION CHROMATOGRAPHY



GEL PERMEATION CHROMATOGRAPHY

A Separation Technique for Testing Polymers



Shows how GPC can be used to investigate both polymer molecular weight distribution and lower molecular weight components.

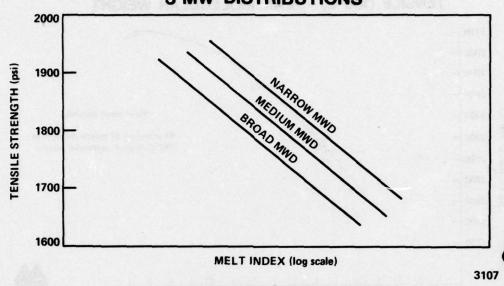
PROPERTIES CORRELATABLE TO MOLECULAR WEIGHT DISTRIBUTION

TENSILE STRENGTH
MODULUS OF ELASTICITY
(BEFORE CROSSLINKING)
RELAXATION TIMES OF
ELASTOMERS
MELT VISCOSITY
BRITTLENESS
HARDNESS
FLEX LIFE

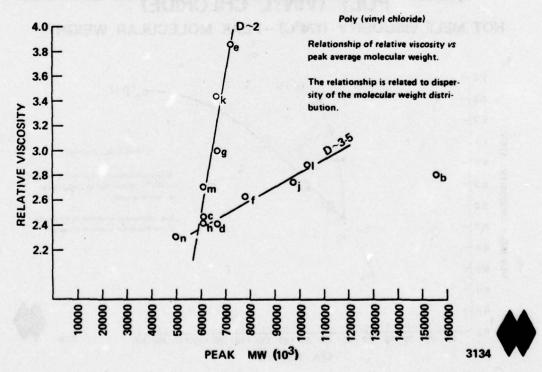
SOFTENING TEMPERATURE
ELONGATION AT TENSILE BREAK
IMPACT STRENGTH
TEAR STRENGTH
LOW TEMPERATURE TOUGHNESS
RESISTANCE TO ENVIRONMENTAL
STRESS CRACKING
DRAWABILITY
COEFFICIENT OF FRICTION



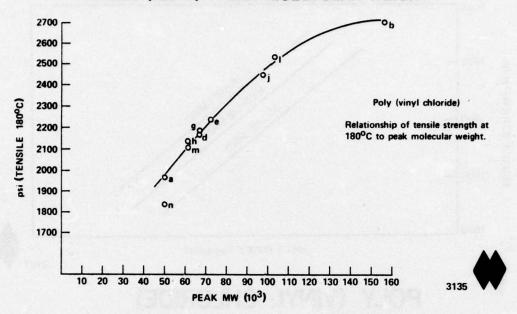
TENSILE STRENGTH VS MELT INDEX 3 MW DISTRIBUTIONS



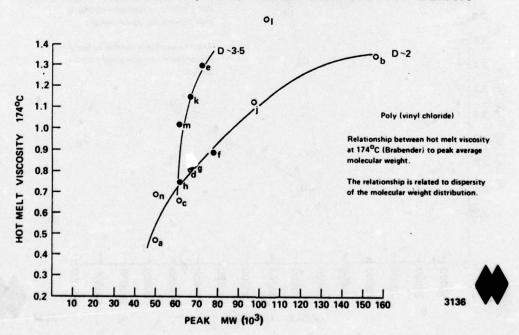
POLY (VINYL CHLORIDE) RELATIVE VISCOSITY - PEAK MOLECULAR WEIGHT



POLY (VINYL CHLORIDE) TENSILE (180°C) - PEAK MOLECULAR WEIGHT

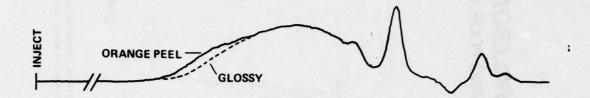


POLY (VINYL CHLORIDE) HOT MELT VISCOSITY (174°C) – PEAK MOLECULAR WEIGHT



POLYMER POWDER COATING

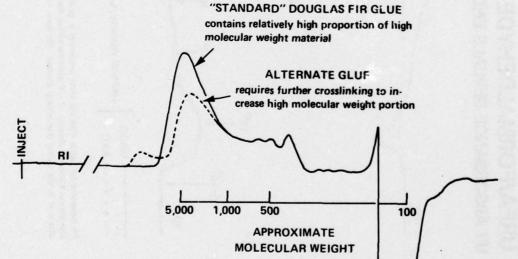
Orange peel vs. glossy batches



Distinguishing between satisfactory and unsatisfactory batches for powder coating.

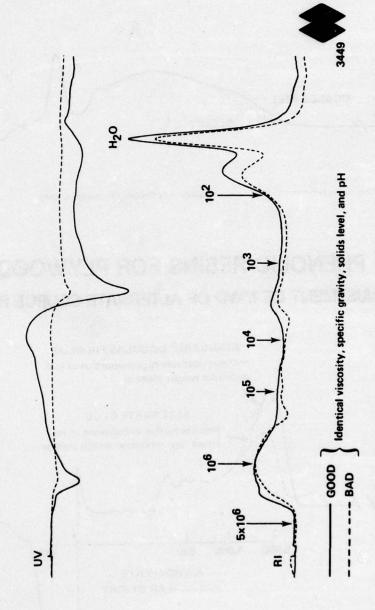


PHENOLIC RESINS FOR PLYWOOD ADJUSTMENT OF MWD OF ALTERNATE SOURCE RESIN



Afternate glue is cheaper and more readily available – however, it doesn't have as much high molecular weight as "Std". It can be made usable to replace "Std" if first "cooked" with additional formaldehyde to raise its molecular weight and make its distribution more like the "Std".

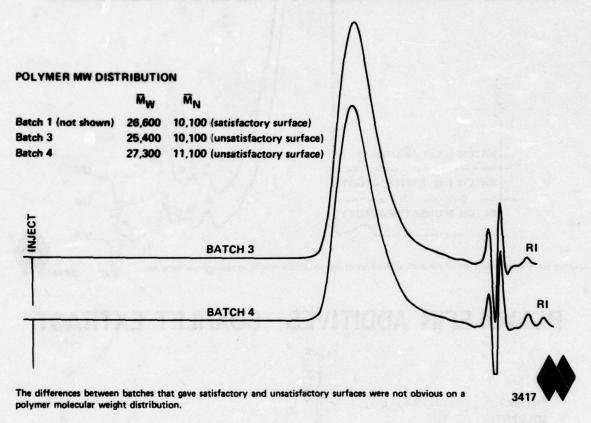
UV ABSORBANCE REVEALS END-GROUP DEFICIENCY GIVING POOR CURE UREA/FORMALDEHYDE RESINS FOR PARTICLEBOARD



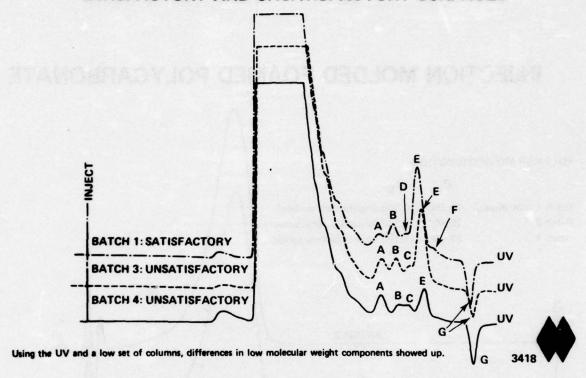
An experimental batch with the same properties as good materials by conventional testing, gave board which literally fell apart. The almost complete absence of UV absorbance for the bad one indicates that there are probably very few end groups that can take part in the curing (hardening) process. No cure, no bonds. It took days to scrape the mess up.

.

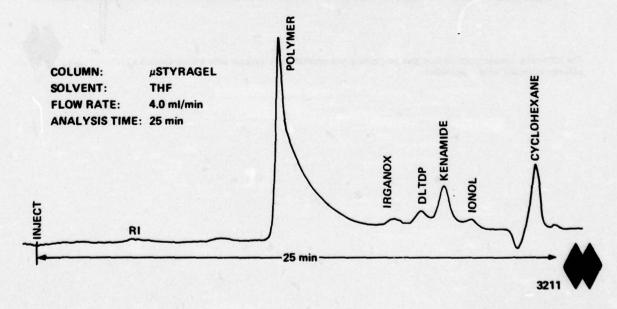
INJECTION MOLDED FOAMED POLYCARBONATE



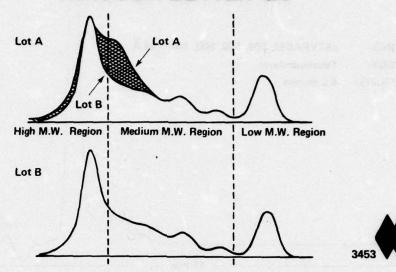
INJECTION MOLDED FOAMED POLYCARBONATE SATISFACTORY AND UNSATISFACTORY SURFACES



POLYOLEFIN ADDITIVES - SOXHLET EXTRACT

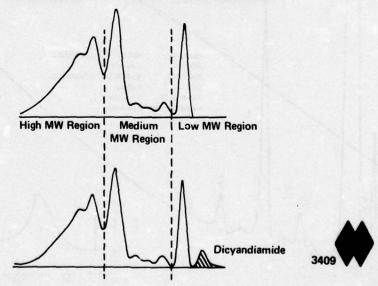


CUTTING REJECT RATES IN PC BOARD PRODUCTION THROUGH BETTER QC

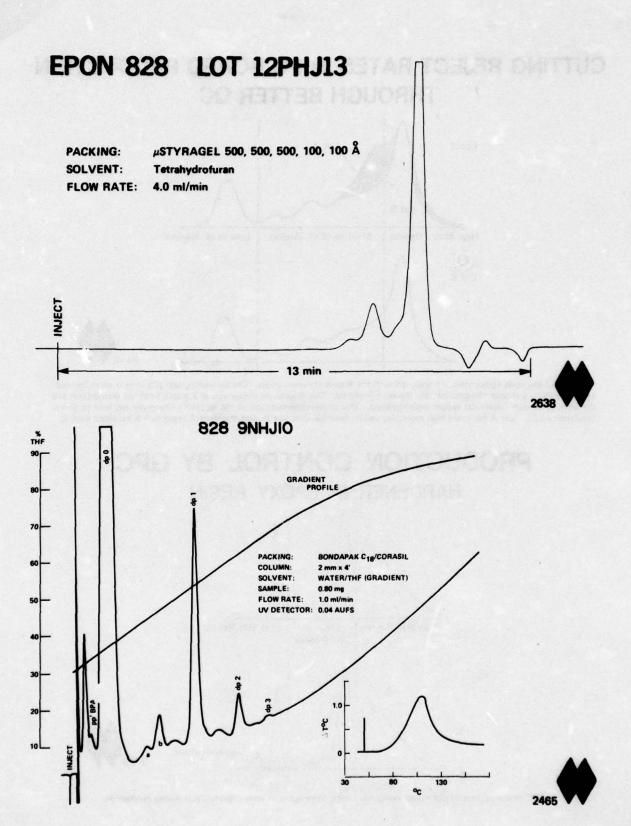


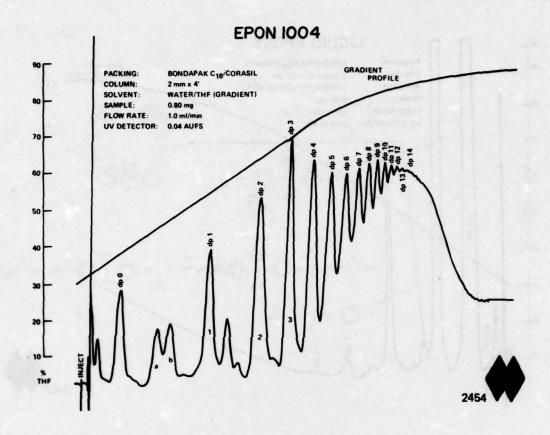
Two lots of the same epoxy resin are analyzed with the Waters chromatograph. The chromatograph produces a curve for each epoxy which is a unique "fingerprint" for the resin analyzed. This fingerprint shows you at a glance both the distribution and the amount of each molecular weight region present. This allows determination of the amount of hardener required to give a satisfactory cure. Lot A has more high molecular weight material than Lot B, and therefore A requires less hardener than B.

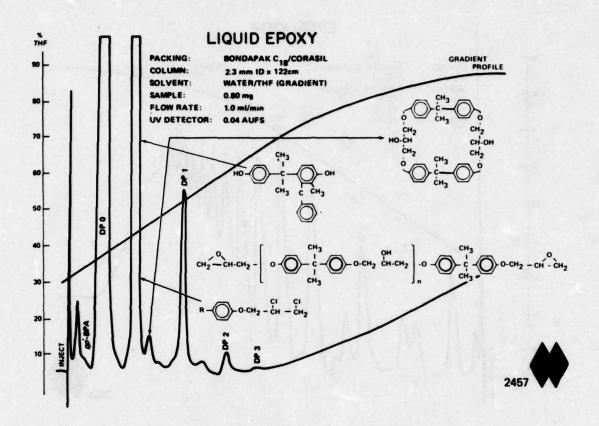
PRODUCTION CONTROL BY GPC HARDENER IN EPOXY RESIN



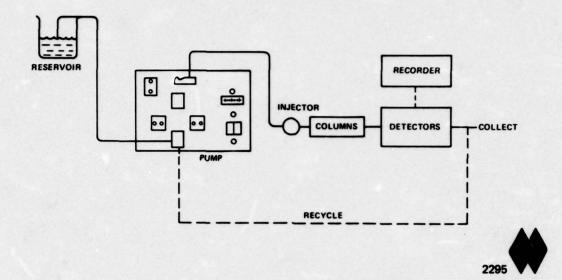
GPC shows up presence at a low molecular weight component in epoxy formulation during production.



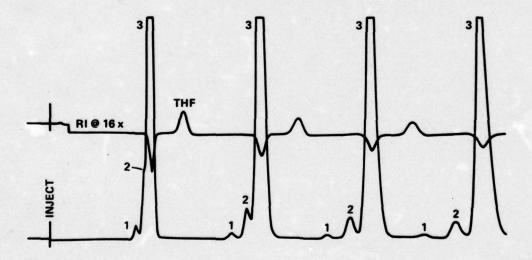




RECYCLE SCHEMATIC



RECYCLE FOR PURIFICATION ON µSTYRAGEL



- 1. IMPURITY
- 2. IMPURITY
- 3. 2,3-DIMETHYLNAPHTHALENE

COLUMN:

120 cm 100Å µSTYRAGEL

FLOW RATE:

2 ml/min

SOLVENT: SAMPLE: Dioxane 2,3-DIMETHYLNAPHTHALENE

DISOLVED IN THE



ANALYSIS OF POLYMER MATERIALS BY LIQUID CHROMATOGRAPHY AND INFRARED SPECTROSCOPY

Silvio C. Pattacini and John J. Stoveken

The Perkin-Elmer Corporation Norwalk, Connecticut 06856

INTRODUCTION

The combination of liquid chromatography (LC) and IR spectroscopy provides a powerful tool for analyzing the composition of polymer mixtures to detect batch-to-batch differences caused during formulation, or changes produced by environmental effects. In this preliminary study, we have used both the normal-phase and reverse-phase modes of LC to separate both polystyrene and epoxy polymer materials. IR spectroscopy was then used to identify some of the separated compounds. The IR spectra were run after the eluted peaks were collected, deposited onto a micro internal reflection plate and mounted in the IR spectrometer (1).

It is important to note that with this approach, the material obtained from analytical LC columns is sufficient to obtain high-quality IR spectra of the separated compounds.

CHROMATOGRAPHY

Gel Permeation Chromatography (GPC) is the traditional chromatographic technique for the analysis of polymeric materials. It is characteristic of this technique that any separation of sample components present is performed solely on the basis of molecular size. Thus, if the differences in molecular size are not great enough, then little or no separation will be achieved. This potential limitation of GPC is illustrated by the GPC analysis of a polystyrene broad range Molecular Weight Standard, NBS-706, shown in figure 1. The first peak represents the polymeric material having an average molecular weight of 254,000. The second peak contains any low molecular weight polystyrene oligomers or imputities. Utilizing the precise flow-rate delivery of a syringe pumping system and electronic data handling, a GPC system and electronic data handling, a GPC system can determine molecular weight and number averages to better than 1% precision (2), but will provide little information on low molecular weight compounds due to the lack of selectivity in size systems.

We found that we could separate polystyrene oligomers on an adsorption chromatographic system and we developed a separation for polystyrene materials up to a molecular weight of two million. Figure 2 illustrates a gradient run where the low molecular weight oligomers elute early in the run (separated), followed by increasing molecular weight material up to 2,000,000 molecular weight which elutes at the end of the run.

If we run the same NBS-706 standard on a similar system (Figure 3), we see that the adsorption technique is much more selective for the low molecular weight materials than is the GPC system shown in (Figure 1). In this run, the polymeric material is the last major peak in the run. The first major component is tentatively identified as a silicone oil

residue from the extrusion process and the following series of peaks appear to represent a series of polystyrene oligomers that are present in this high molecular weight standard.

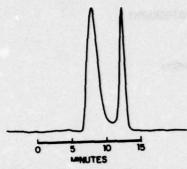


Fig. 1. GPC chromatogram of NBS-706, a broad molecular weight standard, performed on a Vit-X porous glass column set.

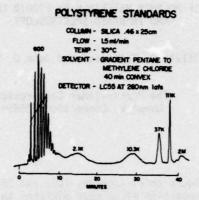


Fig. 2. Gradient separation of polystyrene standards from the individual oligomers to the high molecular weight polymer.

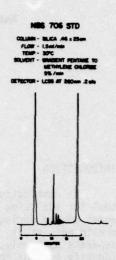
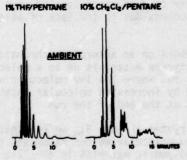


Fig. 3. Gradient separation of NBS 706 showing a non-polar impurity, polystyrene oligomers and the 254,000 MW polymer.

Other potentials of the chromatographic system are illustrated in (Figure 4) for the normal-phase separations of polystyrene 600. The first run shows a separation of the individual oligomers. The second run illustrates the power of this approach in which with only slight change of conditions, we can begin to separate the isomers of each of these low molecular weight oligomers.

SAMPLE: POLYSTYRENE 600
COLUMN: 25 x Q,46cm SQLYENT
PACKING: 5µm SILICA
FLOW: 2mi/min



Chromatogram of polystyrene oligomers illustrating the isomeric separation that is possible under these conditions.

Figure 5 shows a separation of an epoxy resin on a very efficient GPC column that is manufactured in Japan. Here the separation is by molecular size only, with the largest molecules eluting first followed by components in order of decreasing molecular size.

Figure 6 shows the results when this same sample is separated on an adsorption system in which the separation is based on chemical characteristics and not only size. Now the previous 8 peak analysis is shown to contain many more compounds than were evident in the previous analysis, demonstrating the superior selectivity of adsorption chromatography over GPC.

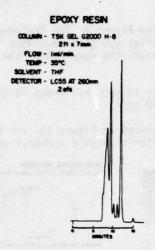


Fig. 5. A high resolution size separation of a commercial epoxy resin.

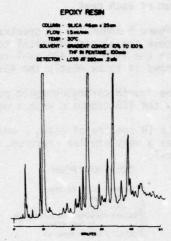
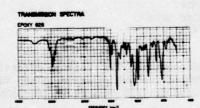


Fig. 6. A chromatographic separation of the same sample run in Fig. 5 showing the increased separating power of the adsorption chromatographic technique.

INFRARED SPECTROSCOPY AND LC

Most of our work has involved the separation and attempts at identification by IR of epoxy precure resins.

We have studied a commercially important epoxy resin, 1009 from 3M Corporation. It is composed of two materials and a catalyst which triggers the curing when the mixture is raised to about 160° C. About 65% of the mixture is a 438 epoxy Novalac, 32% is an 828 Epon and the catalyst present at 3%, is mono ethyl amine-BF3. The IR spectra of the 438 and 828 materials were recorded as smears on a KBr window as shown in Figure 7.



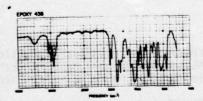


Fig. 7. Infrared spectra of the Epon 828 and DEN 438 used to formulate the 1009 epoxy resin.

The features that are particularly characteristic in comparing the 828 epon with the epoxy Novalac 438 material are the weak, sharp bands in the 1400 and 1100 cm-1 region and by the relative intensities of the 1030, 910 and 830 cm-1 bands. Note in the epoxy Novalac 438 spectrum, the similar intensity of the 1030, 910 and 839 cm-1 bands, the strong band at 1450 cm-1 and the broad band at 1110 cm-1.

The adsorption chromatogram of the 1009 material (Figure 8) shows the early strong peaks correspond to the two principal components of the mixture as evidenced by the IR spectrum of each peak.

Figure 9 shows the IR spectra of peaks 1, 2 and 4 from Figure 8. The features of the first peak are almost identical to the reference 828 material you just saw. Note the bands in the 1100 and 1400 cm-1 region for example. Likewise, the spectrum of the second peak shows it to be mostly the 438 epoxy Novalac.

The fourth chromatographic peak was collected and its IR spectrum shows it to be largely the 438 compound with a weak carbonyl band at 1730 cm^{-1} .

The IR spectra of peaks 5 and 7 in Figure 8 are presented in Figure 10. The fifth peak has a very similar spectrum, again mostly the 438 material with a carbonyl peak 1735 cm-1.

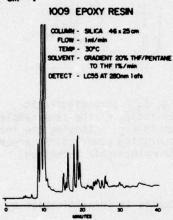


Fig. 8. Gradient chromatogram of the 1009 resin showing two major components (peaks 1 & 2) followed by several smaller components that were collected for infrared analysis.

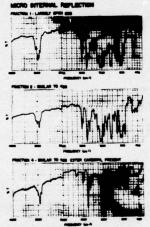


Fig. 9. Micro internal reflection infrared spectra of the two major components (identified as the Epon 828 and DEN 438 respectively) and one of the minor components whose separation was illustrated in Fig. 8.

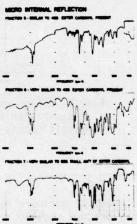


Fig. 10. MIR infrared spectra of three minor components of the 1009 resin.

Fraction six is virtually identical to the 438 spectrum. The relative intensities of the 760 and the 835 cm-1 bands suggest a lower aromatic content relative to the 438 starting material. Note again, the carbonyl ester band at 1735 cm-1 as in fraction 5.

Finally, the seventh peak has the characteristics of 828 Epon precursor. The 1110 cm⁻¹ structure variation may be associated with a phenolic ester group.

We obtained two different sample batches of the 1009-26 resin. These were known to

have some very subtle differences that were due to variations in formulation or due to differing environmental factors during storage.

We then ran these samples on a reverse-phase chromatographic system that has different selectivities than the previous system. By monitoring at 290 nm (an absorbance maximum for the material), we found little difference between the two batches. However, by changing the detector wavelength of 300 nm where we are not sensitive to the epoxy materials, we found some dramatic differences in small components that did absorb at 300 nm. This batch has much more of these materials that are present in the second sun exposed resin.

The pair of peaks that were eluting at the 16.5 minute point in Figure 11 were collected and subjected to IR analysis. As can be seen in the chromatographic comparison, the second component is present in a much higher quantity in the first resin batch than in the sun exposed batch (Figure 12).

The IR spectra of the first peak proves it to be closely related to the 438 material, while the second peak contains some 438 contaminates and some very strong bands that have not been seen in earlier spectra. Please note the very strong carbonyl doublet at 1720, the bands at 1110 and the very sharp band in the vicinity of 700 cm-l in Figure 13.

1009 EPOXY

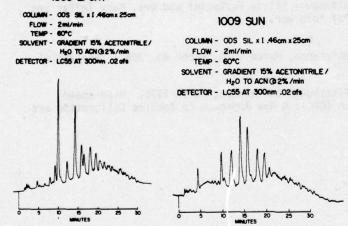


Fig. 11 and 12. Reverse-phase gradient chromatograms of two different batches of the 1009 resin material illustrating differences due either to formulation or storage variation.

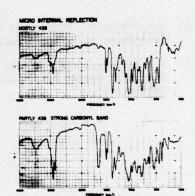


Fig. 13. MIR infrared spectra of the doublet shown at the 16.5 minute in Fig. 12. The second peak, barely evident in Fig. 11, produces a strong carbonyl band (1750 cm-1) and several additional bands (700 cm-1).

APPLICATION

This technique has now provided information on a trace contaminate that would not be available from any other method. The LC has fractionated the epoxy into its varied components and thus, has allowed us to visualize differences between two samples. The IR, particularly when coupled with the computer subtraction techniques, will provide a great deal of structural information that will allow the operator to identify any compound present in the mix.

Time does not permit discussion of the chromatographic or IR conditions used for these analyses - this information is available upon request (LCAS-61). We used the Model 601 LC and new columns whose superiority we believe permitted us to resolve the fractions we have shown. Our IR work utilized the Model 283 microprocessor IR spectrophotometer. The procedure used to prepare the LC fractions for IR have been described in a recent article in our Chromatography Newsletter Vol. 4, No. 1, which is also available upon request. Each LC fraction required less than 15 mins. to prepare for the IR and much of this time is just waiting time. The procedure is simple and rapid.

To summarize, we have developed a highly sensitive and selective technique involving both LC and IR for the analysis and routine quality assurance of a wide variety of polymeric materials. The liquid chromatograph in the adsorption or reverse-phase modes (not the GPC mode), can provide precise separation and quantitation for a wide variety of materials that may be present, including the polymer precursors, oligomers, isomers of the oligomers and additives that are present in the blend. Samples from the LC can then be analyzed by IR spectroscopy to identify the major components and any impurities or unknowns to produce an extremely powerful analytical technique.

I want to thank Drs. Bob Sacher, Jim Sprouse and Bernie Halpin at the Watertown Arsenal for samples and helpful discussions on this work. I also want to acknowledge the help and cooperation of my colleagues Silvio Pattacini and Drs. Mary Zeller and Robert Hannah for the IR portion of this work.

- S.C.Pattacini, Pittsburgh Conference, March 1975, Paper No. 365 'Analytical Techniques in IR Spectroscopy'.
- (2) W.M.MacLean and A.F.Poile, Pittsburgh Conference, March 1975. 'High-Speed Molecular Weight Distribution (GPC); A New Approach to Routine Calibration and Resolution'.

EFFECT OF ESTER IMPURITIES IN PMR-POLYIMIDE RESIN

by Richard W. Lauver

Lewis Research Center Cleveland, Ohio 44135

ABSTRACT

Spectral and chromatographic studies were conducted which established the presence of tri- and tetraester impurities in aged monomer solutions employed in fabrication of PMR-polyimide resin composites. The equilibrium constant and apparent rate of the esterification were determined. It was demonstrated, using differential scanning calorimetry, that the ortho-ester moiety of these impurities does not completely react at typical cure conditions. It is concluded that voids formed in composites fabricated with aged monomer solution are due to gaseous decomposition products evolved by ester impurities and/or unreacted amine during elevated temperature post-cure treatment.

185

INTRODUCTION

The purpose of this investigation was to identify the factors responsible for void formation in PMR-polyimide resin composites fabricated with aged monomer solutions. The high temperature resistant, addition-type, polyimide resin system (designated PMR) developed at Lewis Research Center (Ref. 1) was found to exhibit excellent fabrication characteristics for making low void, high performance composite materials. However, problems appeared during a program (Ref. 2) to develop fabrication technology for a composite fan blade employing the PMR resin. Non-reproducible properties (mechanical strength and thermal stability) due to void formation were observed after elevated temperature postcure treatment (up to 16 hours at 344° C) of the composites.

The in situ PMR approach for synthesis of thermally stable polyimides employs three monomeric reactants (Fig. 1): monomethylester of 5-norbornene-2, 3-dicarboxylic acid (NE), 4, 4'-methylenedianiline (MDA), and dimethylester of 3, 3', 4, 4'-benzophenonetetracarboxylic acid (BTDE). The reaction is postulated to follow the path indicated in Fig. 1. Initially, short chain polyamide-acids are formed on the reinforcing fibers; subsequently, water is eliminated to form the desired polyimide structure. Final curing occurs by addition polymerization of

$$2\left[\left(\begin{array}{c} \begin{array}{c} 0 \\ c \\ - \text{OCH} \end{array}\right) + (n+1) \left[\begin{array}{c} H_{2}N - \bigcirc & 0 \\ - C \\ - C \\ - C \end{array}\right] + \left[\begin{array}{c} 0 \\ - C \\ - C \\ - C \end{array}\right] + \left[\begin{array}{c} 0 \\ - C \\ - C \\ - C \\ - C \end{array}\right] + \left[\begin{array}{c} 0 \\ - C \end{array}\right] + \left[\begin{array}{c} 0 \\ - C \end{array}\right] + \left[\begin{array}{c} 0 \\ - C \end{array}\right] + \left[\begin{array}{c} 0 \\ - C \end{array}\right] + \left[\begin{array}{c} 0 \\ - C \\$$

Figure 1. - Reaction sequence for PMR-polyimide resin.

the norbornenyl endcaps to form the crosslinked structure. The ideal time/temperature/pressure sequence for curing the resin is predicated on completion of the condensation reactions to form the imide prior to the final addition crosslinking. This permits the evolution of condensation products (methanol and water) before the viscosity of the resin greatly increases due to formation of the crosslinked network.

The PMR resin is employed as a high-solids content methanol solution of the monomers. Because both MDA and NE can be commercially obtained as well characterized solids, they can be introduced into the resin reproducibly. In earlier studies (Refs. 1, 3) employing the resin, the BTDE was isolated as a solid. However, the difficulties with isolating the isomer mixture in large quantities led to the direct use of methanol solutions of the monomer for preparation of the resin. The preparation or purchase of bulk quantities of BTDE/methanol solution led in turn to more extended periods of storage prior to use. It was ultimately observed (Ref. 2) that the presence of voids in post-cured composite samples could be correlated with the use of aged BTDE solutions, and this prompted the more detailed study of the PMR resin system described in this report.

EXPERIMENTAL

Reagents. - The monomethylester of 5-norbornene-2, 3-dicarboxylic acid (NE), melting point 97 to 100° C, the 3, 3', 4, 4'-benzophenonetetra-carboxylic dianhydride (BTDA), melting point 215 to 217° C, and the 4, 4'-methylenedianiline (MDA), melting point 90 to 91° C, were commercially available materials used without further purification. Anhydrous, electronic grade methanol was employed. The tetramethylester of 3, 3', 4, 4'-benzophenonetetracarboxylic acid (BTTE), melting point 93 to 94° C, was prepared by refluxing BTDA in methanol for two hours, then bubbling dry HCl through the solution for one hour to force the reaction to completion. The methanol was removed at reduced pressure and the product recrystallized in heptane/ethyl acetate (2:1).

Monomer solutions. - The solutions employed in this study were selected from bulk working solutions prepared for use in composite fabrication. These solutions were, with one exception, prepared by refluxing BTDA in methanol for approximately two hours. The solutions were formulated to give 50 weight percent BTDE at the end of the reaction. Samples were stored at ambient conditions in closed plastic containers (loss of methanol during extended periods of storage appeared minimal). The unique sample was commercially prepared and was 85 weight percent BTDE in methanol.

Instrumental measurements. - Nuclear magnetic resonance spectral were obtained on a commercial, 60 MHz, continuous wave instrument. Data were referenced to internal tetramethylsilane. Sample solutions were diluted approximately four fold with deutero-chloroform for the measurements. Due to the high methanol concentration, the spectral exhibited some inconsistencies in chemical shift. All data was electronically integrated. Solutions of thermally reacted binary mixtures of monomers were prepared in perdeuterodimethylsulfoxide (DMSO).

High pressure liquid chromatography was performed on a microparticulate reverse phase column (column: 2.2 mm × 25 cm; packing: bonded hydrocarbon on 10 micron silica). Constant volume syringe pumps were employed at 150 ml/hr. Spectrophotometric detection was employed at 254 nm wavelength with a sensitivity of 0.5 absorbance units full scale. Sample solutions were diluted approximately forty fold with methanol and injections of about 1 microliter were made using the stop/flow technique. Composition of the solvent was varied continuously from 100 percent water to 100 percent methanol. The gradient program was: 100 percent water for one minute; addition of methanol at 5 percent per minute for two minutes; and, addition of methanol at 10 percent per minute for nine minutes.

Differential scanning calorimetry (DSC) was performed on a commercial thermal analysis unit employing a high pressure DSC attachment. Sample size was approximately 5 mg. Aluminum sample pans were employed; the pans were covered, but not crimped closed. A heating rate of 10° C per minute was used for all runs. A static pressure of approximately 3.8×10^{5} N/m² (55 psi) of dry nitrogen was maintained over the sample.

Infrared spectral measurements were made on a commercial, double-beam spectrometer. PMR resin was cast as a film on a NaCl salt plate for spectral monitoring. The plate was placed in an air circulating oven at 204° C and removed intermittently for spectral measurements.

RESULTS AND DISCUSSION

Analysis of Ester Impurities

Solutions of the monomer BTDE are formed by reacting the dianhy-dride, BTDA, in methanol as shown in the first step of Fig. 2. It was generally assumed that only the first step of the reaction sequence shown in Fig. 2 was of significance because the rate of additional esterification

Figure 2. - Reaction sequence for esterification of 3, 3', 4, 4'-benzophenonetetracarboxylic dianhydride.

is slow. While this assumption may be reasonable for short times, the presence of the higher ester impurities (tri- and tetraester) in a BTDE solution (85 weight percent) aged for 19 months is demonstrated by the liquid chromatogram shown in Fig. 3. The reverse phase separation adequately resolved the three major chemical constituents in the solution. The principal component, the diester, elutes very quickly; two partially resolved peaks due to the isomers of the triester elute after approximately 6 minutes; and, the tetraester elutes last. The elution times for the di- and tetraesters were verified by direct comparison with chromatograms of the pure components. The triester was not isolated, but the assignment is based on: (1) elution time - this component should be bracketed by the di- and tetraesters because of the relative number of polar groups in this series; and (2) relative intensity of the elution peak - assuming similar extinction coefficients for the tri- and tetraesters, there should be (statistically) twice as much tri- as tetraester. Because the

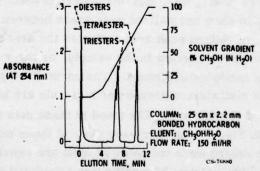


Figure 3. - Liquid chromatogram and elution gradient for an aged BTDE solution (85 weight percent; aged 19 months).

triester was not isolated, its extinction coefficient was not determined and the liquid chromatography data was not analyzed quantitatively. At the experimental conditions employed for these measurements, no higher ester impurity was observed in BTDE solutions which had been aged for one month.

The nuclear magnetic resonance spectra provided a more convenient basis for documenting quantitatively the formation of the higher esters with time. The general features of the spectra were: (1) a complex multiplet due to the phenyl protons of the substituted benzophenone compounds centered near 8 ppm; (2) a broad singlet exhibiting variable chemical shift (5 to 7 ppm) due to the labile protons (ROH, H₂O); (3) a sharp multiplet at 4 ppm due to the methylester protons; and (4) a sharp singlet at 3.3 ppm due to the methyl protons of methanol. The aged solutions did show additional peaks in both the phenyl and the methylester multiplets although, qualitatively, the spectra did not change dramatically because of peak overlap.

Shown in Fig. 4 is a comparison of the spectra for the pure diester (Fig. 4(a)) and an aged BTDE solution (Fig. 4(b)). Neither the phenyl multiplet nor the methylester multiplet was completely resolved at the experimental conditions employed. This did not prevent quantitative analysis of the data, however, because the total integrated peak areas for each multiplet provided sufficient information to determine the equilibrium constant and apparent rate of the esterification. The expected trend in total peak area for the multiplets can be seen in the integral curves shown in Fig. 4. When the areas are normalized to 6 for the phenyl multiplet (six protons on each substituted benzophenone), we see (Fig. 4(a)) that the peak area of the methylester multiplet for the pure diester is 6 (as expected for six protons on the two ester groups). For the pure tetraester, the area would be 12 (expected for four methylester groups). Necessarily, the triester or mixtures of di-, tri-, and tetraesters present in an aged BTDE solution would show normalized peak areas between 6 and 12 (Fig. 4(b)). The normalized peak area indicates the average number of methylester protons per molecule in the sample, or three times the average number of methylester groups. The normalized peak areas and average number of methylester groups per molecule are given in Table I for five solutions of varying age. The trend in these data can be better seen graphically in Fig. 5. Again we see that, at these experimental conditions, higher esters were not detected until one month of storage time had elapsed. The point at 21 months was calculated from the

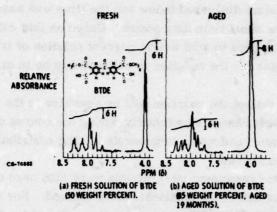


Figure 4. - Nuclear magnetic resonance spectra of phenyl protons (near 8 ppm) and methylester protons (near 4 ppm) with peak integrals.

TABLE I. - NORMALIZED NMR PEAK AREAS AND CALCULATED NUMBER OF ESTER GROUPS FOR AGED BTDE SOLUTIONS

Storage time (months)		nalized k area	Average number of methylester groups per molecule	
	H(phenyl)	H(methyl- ester)		
0	6	6	2.0	
1	6	~6	2.0	
2	6	6.3	2.1	
3.5	6	6.6	2.2	
6	6	7.2	2.4	

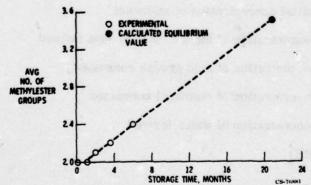


Figure 5. - Increase in number of methylester groups per molecule during storage of 50 weight percent solutions of 87DE.

equilibrium constant discussed below and the time was assigned by extrapolation of the short time data points. Based on this calculated endpoint for esterification in a 50 weight percent solution of BTDE, the apparent half-time for the reaction is estimated to be in excess of eleven months.

The actual rate of the reaction will be sensitive to the pH of the solution, and this must change significantly during the course of the reaction as acid is consumed and water is generated. The contribution of this factor was not examined.

The magnetic resonance integral data were also used to calculate actual concentrations of the additional ester formed. For the oldest solution tested (the 85 weight percent solution, stored for 19 months), it was assumed that equilibrium had been established and the concentration data were used to calculate the equilibrium constant for the net reaction:

The equilibrium constant, K, is defined in terms of known concentrations as:

$$K = \frac{([E] + [HE])([H_2O])}{([A] - [HE])([CH_3OH] - [HE])},$$
 (2)

where

$$[H_2O]$$
 = concentration of water formed
= $[HE]$

For the 85 weight percent solution, the initial molar concentrations were: $[BTDE] = 0.22 \, M$ and $[CH_3OH] = 0.47 \, M$. The integral data from the nuclear magnetic resonance spectrum of the solution indicated 2.7 methylester groups per molecule which means that, on the average, 0.7 of the two available acid groups has reacted. Thus, the fraction of available acid groups reacted, 0.7/2, times the known concentration of available acid groups, $2 \times [BTDE] = 0.44 \, M$, gives the desired concentration value: $[HE] = 0.154 \, M$. Substituting these concentration values in Eq. (2) gives approximately $K = 1.0 \, \text{for the equilibrium constant}$.

Employing this equilibrium constant and the appropriate initial concentrations for the 50 weight percent solution: $[BTDE] = 0.13 \, M$ and $[CH_3OH] = 1.56 \, M$, the equilibrium concentration of additional higher ester can be calculated: $[HE] = 0.195 \, M$. This result was verified by measurement of the nuclear magnetic resonance data for a 50 weight percent solution of BTDE which was accelerated toward equilibrium by acidification with H_2SO_4 . The normalized integral for the methylester showed 3.5 ester groups per molecule or approximately: $[HE] = 0.20 \, M$, which agrees with the calculated value of 0.195 M.

The effect of concentration is evident from these results. At 85 weight percent (where $[CH_3OH]/[available\ acid]\approx 1$), the reaction proceeds until 68 percent of all the carboxyl groups are esterified (an average of 2.7 methylester groups per molecule). However, for the 50 weight percent solution (where $[CH_3OH]/[available\ acid]\approx 6$), the reaction proceeds until 88 percent of the carboxyl groups are esterified (3.5 methylesters per molecule). Thus, the six fold increase in methanol concentration provides significant impetus for additional ester formation. It should be recalled, however, that we have not attempted to account for the kinetic effects of changing pH and it might be that, at short times, the 85 weight percent solution would exceed the 50 weight percent solution in concentration of higher esters due to the greater concentration of acid in the 85 weight percent solution.

Relative Reactivity of Ester Impurities

We postulate that the relationship of the observed impurities to the void formation lies in several possible reactions of the ortho-ester groups to form undesirable intermediates. These fail to form the desired imide structure or react more slowly than the amide-acids of BTDE or NE. Figure 6 illustrates three such intermediates in which the resultant chemical structures have one common feature: These structures are less stable

than the imide ring at elevated temperatures and will decompose or rearrange evolving volatile materials. The evolution of volatiles late in the cure cycle or during post-cure treatment is the apparent cause of void formation.

A previous study (Ref. 4) has shown that ortho-amide and ortho-ester substituted polyamide intermediates require higher temperatures for imidization than the polyamide-acid. Thus, if the impurities react to form amide intermediates (such as those shown in Fig. 6), then these intermediates would imidize more slowly than the bulk of the resin and evolve condensation products late in the cure cycle. Evolution of volatiles by the 'no reaction' path cannot be discounted because the steric barrier imposed by the ortho-ester would be expected to hinder reaction at the carboxyl groups. Hence, volatiles could be produced by decomposition of unreacted amine or ester, or by slow evolution of condensation products as some reation occurs at higher temperatures.

The relative reactivity toward MDA of the ortho-ester moiety (in the tetraester) is qualitatively compared to the acid-esters of BTDE and NE in Fig. 7. The principal features of the differential thermograms for the indicated binary mixtures are: (a) sharp endotherms below 100° C; (b) a large endotherm between 125 and 200° C for the NE/MDA and BTDE/MDA mixtures; and (c) a relatively small broad endotherm between 175 and 300° C for the tetraester/MDA mixture. The features below 100° C are due to the melt of the monomers. No chemical reaction is apparent at this temperature. The nuclear magnetic resonance spectra of the mixtures of monomers showed no changes after the mixtures were heated to 100° C. The large endotherms, (b), are due to the loss of methanol and water as amide and imide are formed. Infrared spectral monitoring of

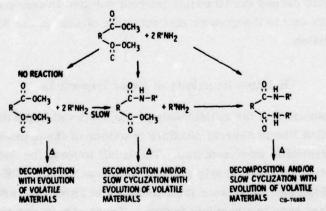


Figure 6. - Possible reactions of ortho-ester groups with amines.

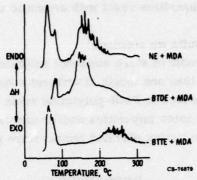


Figure 7. - Differential calorimeter scans of binary

imide formation showed that the reaction is nearly complete (for condensation of the amide-acids) after 15 minutes at 204° C. The large apparent noise level in region (b) of the thermograms is typical of agitation of the sample due to evolution of volatiles. It is significant that the tetraester/MDA mixture shows little or no reaction in the temperature range in which the other monomer mixtures imidize. While the reaction that does occur (feature (c)) was not characterized completely, it was observed that even after raising the sample temperature to 250° C at 10° C per minute, the magnetic resonance spectrum of the mixture still showed some unreacted methylester:

Thus, while these data do not define a single reaction path, they do confirm that the ortho-ester moiety reacts significantly slower than the amide-acids and that those reactions which do occur are not complete at a temperature of 250° C. In a typical cure cycle, the resin is held at 204° C for about one hour for imidization. It is doubtful that the ester impurities would react completely (if at all) during this staging.

SUMMARY OF RESULTS AND CONCLUSIONS

Spectral, chromatographic and thermal studies were conducted to identify the factors responsible for void formation in PMR-polyimide resin composites fabricated with aged monomer solutions. It was demonstrated that:

- (1) Detectable quantities of tri- and tetraester impurities form in 50 weight percent solutions of the diester of 3, 3', 4, 4'-benzophenonetetra-carboxylic acid (BTDE) after approximately one month of storage at ambient conditions.
- (2) The rate of formation of the ester impurities is slow (apparent half time in excess of eleven months), however, their formation is favored in the equilibrated solution.

(3) The ester impurities react with aromatic amines more slowly than the BTDE.

From these results we conclude:

- (1) It is undesirable to store methanol solutions of the monomer BTDE for periods greater than one month at ambient conditions.
- (2) Voids are formed in PMR-polyimide resin composites by gaseous products evolved by ester impurities and/or unreacted amine which react slowly or decompose during elevated temperature post cure treatment.

REFERENCES

- Serafini, Tito T.; Delvigs, Peter; and Lightsey, George R.: Thermally Stable Polyimides from Solutions of Monomeric Reactants.
 NASA TN D-6611, 1972.
- Cavano, Paul J.: Resin/Graphite Fiber Composites. (TRW-ER-7581F, TRW Equipment Labs.; NAS3-15829), NASA CR-121275, 1974.
- Delvigs, Peter; Serafini, Tito T.; and Lightsey, George R.: Addition-Type Polyimides from Solutions of Monomeric Reactants. NASA TN D-6877, 1972.
- Serafini, Tito T.: High-Temperature Resin-Matrix Composites.
 Aerospace Structural Materials. NASA SP-227, 1967, pp. 207-215.

THIN LAYER CHROMATOGRAPHY

C. A. May

Lockheed Missiles & Space Company Sunnyvale, California

In thin layer chromatography (TLC) an adsorbent, such as silica gel, is applied to a supporting glass plate in a thin layer. The solution of the mixture to be separated is deposited about 2 cm from the bottom of the plate by means of a micropipet. The plate is then placed in a closed container containing a layer of solvent about 1 cm deep. The solvent ascends the plate by capillary action carrying the components of the mixture. When the solvent has travelled a convenient distance, the plate is removed and the solvent allowed to evaporate. The locations of the various components can be determined visually. There are a variety of methods which can be used for this purpose. Typically, fluorescent dyes are added to the adsorbent so that UV-light can be used to detect the positions of components. The Rf value, defined as the ratio of the distance travelled by the compound to the distance travelled by the solvent is determined to establish a standard.

Compounds travel various distances up the plate depending on their adsorption coefficients. This is the ratio of the amount of material adsorbed to the amount of material in solution at equilibrium (Rf). As the solvent moves over the adsorbed spot, the equilibrium is shifted and compounds are desorbed, the more tightly adsorbed material to a lesser extent than the more loosely held material. When the material in solution reaches fresh adsorbent, it is adsorbed under new equilibrium conditions. In the case of two compounds the more strongly adsorbed material will displace the less strongly adsorbed material causing the displaced material to form a spot further from the origin. For this analysis, silica gel plates (5 x 20 cm) are commercially available at moderate cost. In fact, the entire setup for TLC can be purchased for around \$150. Generally, the silica gel layer is 0.25 mm thick and contains a fluorescent dye to facilitate visual examination with UV light.

In our work on composite matrices the resin system is separated from the fiber by washing the prepreg with a solvent. A silica gel plate is spotted 2 cm from the bottom with 5 μ l of the solvent solution. Solutions of the resin, a synthetic mixture approximating the formulations and the individual components of the formulation are applied on the same plate for comparison. After the solvent evaporates, the plate is developed for 45 minutes in a vertical position. A developing solvent which worked well on 350°F resin systems is 90/10 benzene/tetrahydrofuran (by volume). This solvent mixture was found, by trial and error, to give the greatest separation of the resin system components. After the developing solvent has evaporated, the spots are located under UV light.

A detection reagent specific for epoxy resins can also be used. It is prepared as follows:

25g NaBr
1.25g bromcresol purple
25ml benzyl alcohol
6.25ml water
188ml methanol
Titrate to a yellow end point with NaOH

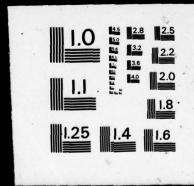
The reagent is sprayed or brushed onto the plate and dried. Epoxies show up as blue spots on a yellow background. The disadvantages of the reagent as compared to UV detection are the fading of the spots after a few days and the fact that it may not be possible to detect curing agents.

To facilitate positive identification of the individual components, a preparative TLC is used. The plate is larger (20 x 20 cm) and the silica gel layer is thicker (2.0 mm). The plate is spotted 2 cm from the bottom in a continuous band, hence, the sample is considerably larger. The plate is developed in the same manner. After the bonds of individual components are located by ultraviolet light, the silica gel in these regions is scraped from the plate. The component is then eluted from the silica gel with a solvent and the infrared spectrum obtained. In this manner a wide variety of components of a formulation can be separated, detected and identified.

TLC should prove to be a valuable quality assurance tool. The method is easy to run and is economic in both time and materials. A check on incoming material would immediately detect formulative material substitutions. Then, if required, the new component could be identified by infrared spectroscopy.

ARMY MATERIALS AND MECHANICS RESEARCH CENTER WATERTO--ETC F/G 11/9 PROCEEDINGS OF THE TTCP-3 CRITICAL REVIEW: TECHNIQUES FOR THE C--ETC(U) AD-A036 082 JAN 77 AMMRC-MS-77-2 NL UNCLASSIFIED 3 OF 4 El

3 of 4 DA036082



USE OF SEPARATION METHODS FOR QUALITY ASSURANCE OF POLYMERIC MATERIALS

C. D'Oyly-Watkins

Materials Quality Assurance Directorate, Ministry of Defence, Woolwich

INTRODUCTION

The process of quality assurance of materials by chemical means can be divided into three main stages all of which involve the analysis of samples usually by instrumental methods.

Firstly the properties of the material must be examined and the effects of variation in its composition studied so that a specification can be produced defining the composition required to satisfy a particular application. The specification will usually include details of test methods which should be used for ensuring that the material supplied is within the required limits.

Secondly check samples of materials must be examined from time to time to ensure that production is within specification and that the manufacturer's quality assurance system is satisfactory.

Thirdly faults and defects occurring in stores must be investigated in order to discover the cause of failure. If this is traced to a particular component it can then be decided if the specification for that component requires modification.

Instrumental analytical techniques such as the various forms of atomic and molecular spectroscopy are now widely used. These are of particular value for the third stage where sample sizes are often very small and it is necessary to obtain as much information as possible from a single sample. Most of the techniques employed give results which are easier to interpret if the material being examined is a single compound. Separation methods are therefore needed to separate the components of complex samples prior to their examination by spectrographic methods. They can also often provide direct information on the qualitative and quantitative composition of the sample.

The object of this paper is to discuss three techniques which are used in my Establishment and have proved of considerable value, particularly for samples which contain polymeric constituents.

PYROLYSIS GAS LIQUID CHROMATOGRAPHY

Gas chromatography is now very widely used and no further description of the equipment or the principles involved need be given here. Polymeric materials however cannot be separated or identified directly by this method because of their lack of volatility, but if the material is first pyrolysed and the resultant mixture of vapours passed through a gas chromatograph the products of the pyrolysis can be separated. The nature of the starting material can then in many cases be deduced, either by comparison of the pattern of peaks produced from the sample with that obtained from known materials or by the actual identification of the pyrolysis products using methods such as mass spectrometry.

Equipment

Chromatographs. Pye Fl1 and Perkin Elmer 900.

Pyrolysers. Perkin Elmer Bodenseeverk Pyrolysis unit.

Pye Curie Point Pyrolyser.

Hamilton multi purpose sampling system.

Mass Spectrometer. Perkin Elmer/Hitachi RMU 7.

Method

A small sample of the material being examined is heated rapidly to a temperature (usually between 500°C and 1000°C) sufficient to cause decomposition and the gaseous products produced are swept on to the column by the continuously flowing carrier gas (helium). The pyrolyser is normally mounted at the normal injection point of the system.

We have used three types of pyrolyser.

(a) Platinum helical coil. This consists of a spiral of platinum wire in which the sample is wedged and heated by passing a current through the wire. The temperature reached is controlled by adjusting the current to a suitable value. Pyrolysis can be carried out in stages by increasing the current after a suitable interval.

(b) <u>Curie Point Pyrolyser</u>. The sample is mounted on the end of a wire of magnetic material which is heated by induction. At the Curie point the magnetic properties of the wire disappear and no further heating occurs until the temperature has fallen below this critical point. A range of pyrolysis temperature can be obtained

by using wires of different composition and Curie point.

(c) Furnace Pyrolyser. The sample is placed in a boat and inserted into a furnace tube through which the chromatograph carrier gas passes. Heating is by external coil and the temperature can be thermostatically controlled. A capillary tube connection carries the products of pyrolysis to the chromatograph injection point.

Table 1 lists the advantages and disadvantages of these three pyrolysers.

When positive identification of the pyrolysis products is required a chromatograph permanently coupled to the mass spectrometer via a jet separator is used.

The jet separator permits the greater part of the carrier gas, whose volume would cause too great an increase in pressure in the mass spectrometer, to be pumped away while permitting all the heavier sample vapour to enter the spectrometer.

Applications

May, Pearson and Scothern (1) described the pyrograms produced by sixtyfive polymers and polymer mixtures. Using similar equipment, comprising a Pye Fll chromatograph and Curie point pyrolyser, we now use this method on a semi-routine basis. Examination of further column systems has shown that, as stated in the original paper, Poropak Q gives the most reproducible pyrograms for the widest range of polymers.

It has been found that the presence of plasticisers, oil extenders, additives, liquid diluents etc can modify the pyrogram so that in some cases the major identification peak which is often the monomer completely disappears. For positive identification of the polymer it is therefore advisable that such components are first removed by solvent extraction or other means.

Pyrolysis GC using a helical platinum filament pyrolyser has been used to provide unambiguous identification of sub-milligram amounts of 19 different rubber vulcanisates. The results are described in a paper by Foxton, Hillman and Mears (2). Additives present in the vulcanisates did not interfere and preliminary solvent extraction was not necessary in this case. Temperature programming of the column and the use of two stationary phases was necessary to achieve satisfactory separation in all cases.

TABLE 1

COMPARISON OF PYROLYSERS

Platinum Coil Advantages.

- (a) Simple to use.
- (b) Temperatures up to 1500°C can be obtained.

Disadvantages.

- (a) Platinum oxidises and hardens when cleaned in air thus changing its thermal properties and hence the reproducibility.
- (b) Difficulty in mounting small samples on coil.
- (c) Some types have a marked temperature gradient.

Curie Point

Advantages .

- (a) Simple to use.
- (b) Reproducible temperatures obtained.

Disadvantages.

- (a) Only a limited number of temperatures available.
- (b) Difficulty in mounting small samples on wire.
- (c) One step pyrolysis only.

Furnace

Advantages.

- (a) Sample can be accurately weighed.
- (b) Can be used for powders.
- (c) Accurate temperature check at point of pyrolysis.
- (d) Mon-volatiles stay in boat and do not contaminate column.

Disadvantages.

- (a) Temperatures only up to 800°C.
- (b) Products tend to condense on cold spots in furnace.
- (c) Can cause excessive breakdown to small fragments which are less characteristic than larger ones.

Squalene programmed from 50-130°C gave good separation in most cases but a few synthetic rubbers which produce only highly volatile pyrolysis products require a Poropak Q column programmed from 50-180°C.

Epoxide resins are now used in a variety of systems for adhesives, electrical insulation, surface coatings etc and it is often necessary to check the composition of materials employing these systems when failures occur. Heathcote (3) as a first part of an investigation on the analysis of such systems has looked at pyrograms produced from DGEBA (Diglycidyl ether of bisophenol A) with 13 different hardeners. He has developed a system for the identification of the hardener by examination of the peaks in the pyrogram (Fig. 1). A furnace pyrolyser was used in this case since pyrolysis of epoxy resin systems produces an appreciable amount of high boiling compounds. With the platinum coil or Curie point pyrolyser these are swept on to the column where they accumulate and eventually change its characteristics. With the furnace they tend to remain within the pyrolyser. Fairly large samples (1 mgm) were used and the separation was carried out using an FFAP (Carbowax 20 m crosslinked with nitroterephthalic acid) column programmed from 35-250°C at 15° a minute. The large peaks arising from the resin itself were allowed to go off scale and the hardeners could be identified by means of the smaller peaks which then become apparent. Of the 13 hardeners examined all could be

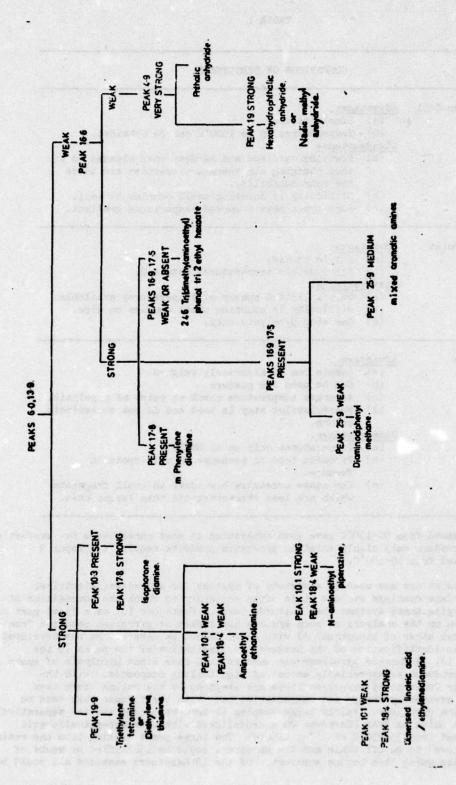


Fig. 1. Identification scheme for epoxide resin hardeners

.

9

identified with the exception that triethylene tetramine could not be distinguished from diethylene triamine nor could hexahydro phthalic anhydride from nadic methyl anhydride.

Five proprietary high strength adhesives all based on bisphenol A, epichlorhydrin and dicyandiamide in differing amounts with various inert fillers were examined by McIntosh (4). Pyrolysis GC alone having failed to differentiate between them the components present in the pyrolysates were identified, as far as possible, using combined GC-MS. All but two of the adhesives could then be distinguished by the presence of unusual pyrolysis products such as chloroaniline, diphenyl ether and N,N-dimethyl acetamide or by the presence of accelerating agents. N'-chlorophenyl-N,N'-dimethyl urea and N'-dichlorophenyl N,N-dimethyl urea. The two undistinguishable samples contained differing amounts of the same accelerating agent and were later distinguished by the use of gel permeation chromatography.

GEL PERMEATION CHROMATOGRAPHY

This again is a well established technique which produces separation by virtue of molecular size. It is a specialised form of high pressure liquid chromatography using columns packed with porous highly crosslinked polystyrene beads ("Styragel"). The eluting solvent is organic, usually tetrahydrofuran, and the detector usually a differential refractometer. Separation of mixture components is achieved because smaller molecules can penetrate more deeply into the pores of the Styragel than can larger ones and therefore have a longer residence time on the column. The range of molecular size which can be separated with any particular pore size is very limited so a number of columns each containing stationary phase of different pore size are commonly used in series. Several such sets of columns are needed to cover the whole range of materials to which this technique can be applied.

Equipment

Chromatograph. Waters Associates, Model 200.

Method

A pumping system and buffer reservoir provide a supply of moving phase solvent at high pressure and usually at elevated temperature. This is fed to two column systems in parallel, one for sample separation and the other to provide reference solvent for the differential refractometer. Samples are introduced into the system either with a syringe or by the use of a sample loop. Solvent emerging from the sample side of the system after passing through the detector is collected in a siphon tube. Each time the siphon empties, a voltage is superimposed on the detector output producing a blip on the recorder trace. By counting these blips the elution volume at any point on the trace can be measured. Separated sample fractions can be collected at the siphon outlet.

Applications

The use of this technique is two-fold firstly it can be used for the separation of mixtures, particularly those containing polymeric and non-polymeric components and secondly it can be used for measuring the molecular weight distribution of a polymer or similar material.

For applications involving separation of components or a simple comparison of samples, visual examination of the chromatogram and measurement of the retention volume is all that is necessary. For the determination of molecular weight distributions, the column must be calibrated by the use of narrow range polystyrene samples. This calibration can then be corrected for a particular sample material by one of three 'universal calibration' methods. These are based on literature or calculated values of extended chain length (Q-factor), hydrodynamic value (Benoit method) or unperturbed dimensions (Dawkins). All three methods have been reviewed in a paper by Dawkins (5).

The number $(\bar{M}n)$, weight $(\bar{M}v)$ and viscosity $(\bar{M}v)$ average molecular weights and the polydispersity $(\bar{M}v/\bar{M}n)$ may also be calculated.

Determination of molecular weight distribution has been used to characterise polymers in studies of batch to batch variations and to investigate degradation processes eg. of oil additives in engine testing or in simulated laboratory shear tests (6).

As a quantitative technique it has been used for the determination of total polymers in industrial mixes eg. nitrocellulose in nitrocellulose-nitroglycerine-water pastes (7) and viscosity improvers in oils.

As a small scale preparative method it can provide samples of separated polymers etc. for further investigation by other methods. This has been used for the separation of polymeric viscosity improvers in oils, and subsequent identification by pyrolysisgas chromatography.

An example of the use of GPC for determination of molecular weight distribution is in the examination of ethyl cellulose. This material is extruded as tubes which are used to provide an inhibitive coating for rocket motors. Some batches produce a melt defect known as 'sharkskin' which appears as a rough and hazy surface finish. Both 'good' and 'bad' materials passed the normal specification tests and gave similar (Mv). Although a number of techniques have been tried in order to distinguish those materials only by gel permeation was any difference detected. Examiniation of the chromatograms showed (Fig. 2) that the 'bad' material has a narrower weight distribution than the satisfactory batches. Other factors, such as lower plasticiser content are now known to contribute, but broadening of the molecular weight distribution by blending with lower molecular weight material has been found to give an improved result.

The determination of polyethylene in admixture with micro crystalline wax (9), both of which are similar in composition and differ only in molecular weight, provides a good example of the capabilities of GPC as an analytical method for total polymer content (Fig. 3). This wax mixture is used as a desensitiser for explosives. During a proofing trial variations in performance were detected which were attributed to lack of homogeneity of the mixed wax. Nine samples of the wax blend taken throughout the processing of a melt gave polyethylene figures (15.7%, 15.8%, 16.0%, 15.8%, 16.3%, 15.8%, 15.9%, 16.5%) which in fact show a remarkable degree of homogeneity for a very simple production process. Repeatability was good even though the poor solubility of polyethylene requires the use of a hot solvent (o-dichlorobenzene at 80°C) which normally gives maximum difficulty in quantitative work.

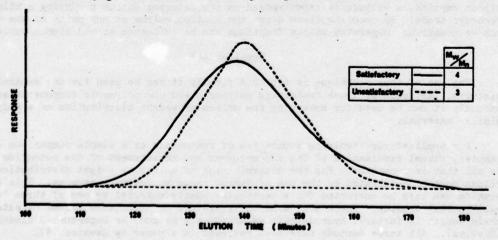


Fig. 2. Molecular weight distribution of ethyl cellulose

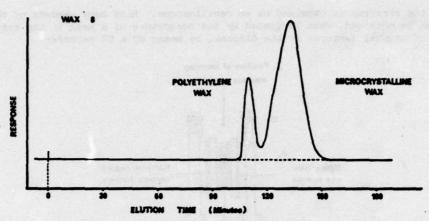


Fig. 3. Determination of polyethylene in admixture with microcrystalline wax

EVOLVED GAS ANALYSIS BY MASS SPECTROMETRY (EGAMS)

This method is comparable to the normal thermal degradation methods (TGA, DTA and DSC) in which the polymer is progressively decomposed by linear heating and the evolution of volatile products is detected by heat evolution or absorption or by weight loss.

With EGAMS however the sample is heated directly in the source region of a mass spectrometer and evolution of volatile products can be seen by an increase in the total ion current of the spectrometer. Positive identification of the evolved vapour can then often be achieved by examination of the mass spectrum which it produces.

Equipment

Mass Spectrometer.

Bendix Time-of-Flight, Model 12.

Temperature Controller.

Stanton Redcroft Linear Temperature Controller, Model LVP-C.

Method

A small sliver of the sample (approximate dimensions 5 mm \times 0.5 mm \times 0.5 mm) is placed in the top half of a small silica tube. This tube has a central septum which enables it to be placed on the top of the thermocouple in the direct inlet probe of the mass spectrometer (Fig. 4). Here it is now sited within the modified furnace of the probe and can be introduced via a vacuum lock into the source region of the mass spectrometer. The final position of the top of the sample tube is a few millimetres from the ionising electron beam of the spectrometer.

The sample is then heated by current supplied to the furnace which is a platinum sputtered alumina cylinder. The linear programmer is controlled by feedback from the thermocouple which also provides an indication of the temperature at any time (Fig. 5).

Heating rates of 5 or 10°C/min are normally used and temperatures up to 1000°C can be achieved, although 400°C is normally sufficient for most polymer samples. Some arcing, which can cause problems, occurs within the spectrometer as the temperature is raised above 500°C.

The total ion current of the spectrometer is monitored continuously, giving a trace of amount of evolved material versus time (temperature) on a pen recorder. Because of the high repetition rate of the TOF instrument (10,000 spectra/sec) a continuous

display of the spectrum is obtained on an oscilloscope. Hard copy records of the spectrum can be obtained, when indicated by the occurrence of a peak in the total ion current or of unusual features in the display, by means of a UV recorder.

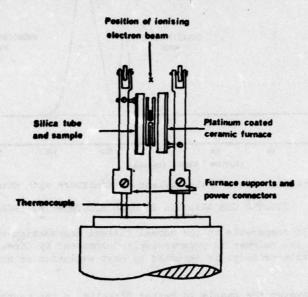
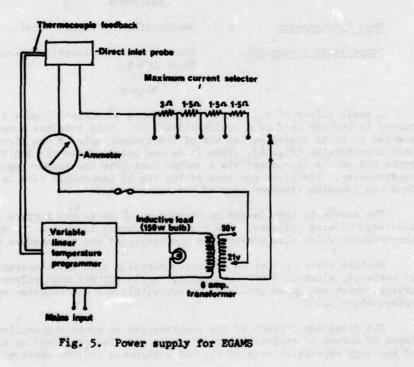


Fig. 4. Furnace and sample holder for EGAMS



Applications

The combination of mass spectrometry with thermogravimetry was first described by Zitomer (10) and the use of EGAMS itself by Murdoch and Rigby (11).

It was first used in the department for the characterisation of nylons and has since been used for a variety of purposes including the analysis of polyurethane foams (12), silicone rubbers and phenylformaldehyde resins.

As a method it is reasonably quick and easy to use. It requires a minimum of sample preparation and a minute amount of sample. Compared to pyrolysis GC the breakdown is less and the fragments involved are larger and more characteristic of the starting material. For example in the case of polyurethanes it is often possible to identify the blowing agent and the isocyanate used and to characterise the polymer as a polyester or polyether type with only a few milligrams of sample.

Some problems have been experienced with poor reproducibility of the thermal trace and considerable variation in the relative peak heights of the materials evolved. This is possibly due to non-uniform heating and may be improved by better temperature programming and a constant sample size.

A trace obtained from a polyester type polyurethane elastomer preformed from known starting materials is shown in Fig. 6. The materials used were:

Polyethylene adipate (M.W. 2000)	1.0 moles
4,4' diphenyl methane diisocyanate	3.3 moles
1.4 butane diol	2.0 moles

The temperature was increased at 5°C/min up to 100°C and then at 10°C/min. Spectra were recorded at the points lettered on the trace and were identified as due to:

- A. Residual moisture
- B. Carbon dioxide
- C. 1,4 butane diol
- D. 4,4' diphenylmethane diisocyanate
- E. Ethylene glycol
- F. An adipate type compounds (peaks at m/e 84, 111, 129).

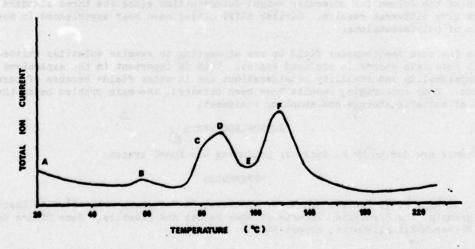


Fig. 6. EGAMS trac from a polyurethane elastomer

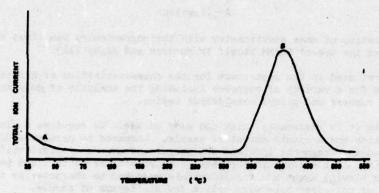


Fig. 7. EGAMS trace from P.T.F.E.

A trace obtained from an unknown material is shown in Fig. 7.

Spectra taken at the lettered points show:

- A. Moisture and a trace of carbon dioxide.
- B. Tetrafluoroethylene with a trace of hexafluoropropane.

The sample was identified as a polytetrafluoroethylene.

CONCLUSION

Three instrumental analytical techniques have been described and examples of their use to examine complex organic materials have been outlined.

Current problems include an attempt to identify silating agents on glass and quartz fibres. Some preliminary work has been carried out but so far it has not been possible to detect any differences.

Gel permeation is being used as part of a large program for characterising propellant grade nitrocellulose. The major difficulty experienced here is in calibration of the column for molecular weight determination since the three standard methods give different results. Similar difficulties have been experienced in the examination of polyisobutylene.

In the mass spectrometry field we are attempting to examine volatiles emitted from plastic materials stored in confined spaces. This is important in the explosives field for compatibility and stability considerations and in other fields because of corrosion problems. Some encouraging results have been obtained, the main problem being the design of suitable storage and sampling equipment.

ACKNOWLEDGEMENTS

Thanks are due to Mr R. Dunk for producing the EGAMS traces.

REFERENCES

- R. W. May, E. F. Pearson and M. D. Scothern, "A Reference Collection of Chromatograms of the Pyrolysis Products of some Paints and Plastics," Home Office Central Research Establishment, Report No. 54.
- A. A. Foxton, D. E. Hillman and P. R. Mears, "Identification of Rubber Vulcanisates by Pyrolysis Gas Chromatography," CI Memorandum No. 236.

- P. C. Heathcote, "Identification of Epoxide Resin Systems by Pyrolysis Gas Liquid Chromatography, Part 1 Epoxide Curing Agents, M.Q.A.D. Report No. 230.
- B. McIntosh, "The Use of Mass Spectrometry to Characterise Adhesive Films," M.Q.A.D. Technical Paper No. 635.
- J. V. Dawkins, "Calibration Procedures in Gel Permeation Chromatography," Br. Polymer J., <u>h</u>, (1972), p. 87-101.
- D. E. Hillman, Miss H. M. Lindley, J. I. Paul and D. Pickles, "Application of Gel Permeation Chromatography to the Study of Shear Degradation of Polymeric Viscosity Improvers used in Automotive Engine Oils," Brit. Polymer J., 1975, I, p. 397-407.
- D. E. Hillman and J. I. Paul, "Determination of Total Polymers in Industrial Materials by Gel Permeation Chromatography ("Exclusion Limit Chromatography")," J. Chromatog., 108, (1975), p. 397-400.
- A. P. Brookshaw, D. E. Hillman and J. I. Paul, "Gel Permeation Chromatographic Evaluation of Ethyl Cellulose Extrudates Exhibiting "Sharkskin Effect"," Brit. Polymer J., 5, (1973), p. 229-239.
- D. E. Hillman, "Characterisation and Analysis of Waxes by Gel Permeation Chromatography," Anal. Chem., <u>43</u>, 1007, (1971).
- F. Zitomer, "Thermogravimetric-Mass Spectrometric Analysis," Anal. Chem., 40, (1968), p. 1091-1095.
- I. A. Murdoch and L. J. Rigby, "Thermal Volatisation Analysis by Mass Spectrometry," Dynamic Mass Spectrometry Vol. 3, (1972), p. 244-265, (London, Heyden), Ed. by D. Price.
- 12. C. Reed, "Evolved Gas Analysis of Polyurethane Foams by TOF Mass Spectrometry," Brit. Polymer Journal, 6, (1974), p. 1-11.

3

SESSION III: THERMAL AND THERMAL MECHANICAL METHOD

Chairman: H. Schwartz Air Force Materials Laboratory, USAF

APPLICATIONS OF COMBINED PYROLYSIS-GAS CHROMATOGRAPHY-MASS SPECTROMETRY TO THE ANALYSIS AND EVALUATION OF POLYMERIC MATERIALS
C. Merritt, Jr., U.S. Army Natick R&D Command

APPLICATIONS OF THERMAL METHODS OF ANALYSIS
J. M. Barton, W. A. Lee, and W. W. Wright, RAE, Farnborough, England

DIFFERENTIAL SCANNING CALORIMETRY APPLICATIONS IN THE THERMAL, KINETIC, AND RHEOLOGICAL CHARACTERIZATION OF THERMOSETTING SYSTEMS M. R. Kamal, McGill University, Canada

CHARACTERIZATION OF THERMOSETTING EPOXY SYSTEMS BY TORSIONAL BRAID ANALYSIS J. K. Gillham, Princeton University

POLYMER CHARACTERIZATION USING DIFFERENTIAL SCANNING CALORIMETRY W. D. Bascom and P. Peyser, Naval Research Laboratory

APPLICATIONS OF COMBINED PYROLYSIS-GAS CHROMATOGRAPHY-MASS SPECTROMETRY TO THE ANALYSIS AND EVALUATION OF POLYMERIC MATERIALS

C. Merritt, Jr.

US Army Natick Research & Development Command Natick, Massachusetts 91760 USA

Several excellent reviews of the principles of combined pyrolysis-gas chromatographic mass spectrometric analysis are available in the literature (1-3). This paper, accordingly, will be restricted to a description of the applications of the technique that have been made to problems relating to studies of polymeric materials of concern to the Army Materials and Mechanics Research Center.

A schematic diagram of the analytical system is seen in Figure 1. Pyrolysis may be accomplished by several means under a variety of conditions. The thermal degradation products from solids pyrolyzers such as resistive type heater wires or ferromagnetic (Curie point) wires may be introduced to the GC/MS analysis system at the points indicated by arrows. The products from a boat pyrolyzer may be similarly introduced. The conditions of temperature and atmosphere may be carefully controlled if desired. A vapor phase pyrolyzer (Pyrochrom) is also incorporated. Pyrolysis products are normally swept onto a cold chromatography column with helium carrier gas as they are formed. Upon completion of the pyrolysis, a column temperature program is initiated to separate and elute the components. The eluents are then identified by means of the mass

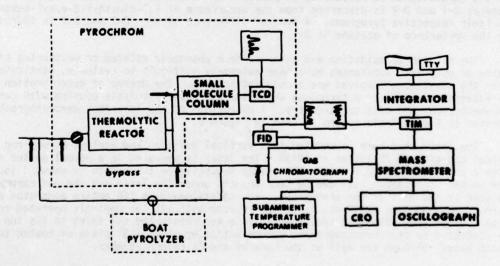


Figure 1

spectrometer. A photograph of part of the system is seen in Figure 2. The combined vapor phase and solids phase pyrolyzer is seen at the left of the chromatograph. The heater furnace for the boat pyrolyzer is attached to one of the GC inlet ports. The time of flight mass spectrometer ion source may be seen at the top right.

Another system has been configured for TGA/GC/MS analysis. A photograph of this system is shown in Figure 3. The TGA cell is mounted beside the gas chromatograph at the left. The mass spectrometer is a double focussing magnetic deflection type and utilizes a small (8K) computer system for data acquisition.

In order to avoid secondary reactions of the pyrolysis products it is desirable to provide for a fast temperature rise time, to rapidly sweep out the products and to employ small samples. A specially devised sample probe to achieve these objectives is shown in Figure 4. The sample $(1-5\,\mu\mathrm{g})$ is placed in the small cavity near the end (left) and the probe, after connecting to the heater chamber, is inserted quickly into the hot zone. The temperature employed for most of the analyses of polymers described below was 950°C.

Chromatographic separations were performed on a 1/8 in. x 4 ft. stainless steel column packed with 1% SE30 on Chromosorb. The column was programmed from -50°C to 250° C at 20° C per minute.

The pyrolysis/GC/MS system has been used for a wide variety of studies of polymer characterization, but only a few examples can be given here. One of these is the analysis of products from the pyrolysis of carbon fibers. A summary of the composition of components evolved from several different carbon fiber samples is seen in Table I. Two parameters are seen to be significant in characterizing the fibers, viz., the amount of $\rm CO_2$ evolved and the occurrence of various aliphatic and aromatic hydrocarbons. These factors may be ultimately related through correlation studies to the structure of the fiber.

Another application of pyrolysis/GC/MS is depicted in Figure 5 in which the type of additive, curing agent, and other modifications of EPON 828 resins may be discerned from differences in the pyrolytic decomposition products. Common components are seen in the chromatogram corresponding to sample D-3. A change in the resin composition in samples D-1 and D-2 is discerned from the occurrence of 1,3-dimethyl-2-ethyl-benzene, in their respective pyrograms. A further difference between D-1 and D-2 is indicated by the appearance of acetone in D-1

The effects of oxidation and other surface phenomena related to weathering and aging of polymeric substances have been extremely difficult to evaluate, particularly when the substances involved are highly intractable. The degree of deterioration can be assessed however, by a technique which employs laser pyrolysis coupled with gas chromatography and mass spectrometry. A photograph of the laser/gas chromatograph portion of the analysis system is seen in Figure 6.

The laser used here is mounted in a vertical position and employs a ruby rod with an output capacity of 25 joules at 6943Å. The laser is operated in a normal pulsed mode with a pulse width of 2.7 msec - The energy impinging on the sample is about 4 joules per pulse. The sample cell can be seen mounted under the laser and the gas chromatograph is seen at the left of the photograph. For safety measures the entire apparatus as seen here is mounted in a small optically sealed room with all the controls operated remotely from the outside. The mass spectrometer is a quadrupole and the inlet to its ion source is connected to the chromatographic column outlet by about a 6" piece of heated tubing which passes through the wall at the back of the GC column chamber.



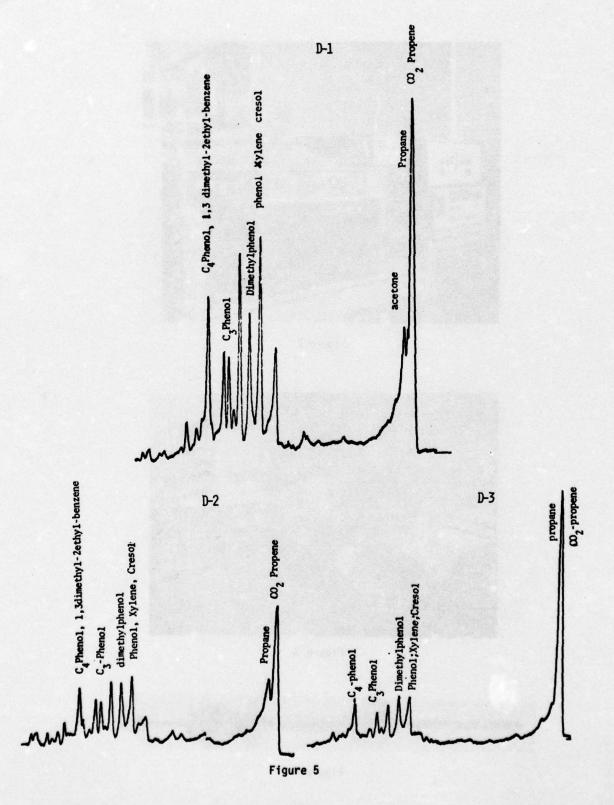
Figure 2



Figure 3



Figure 4



.

Table I. MS ANALYSIS OF VOLATILES-(DETERMINED ON WATERFREE BASIS)

Carbon Fiber Sample	CO ₂	Methane	Propane	Propene	Benzene	Toluene	Dimethyl- benzene	Naphtha- lene	Methyl- naphtha- lene	Estim. CO ₂ Evolved as % of Sample Wt.
1	100									1.58
2	100									1.00
3	100									0.06
4	100									0.05
5	48	23.0	0.5	2.0	9.5	8.3	2.9	2.9	2.8	2.34
6	100									0.07
7	100									0.02
8	32	20.0	19.0	20.0	7.0	2.0				0.35
9	100									0.13
10	100									0.16
11	48	2.0	14.3	15.0	14.4	6.4				0.36



Photograph of laser and cell assembly.

Figure 6

A detail of the pyrolysis sample cell is seen in Figure 7. The sample cell consists of a stainless steel chamber with a quartz window for admitting the laser beam. A top view of the cell chamber is seen in the insert at the left with a view of a sample piece of the fiberglass epoxy resin composite in position. A switching valve was incorporated in the assembly to allow the helium stream to flow through the cell or to bypass it. In use, the cell was also enclosed in a heater which was operated at 250°C and the pyrolysis products were swept by helium carrier gas onto the GC column through heated transfer lines.

After mounting the sample in the cell - and purging of air - the laser was first focussed by means of an auxiliary ocular viewing lens to bring the beam into sharp focus on the surface of the sample, but it was then defocussed to a predetermined degree to achieve an optimum area that would yield the maximum amount of volatile product. This was determined by trial and error using representative samples and was found to be a spot about 1-2mm in diameter. The depth of penetration was determined by electron microscope examination of exposed samples to be about 50Å which corresponds very well, with the depth of surface deterioration due to weathering which was also about 50-100Å.

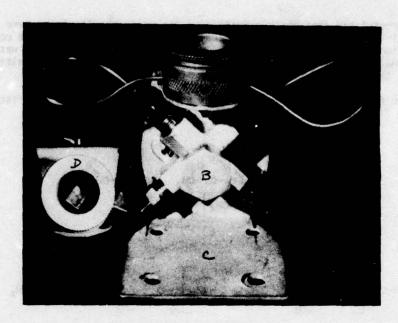
In this study the pyrolysis products were separated on a 50-ft. x 0.02 in. support coated open tubular column coated with 3% SE30. The column was operated in a subambient temperature mode at -180°C during collection of the pyrolysis products and programmed from -180 to +200 during elution. No molecular separator was used in coupling the GC to the mass spectrometer, but a restrictor was used to control the pressure drop, and a small portion of the eluate was split off to a flame ionization detector for recording the chromatograms.

The objective of the laser pyrolysis analyses was to develop a means of evaluating the extent of weathering of the fiberglass epoxy resin composite materials; i.e., from the chemical composition of the pyrolysis products to gain some insight to the mechanism of deterioration.

Figure 8 shows some of the samples of epoxy composite material that were studied. The samples in the top row are representative of the material before it is pyrolyzed in the laser cell. The one in the top left corner has not been weathered, but the other three have been exposed, respectively from left to right, for 6, 12 and 18 months to a combined tropical and maritime environment in the Panama Canal Zone. These test panels as well as others exposed at several other test sites (see Table II) show severe visual deterioration especially after the twelve and 18 months exposure periods. Fiber blooming can be seen on all the exposed test panels and 3-9% of the resin was found by gravemetric analysis to have volatilized. The samples seen in the bottom row of Figure 8 are representative of the effect of exposure to the laser beam. Although there is considerable charring, it is somewhat misleading because copious amounts of CO₂ and H₂O are evolved during pyrolysis and there is obviously some carbonaceous residue. The significant components are far less abundant, but much more revealing with respect to what is occurring. For example, the unweathered sample yields no other products but CO₂ and H₂O upon laser pyrolysis under the conditions employed here.

Table II. TEST SITES

Site	Type of Environment
Ft. Sherman, Panama, open field	Sun, hot, humid
Ft. Sherman, rain forest	Hot, humid, microbiological
Ft. Sherman, breakwater	Sun, hot, humid, salt content
Chiva Chiva, Panama	Sun, hot, humid
Maynard, Mass	Temperate



Photograph of pyrolysis cell.

A. Cell chamber. B. By-pass valve. C. Mounting stand. D. Top view
Figure 7

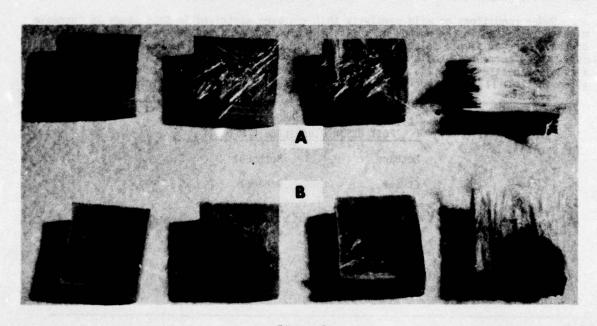


Figure 8

It may be postulated that photo-oxidation of the resin results in rupture of the polymer cross linking and the formation of smaller resin chains which can be correlated with deterioration of the critical mechanical properities of the resin. It was hoped that chemical analysis of the pyrolysis products might also yield some definitive information about the nature of this process

The generic formulas for the two resins of which the composite is comprised in addition to the fiberglass are:

EPON 828

DEN 438 is seen to have a carbon skeleton whereas the EPON 828 has a skeleton with repeating ether linkages. It may also be postulated that the ether linkages, both in the skeleton of the DEN resin and of the side chains of the EPON resin may be ruptured by UV radiation. The effect with time would be to decrease the molecular weight and size of the polymer, and to increase the number of terminal groups.

Under conditions of mild pyrolysis that has been contrived in this study an increase might be expected in the number of volatile compounds produced in the surface layers of the weathered sample relative to the number produced from the basic resin. Moreover, these compounds should be predominantly oxygenated compounds such as ketones, alcohols and ethers. A list of the most abundant pyrolysis components observed is given in Table III. The expected oxygenated components are seen on the right and several,

Table III. LIST OF VOLATILE PRODUCTS FROM EXPOSED EPOXY RESIN/FIBERGLASS COMPOSITE

Methane	Methano1
Ethane	Ethano1
Benzene	Acetone
Toluene	Pheno1
Ethylbenzene	Acetophenone
2-pheny1propane	Phenylethyl ether

perhaps, equally expected hydrocarbon fragments, are seen on the left. The possible origin of some of these components may be depicted as follows:

It may be naive to indicate various fragments splitting out in this manner but it is not intended to portray any proposed mechanisms. The scheme does point out, however that no components are found which are not consistent with the hypothesis of UV degradation of the polymer increasing the number of side groups that can be split off by subsequent pyrolysis. Moreover, all the expected fragments are found.

The most significant observation is that these components are not found upon pyrolysis of unweathered samples, and that they increase with the amount of weathering.

Figure 9 shows a graph of the amount of several pyrolysis components produced from the surface of weathered test panels at one of the exposure sites for a combined tropical-maritime environment. These data correspond to the test panels shown in Figure 8.

Figure 10 shows another graph of the amount of pyrolysis components as a function of exposure time. These data were obtained from test panels that were exposed at another location in Panama that was classified as tropical only. The results are essentially the same.

The formation of volatile compounds by pyrolysis from the weathered polymer surfaces can perhaps be utilized as a test measure of resin deterioration. Characteristically, the polymer chemist has used physical testing methods to evaluate the degree of deterioration produced by weathering. Some typical data for tensile strengths are seen in Table IV.

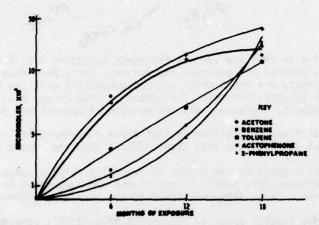
Table IV. COMPARISON OF TENSILE STRENGTHS FOR THE VARIOUS TEST SITES*

	6 Months		12 Months	
Test Sites	Change	cv	Change	cv
Open field	-6.1	3.5	0.3	5.2
Chiva Chiva	-1.1	2.5	-13.8	5.3
Breakwater	-7.1	2.6	-6.0	9.5
Maynard	4.9	7.5	-22.0	4.4
Rain forest	-2.2	7.4	-6.0	9.5

*As % change - unexposed initial control = $735 \text{ psi x } 10^{-2}$.

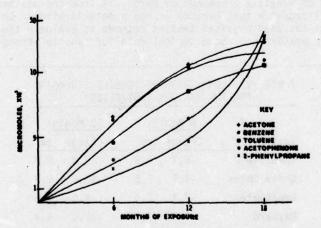
Similar data have been obtained for sheer strength and flexure strength (4). For all these properties there appears to be a great inconsistency among the data obtained at various test sites. Pyrolysis data, on the other hand, appear to provide more uniform agreement. In Figure 11 it may be seen that the release of volatile compounds by laser pyrolysis from the surface of the composite is apparently a function of the extent of deterioration. It is especially noteworthy that the results of exposures at a variety of test sites are in quite good agreement.

These studies have indicated that some of the surface phenomana associated with weathering of epoxy resin/fiberglass composites may be eluciated by means of a combined laser pyrolysis, gc/ms technique. The method is expected to have continued application in several related studies of similar behavior in other polymeric systems and in particular, to be useful wherever it is necessary to examine the composition and microstructure of surfaces or minute areas of polymeric substances.



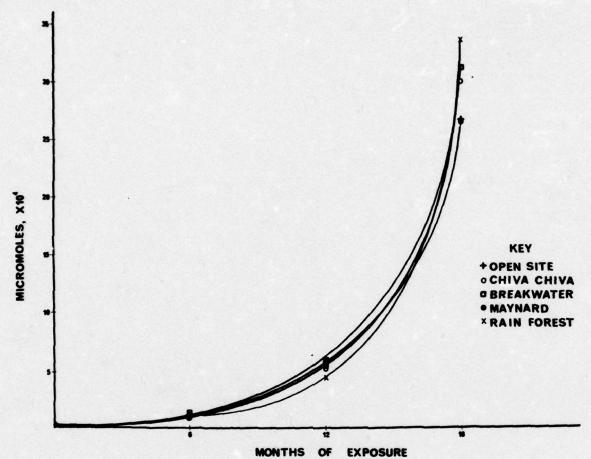
Graph of amount of volatile component produced by laser pyrolysis as a function of duration of exposure at test site "breakwater".

Figure 9



Graph of amount of volatile component produced by laser pyrolysis as a function of duration of exposure at test site Chiva Chiva.

Figure 10



Graph of total gas evolution from lasing event as a function of exposure time.

Figure 11

REFERENCES

- 1. R.L. Levy, Chromatogr. Rev. 8, 49-89 (1967)
- D.A. Leathard and B.C. Shurlock "Identification Techniques in Gas Chromatography",
 John Wiley & Sons, Ltd., London, (1970), p.123.
- S.G. Perry in "Advances in Chromatography", Vol. 7., J.C. Giddings and R.A. Keller, eds., Marcel Dekker, Inc., New York (1968) p.221.
- 4. C. Merritt, Jr., R.E. Sacher and B.A. Petersen, J. Chromatog, 99, 301-308 (1974).

APPLICATIONS OF THERMAL METHODS OF ANALYSIS

J. M. Barton, W. A. Lee and W. W. Wright

Materials Department, Royal Aircraft Establishment, Farnborough, Hants

INTRODUCTION

Thermal and thermomechanical methods of polymer characterisation and evaluation have been developed and have achieved wide acceptance over the past 10-15 years. The various techniques are in many ways complementary and each has its own advantages and disadvantages. Materials Department, RAE, is equipped to carry out thermogravimetry, differential thermal analysis and differential scanning calorimetry, thermomechanical analysis, torsional braid analysis, automatic dilatometry, electrothermal analysis, pyrolysis/gas chromatography/mass spectrometry, stress relaxation measurements, and dynamic mechanical measurements using a torsional pendulum or dynamic viscoelastometer. This paper briefly reviews work using the six techniques underlined. In each case the approach has been to outline, (a) the purpose for which the technique was used, (b) the information desired and (c) the advantages and limitations of the method.

THERMOGRAVIMETRY (TG)

The major use of thermogravimetry on polymers has been the assessment of thermal stability. Subsidiary uses have been the measurement of the relative efficiency of antioxidants and the monitoring of curing conditions for condensation polymers.

Thermal stability assessment may be directed towards comparison of the heat resistance of different polymer structures, or may serve as an accelerated test for life-time prediction. In the latter case, the method only has real quantitative significance if breakdown is by a single well defined mechanism and if the retention of the properties of interest is directly related to weight loss. The test may nevertheless be used as a preliminary screening procedure to eliminate those materials, which will obviously not withstand the required conditions.

Much emphasis in this field has been placed upon dynamic methods of analysis i.e. at different rates of temperature rise, and the reported ways of analysing the test data are legion. We view dynamic data with considerable reservation as many instances have been observed, where orders of stability as determined by this method are not confirmed when isothermal tests are carried out.

The advantages of thermogravimetry are that it is a quick and easy test to make, instrumentation and data analysis can be fully automated and only small quantities of material in a non-specific form are required. The major disadvantage is that it only records phenomena, which are associated with weight loss. This can be illustrated from polyimide chemistry. Polyimides are attacked by bases — a drawback for some applications, but analytically very useful as by treatment of a polyimide with hydrazine hydrate it is possible to recover quantitatively the diamine used in the preparation and the

cyclohydrazide derivative of the dianhydride. A polyimide film can therefore be aged and then broken down chemically to determine how much of the original structure remains. The results [Figure 1] show that at only 2-3% weight loss approximately 50% of the diphenyl ether and 30% of the pyromellitimide units in the original polymer chains had been chemically modified (1). This raises the question of the extent of this sort of reaction in other high temperature polymer systems, which do not have such a convenient method of chemical analysis.

Whilst on the subject of polyimides, thermogravimetry has proved very useful for monitoring the cure of the condensation type. Weight loss determinations have been made for the time/temperature profiles used throughout the curing cycle (i.e. for precure, cure and postcure). Significant differences were observed in the characteristics of different experimental batches of resin and as a result a simple quality control test based on a rising temperature experiment [Figure 2] was developed (2). Quality control of prepreg was also possible, weight loss measurements being used to ascertain the amount of precure that had taken place and whether, as a consequence, changes were required in the subsequent moulding conditions. These techniques can be applied in principle to any curing reaction involving weight loss.

DIFFERENTIAL SCANNING CALORIMETRY (DSC)

The advantage of this technique over thermogravimetry is that it is sensitive to any reaction involving a change in heat content and this makes it especially useful for monitoring curing reactions. It also detects transitions such as Tg, Tm, Tcrystallisation and Tdecomposition. The MOD had for many years a Sub-Committee dealing with the problem of assessing the degree of cure of polyester and epoxy resins in glass reinforced plastics. All promising techniques were evaluated, many in co-operative programmes, and it was concluded that DSC was probably the most useful technique for this purpose.

Our main uses of DSC have in fact been for the study of the cure of laminating resins (epoxies and polyimides) and adhesives and for the determination of transition temperatures. Advantages of the technique are that it measures a parameter directly related to a curing reaction, the estimation is relatively rapid and only small amounts of material of non-specific form are required. Disadvantages are that it gives no indication of changes, which may be occurring in mechanical properties. The transition temperatures recorded are very dependent upon the heating rate and the thermal history of the sample and hence care is needed in the interpretation of the results. Transition temperatures below Tg are hardly detectable, but these can be very important in relation to energy absorption processes e.g. impact strength and ductility.

In fibre reinforced composites, the mechanical and physical properties are dependent upon the state of cure of the resin. The production of components with consistent and reproducible properties therefore requires the resin to be crosslinked to the same degree when ever fabricated. If the resin is slightly undercured, this may not be apparent from the initial property levels, but may well be reflected in a reduced life-time of the component when stressed under adverse environmental conditions.

In a study (3) of an epoxy resin system it was shown that measurement of the heat of reaction was a quite sensitive method for following cure up to about 90% conversion, but that beyond this point determination of Tg was a more precise method [Figure 3]. Isothermal cure curves when plotted on a log scale could be approximately superimposed to give a master curve by horizontal shifts along the log time axis [Figure 4]. The shifts were related to the overall activation energy for the curing process and this allowed the prediction of isothermal cure curves at various temperatures from experimental data obtained at a single temperature. It was also shown that isothermal cure curves can be predicted to a fair approximation from the results of dynamic DSC experiments. This enabled a profile of the cure characteristics of the system to be built up from only two experiments.

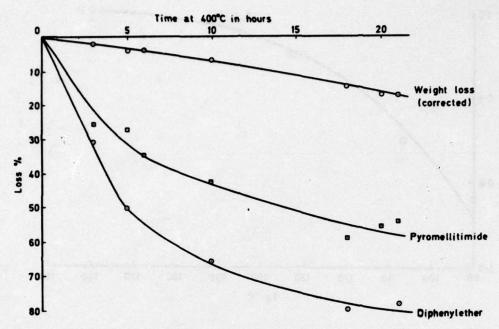


Fig.1 Change in yield of pure components with time of ageing of polyimide film at 400°C

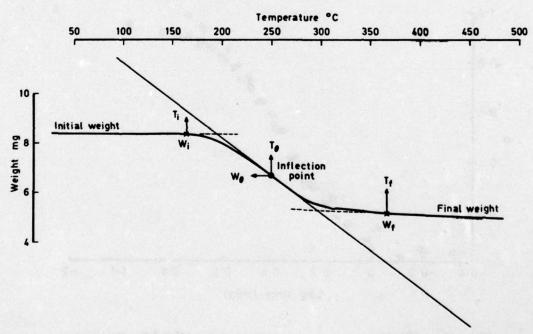
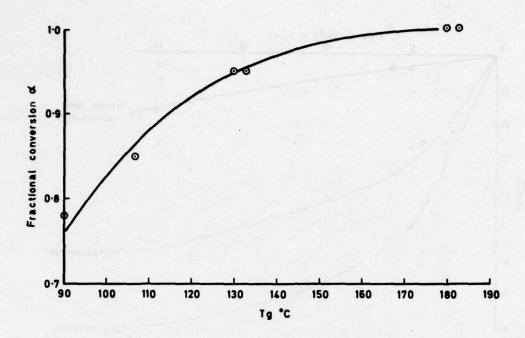


Fig. 2 Dynamic weight loss curve for polyimide resin at 10°C / minute heating rate



.

Fig. 3 Dependence of Tg on fractional conversion from isothermal experiments

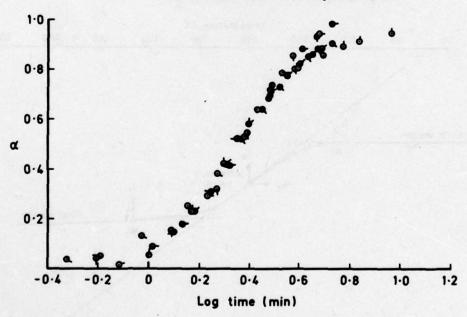


Fig. 4 Master cure curve at 179°C from superposition of isothermal curves

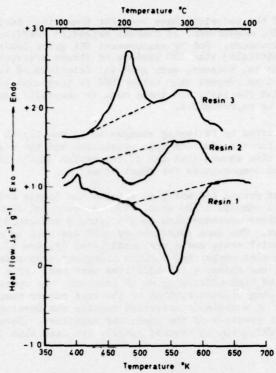


Fig.5 DSC scans on uncured polyimide resins.
For clarity Y~axis shifts have been
applied to the curves as follows.
Resins 1 & 2, +0.6; Resin 3, +1.2 J.s⁻¹.g⁻¹

Three commercially available addition-type polyimides were also studied (4) using as well as DSC, thermogravimetry and penetrometer (thermomechanical analysis) tests. Differences in curing characteristics are illustrated in Figure 5. The overall results showed that

- (a) Resin 1 followed first order kinetics up to about 60% conversion. It was possible to lose a component of this material by volatilisation.
- (b) Resin 2 followed second order kinetics up to 30% conversion. It began to cure in a lower temperature range than Resin 1, but was not fully cured on heating to 350°C, a temperature well above the recommended cure cycle.
- (c) Resin 3 was in the amic acid form as supplied and cure was accompanied by significant weight loss due to the cyclisation process.

Differences such as these have a marked effect upon the processing required and hence on properties and subsequent behaviour.

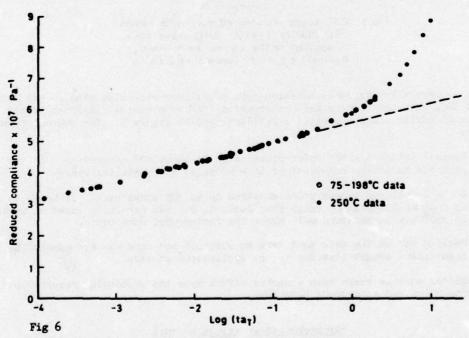
THERMOMECHANICAL ANALYSIS (TMA)

Besides measurement of transition temperatures, thermomechanical analysis may also be used for determination of modulus, of creep under load at various temperatures and of solvent swelling characteristics of rubbers. The last determination leads to the derivation of the length of chain between crosslinks in an elastomer.

Our main uses of the technique have been for transition temperature measurement — as a complement to DSC, measurement of thermal expansion coefficients and assessment of the properties of elastomers. For Tg measurement TMA gives lower values [up to 20°C for highly crosslinked materials] than DSC because of stress activation of relaxation processes. The method is, however, very good for detection of transitions below Tg and is more sensitive in this respect than either DSC or torsional braid analysis. Small samples only are needed for test, but these must be carefully prepared if the mechanical data obtained are to be reproducible.

Cure can be monitored by following changes in Tg exactly as with DSC. Both techniques were used for the addition-type polyimides and the results paralleled each other. The TMA data also showed that one of the resins should offer superior performance under load at elevated temperatures for short times.

The technique has proved its worth as a rapid and simple method for characterising elastomers using small samples of material (5). A spherical penetrometer test gave the modulus of the rubber corresponding to the Young's modulus determined by tensile loading at low strains. The same penetrometer test was used to measure creep at elevated temperatures and a master creep curve was constructed [Figure 6]. The method was applied to fluoroelastomer samples containing various inorganic compounds as hydrogen fluoride (HF) acceptors and it was shown, which additives were best for a combination of high resistance to creep and high efficiency as HF acceptor. By operating in the expansion mode the solvent swelling characteristics of the same rubber samples were determined and it was confirmed that an acceptable crosslink density was developed during cure of the fluoroelastomer in the presence of the preferred additives. Because very small samples are used, swelling equilibrium is reached quickly (in less than two hours).



Master creep curve at 250°C from superposition of reduced data at 75°, 98°, 147°, 172°, 198°C in nitrogen on data at 250°C in oxygen

TORSIONAL BRAID ANALYSIS (TBA)

Another technique which can be used for determination of transition temperatures, although it does not distinguish between Tg and Tm as say DSC does. Measurement is made of the complex modulus of a fibre/resin combination and only relative not absolute values can be obtained. The measurement is, however, much more directly related to the composite situation than any of the other techniques so far considered, as the actual resins and fibres of interest may be used in making up the braid. Because of the fibre support, polymers can be studied in the liquid state above Tg.

Our major use of TBA has been for the study of the cure of epoxy and polyimide resins and for assessing the effect of heat, or water uptake, upon mechanical properties. A drawback of the technique is that a sample must either melt, or dissolve in a solvent for braid impregnation and hence the method cannot be applied to already cured components. The effect of heat upon the mechanical properties of some aromatic fluoropolyimides has been studied (6). The loss peak heights were observed to diminish and the temperatures at which the peaks occurred to increase with increase in temperature [Figure 7]. The heights also diminished initially with time of heating at constant temperature, but then stabilised, further decreases only resulting if the temperature was raised. By 360°C the loss peaks were virtually non-existent. These changes must be associated with chain stiffening brought about either by crosslinking, or cyclisation reactions. The deliberate introduction into some of the polyimides of functional groups capable of crosslinking did not, however, increase the rate of diminution of the loss peaks.

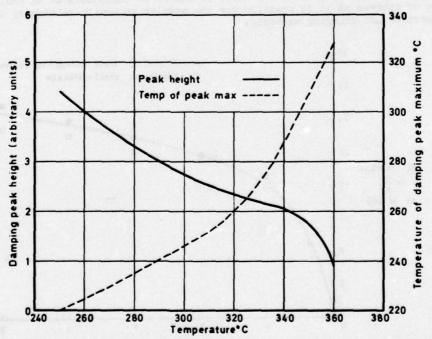


Fig. 7 Change in height and temperature of damping peak with temperature for a fluoropolyimide

STRESS RELAXATION MEASUREMENTS

Stress relaxation measurements are widely used for assessing the stability of rubber vulcanisates at elevated temperatures. The stressing may either be continuous, when the rate of network scission reactions is measured, or intermittent when the overall change in network structure resulting from both scission and crosslinking reactions is recorded. By such measurements it is possible to ascertain whether scission occurs primarily in the polymer chain, or in the crosslinks. The technique is effectively limited to elastomeric systems and requires that a sheet of material can be made from which test-pieces can be cut. A study can be fairly laborious as behaviour must be studied over a range of temperatures and times.

We have used the technique most extensively for assessment of the thermal stability of different rubbers and for determining the relative efficiencies of antioxidants; for these purposes it has proved very successful. Attempts have also been made to utilise the results for prediction of the long term stability of a rubber over a range of temperatures in either an unstrained or strained condition. This is not easy because of the difficulty of fitting kinetic equations to relaxation curves obtained at elevated temperatures in a form suitable for extrapolation to longer times at lower temperatures. In addition, rubbers differ widely in their relaxation behaviour and a standardised approach to the analysis of stress-relaxation curves has not yet been evolved. experiments were made with polychloroprene and a copolymer of butadiene and acrylonitrile (7). It was possible to extrapolate the results of intermittent stressrelaxation experiments at elevated temperatures to room temperatures and, in so doing, to describe the rate of change of modulus with time at that temperature. Good correlations were found between changes predicted in this way and those observed in shelfstorage experiments [Figure 8]. This in itself is inadequate as an indication of storage life of rubbers as it is possible for the modulus to remain relatively constant, whilst properties are changing markedly.

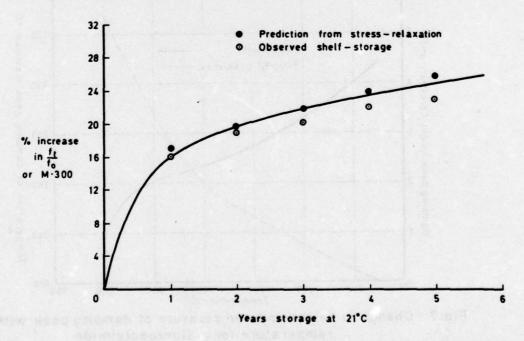


Fig. 8 Comparison of modulus changes predicted from stress-relaxation experiments and those observed during shelf-storage

More success has been achieved with butyl rubbers (8). For a sulphur accelerator cured system it was shown that the reactions leading to changes in network structure at or near room temperature were predominantly non-oxidative in nature. Hence oxygen bomb, or conventional oven ageing tests are inappropriate for assessing suitability of this formulation for use, or storage, under these temperature conditions. Results of intermittent stress-relaxation tests in nitrogen, however, give useful indications of the long term stability of the vulcanisate when stored in the unstrained condition. More interesting was the finding that by using a two network model for the ageing rubber under 20% strain, it was possible to calculate from the relaxation results "permanent set" values, which agreed well with compression set values obtained during long term storage under ambient conditions [Figure 9]. This agreement encourages the hope that accelerated ageing techniques, when carried out under the right conditions can be of value in the difficult area of assessing life in storage or in use of a continuously strained rubber.

DYNAMIC VISCOELASTIC MEASUREMENTS

With the Rheovibron direct-reading viscoelastometer absolute measurements can be made of the complex dynamic tensile modulus and of the mechanical loss factor at different frequencies. With suitable modifications the tensile shear modulus and the corresponding loss factor can also be obtained.

We have used the apparatus to examine the effects of exposure to high humidity upon the dynamic mechanical properties of epoxy-polyamide and fluoropolyimide adhesives. Only small test-pieces are required, but measurements have to be made over a range of test lengths of the specimens to obtain a correction factor, which is applied to the measured values of the dynamic forces. This has to be done to allow for the error imposed on the measurements by the modulus of elasticity and displacement of the Rheovibron stress gauge and its chuck during passage of a sinusoidal wave. Accurate measurements of the dimensions of test-pieces are required. The apparatus is not easy to set up and some determinations are tedious to make. Automation of the instrument would overcome this.

Exposure of an epoxy-polyamide adhesive in film form to high humidity resulted in a large water pick-up (11-14%) and a substantial decrease in the complex dynamic tensile modulus (9). Figure 10 shows the effect of exposure to a laboratory environment; at 43°C and 97% RH the modulus fell to approximately 0.33 GN/m². If the water were then removed, the original value of the modulus was restored. No corresponding effects of moisture were observed for fluoropolyimide adhesives. DSC measurements on the same epoxy-polyamide samples showed that the Tg was lowered by a maximum of approximately 40°C on exposure and that the original value was regained on drying out. In contrast to these reversible changes observed in the adhesive film, bonded joints made with the adhesive suffered losses in strength, when aged in humid conditions, which could not be restored by removal of water. The mode of failure of the joints changed progressively from wholly cohesive to predominantly adhesive with moisture absorption. The results, therefore, indicate that the primary role of water in joint degradation was to displace adhesive from the metal substrate and not to induce cohesive failure of the adhesive itself. Attempts to improve durability with this adhesive must therefore be directed to increasing the moisture resistance of the interface by the use of surface pretreatments and primers capable of rendering the metal surface less susceptible to attack by moisture, or by the use of adhesion promoters whose primary role would be to increase the extent of covalent bonding between the adhesive and the metal substrate.

CONCLUSIONS

In the table we have attempted to summarise the salient features of the six techniques discussed. The table shows where the techniques complement one another and what are some of the advantages and disadvantages of the individual methods. Obviously the application of a number of tests rather than just one to a polymer results in a much

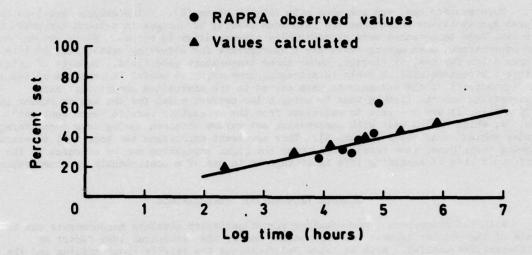


Fig. 9 Long term permanent set in butyl rubber at room temperature

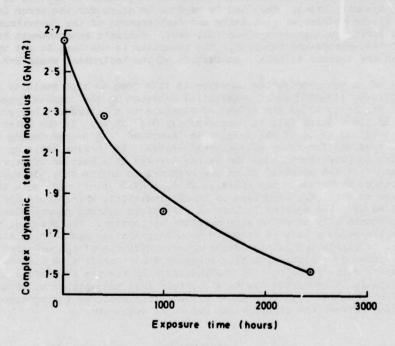


Fig.10 Effect of laboratory environment (20°C, 34% RH) on the complex dynamic tensile modulus of an epoxy-polyamide adhesive

COMPARISON OF THERMOANALYTICAL METHODS

) .

	TG	DSC	TMA
Parameters measured	Weight loss	Differential heat flow	Penetration under load. Thermal expansion.
Main uses	Measurement of (a) Thermal stability (b) Efficiency of antioxidants (c) Cure (of some resins	Measurement of (a) Transitions (b) Cure (c) Efficiency of antioxidants (d) Purity	Measurement of (a) Transitions (b) Cure (c) Modulus (d) Creep (e) Thermal expansion (f) Swelling behaviour
Advantages	Quick. Easy. Small samples, no specific form	Quick. Small samples, no specific form. Sensitive to any thermal reaction. Parameter measured directly related to cure.	Quick. Small samples. Measures transitions below Tg.
Disadvantages	Weight loss only recorded.	Results depend on thermal history of sample. Transitions below Tg not detected. Thermal changes only recorded.	Transitions measured affected by stress applied. Samples need careful preparation.

TBA	Stress-relaxation	Dynamic mechanical
Modulus of braid. Mechanical loss.	Change in stress for fixed strain.	Dynamic tensile modulus. Mechanical loss.
Measurement of (a) Transitions (b) Cure (c) Modulus (d) Effect of environment on mechanical properties	Measurement of (a) Thermal stability of rubbers (b) Efficiency of antioxidants	Measurement of (a) Modulus (b) Effect of environment on mechanical properties
Directly related to composites. Polymers can be studied in liquid state above Tg. Modulus can be followed through cure to degradation.	Indicates where chain scission occurs.	Gives absolute values of modulus.
Samples must melt, or dissolve, for braid to be made. Gives only relative moduli. Does not distinguish between Tg and Tm.	Limited to elastomers. Laborious. Needs sheet for specimens.	Laborious. Needs sheet, or film for specimens. Accurate testpiece dimensions required. Tests must be made over range of lengths.

fuller and more definite characterisation. The particular features of a polymer defined by these thermoanalytical techniques are:

1. Transition temperatures and the effect of environment upon these.

Note that Tg is related to the maximum temperature of use of a thermoplastic and the minimum temperature of use of an elastomer. For a thermoset large changes in mechanical properties may also occur at Tg and this would then represent a limiting temperature for use. Sub-Tg transitions may be of importance for impact and toughness properties.

2. Curing cycle and degree of cure of a crosslinked system.

Cure affects mechanical properties and the retention of these under various environmental conditions.

- 3. Thermal stability.
- Certain physical and mechanical properties e.g. modulus, creep, thermal expansion.

All of the methods cited can normally be applied to a base polymer, or a particular formulation of it. They are not strictly non-destructive tests, but the quantity of material needed in many cases is so small that it could be taken from a component without detriment. For monitoring of service life it would be necessary first of all to ascertain precisely what are the relationships between the properties of crucial interest and the change of these in use, and the parameters measured by the thermoanalytical techniques.

REFERENCES

- R. A. Dine-Hart, D. B. V. Parker and W. W. Wright, "Oxidative Degradation of a Polyimide Film" III Kinetic Studies. Br. Polym. J. 3, 235 (1971).
- J. M. Barton, "Thermoanalytical Investigation of the Cure of a Melt Processable Polyimide System" Part 2. Thermogravimetry as a Method for Monitoring Batch Variability.
 RAE Technical Report 72113 (1972).
- J. M. Barton, "Investigation of the Cure Process in an Aromatic Amine Cured Epoxide Resin by Thermoanalytical Techniques".
 RAE Technical Report 72182 (1972).
- 4. J. M. Barton and G. J. Knight, "The Thermal Analysis of some Addition Type Polyimides" RAE Technical Report 75082 (1975).
- J. M. Barton, "Thermomechanical Analysis of Viton B Rubber: The Effect of Additives on Creep at High Temperatures".
 RAE Technical Report 73125 (1973).
- 6. J. H. Sewell, Unpublished RAE work (1973).
- D. K. Thomas and B. B. Moore, "The Prediction of Shelf-Storage Life in Rubbers from Accelerated Heat Ageing Tests" Part 2. Stress-Relaxation Tests. RAE Technical Report 68016 (1968).
- D. K. Thomas, "Stress-Relaxation Studies in Butyl Rubber". RAE Technical Report 74108 (1974).
- 9. R. I. Butt and J. L. Cotter, Unpublished RAE work (1975).

DIFFERENTIAL SCANNING CALORIMETRY APPLICATIONS IN THE THERMAL, KINETIC, AND RHEOLOGICAL CHARACTERIZATION OF THERMOSETTING SYSTEMS

Musa R. Kamal

Chemical Engineering Department
McGill University, Montreal, Canada

ABSTRACT

Differential scanning calorimetry (DSC) is a versatile tool for the study of the cure of thermosetting systems. Isothermal and scanning DSC studies yield information about the rate of exothermic heat generation, the rate of cure, the variation of the degree of cure with time, and specific heat. This information is quite useful in the study of the thermal history and the distribution of the degree of cure in time and space in thermoset products. Also, kinetic data obtained from DSC analysis may be integrated with rheological data to yield information about the activation energy for viscous flow and to isolate the effects of temperature, degree of cure, and shear rate on the viscosity of thermosetting melts. It is proposed that these techniques may be extended to study the thermo-mechanical behavior of thermosetting solids and composites.

INTRODUCTION

Thermosetting reactions have been studied with the help of swelling measurements (1,2), spectroscopic analysis (3-11), rheological measurements (12-21), torsional and flexural braid analysis (22-27), electrical conductivity measurements (8,28), and a variety of other techniques. However, thermal analysis of the type normally obtained with the differential scanning calorimeter (DSC) has the advantage of simultaneously yielding thermal and kinetic data for the reacting system. Differential scanning calorimetry has been used by a number of workers in both the isothermal (8,18,29-36) and non-isothermal (18,32,33,37-39) modes to study the cure kinetics and thermal properties of thermosets. The attraction of DSC measurements lies in the generally valid assumption that the rate of heat generation is proportional to the rate of the cure reaction. This situation allows for a simple derivation of kinetic data from DSC measurements.

In the isothermal mode, DSC measurements may be employed to determine the cumulative and rates of heat generation as functions of time and temperature. Such information is usually valuable in process and equipment design for the manufacture of thermoset products. Isothermal DSC data are also useful in deriving the kinetic parameters for the cure reaction. Naturally, the utility of the kinetic parameters and their validity depend on the application of a realistic kinetic model to describe the reactions which prevail during cure. With the aid of such a model, kinetic rate constants and cure activation energies may be estimated.

Scanning (non-isothermal) DSC studies have been used by some workers (31) to estimate kinetic parameters. However, the procedure tends to be more complex than in the case of isothermal measurements. Furthermore, unless care is taken in the analysis of the data, the direct utilization of scanning studies for kinetic characterization could be misleading, since some unrealistic kinetic models could fit scanning results without necessarily fitting isothermal cure data. However, scanning experiments could be employed in conjunction with isothermal experiments to determine the variation of the specific heat of thermosetting systems with temperature and cure level. Also, data obtained from both isothermal and non-isothermal experiments are valuable in the analysis of commercial systems employed in the cure of thermosets to determine the thermal history and the distribution of degrees of cure as a function of time and position in commercial moldings.

Finally, DSC measurements are useful in the understanding and analysis of the thermo-mechanical behavior of thermosetting systems, in both the molten and solid states. In the melt, coupling DSC data with rheological measurements helps in the estimation of the activation energy of viscous flow and in isolating the effect of shear rate on viscosity. Similarly, since in many cases some post-curing occurs during the thermo-mechanical testing of thermoset solids and composites, DSC data could be coupled with thermo-mechanical measurements to isolate the effects of reaction from purely mechanical and thermal effects.

In the following discussion, some of the applications of DSC measurements to the characterization of the energetics, kinetics, and melt rheology of thermosetting systems are considered.

ISOTHERMAL CURE DATA

Isothermal Heats of Reaction

Figure 1 shows a set of DSC thermograms obtained during the isothermal cure of various epoxy systems consisting of a commercial diglycidyl ether of bisphenol A (Dow Chemical Resin, DER 332) and m-phenylene diamine (m-PDA; Aldrich Chemical Co; 99% pure) (36). The system containing stoichiometric quantities of epoxide and diamine is referred to as EPO-1.0, where the number B = 1.0 reflects stoichiometric quantities of ether and diamine. Other numbers, e.g., B = 1.5, refer to different ratios of diamine to epoxide, i.e., 1.5 times the stoichiometric ratio in this case. By assuming that the rate of heat generation is proportional to the rate of reaction, the data of Figure 1 may be employed to yield information regarding the variation of the rate of reaction with reaction time and temperature. Integral curves obtained by calculating the areas under the various curves of Figure 1 as a function of time yield information regarding the variation of the integral heat of reaction and the corresponding cure level with time. Finally, integral and rate of heat of reaction data can be used to show the dependence of the rate of cure on cure level and temperature.

A number of observations may be made regarding DSC thermograms obtained for cure reactions. Firstly, it is observed that cure thermograms exhibit a peak at some intermediate level of cure. The peak may be explained by the combined effects of the auto-catalytic nature of cure reactions, which contributes to the increase in rate of polymerization at the low cure levels, and the onset of a diffusion controlled reaction mechanism above the gel point, which contributes to a lowering of the measured reaction rate. Careful analysis of the location of the peak suggests that it occurs at the gel point of the reaction mixture. This is supported by the observation that

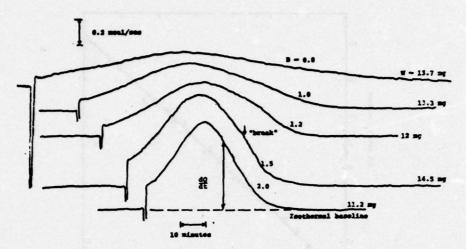


Figure 1. Typical DSC exotherm curves showing the effect of the stoichiometric m-FDA ratio, B, on the isothermal cure rate of DER-332 at 355 K for different sample weights, W.

the cumulative heat of cure from the beginning of cure to the peak is a constant value, which is independent of temperature for a given resin system (36). More conclusive evidence is provided by the good correlation obtained between kinetic gel times determined from the position of the peak in the DSC thermogram and the rheological gel time determined for the same system on the basis of viscosity measurements. The rheological gel time is taken as the time at which the rate of rise of isothermal viscosity. of the system, which is measured with the aid of a cone-and-plate rheometer, increases abruptly to very high levels of viscosity characteristic of rubbery materials. A comparison between the kinetic and rheological gel times is shown in Figure 2 (36). Figure 2 also shows that good agreement is obtained between the above gel time and the one determined from torsional braid analysis (TBA) for the same system (26).

The second important observation in relation to isothermal DSC thermograms concerns the total area under the isothermal rate of cure curve, $\mathbf{Q}_{\mathbf{T}}.$ It is observed that $\mathbf{Q}_{\mathbf{T}}$ increases with the cure temperature, reaching an asymptotic constant value, $\mathbf{Q}_{\mathbf{U}},$ at high temperatures exceeding a value, $\mathbf{T}_{\mathbf{U}},$ which depends on the resin system. Figure 3 shows typical results for EPO-1.0 and EPO-1.5 (36). These results suggest that isothermal cure in the DSC at temperatures below $\mathbf{T}_{\mathbf{U}}$ does not yield a completely cured system. Instead, a level of residual reactivity may be associated with the quantity $(\mathbf{Q}_{\mathbf{U}}\text{-}\mathbf{Q}_{\mathbf{T}}).$ The relative residual reactivity defined as $(1-\mathbf{Q}_{\mathbf{T}}/\mathbf{Q}_{\mathbf{U}})$ appears to decrease exponentially with temperature (36).

Isothermal Cure Kinetics

When the differntial scanning calorimeter is used in the kinetic analysis of thermosetting reactions, it is important to employ a realistic kinetic model to describe the critical reactions occuring during cure. A suitable model must be consistent with the assumptions employed in the analysis and must yield results which are in reasonable agreement with experimental data. Some models which have been found suitable for the treatment of cure studies of a variety of systems are described below.

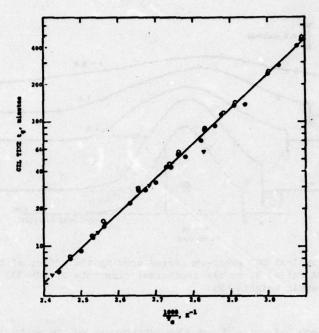


Figure 2. Arrhenius plot of gel time for EPO-1.0 during isothermal cure at T_c ; (0) kinetic gel time from DSC, (0) rheological gel time from viscosity measurements, (V) mechanical gel time from TRA, (Reference 26).

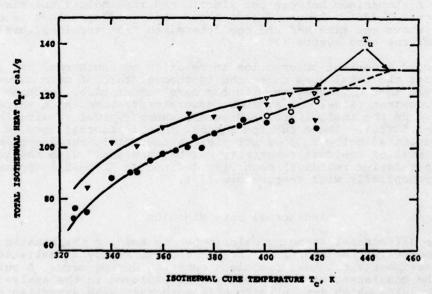


Figure 3. Total heat of reaction, Q_T , at different isothermal cure temperatures, T_C , for EPO-1.0 (0,0) and EPO-1.5 (∇ , ∇).

Ideally, the kinetic model should be derived directly from a treatment of the relevant reactions occuring during cure. However, since the cure reaction is rather complex, especially in the latter stages which follow the gel point, it is not always possible to obtain exact kinetic relationships. For example it has been shown (36) that the early stages of the polymerization reaction between an epoxide and a primary amine may be described by the following equation.

$$\frac{d\alpha}{dt} = (K_1 + K_2\alpha) (1-\alpha) (B-\alpha)$$
 (1)

where α is the fraction of the original epoxide reacted at time t, B is the initial ratio of diamine equivalents to epoxide equivalents, and K_1 and K_2 are rate constants. By fitting experimental DSC data to Equation (1), the rate constants K_1 and K_2 may be estimated at various temperatures, and thus, the kinetic rate equation governing the reaction is obtained. The activation energies of the respective reactions associated with K_1 and K_2 may be obtained from Arrhenius plots of data obtained at various temperatures, as shown in Figures 4 and 5. On the basis of these plots, the following relationships are derived for EPO-1.0.

$$K_1 \text{ (min}^{-1}) = 5.53 \times 10^8 \exp(-19.4 \text{ k cal. mol}^{-1}/\text{RT})$$
 (2)

$$K_2 (min^{-1}) = 8.06 \times 10^5 \exp(-11.4 \text{ k cal. mol}^{-1}/\text{RT})$$
 (3)

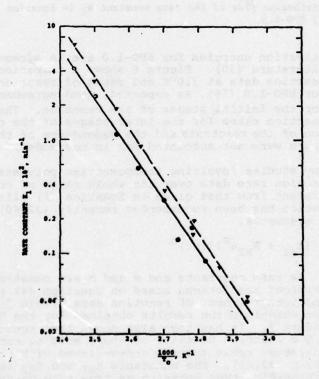


Figure 4. Arrhenius plot of the rate constant K, in Equation (1); (0) EPO-1.0, (7) EPO-1.5.

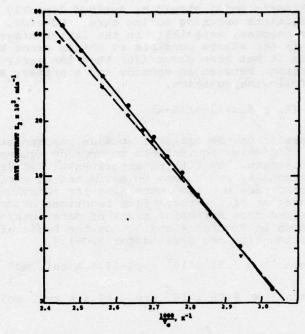


Figure 5. Arrhenius plot of the rate constant K_2 in Equation (1); (0) EPO-1.0, (∇) EPO-1.5.

The calculated activation energies for EPO-1.0 are in agreement with values reported in the literature (30). Figure 6 shows a comparison between experimental rate of reaction data at 330°K and rates of reaction as calculated by Equation (1) for EPO-1.0 (36). As expected, good agreement (within ± 5%) is obtained for the initial stages of the reaction. The model, however, predicts higher reaction rates for the later stages of the cure reaction since the diffusion of the reactants and the dependence of the rate constants on the extent of cure were not accounted for in the model.

Since, in many studies involving thermosetting polymers, it is desirable to obtain reaction rate data over the whole range of cure levels, a rate equation different from that given in Equation (1) will be required. The following equation has been recommended recently (32,40) on the basis of semi-empirical arguments.

$$\frac{d\alpha}{dt} = (\kappa_{R1} + \kappa_{R2}\alpha^{m}) (1-\alpha)^{n}$$
(4)

Where K_{R1} and K_{R2} are rate constants and m and n are constants independent of temperature. Typical predictions based on Equation (4) yield rate of heat generation and integral heat of reaction data within $^+$ 5% of experimental results. An example of the results obtained for the EPO-1.0 system is shown in Figure 7. It has been also shown that Equation (4) is useful in describing the reaction behavior of epoxy molding compounds (41,42) and unsaturated polyester resin systems cross-linked with styrene and a free radical catalyst (32,43). The constants K_{R1} and K_{R2} appear to obey the Arrhenius relationship, thus behaving as true rate constants. Equation (4) is significantly superior to other empirical equations which postulate first order or n-th order cure reaction mechanisms, since such equations do not predict a peak in the reaction rate, as indicated by DSC studies.

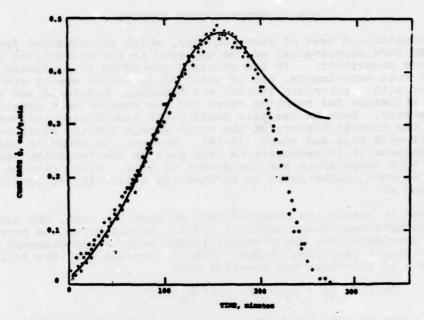


Figure 6. Comparison between experimental (0) and calculated (---) isothermal cure rates for EPO-1.0 at 330 K using the model of Equation (1).

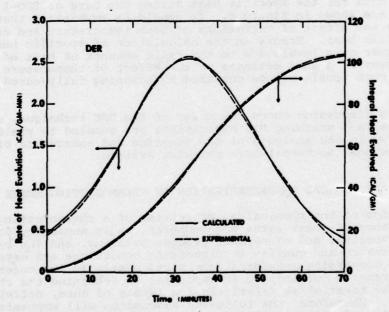


Figure 7. Comparison between experimental and calculated isothermal cure rates for EPO-1.0 at 367 K using the model of Equation (4).

NON-ISOTHERMAL CURE STUDIES

The kinetic and heat of reaction data, which are obtained from isothermal DSC cure experiments, may be employed in the analysis of non-isothermal cure experiments. In the standard procedure of analyzing non-isothermal cure experiments, the relevant equations of energy are solved in conjunction with appropriate initial and boundary conditions and with the necessary allowance for reaction rates and the rate of heat generation by the reaction. Such an analysis could yield significant information regarding the thermal history of the cured sample and the distribution of cure levels with time and space (44-46). However, in order to carry out such an analysis it is necessary to have data on the variation of specific heat with both temperature and the extent of cure. Also, data on the variation of thermal conductivity or diffusivity under similar conditions would be needed.

In order to obtain the required data on specific heat, DSC scanning experiments have been found useful (32,43). According to the proposed numerical procedure, the experimental linear scan is approximated by a sequence of equal isothermal steps. This is coupled with the following heat balance to calculate the specific heat

$$Cp(\alpha,T) \frac{dT}{dt} - \dot{Q}_{s}(\alpha_{o},T_{o},T,S) - \dot{Q}_{R}(\alpha,T)$$
 (5)

where Cp is the specific heat of the sample, \dot{Q}_{S} is the experimentally recorded rate of heat input to the system, and \dot{Q}_{R} is the rate of heat generation by the curing reaction at the prevailing degree of cure, α , and temperature, T. Also, α_{O} and T_{O} refer to the initial degree of cure and temperature, respectively, and S is the scanning rate, which is usually held constant.

Typical data for the specific heat during the cure of EPO-1.0 epoxy resin system are shown in Figure 8. It should be emphasized that the curves represent the net effect of variations of both temperature and degree of cure on specific heat. Errors in the calculation of specific heat become larger at higher cure levels due to the small amounts of heat of reaction involved. However, a good estimate of the effect of temperature on specific heat at high cure levels may be obtained by scanning fully-cured samples in the DSC.

The above discussion shows the power of the DSC technique, especially when isothermal and scanning DSC experiments are coupled to yield information of value in the analysis of the kinetics and energetics of both isothermal and non-isothermal cure reaction systems.

THE RHEOLOGICAL CHARACTERIZATION OF THERMOSETTING MELTS

A knowledge of the rheological properties of a thermosetting material over a wide range of shear rates and temperatures is necessary for understanding, diagnosing, and overcoming process problems, and for relating product performance and quality to processing conditions and material properties. From processing considerations, particularly in the cases of injection and transfer molding, it is important to determine the rheological behavior of the material at relatively low levels of cure, definitely before the gel point. Therefore, the following discussion will emphasize the viscous behavior of thermosetting melts at relatively low levels of cure.

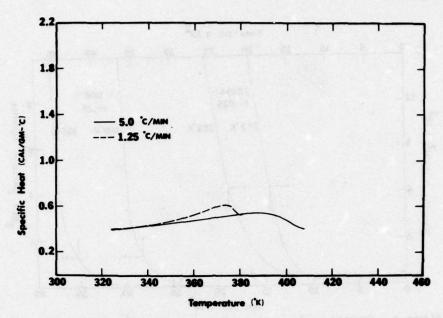


Figure 8. Variation of specific heat of EPO-1.0 during scanning at dif-

Usually, viscosity measurements are carried out in either rotational or capillary devices. One of the most versatile rotational devices is the cone-and-plate viscometer. Cone-and-plate viscometry is limited to the low shear rate regime due to the loss of material and flow instabilities encountered at moderate rates of shear. In order to obtain information on the high shear rate viscous behavior, a split-barrel capillary rheometer may be employed (42).

Typical viscosity-time isotherms for EPO-1.0 and a commercial epoxy molding compound (Fiberite E-8354J) are shown in Figure 9 (42). These data were obtained with the Rheometrics Mechanical Spectrometer. The apparent viscosity changes only slightly with time until the cross-linking reaction becomes significant. Near the gel point, the viscosity rises rapidly with time until the material is transformed to a rubbery, and then a hard mass.

Several writers have reported on the flow characteristics of thermoset systems during the cure reaction by treating data similar to those given in Figure 9 (12,16,7,19-21,47-55). However, in most cases, rheological data were analyzed independently of kinetic data or on the basis of inadequate kinetic models. Recently, experimental and analytical procedures were recommended for a systematic integration of rheological and kinetic data for thermosetting resins (18,43,56). It has been shown that such integration yields useful information regarding the activation energy of viscous flow at various levels of cure. The critical aspect of the proposed procedure consists of coupling viscosity-time data obtained with the rheometer to degree of cure-time data obtained with the differential scanning calorimeter. Thus, the data shown in Figure 8 may be redrawn to yield curves depicting the dependence of viscosity on degree of cure at various temperatures. By making Arrhenius plots of the logarithm of viscoisty vs. the inverse of the absolute temperature, as shown in Figure 10, the activation energy of viscous flow may be estimated at various levels of cure, a,

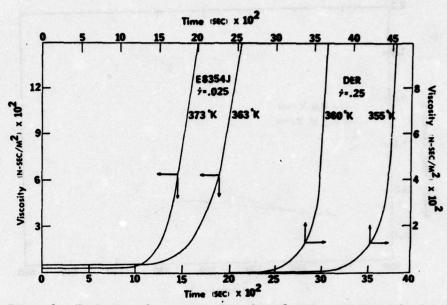


Figure 9. Variation of apparent viscosity of epoxy systems with time during isothermal cure.

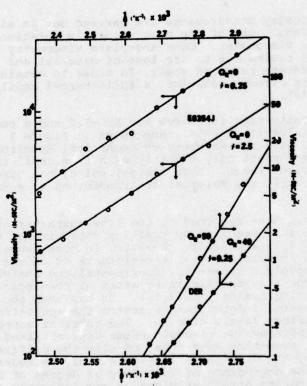


Figure 10. Variation of apparent viscosity of epoxy systems with temperature at constant shear rate and degree of cure.

or the equivalent cumulative heats of cure, Q_R (42). Table 1 summarizes activation energy data for the epoxy resin DER-332, obtained at a shear rate of 0.25 sec. (42). As expected, the activation energy of viscous flow rises as the degree of cure increases. The technique may be extended to isolate the effect of shear rate on the viscosity of reacting thermosetting systems.

CONCLUSION

The above discussion demonstrates the utility of the differential scanning calorimeter in supplying valuable information about the energetics and kinetics of thermosetting reactions. However, the value of the kinetic data and its utility in understanding other aspects of the behavior of thermosets depend on the validity of the kinetic model which is employed in the kinetic analysis. It has been shown above that the understanding of the flow behavior of thermosetting melts is enhanced significantly when kinetic, thermal, and rheological data are integrated in an appropriate manner. It is expected that these procedures may be extended in a similar fashion to study the thermomechanical behavior of thermosetting solids and composites.

ACKNOWLEDGEMENTS

The author wishes to express his thanks to Mr. S. Sourour and Mr. M.E. Ryan from the Chemical Engineering Department; McGill University for their contributions to developing many of the techniques discussed above.

TABLE 1
PLOW ACTIVATION ENERGY FOR DER-332

QR		ΔEη	
CAL/GRAM	J/KG	KCAL/MOLE	J/MOLE
30	1.26 x 10 ⁵	7.8	3.26 x 10 ⁴
40	1.67 x 10 ⁵	10.1	4.23 x 10 ⁴
50	2.09 x 10 ⁵	13.4	5.61 x 10
60	2.51 x 10 ⁵	16.2	6.78 x 10 ⁴
70	2.93 x 10 ⁵	21.7	9.08 x 10 ⁴
80	3.35 x 10 ⁵	39.5	1.65 x 10 ⁵

REFERENCES

- 1. B.M.E. Van der Hoff, Applied Polymer Symposia, 7, 21 (1968).
- 2. J. Barton, J. Polymer Sci., Part A-1, 6, 1315 (1968).
- 3. J.C. Illman, J. Appl. Polymer Sci., 10, 10, 1519 (1966).
- 4. R. Jenkins and L. Karre, J. Appl. Polymer Sci., 10, 2, 303 (1966).
- 5. T. Imai, J. Appl. Polymer Sci., 11, 7, 1055 (1967).
- T.F. Saunders, M.F. Levy and J.F. Serino, J. Polymer Sci., Part A-1, 5, 7, 1609 (1967).
- 7. P. Fijolka and Y. Shabab, J. Polymer Sci., Part A-1 6, 5, 1217 (1968).
- M.A. Acitelli, R.B. Prime and E. Sacher, Polymer, 12, 5, 335 (1971).
- 9. M.G. Rogers, J. Appl. Polymer Sci., 16, 8, 1953 (1972).
- J.L. Koenig and P.T.K. Shih, J. Polymer Sci., Part A-2, <u>10</u>, 4, 721 (1972).
- 11. R. Fountain and T.W. Haas, J. Appl. Polymer Sci., 19, 6, 1767 (1975).
- 12. A. Shimazaki, J. Appl. Polymer Sci., 12, 2013 (1968).
- 13. R.E. Cuthrell, J. Appl. Polymer Sci., 12, 4, 955 (1968).
 - Yu. V. Zherdev, M. Yu. Korindyasova and T.S. Tatarenko, Soviet Plastics 4, 17, (1969).
 - A.E. Moehlenpah, A.T. Dibendetto and O. Ishai, Polymer Eng. Sci., 10 3, 170 (1970).
 - 16. D. Craig, Soc. Plastics Engrs. Technical Papers, 18, 533, (1972).
 - 17. F.G. Mussatti and C.W. Macosko, Polymer Eng. Sci., 13, 3, 236 (1973).
 - M.R. Kamal, S. Sourour and M. Ryan Soc. Plastics Engrs. Technical Papers, 19, 187 (1973).
 - 19. R.P. White Jr., Polymer Eng. Sci., 14, 1, 50 (1974).
 - 20. P.E. Willard, Polymer Eng. Sci., 14, 4, 273 (1974).
 - 21. M.B. Roller, Polymer Eng. Sci., 15, 6, 406 (1975).
 - 22. A.F. Lewis, and J.K. Gillham, J. Appl. Polymer Sci., 6, 22, 422 (1962)
 - 23. J.K. Gillham and A.F. Lewis, J. Appl. Polymer Sci., 7, 6, 2293 (1963)
 - 24. J.K. Gillham and M.B. Roller, Polymer Eng. Sci., 11, 4, 295 (1971)
 - 25. J.K. Gillham and H.C. Gillham, Polymer Eng. Sci., 13, 6, 447 (1973).
 - P.G. Babayevsky and J.K. Gillham, J. Appl. Polymer Sci., <u>17</u>, 7, 2067 (1973).

- J.K. Gillham, J.A. Benci and A. Noshay, J. Appl. Polymer Sci., <u>18</u>, 4, 951 (1974).
- G.S. Learmouth and G. Pritchard, J. Appl. Polymer Sci., <u>13</u>, 10, 2119 (1969).
- K. Horie, I. Mita and H. Kambe, J. Polymer Sci., Part A-1, 8, 10, 2839 (1970)
- K. Horie, H. Hiura, M. Sawada, I. Mita and H. Kambe, J. Polymer Sci., Part A-1, 8, 6, 1357 (1970).
- 31. P.E. Willard, Polymer Eng. Sci., 12. 2, 120 (1972).
- 32. M.R. Kamal and S. Sourour, Polymer Eng. Sci., 13, 1, 59 (1973).
 - 33. E. Sacher, Polymer, 14, 3, 91 (1973).
 - 34. R.B. Prime, Polymer Eng. Sci., 13, 5, 365 (1973).
 - 35. H. Kubota, J. Appl. Polymer Sci., 19, 8, 2279 (1975).
 - 36. S. Sourour and M.R. Kamal, Thermochimica Acta, 14, 41 (1976).
 - 37. O.R. Abolafia, Soc. Plastics Engrs. Technical Papers, 13, 610 (1967).
 - 38. R.A. Fava, Polymer, 9, 137 (1968).
 - R.B. Prime, R.S. in Porter and J.F. Johnson, editors, Analytical Calorimetry, Plenum Press, New York (1970).
 - M.R. Kamal and S. Sourour, Soc. Plastics Engrs. Technical Papers, <u>18</u>. 93 (1972).
 - M.R. Kamal and M.E. Ryan, "Considerations in The Modeling of Thermoset Injection Molding", paper presented at the American Institute of Chemical Engineers Annual Meeting, Chicago, Illinois, Nov. 28-Dec 2, 1976.
- 42. M.E. Ryan and M.R. Kamal, "Thermo-Rheological Analysis of Thermosetting Resins and Molding Compounds", paper presented at the VIIth International Congress on Rheology, Gothenburg, Sweden, August 23-27, 1976.
- 43. M.R. Kamal, Polymer Eng. Sci., 14, 3, 231 (1974).
- J.D. Domine and C.G. Gogos, Soc. Plastics Engrs. Technical Papers, <u>22</u>, 274, (1976).
- E. Broyer and C.W. Mocosko, Soc Plastics Engrs. Technical Papers, 22, 563 (1976).
- 46. Y. Tanaka and H. Kakiuchi, J. Appl. Polymer Sci., 7, 1063 (1963)
- 47. Y. Tanaka and H. Kakicuhi, J. Appl. Polymer Sci., 7. 1951 (1963).
- 48. T Imai, J. Appl. Polymer Sci., 11, 575 (1967)
- J.H.L. Henson, A.J. Lovett, and G.S. Learmonth, J. Appl. Polymer Sci., <u>11</u>, 2543 (1967).

- G.S. Learmonth and G. Pritchard, Soc. Plastics Engrs. J., 24, 11, 47 (1968).
- 51. P.J. Heinle and M.A. Rodgers, Soc. Plastics Engrs. J., 25, 6, 56 (1969).
- 52. N.N. Danilkin and I.F. Kanavets, Soviet Plastics, 1, 27 (1970).
- W.G. Frizelle and J.S. Norfleet, Soc. Plastics Engrs. J., <u>27</u>, 11, 44 (1971).
- 54. W.H. Beck Jr., Soc. Plastics Engrs. J., 27, 5, 43 (1971).
- 55. M.E. Ryan, M.Eng. Thesis, McGill University, 1973.
- 56. R.C. Progelhof and J.L. Throne, Polymer Eng. Sci., 15, 9, 690 (1975).

to the second the second of the second

CHARACTERIZATION OF THERMOSETTING EPOXY SYSTEMS BY TORSIONAL BRAID ANALYSIS

John K. Gillham

Polymer Materials Program, Department of Chemical Engineering

Princeton University, Princeton, New Jersey 08540

SYNOPSIS

An automated torsional pendulum has been used to investigate the cure, transitions and effect of water vapor on epoxy systems. The findings include: 1) that the thermosetting process is characterized by two transition temperatures (T_{gg} and T_{go}) and 2) that a reversible transition [$T_{H20} = -70$ °C (1.6 Hz)] is induced by exposure of an epoxy system to water vapor.

INTRODUCTION

The first part of this communication generalizes earlier results on the cure and transitions of epoxy systems. The second part reports new results on a low temperature water-induced transition.

EXPERIMENTAL

Torsional Braid Analysis (TBA)

An automated torsional pendulum has been developed which permits monitoring of the changes which occur throughout cure and of the transitions which occur in the cured material with change of temperature and environment (1).

The specimen for studying cure is made by impregnating a glass fiber braid in a solution of the reactive system. After mounting, the specimen is intermittently set into torsional oscillation to generate a series of freely damped waves. The frequency of oscillation is about 1 Hz. The character of these waves provides a monitor of changes. Two mechanical functions, rigidity and damping, are obtained from the frequency and decay constants which characterize each wave. A schematic diagram of the pendulum is shown in Fig. 1. This adaptation of the torsional pendulum approach for characterizing small quantities of polymer has been developed under the name "torsional braid analysis (TBA)" (1). The apparatus also serves as a conventional torsional pendulum.

The experiment provides plots of relative rigidity $(1/P^2)$, where P is the period in seconds) and logarithmic decrement $(\Delta = \ln A_1/A_{1+1})$, where A_1 is the amplitude of the 1^{th} oscillation) of freely damped waves. The relative rigidity is directly proportional to the in-phase shear modulus (G'); the logarithmic decrement is directly proportional to the ratio of the out-of-phase shear modulus (G") to G'. G' and G" are material parameters of the specimen which characterize the storage and loss of mechanical energy on cyclic deformation.

Specimens were exposed to various levels (ppm) of water vapor in a flowing stream

of helium which was formed by mixing dry and saturated streams of helium in various proportions. After conditioning at a definite temperature for a measured period of time thermomechanical TBA data were obtained on cooling to -190°C and subsequent heating. The TBA apparatus serves as an efficient trap for water on cooling below 0°C and so the conditioning atmosphere could be used in the testing.

RESULTS AND DISCUSSION

Cure and Transitions

The experimental results for the cure of an epoxy system at a series of constant temperatures can be used to obtain the gelation time and the vitrification time vs cure temperature. These transformation times correspond to peaks in the mechanical damping curves; they also correspond to points of inflection in the rigidity curves (see Fig. 2). Schematic results for isothermal cure of a typical system relating the time to gelation and the time to vitrification to the temperature of cure are summarized in Fig. 3.

It is apparent from Fig. 3 that there are three types of behavior depending on the temperature of cure (2). At high temperatures the liquid gels but does not vitrify. At low temperatures the liquid vitrifies and need not gel -- if reactions are quenched at low degrees of reaction by vitrification. At intermediate temperatures the liquid first gels and later vitrifies (Figs. 2 and 3). The time to gelation decreases exponentially with temperature since the degree of reaction at the point of gelation is constant. On the other hand, it is noted that the time to vitrify passes through a minimum which occurs at intermediate temperatures of cure (3, 4). This reflects competition between the increased rate constants for reaction and the increased degree of crosslinking (and therefore of reaction) required for vitrification at higher temperatures. The temperature at which gelation and vitrification occur together is defined as T_{gg} (Fig. 3) (2). Vitrification can occur before gelation (Tcure < Tgg) simply by an increase of molecular weight. Gelation occurs without vitrification when cure is performed above the maximum softening point of the system, Tgm (Fig. 3). It is also apparent that if reactions cease at vitrification, the softening temperature (glass transition temperature, Tg) of the system after cure will equal the temperature of cure. The vitrification curve therefore gives the time to reach the softening temperature which the system can achieve by curing at T_{cure}. In particular, T_{gg} is the glass transition temperature of the reactive system at its point of gelation (2). A diagram such as Fig. 3 summarizes much of the behavior of the thermosetting process and in particular shows that it is characterized by two temperatures, T_{gg} and T_{gw} . In contrast, thermoplastic materials are characterized only by T_{gw} since gelation does not occur in their formation. The temperatures T_{gg} and T_{gw} are critical parameters which will vary from system to system.

From the practical point of view the diagram (Fig. 3) explains a number of practices in the field of thermosets. Examples follow.

- Finite vs infinite shelf-life: if the storage temperature is below Tgg, a reactive material will convert to a vitrified solid which is stable and can be later "melted" and processed; above Tgg the material will have a finite shelf-life since gelation will occur before vitrification. (A gelled material has "memory" and even if soft does not flow.) This concept lies at the basis of a widespread technology which includes thermosetting molding compounds and "prepregs" with latent reactivity.
- Post-cure: if $T_{\rm cure} < T_{\rm gw}$ a reactive material will vitrify and full chemical conversion may be prevented; the material will then need to be post-cured above $T_{\rm gw}$ for development of optimum properties. As an example, Fig. 4 presents the thermomechanical data after isothermal reaction at an arbitrary temperature for a finite period of time and also after heating the same specimen to well above $T_{\rm gw}$ (5). Using the transitions as a measure of material properties (see Fig. 4), it is apparent that the extent of cure affects not only the value of the glass transition but also properties at temperatures well below it. For the manufacture of objects of large size, it is usually necessary

to go through a two-step process because of the exothermic nature of the reactions.

Influence of reactants: the inherent reactivity of the functional groups together with the geometry and polarity of the growing chain segments will determine the transition temperatures (T_{gg} , T_{g} , $T_{g\infty}$) of each particular system and therefore the types of behavior which will be experienced during cure and after cure. For example, for highly crosslinked or rigid-chain polymeric structures $T_{g\infty}$ can be above the limits of thermal stability. In these cases the thermoset materials need not have measurable glass transition temperatures. In contrast, if $T_{g\infty}$ is below room temperature, the polymer systems will be used as elastomers.

Effect of Water Vapor

The above general results stemmed from examination of a number of epoxy systems with known chemical reactants (2, 3, 4). The present section deals with a proprietary epoxy system which is currently used on aircraft and space vehicles.

A 10 percent solution of the resin was obtained by extraction with acetone at room temperature of a "prepreg" composite material (NARMCO'S RIGIDITE(R) 5209 - UCC Thornel 300) supplied by the formulator. After mounting in the TBA apparatus, the impregnated braid specimen was taken through the cure cycle recommended by the manufacturer (the final stage involved heating at 127°C for 100 minutes). After cooling the cured specimen to -170°C, its thermomechanical behavior was obtained from measurements made during the temperature sequence $-160^{\circ} + 170^{\circ} + -190^{\circ}$ C ($\Delta T/\Delta t = 1.5^{\circ}$ C/min). The results (Fig. 5) show that reactions occurring above the maximum temperature used in the specified cure produced an increase in Tg. By further heating in a similar manner to 200°C the Tg was increased from its original value of 138°C (Fig. 5) to 151°C. Two transitions (< Tg) are also apparent in the data of Fig. 5. That at ca. ~98°C is broadened by post-cure (Fig. 5) and that at ca. 80°C (Fig. 5, shoulder) disappears on further temperature cycling (cf Figs. 5, 6 and 8). Investigations of the effect of water vapor were performed on the same specimen after being further heated at 170°C for 12.5 hr (Tg $^+$ 155°C) in an attempt to fully react the material prior to exposure to water vapor. Exposures were made at different levels (ppm) of water in two conditioning isothermal atmospheres (170°C and 30°C) prior to obtaining the thermomechanical spectra.

The effect of water vapor on the thermomechanical behavior is shown in Fig. 6. In particular, the presence of a loss peak at -68°C (1.6 Hz) and a decrease in intensity of the original low temperature peak are noted. The intensity of the water transition increased with concentration of water in the conditioning atmosphere (Fig. 7) and with decreasing temperature (30°C vs 170°C). Subsequent heating in a dry atmosphere (at 170°C) resulted in elimination of the water transition and in a thermomechanical spectrum (Figs. 7, 8) which was similar to that of the pre-exposed specimen. Using the intensity of the water peak as an index of the quantity of water absorbed, exposure at 30°C resulted in greater pick up of water than exposure at 170°C at the same conditioning level (ppm H₂O).

The decrease in water absorption with increasing conditioning temperature suggests that a complex forms between water and specific chemical sites in the epoxy. The concomitant decrease in intensity of the low temperature secondary transition of the epoxy which accompanies the increase in intensity of the $\rm H_{2}O$ transition suggests further that the two relaxations are coupled. Addition of $\rm H_{2}O$ to a localized flexible segment (e.g. \sim C-C-C-O- \bigcirc \sim)

OH

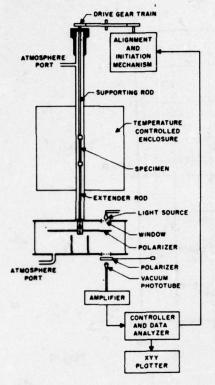
increases its size and restricts its motion until higher temperatures. Other epoxy systems (6) reveal a water-vapor-induced loss peak the temperature of which depends on chemical structure. Examination of an unfilled epoxy specimen using the TBA apparatus as a conventional torsional pendulum (6) showed the presence of a water transition, the presence of which must have been the consequence of an epoxy-water interaction.

REFERENCES

- 1. J. K. Gillham, A.I.Ch.E. J., 20, 6, 1066 (1974).
- 2. P. G. Babayevsky and J. K. Gillham, J. Appl. Polym. Sci., 17, 2067 (1973).
- 3. J. K. Gillham, J. A. Benci and A. Noshay, J. Polym. Sci., Sym. No. 46, 279 (1974).
- 4. C. A. Glandt and J. K. Gillham, Polym. Preprints, Amer. Chem. Soc., 16(1), 694 (1975).
- 5. J. K. Gillham, Polym. Eng. Sci., 16, 353 (1976).
- 6. J. K. Gillham and C. A. McPherson, Unpublished manuscript (1976).

FIGURE CAPTIONS

- Fig. 1. Automated TBA torsional pendulum. An electrical signal is obtained using a light beam passing through a pair of polarizers, one of which oscillates with the specimen. The pendulum is aligned and oscillations are initiated by a dedicated analog computer which also processes the damped sine waves to provide the mechanical rigidity and mechanical damping data which are plotted in immediate time on an XYY plotter.
- Fig. 2. Mechanical rigidity and mechanical damping vs time during cure of an epoxy system at a constant temperature ($T_{gg} < T_{cure} < T_{ge}$). The first peak in the damping curve represents gelation, the second vitrification.
- Fig. 3. Time to gel and time to vitrify vs isothermal cure temperature for an epoxy system. (The dashed sections of the curves represent extrapolation of experimental data). Note the two critical temperatures, T_{gg} and $T_{g\infty}$.
- Fig. 4. Epoxy system: effect of cure on transitions.
- Fig. 5. RIGIDITE 5209: effect of cure on transitions.
- Fig. 6. RIGIDITE 5209: effect of water vapor. [Hysteresis above 0°C is the consequence of elimination of water during heating.]
- Fig. 7. RIGIDITE 5209: effect of water vapor. Specimens were exposed overnight at 30°C to the humid atmospheres before taking measurements on further cooling. [The small gap in the data at 30°C resulted from overnight conditioning after cooling from 170° to 30°C.]
- Fig. 8. RIGIDITE 5209: after removal of water.



0.5 -0.5 -1.5 -2.5 -2.5 -2.5 -2.5 -2.5 -2.5 -3.0 -1.5 -1.5 -1.5 -1.5 -1.5 -1.5 -1.5 -1.5 -1.5 -1.5

Fig. 2

Fig. 1

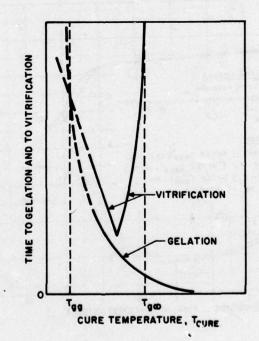


Fig. 3

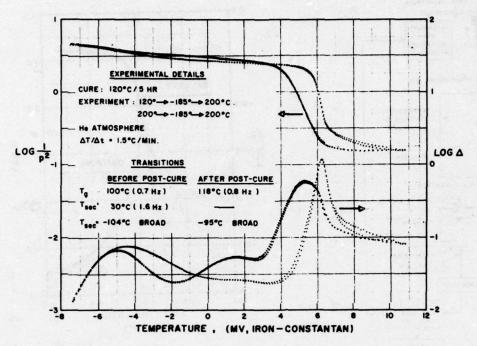


Fig. 4

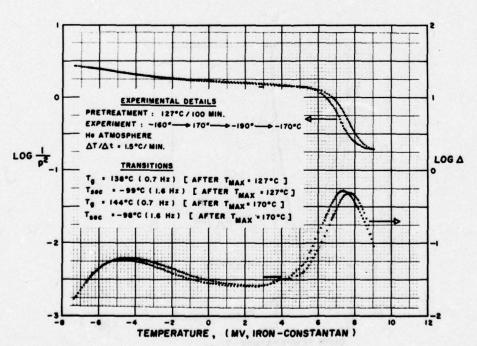


Fig. 5

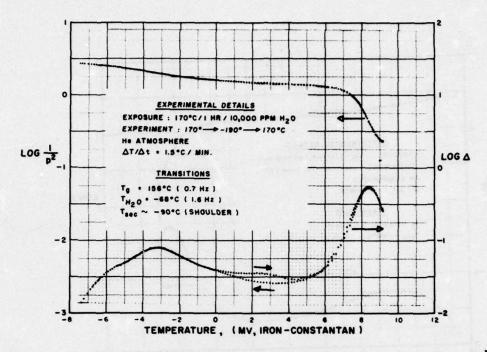


Fig. 6

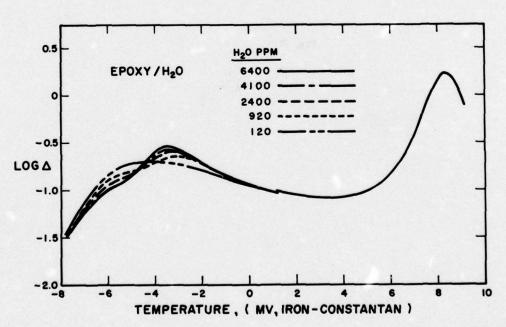


Fig. 7

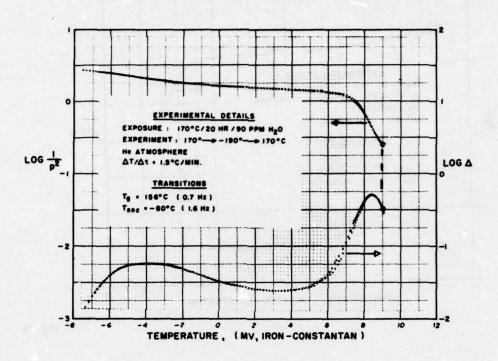


Fig. 8

POLYMER CHARACTERIZATION USING DIFFERENTIAL SCANNING CALORIMETRY

W. D. Bascom and P. Peyser

Naval Research Laboratory Washington, D. C. 20375

INTRODUCTION

Among the methods in use for the thermomechanical characterization of polymers, differential scanning calorimetry (DSC) has notable versatility. The technique can be used to determine "static" properties such as the glass transition temperature (T_g), melting point, and heat capacity and also dynamic properties including reaction kinetics and heating rate effects. Even when these properties or effects are very subtle, DSC has the sensitivity to measure them accurately and the technique has benefited in recent years from advanced data analysis methods and computer controlled data processing. In this paper we wish to describe some of our experiences with DSC not with the intent of covering the subject comprehensively but to illustrate its utility and some of the problem areas.

The material properties measurable using DSC are shown schematically in Figure 1 taken from the Perkin-Elmer Corp. manual for their DSC-2 instrument. Essentially, DSC measures energy change per unit time as a function of time either at constant temperature (isothermal mode) or at some fixed heating rate (scanning mode). The commercial equipment presently available from a variety of manufacturers is of high quality; well engineered and easily calibrated and operated. Moreover, there are computational correction techniques that can be applied to give a level of accuracy better than normally expected from current equipment.

We have a modest but intensive effort in DSC which has been devoted to studying the cure kinetics of simple epoxy resin systems (1,2) and more recently the glass transition temperature of polymers (3). The work is a fundamental research effort aimed at both polymer characterization and refining the DSC technique and appropo of the latter much attention has been given to developing computer methodology for data reduction.

KINETIC STUDIES

The kinetics of polymerization are determined by scanning a small sample of the reaction mixture isothermally or at various fixed heating rates. A typical DSC output is shown in Figure 2 where the heat flow rate is plotted against sample temperature. As is discussed below, the cumulative reaction heat at any given time must be determined accurately so it is important to establish an accurate base line. Actually, there are two baselines: one is for a scan of two empty pans through the temperature range of interest at a specific heating rate and the other is due to the change in specific heat between the start and the finish of a run as indicated in Figure 2. The "empty pan"

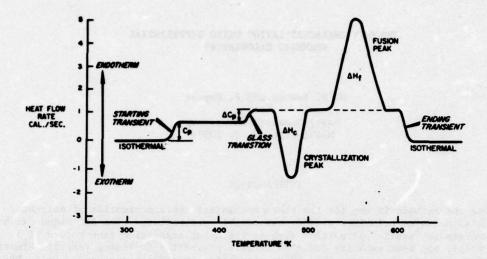


Figure 1: Schematic representation of DSC output (reproduced from Operators Manual, DSC-2, Perkin Elmer Corp., Norwalk, Conn.)

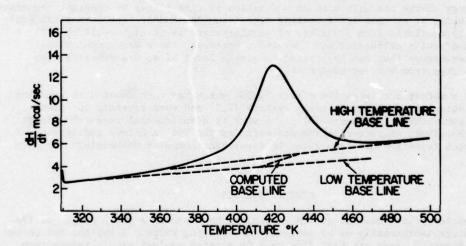


Figure 2: Typical DSC scan (dynamic mode) at 5°/min heating rate showing shift in baseline due to change in specific heat of the sample.

baseline is measured just before the experiment and the data is stored in a computer memory for later, point-by-point subtraction from the experimental data. To deal with the change in specific heat a computer program was developed in which it is assumed that the baseline changes from initial to final condition in proportion to the cumulative heat flow. The procedure is to collect the DSC output at 0.2°K intervals, assume an arbitrary baseline, and convert to h/H, where H is the cumulative heat and H, the total heat, i.e., the area under the curve of Figure 2. The "empty pan" background is subtracted and the data smoothed by a 5-point smoothing program. Correction for the experimental background is made by an iterative program that assumes the change in background is proportional to H/H, and the process is continued until H_T approaches a constant value, i.e. about three iterations.

The underlying assumption of DSC reaction kinetics is that the extent of reaction at any time is proportional to the evolved heat of reaction. The Arrhenius equation becomes

$$k = \frac{1}{H_T} \frac{dH}{dt} = A \exp E_a / RT \left(\frac{H_r}{H_T}\right)^n$$

where A is the frequency factor, E athe activation energy, $H_{\rm c}=(H_{\rm c}-H)$ and n the reaction order. The simplest way of treating DSC data is to put equation 1 into logrithmic form and plot lnk \underline{vs} 1/T for some assumed value of n. Such a plot is given in Figure 3 from a study (2) of the polymerization of diglycidyl ether bisphenol A (DGEBA) and hexahydrophthalic anhydride (MHPA) catalyzed with benzyldimethylamine (BDMA). The data fit to the simple Arrhenius kinetics is quite good; surprisingly so for polymerization of a thermosetting resin which generally follow complex kinetics (4) requiring multiparameter equations to give an adequate fit to the data. However, studies of anhydride-epoxy resin polymerizations by DSC and other methods have generally found simple kinetics at least during the early stages (2).

The reaction parameters can be obtained from DSC data, still within the Arrhenius model, by analysis other than the direct application of equation 1. These analyses, most of which were developed for thermal gravimetric analysis (5), are based on manipulation of equation 1 and their application to a given set of data can sometimes reveal features of the reaction that data analysis by a single method might miss. Data taken in the seamning mode can be treated by noting that at the maximum point of the DSC curve, d $^{\rm H}/{\rm dt}^2=0$, and differentiation of equation 1 gives an expression for $\rm E_{a/n}$ in terms of the heating rate and H. Similarly, since the Arrhenius equation is independent of heating rate, data compared at constant fraction reacted for different heating rates can be plotted to give E $_{a}/{\rm R}$. Finally equation 1 can be transformed according to the method of Freeman and Carroll (5,6) to obtain an expression that gives E and n independently. The results of using these four methods on the DGEBA/HHPA/BDMA data are given in Table 1 and the good correlation between the computational methods is evident.

This reaction was also studied in the isothermal mode where the sample is heated rapidly to and held at some fixed temperature. The form of the isothermal DSC output is illustrated in Figure 4. This method suffers from the fact that the heat flow in the early stages of reaction cannot be accurately determined. This problem is circumvented if the selected temperature is low enough that equilibration can be reached quickly but high enough that the reaction goes to completion. At a properly selected temperature equilibration can be reached before 10% of the reaction has occurred.

In the isothermal study of the DGEBA/HHPA/BDMA system data analysis again based on the Arrhenius model gave $\rm E_a$ = 21 kcal/mole and n \gtrsim 1 in good agreement with the dynamic results. Actually, the isothermal study indicated a significant temperature dependence for the reaction order which had not been evident from the dynamic studies.

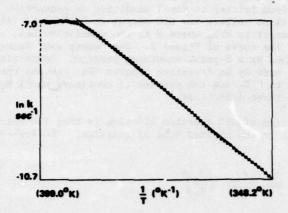


Figure 3: Arrhenius plot of DSC data for a dynamic mode scan of an epoxy resin: DGEBA/HHPA/BDHA (reference 2)

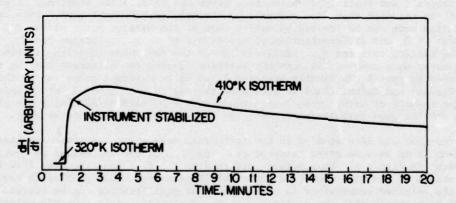


Figure 4: Typical DSC scan (isothermal mode). Note stabilization of reaction during heat up.

A similar kinetics study was made of the cure of DGEBA resin with nadic methyl anhydride (NMA) and BDMA as catalyst. This work demonstrated the value of a complete analysis of DSC data. The lnk vs 1/T results are plotted in Figure 5 for a dynamic scan and the data give clear evidence for an abrupt change in kinetics of about 12% completion. The results using the four computational methods are given in Table II. The change in kinetics was detected when the data were treated by the Freeman-Carroll method and from Arrhenius plots (Figure 5) but would not have been recognized from the maximum term or variable heating rate treatments alone.

Our explanation for the change in kinetics (1) is that the reaction becomes diffusion controlled after 10-12% completion. A similar discontinuity did not occur for the HHPA-cured system possibly because the molar volume of HHPA is 70% less than the molar volume of NMA.

THE CLASS TRANSITION TEMPERATURE

The temperature intersection of the enthalpy (or molar volume) curves of the glassy and rubbery (supercooled liquid) state defines the glass transition temperature, Tg. Since DSC measures the slope of the change in internal energy with temperature it is ideally suited for Tg measurements. The discontinuity in the temperature-enthalpy curve is illustrated in Figure 6. In the rubbery state the relaxation times are short (relative to experimental times) so that above Tg most polymers quickly reach the equilibrium state; i.e., line 22. If the material could be cooled along 22 at an infinitely slow rate the internal energy would reach the equilibrium solid state; line 11. At finite cooling rates the material reaches some meta stable, nonequilibrium glassy state (1'1') having residual enthalpy or free volume above that of the equilibrium glass. Accordingly, the measured Tg (Tg, 1') is greater than the true (equilibrium) Tg (Tg,1).

The DSC output for a transition through Tg is illustrated in Figure 7. The small exotherm at the beginning of the transition (usually not seen in DSC), the slope of the rise in dH/dt and the endotherm at the end of the transition are the result of kinetic effects and clearly make a direct identification of Tg highly uncertain. However, the transition temperature can be determined with good precision from a DSC trace using the method of Guttman and Flynn (7,8). They find the difference in enthalpy content between state 1 (glassy) and state 2(rubbery) at temperatures T_3 and T_4 respectively. This residual area which is the shaded area of Figure 7 including the endotherm is then related to Tg through the heat capacities (dH/dT) of the two states.

In our determinations of Tg, the DSC output is corrected for the instrument baseline and the data is smoothed and plotted. The straight lines for the initial and final states are determined, the range of integration for application of the Guttman-Flynn equation is selected and both Tg and Δ Cp at the glass transition are computed. The results must be corrected for thermal lag of the equipment and this is done by determining for each sample the difference in Tg on heating vs cooling through the transition at some specific heating-cooling rate. One-half of this difference is taken as the thermal lag correction. This method gave the same correction as the method recommended by Flynn (9) of plotting heating rate vs Tg and extrapolating to zero heating rate.

Our recent work with the DSC on Tg has been on the effect of filler on the glass transition. The literature abounds with contradiction on whether the presence of a filler raises, lowers or has no effect on Tg. We suspected that the thermal history of the polymer specimens played some role in these discrepancies. Notably, the rate at which the polymer had been brought through the transition. Consequently, we have studied the effect of cooling rate on Tg for filled and unfilled polymers. In Figure 8 the results are given for polystyrene and polystyrene-silica and as Wunderlich (10) has already shown the relationship is essentially linear. The interesting point is that the plots for the filled and unfilled material have different slopes indicating a

TABLE I

KINETIC PARAMETERS FOR THE DGEBA/HHPA/BDMA
POLYMERIZATION USING DIFFERENT COMPUTATIONAL METHODS

METHOD	REACTION ORDER, n	E _a CAL/MOLE	
ARRHENIUS	1 (ASSUME)	24.9 ± 1.3	
MAXIMUM TERM*	1 (ASSUME)	24.3 ± 1.1	
VARIABLE HEATING RATE	1 (ASSUME)	26.0 ± .8	
FREEMAN-CARROLL	1.14 ± 0.10	22.2 <u>+</u> 2.2	

^{*} GIVES Ea/n

TABLE II

KINETIC PARAMETERS FOR DGEBA/NMA/BDMA
POLYMERIZATION USING DIFFERENT COMPUTATIONAL METHODS

METHOD	REAC	TION ORDER, n	Ea,	CAL/MOLE
ARRHENIUS ARRHENIUS		(ASSUME) (ASSUME)		14.7 37.9
MAXIMUM TERM*		(ASSUME)		20.2 40.4
VARIABLE HEATING RATE				19.4
FREEMAN-CARROLL		1.3 2.1		13.6 40.5

^{*} GIVES Ea/n

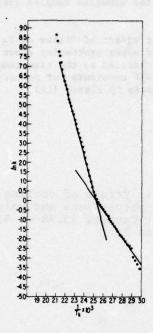


Figure 5: Arrhenius plot of DSC data for a dynamic mode scan of an epoxy resin: DGEBA/NMA/BDMA. Note the change in kinetics during the reaction (reference 1)

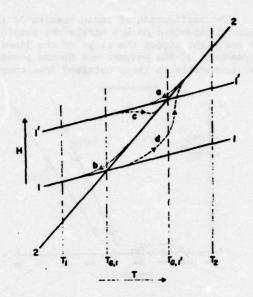


Figure 6: Enthalpy temperature schematic. Note lower Tg for lower er enthalpy state. Lower case letters and dotted lines refer to transitions that may occur due to the kinetics of cooling or heating (reference 8).

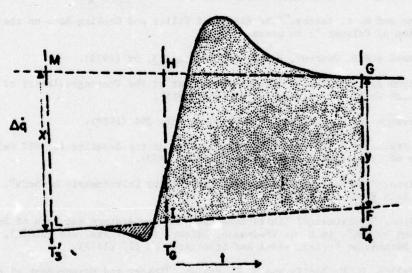


Figure 7: Schematic of DSC output for the Tg transition (reference 8).

crossover at sufficiently low cooling rate. The results for annealed samples (very low cooling rates) appear to confirm this crossover.

The implication of these results is that the apparent effect of filler on Tg is clearly dependent on how slowly the sample had been cooled after processing above Tg. As one might expect the slope of the lines in Figure 8 is related to the time-temperature dependence of the polymer and it was possible to compute WLF constants for polystyrene (3) comparable to those obtained from compliance measurements by Plazek (11).

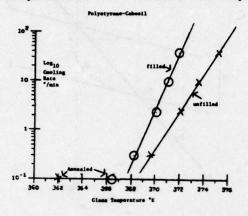


Figure 8: Effect of cooling rate on Tg of polystyrene and polystyrene + Cabosil (3.48 wt %) (reference 3).

REFERENCES

- P. Peyser and W. D. Bascom, "Kinetics of an Anhydride Epoxy Polymerization as Determined by DSC", in R.S. Porter and J.F. Johnson, Editors, Analytical Calorimetry, Vol. 3, p. 537, Plenum Press (1974).
- P. Peyser and W. D. Bascom, "Kinetics of Epoxy Resin Polymerization Using DSC", J. Appl. Polym. Sci., accepted for publication.
- P. Peyser and W. D. Bascom, "The Effect of Filler and Cooling Rate on the Glass Transition of Polymers", in press.
- 4. M. R. Kamal and S. Sourour, Polym. Eng. & Sci. 13, 59 (1973).
- J. H. Flynn and L. A. Wall, "General Treatment of the Thermogravimetry of Polymers",
 J. Research Natl. Bur. Standards 70A, 487 (1966).
- 6. E. S. Freeman and J. Carroll, J. Phys. Chem. 62, 394 (1958).
- C. M. Guttman and J. H. Flynn, "On the Drawing of the Baseline for DSC Calculation of Heats of Transition", Anal. Chem. 45, 408 (1973).
- J. H. Flynn, "Thermodynamic Properties from DSC by Calorimetric Methods", Thermochimica Acta 8, 69 (1974).
- J. H. Flynn, "Instrumental Limitations upon the Temperature and Rate of Energy Production by DSC", in H. G. Wiedemann, Editor, Thermal Analysis (3ICTA), Vol. 1, Birkhauser Verlag, Basel and Stuttgart, p. 127 (1972).
- B. Wunderlich, D. M. Bodily and M. H. Kaplan, "Theory and Measurement of the Glass-Transformation Interval of Polystyrene", J. Appl. Phys. 35, 95 (1964).
- D. J. Plazek and V. M. O'Rourke, "Viscoelastic Behavior of Low Molecular Weight Polystyrene", J. Polym. Sci. <u>A2</u> 9, 209 (1971).

SESSION IV: DIELECTRIC ANALYSIS

Chairman: L. Krichew National Defence, Canada

DIELECTRIC AND CALORIMETRIC MONITORING OF THE RESIN MATRIX DURING THE CURE OF COMPOSITE STRUCTURES
C. A. May, Lockheed Missiles and Space Co.

ETMA: ELECTRICAL, THERMAL AND MECHANICAL ANALYSES OF POLYMERS: THEORY AND USES S. Yalof, Tetrahedron Associates, Inc.

THERMAL ANALYSIS OF PMR-POLYIMIDES BY DIELECTROMETRY R. E. Gluyas, NASA Lewis Research Center

DIELECTRIC AND CALORIMETRIC MONITORING OF THE RESIN MATRIX DURING THE CURE OF COMPOSITE STRUCTURES

Clayton A. May Lockheed Missiles & Space Co., Inc. Sunnyvale, California

The fabrication of high quality aerospace structures from composite materials requires well designed curing cycles on materials of well defined physiochemical structures. A thorough knowledge of what is happening physically and chemically during the cure not only dictates the cure cycle, but also defines the starting material. We have found that a combination of dynamic dielectric analysis (DDA) and differential scanning calorimetry (DSC) is a very effective tool for these purposes.

Three types of DDA measurements can be made, iongraphing, electrical dissipation factor, and phase angle determination, as the cure progresses. Iongraphing is a relative simple technique and also affords the least information on the significant events of a cure cycle. Accordingly, since there are more precise techniques available, it is used only sparingly in our laboratories. Dissipation factor and capacitance measurement (Audrey) is the most widely used because of the ready availability of commercial instrumentation. A third method involves direct measurement of the phase angle and vector voltage. In this case the instrumentation can be built up using off-the-shelf instrumentation. A comparative evaluation of the these latter two techniques is in progress. It has also been noted that the circuit design of the Audrey equipment will permit phase angle measurements.

The Audrey technique generally involves the measurement of the changes in capacitance and power factor as a function of changes in cure time and temperature. The most useful of these properties with epoxy resin systems is the dissipation or power factor. A typical curve shows two maxima as the resin cures. The first of these is attributable to the flow of the matrix resin, the second to the chemistry of the cure. Gellation of the matrix occurs on the second peak but the exact point varies with the chemical structure of the resin system. When the dissipation factor reaches a constant value beyond the second peak, the cure is complete. The valley between the peaks is the low viscosity region. Process changes such as the application of pressure to consolidate the laminates are normally made during this period.

The major drawback to the valley between the two peaks is that the power factor is an extremely small number and does not signal accurately the minimum matrix viscosity. The magnitude of the signal and the location of the minimum viscosity point can be key to automated processing. It could dictate not only when to apply the consolidation pressure but also the amount of pressure required for a high quality part. Current efforts with the phase angle technique indicate that this method may more clearly define the time and a relative magnitude of the minimum viscosity point.

The dielectric monitoring measurements also vary as the chemical structure of the resin system changes. For instance, as the resin system B-stages the matrix flow peak and cure peak move closer together. The addition of an accelerator to a resin-curing

agent combination changes the shape of the power factor curve. Different resin-curing agent systems give different fingerprints. Thus this technique is also useful as a starting material quality assurance method.

An obviously valuable addition to the DDA data would be further knowledge of what is occurring chemically during the cure. This type of data can be obtained from differential scanning calorimetry. DSC measures the heat of reaction between resin and curing agent. From this data it is possible to determine the hold temperatures which will avoid exotherms assuring uniform cure rates, define the proper temperatures and times for debulking operations, and, like DDA, to indicate when the cure is complete.

Similar to DDA, DSC data also indicate chemical structure and B-stage changes. The glass transition temperatures of prepreg (T_g) , as measured by this technique, are indicative of the degree of B-stage. The shape of the DSC exotherm curves are highly responsive to accelerator concentrations in epoxy resin curing agent system. Different resin-curing agent combinations change the shape of the DSC curves. Here again, this technique not only helps derive cure cycles, but also can detect chemical structure changes in a matrix system. It also defines when a cure is completed. DSC is also a good starting material quality assurance procedure.

Dynamic dielectric analysis and differential scanning calorimetry are useful techniques for assessing the physical nature of an epoxy resin matrix at various stages during the cure. Together they form an excellent method for deriving new cure cycles as well as controlling the cure cycle. DDA can be related to the rheological changes which occur in the matrix as it cures. DSC compliments this data by defining where the cure begins and how rapidly the resin and curing agent react as a function of the curing cycle. The combination of these two procedures affords an excellent picture of the curing process and the quality of the starting resin matrix.

ETMA: ELECTRICAL, THERMAL AND MECHANICAL ANALYSES OF POLYMERS: THEORY & USES

Stanley Yalof, President

Tetrahedron Associates, Inc., San Diego, CA

INTRODUCTION

The past two decades have provided the analytical chemist with many powerful analytical techniques: NMR and advanced IR spectroscopies, the various chromatographies, dynamic mechanical test systems, the broad field of thermal analysis, joined in the last decade with the application of dielectric spectroscopy to problems of research and production. These analytical tools have evolved separately, without any overview relating one to another.

It seems that these methods should be linked, all involving the response of a material to an applied stress, which we call relaxation behavior. This interrelationship between electrical, thermal and mechanical behavior, or ETMA, answers such questions as to how DTA, dynamic mechanical and dynamic dielectric measurements are related, bringing out expected and unsuspected connections between methods, giving us insights into the significance of some traditional approaches such as mechanical property-testing.

Because I have the good fortune to have Dr. Clayton May follow me as a speaker, I will concentrate on the background and leave him to discuss his experimental findings.

BACKGROUND

The importance of thermal history to polymer curing and mechanical behavior is becoming increasingly appreciated through work in mechanical, dielectric and thermal analyses. A major step in conceptualizing these systems into a single body of theory was begun by Professor Peter Hedvig of the Research Institute for Plastics, Budapest.

About 10 years ago I found that materials behaved nothing like what the process schedules said they should, and I concluded that it was essential to be able to follow a process directly. It became apparent that of all available techniques, dielectric analysis was unique in its ability to operate outside of a test cell, in real time. We developed a dielectric system known as Audrey, short for automatic dielectrometry which was applied to a variety of applications ranging from basic research to production control.

Gradually, we and our customers found a surprisingly wide variety of problems which were amenable to dielectric spectroscopy: the measurement of monomers; the measurement of polymer cooks (Figure 1); the extent of cure analyses of the various polymers (Figure 2); thermoplastic behavior (Figure 3); moisture absorption, etc. It appeared that the method was applicable to almost any circumstance where there was a viscoelastic thermoplastic or thermoset change. There are several non-polar thermoplastic compounds such as PTFE and PE (but even they will respond to frequency and temperature sweeps).

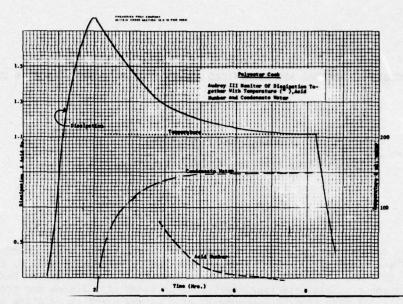


Figure 1. Showing a change of dissipation with initial heating, followed by a decrease as molecular weight builds up. Traditional measures of following cooks, evolved water and acid number, are also plotted.

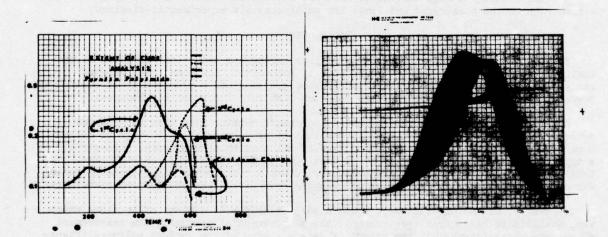


Figure 2. Curing changes for a PI during a 3 step process. The 2nd and 3rd cycles have been amplified 2 and 4 fold, respectively.

Figure 3. Zytel nylon thermoplastic changes with temperature. Note that the dissipation peak centers on the change of C.

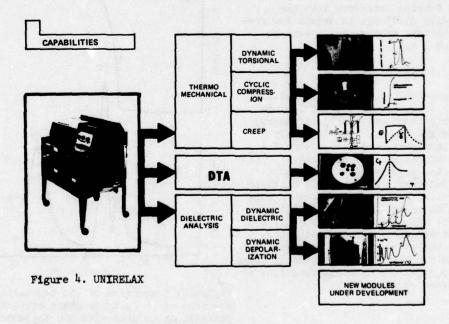
One bothersome problem was the lack of a clear, general understanding of the relationship between dielectric and mechanical properties. There was no shortage of good studies relating mechanical and dielectric behavior for specific materials [1,2]. Williams, Landel and Ferry interrelated dielectric and mechanical response in their landmark "WLF equations" [3], but there still wasn't a good general interconnection. A turning point came with the publication of information on the UNIRELAX system by Dr. Peter Hedvig [4]. UNIRELAX, shortfor Universal Relaxation Spectroscopy, will measure several of the various forms of theoretically related relaxation behavior; dynamic dielectric spectroscopy, dynamic mechanical behavior, thermomechanical behavior, thermal analysis and dynamic depolarization (DPS) by a single instrument, under strictly controlled repetitive conditions (Figure 4). But the most interesting aspect of this instrument is its recognition of the theoretical equivalence and similar needs of relaxation testing disciplines, where a central system will provide both test control and data analysis.

ETMA

The ETMA methods are related through the relaxation effect, where the rate of deformation of a material under the action of a stress is studied. Stresses can be electrical, thermal or mechanical in origin. A theoretical background is evolving for these methods, which permits us to interrelate one technique to another, filling in the details of a materials behavior.

A. Electrical Methods

Electrical methods involve the application of an electrical stress to a material to produce a flow of charge. The energy required to store this charge is related to capacity C and dielectric permittivity E' and the amount of energy dissipated per cycle to dissipation D. Dielectric response, both C and D depend upon molecular architecture and the motions of molecules around a central attachment, e.g., the motion of side chains attached



to a giant molecule. There are both frequency dependent and independent responses, related to by molecular weight and shape, ionic transport of charges, etc.

B. Mechanical Methods

When we impose a mechanical stress on a material, we cause a portion of it to extend in the direction of stress. We call this response strain. Energy can be stored, e.g. storage modulus, or it may be dissipated by some heat mechanism, e.g. the mechanical dissipation. UNIRELAX will perform testing in either the dynamic regime with a dynamic torsional cell or in the thermomechanical regime, with such test methods as stress relaxation, creep, penetration and flow viscometry.

C. Depolarization Analysis

In the past several years it has been observed that under a strong electric field, microcurrents can be induced to flow across a dielectric material, with charges tending

to accumulate at discontinuities in a manner akin to the accumulation of particles borne by river water around fallen trees and rocks. If we cool down this sample, remove the field, and then rewarm it with a precisely controlled heat-up rate, a rather detailed discharge pattern may be observed [5] which provides a fascinating view of material heterogeneities. DPS correlates quite well with dynamic dielectric, dynamic mechanical, and thermomechanical testing, as shown in Figure 5; and of course it offers its special insights too.

Dr. Hedvig has determined that depolarization spectra can be translated by a simplified Fourier transform into the experimentally difficult to obtain low frequency dielectric measurements, between 1×10^{-4} and 1 Hz.

D. Thermomechanical

Thermomechanical tests are considered near-static or quasi-static, and include creep, penetration, capillary viscometry, etc. These methods are experimentally simple to implement, and give a surprising amount of information. Very recently, Peter Forgacs at the Research Institute for Plastics, Budapest, has developed a cyclic creep technique, which almost seems a contradiction in terms, where a sample is periodically unloaded from its stress, and the rate of deformation change with the removal of the stress load is measured, plotted and the results mathemetically transformed into dynamic mechanical functions and the WLF master curve.

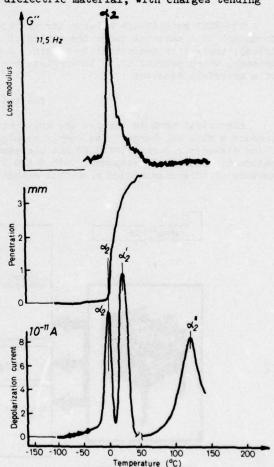


Figure 5. Comparison of the depolarization spectrum of the elastic phase extracted from Hostalit in toluene with the thermomechanical curve (penetration) and with the dynamic mechanical absorption spectrum (loss modulus).

CROSS-CHECKING AGAINST NMR

Although NMR is not a UNIRELAX technique, requiring a very special experimental configuration, still it is a relaxation technique, whose results are often relatable to other relaxation methods.

NMR's utility in studying molecular motions in condensed matter is based on the fact that NMR behavior is affected by the mobility of the nonparamagnetic environment and also by the motions of the nuclear spins themselves.

Molecular motion affects nuclear magnetic resonance in two ways: through the thermal motion of the nonmagnetic lattice (the T_1 process) and through the motions of the dipoles themselves (the T_2 process).

In an NMR model (12) derived for spherical molecules in a liquid medium, the T_1 and T_2 processes are ascribed to random thermal motion of the units being spun. By measuring

the temperature dependence of T_1 and T_2 , the different forms of molecular motion can be determined and these results can be compared with findings from dielectric and mechanical relaxation studies.

For example, the relaxation behavior of commercial amorphous and 95% isostatic PMMA was investigated by Hedvig with NMR, mechanical, dielectric, and dynamic depolarization spectroscopy (Figure 6). Several forms of molecular motion were picked up: an alpha form, due to the glass rubber transition, which is very sensitive to thermal history and is connected to the vibration of chain segments involving structural changes; a beta form that has been ascribed to the rotation of the polar ester groups around the carbon-to-carbon bond linkages to the polymer chain; the gamma process, (which doesn't appear in the dielectric spectrum, so it was therefore concluded that it didn't contain polar groups, was due to the rotation of the alpha-methyl group linked to the main chain, and was not at all affected by the degree of crystallinity.)

There are additional frequency dependent peaks in the mechanical and dielectric spectra between -100° and -50°C that have been traced to absorbed water.

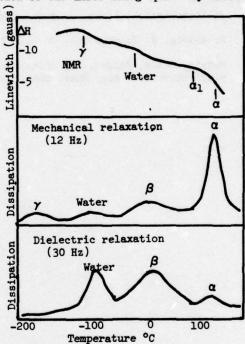


Figure 6. Comparison of the dielectric, mechanical, and NMR spectra as a function of temperature at 30 Hz, 12 Hz, and 20 MHz,

The ester-methyl group rotation is frozen only at very low temperatures. This transition was detected at about 4°K by wide-line NMR, indicating a very low potential barrier.

It was concluded from the preceding work that mechanical and dielectric spectroscopies give a fairly clear picture of molecular motion for PMMA, and that NMR only provided additional information for the $4^{\circ}K$ transition.

CONCLUSIONS

All of the ETMA methods are unified by the common thread of relaxation behavior. As we have shown, their bases are not only interrelated through theory and various transformations, but also through a comparison of experimental findings. These tools allow us to explore the origins of responses, electrical, thermal, mechanical, to optimize processes, and to bring together the fields of materials science and provess control.

REFERENCES

- Yalof, S.A., Wrasidlo, W.A., "Cross-Checking Between Dielectric Measurements, DTA and other Methods of Thermal Analysis," J. Appl. Poly. Sci., 16, 2159-73 (1972).
- Yalof, S.A., "The Relationship Between Mechanical and Dielectric Properties of Polymers," Fourth Nat. SAMPE Tech. Conf., Oct. 17, 1972, Vol. 4, pp. 391-7.
- 3. Williams-Landell-Ferry, J. Amer. Chem. Society, pp. 77, 3701 (1955).
- 4. P. Hedvig, J. Polymer Sci, C. No. 33 pp. 315 (1971).
- Hedvig, Peter, Foldes, E., "Dielectric Depolarization Sectra of Toughened Polyvinyl Chloride," Ang. Makro Chem., 35, 147-57 (1974).

THERMAL ANALYSIS OF PMR-POLYIMIDES BY DIELECTROMETRY

by Richard E. Gluyas

Lewis Research Center

ABSTRACT

A preliminary study was conducted to determine the dielectric properties of glass fabric reinforced composites as influenced by the reactions occurring during the preparation of crosslinked polyimides by the PMR process. The variables studied included: formulated molecular weight, staging temperature and time; rate of temperature increase to cure temperature; and cure temperature and time. The changes of capacitance and, particularly, of dissipation factor were found to be strongly dependent on each of the variables studied.

SUMMARY

The dielectric properties (especially the dissipation factor) of glass fabric reinforced composites as influenced by the reactions occurring during thermal processing of monomer reactants (PMR) to high temperature resistant polyimides are described in this report. The effects of the following variables are presented and discussed: 1) the heating and reheating (after air drying) of glass cloth impregnated with a methanol solution of the three monomers BTDE, MDA, and NE (see table I); 2) staging temperature and time; 3) resin composition (i.e., relative amounts of the three monomers); and 4) heating rate, maximum cure temperature, pressing pressure, and measurement frequency. It was found that all of these variables caused changes in the electrical property behavior. Based on this it is concluded that measurement of dielectric properties under controlled test conditions is a promising method for characterization of this class of materials during reaction.

INTRODUCTION

A class of highly processable, high temperature resistant polyimides has been developed at the NASA Lewis Research Center. These unique addition-type polyimides can be used as matrix resins in fiber reinforced composites, as adhesives, and as molding powders. The advantages of these polyimides over commercially available condensation-type polyimides include: 1) processing versatility, 2) improved high temperature performance, 3) greater safety to fabricators, and 4) lower costs.

The process for fabricating fiber-reinforced composites using this class of polyimides as the matrix material consists of applying monomeric reactants in solution to the fiber (e.g., glass or graphite) and of effecting polymerization in situ by a combination of heat and pressure. For convenience this has been called the PMR process (polymerization of monomer reactants) and is reviewed in ref. 1. A number of variables can be manipulated in this process including: 1) the temperature-time-pressure program, 2) the composition of the monomer-solvent mixture, 3) the specimen geometry, and 4) fiber type and amount.

TABLE I. - STRUCTURES OF PMR MONOMERS AND OF A POLYSULFONE

Abbreviation	NE	BTDE	MDA	PES
Name	Monomethyl ester of 5-norbornene-2, 3-dicarboxylic acid	Dimethyl ester of 3, 3', 4, 4'- benzophenonetetracarboxylic acid	4, 4' -methylenedianiline	Poly(ether-sulfone) from bisphenol-A and bischlorophenyl sulfone
· Structure	C-OMe	O O		

A variety of techniques are being employed to identify the critical processing variables, to identify the critical processing variables, to obtain an improved understanding of the physical and chemical changes occurring during the process, to aid in selection of the proper combination of conditions for ''tailor-making'' composites with desired properties, to aid in quality control, and to develop practical methods for monitoring the state of composites during processing.

The purpose of this report is to describe a preliminary study of the influence of the reactions occurring during the preparation of crosslinked polyimides by the PMR process on the dielectric properties (particularly the dissipation factor) of glass fabric reinforced composites. For convenience, glass fabric was used instead of graphite fiber for this study of resin behavior primarily because the electrical conductivity of graphite necessitates a somewhat more complicated test specimen-electrode configuration. The variables investigated include: 1) the formulated molecular weight (i.e., the ratio of monomers (see ref. 1), 2) "staging" time and temperature (staging refers to a low temperature heat treatment preliminary to forming under pressure at higher temperatures), 3) the time-temperature program for the "curing" process (i.e., heating rate and maximum temperature effects), 4) applied pressure, 5) temperature recycle, and 6) measurement frequency.

Although dielectrometry has been applied to polyimides by others (see for example, refs. 2 and 3), a systematic screening of the effects of all of these variables has not been done.

EXPERIMENTAL

Materials

The materials used in this study included the monomers for preparing PMR polyimides: 1) monomethyl ester of 5-norbornene - 2, 3-dicarboxylic acid (NE), 2) 4, 4'-methylenedianiline (MDA), and 3) the dimethyl ester of 3, 3', 4, 4'-benzophenonetetracarboxylic acid (BTDE) (see table I). These were obtained from commercial sources except for the BTDE which was prepared from the anhydride (BTDA) by refluxing with enough methanol to form a 50 weight percent solution of BTDE in methanol. Other materials used were: 1) anhydrous methanol as solvent to prepare 50 weight percent solutions of the monomers, 2) heat cleaned glass fabric for preparation of composites, 3) Kapton film as an electrical insulating material, and 4) aluminum foil for electrodes.

Also a commercial polysulfone (see table I) was included as an example of a high temperature thermoplastic polymer. Methylene chloride (CH_2Cl_2) was used as the solvent for the polysulfone.

Preparation of Composite Specimens

Solutions containing 50 percent by weight solids in anhydrous methanol were prepared using the monomers NE, MDA, and BTDE in the desired combinations and ratios. Solutions of the three monomers were prepared with formulated molecular weights (FMW) of 1000, 1250, 1500, 1750, and 2000 (corresponding to PMR 10, PMR 12.5, PMR 15, etc.) The expression used for FMW is:

$$FMW = n \ MW_{BTDE} + (n + 1) \ MW_{MDA} + 2 \ MW_{NE}$$

$$- 2(n + 1) \left(MW_{H_2O} + MW_{CH_3OH}\right)$$

where MWBTDE, MWMDA etc., are the molecular weights of the materials indicated in the subscripts (see ref. 1). Thus the molar ratios of NE:MDA:BTDE equal 2:(n + 1):n. Also, solutions having molar ratios of 2:1 for NE:MDA and 1:1 for BTDE:MDA were prepared as well as a solution of MDA by itself. The composites were prepared by impregnating glass fabric with the solutions and allowing to dry in air for several days. The weight of solid monomer was about 0.023 grams per square centimeter of fabric (0.15 grams per square in.). This material is subsequently referred to as "unstaged". In the case of the polysulfone, 10 grams were dissolved in 80 mls. of CH2Cl2, applied to glass cloth, and air dried. The dried composite material was cut into approximately 3 cm squares. ''Staged'' PMR composites were prepared by heating "unstaged" composite material in a hot air oven to remove residual solvent and to imidize (see ref. 4). Most of the specimens were staged for one hour at 204° C. The thickness of specimens staged at 204° C for one hour was 0.052 ± 0.005 cm $(0.020 \pm 0.002$ in.). Some specimens were staged for times ranging from 5 minutes to 3 hours and at temperatures ranging from 1210 to 2320 C to study the effects of staging conditions on electrical properties during subsequent heat treatment.

APPARATUS AND PROCEDURE

The apparatus used in this work is shown schematically in fig. 1 and includes: 1) a commercial dielectrometer (ref. 5) that will continuously measure both the capacitance (from 0 to 500 pf) and the dissipation factor (from 0 to 1) at a frequency in the range from 0.1 to 1.0 kHz. 2) an XYY' recorder, 3) a shielded test cell for dielectric specimens, 4) a press with 11.4 cm (4 1/2 in.) square heated platens capable of operation up to a temperature of about 350° C and a pressure of about 8.3×10⁶ N/m² (1200 PSIG), and 5) a temperature controller with capability of generating linear ramps ranging from 10 to 9° C per minute. (Note: The dissipation factor, DF or tan δ, is defined as the ratio of loss current to charging current. This assumes that the dielectric material corresponds in its electrical behavior to a capacitor with a resistor in parallel-i.e., an RC circuit). Primary emphasis was given to measurement of changes in dissipation factor because there was expected to be relatively little effect of sample thickness or area on the dissipation factor compared to the effect on capacitance.

The dielectric specimen usually consisted of three 2.54 cm (1 in.) square pieces of the impregnated glass fabric stacked to form a laminate. This laminate was contacted, in the case of staged material, by using 2.54 cm (1 in.) square pieces of aluminum foil as plates to form a capacitor. In cases where unstaged material was studied, an additional layer of 0.0025 cm (0.001 in.) thick Kapton was placed on each plate in series with the capacitor. This was done because otherwise the maximum dissipation factor for unstaged material often exceeded the range of the dielectrometer.

The temperature of one of the platens of the press was sensed by a thermocouple which served as input to the temperature controller and to a digital temperature readout. The temperature of the specimen lagged that of the controller. Temperature correction factors for each of the heating rates used were determined experimentally using a thermocouple in the specimen. This was done to avoid the inconvenience of placing a thermocouple inside the specimen cell for every run. Usually a temperature gradient of 9° C per minute was employed to a maximum temperature of 317° C, but rates of 3° C per minute and 24.5° C per minute (not linear) and maximum temperatures of 290° C and 345° C also were tested for qualitative comparison. During a run, the pen carriage of the recorder was swept along the x-axis at a constant rate

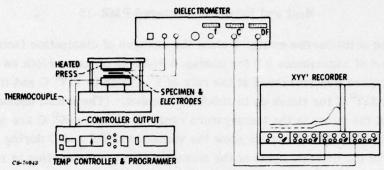


Figure 1. - Dielectric measurements apparatus.

of 0.025 cm (0.01 in.) per second and the DF and C outputs of the dielectrometer were recorded as Y and Y' by the two recorder pens (usually both at a sensitivity of 0.04 volt per cm (0.1 volt per in.) corresponding to a capacity change of 19.7 pf per cm (50 pf per in.) and a DF change of 0.04 per cm (0.1 per in.)). Pressure was applied to the specimen at the beginning of a run and, for the purposes of this study, was not varied during any single run. This pressure usually was $1.7 \times 10^5 \text{ N/m}^2$ (25 PSIG) but pressures of $6.9 \times 10^5 \text{ N/m}^2$ (100 PSIG) and $2.8 \times 10^6 \text{ N/m}^2$ (400 PSIG) also were used. The thickness of a three-ply specimen after a typical run (PMR 15 staged at 204° C for 1 hour and then heated at 9° C/min to 317° C at 1.7×10^{5} N/m²) was 0.064 cm (0.025 in.).

RESULTS

The next several sections present the experimental results on the effects of several variables on the dissipation factor and, in some cases, the capacitance of the materials under study. Generally, only relative changes in the values of DF and of C are shown on the figures in this report. Also in several instances, for ease of comparison, several curves are plotted in the same figure by displacing them in the direction of the y-axis. Sections on the following topics are included: 1) effect of heating and reheating of unstaged PMR-15; 2) effect of staging temperature and time on PMR-15; 3) effect of resin composition; and 4) effects of heating rate, maximum temperature, pressing pressure, and frequency.

Heat and Reheat of Unstaged PMR-15

The solid curves on fig. 2 show the changes of dissipation factor (DF) and of capacitance (C) for unstaged PMR-15 on glass cloth as the temperature was increased at the rate of 9° C/min to 317° C and then held at 317° C for times up to about 15 minutes. (The initial unchanging parts of the curve in the temperature range of 22° C to 60° C are not shown). The dashed curves show the variation of DF and C during a repeat of the thermal cycle of the same specimen after cooling to room temperature, 22° C. During the initial heating of the specimen, three major peaks occurred in the dissipation factor at 93° C, 157° C, and 303° C and one major peak occurred in the capacitance between 93° C and 157° C with a maximum at about 140° C. A smaller peak in the capacitance curve is observed at about 290° C. Upon cooling to room temperature and reheating, none of the peaks appear. There are, however, small permanent changes in C and DF.

The data just presented show the results of heating and reheating of unstaged PMR-15 to 317° C at a rate of 9° C/min. It was of interest to see if heating a specimen through the first peak in the DF (at 93° C) caused some permanent change in the resin. Figure 3 shows the effect on DF and C of heating unstaged PMR-15 to 115° C at the rate of 9° C/min, quickly cooling to room temperature, and then reheating to 1150 C at 90 C/min. Apparently no permanent change as detected by the DF or C resulted from this treatment. Figure 4 shows the response of DF and C to the melting of MDA. A sharp increase in DF and C is followed by a gradual increase as the viscosity of the melt decreases with increase in temperature. (This determination of the melting point of MDA also served as a check on the temperature correction used in these experiments.) Heating of unstaged PMR-15 at 9° C/min to 195° C and thus through the second peak in the DF at 157° C (see fig. 5) resulted in a permanent change in the electrical behavior of the material as shown by the change in the DF and C curves on reheating the specimen.

For a comparison to the behavior of PMR-15, fig. 6 shows the variation of C and DF for a thermoplastic resin, polysulfone P-1700, during three thermal cycles of the same specimen at a heating rate of 9° C/min to 250° C. All three runs show essentially the same DF and C response and thus no permanent change in the resin. A small difference in the leading edge of the 202° C peak on the first heating is believed to be due to the specimen/electrode interface. This type of the specimen is also noted on the first heat of the polyimide specimens.

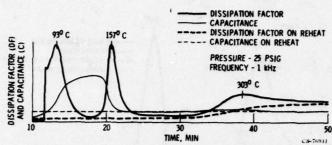
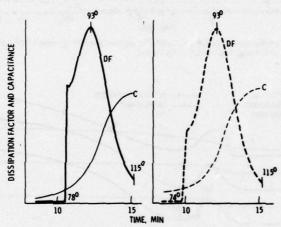


Figure 2. - Variation of dissipation factor and capacitance of unstaged PMR-15 on glass cloth during heating and reheating to 317° C at 9° C/min (3 pty - 1 in. 2, 2 mils Kapton.



(a) HEAT TO 1150 C AND QUENCH.

(b) REHEAT TO 1150 C.

Figure 3. - Effect of thermal cycle on 93° C peak of DF of PMR 15 heated to $115^{\rm o}$ C at 9° C/min (f = 1 kHz, P = 25 psig, 3 pty ~ 1 in, 2 , 2 mils Kapton).

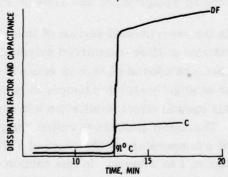


Figure 4. - The change of DF and C on melting of MDA at a heating rate of 9th C/min (f = 1 kHz, P = 25 psig, 3 ply - 1 in.-).

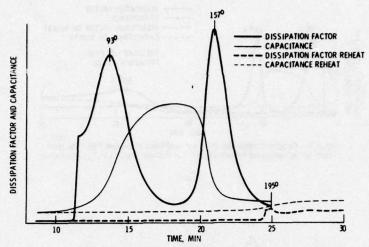


Figure 5. - Effect of thermal cycle on 93° C and 157° C peaks of DF of PMR 15 heated to 195° C at 9° C/min (f = 1 kHz, P = 25 psig, 3 ply - 1 in. $^{\circ}$, 2 mils Kapton).

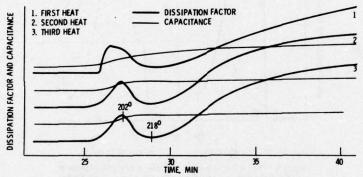


Figure 6. - Effect of 9^{0} C/min grad. to 250^{0} C and reheating on DF of P-1700 polysulfone, a high temperature thermoplastic (f = 1 kHz, 50 psig, 3 ply - 1 in. 2).

Effect of Staging Temperature and Time on PMR-15

As pointed out in the experimental section of this report, two of the steps in the fabrication of fiber-reinforced polyimide matrix composites by the PMR process consist of solvent removal by air drying at room temperature or at slightly elevated temperature ($\sim 60^{\circ}$ C) followed by heating in a hot-air oven to effect imidization and removal of condensation products. This latter process is called "staging" and typically is performed at a temperature in the range of 121° to 204° C and for a time in the range of 1 to 3 hours. In this section the effects of the two principal staging variables, temperature and time, on the subsequent changes in DF of the PMR-15 during heating to 317° C at 9° C/min are presented.

Figure 7 shows the effect on variation of DF of five staging temperatures ranging from 121° to 232° C for a constant staging time of one hour. As the staging temperature increases the temperature at which the first increase in DF occurs becomes greater (ranging from 160° to 225° C), and for the three lowest staging temperatures an additional peak appears in the 222° to 229° C range. Finally, the peak occurring in the 298° to 302° C range has its maximum at essentially the same temperature for all five staging temperatures but the relative height of the maximum for the 232° C staged material is about one-half that of the others.

The effect of change in staging time from 5 to 180 minutes for a constant staging temperature of 204° C on variations of DF is shown in fig. 8. The temperature of initial increase in DF shows only a minor change with staging time (204° to 213° C). The curves for the 5 and 15 minute staging times show second peaks at 233° and 255° C, respectively. The third or high temperature peak occurs at essentially the same temperature for all staging conditions (i.e., at 296° to 299° C). Also this peak has about the same relative height in all cases.

The final figure for this section (fig. 9) shows the changes in DF and C for PMR-15 (staged at 204° C for 1 hour) as the temperature is increased from room temperature to 317° C at 9° C/min, held at 317° C for about 15 minutes, cooled, and recycled. The sensitivity on the capacitance scale is 10 times that indicated on previous figures. As previously noted for unstaged material a permanent change in DF and C occurs as a result of the first heat treatment. And the DF and C each appear to approach a constant value asymptotically with time at 317° C.

Effects of Resin Composition

The variation of dissipation factor with temperature during 9° C/min heating to 317° C is shown in fig. 10 for staged specimens of PMR-polyimide of formulated molecular weights (FMW) 1000, 1250, 1500, 1750, and 2000. The temperature at the first break in the DF curve increases from 188° to 227° C as the FMW increases from 1000 to 2000. The temperature at the maximum DF appears to increase slightly with molecular weight. The height of the DF maximum decreases with increasing molecular weight in the ratio of 3.1:2:1.8:1.2:1.

A comparison of the DF curves for staged PMR-15, 2NE/MDA; and BTDE/MDA is shown in fig. 11. The most important detail to notice is that the curve for BTDE/MDA shows no discernable maximum.

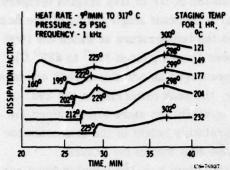


Figure 7. - Effect of staging temperature on the change of DF with temperature and time of PMR-15.

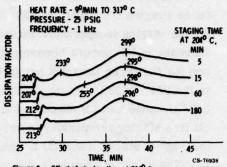


Figure 8. - Effect of staging time at 2040 C on change in DF with temperature and time for PMR-15.

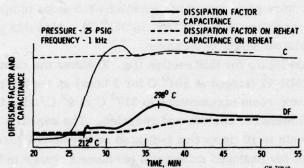


Figure 9. - Variation of DF and C of PMR-15 staged at 204° C for one hour during heating and reheating to 317° C at 9° C/min.

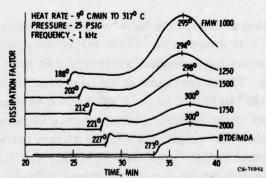


Figure 10. - Effect of formulated molecular weight on the change of DF with temperature and time of PMR-PI staged at 2040 C for one hour.

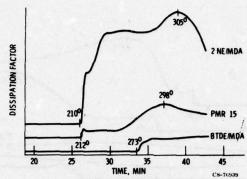


Figure 11. - Comparison of DF changes with temperature and time for three monomer mixtures (staged 205° C/1 hr. HTG rate 9° /min to 317° C, f = 1 kHz, P = 25 psig, 3 ply - 1 in. 2).

Effects of Heating Rate, Maximum Temperature, Pressure, and Frequency

The effect of variation of heating rate, maximum temperature, pressure, and frequency were briefly examined and are discussed below. The effects of different heating rate on the dissipation factor of staged PMR-15 are summarized in fig. 12. (Note that the curve for the 3° C/min heating rate is plotted in three segments.) The major differences caused by change in heating rate are in the high temperature maximum. The maximum occurs at different temperatures and, in the case of the 3° C/min heating rate, the maximum is much lower in height.

The effects of maximum cure temperatures of 290°, 317°, and 345° C are shown in fig. 13. As expected there is no change in the temperature of first increase in DF. But the maximum of the high temperature peak undergoes a shift from 281° to 326° C as the maximum cure temperature is increased from 290° to 345° C. Also the height of the peak increases with temperature in the relative ratios of 1:1.8:2 as the temperature increases from 290° to 345° C.

The only result of increasing pressing pressure from 1.7×10⁵ N/m² (25 psig) to 2.6×10⁶ N/m² (400 psig) was to lower the temperature at which the first increase in dissipation factor occurred (see fig. 14).

The effect of a frequency change from 1000 Hz to 100 Hz on the DF of staged PMR-15 is shown in fig. 15. The dissipation factor at the maximum increased from about 0.2 to 1 for the specimen and conditions selected.

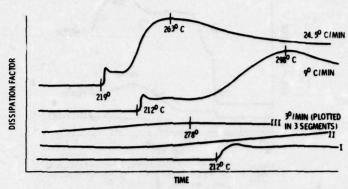


Figure 12. - Effect of heating rate on DF change with temperature and time for PMR 15 staged at 2040 C for one hour (max, temp. 3L70 C, f = 1 kHz, P = 25 psig, 3 ply = 1 in. $\frac{2}{3}$.)

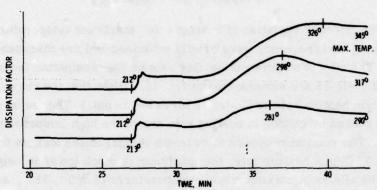


Figure 13, - Effect of maximum cure temperature on DF change with temperature and time for PMR 15 staged at 200° C for one hour (heat rate 9° C/min, f = 1 kHz, P = 25 psig, 3 ply - 1 in.).

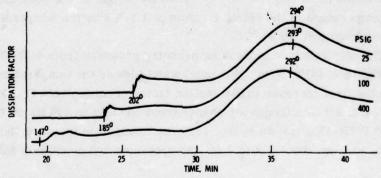


Figure 14, - Effect of pressure on change of DF with temperature and time for PMR 12, 5 staged at 204° C for one hour (heat rate 9° C/min to 317° C; f = 1 kHz, 3 ply - 1 in.).

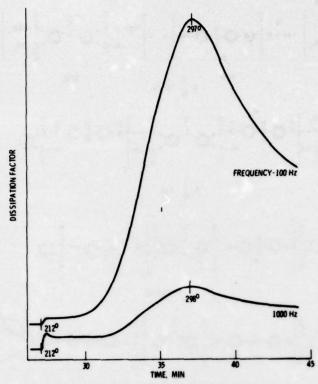


Figure 15. - Effect of frequency on DF change with temperature and time for PMR 15 staged at 204° C for one hour theat rate 9° C/min to 317° C max, P = 25 psig. 3 pty - 1 in. 4).

DISCUSSION OF RESULTS

A simplified outline of the chemistry of the PMR-polyimide reaction sequence as it is understood at present is shown in fig. 16. First, condensation reactions occur between the amine and the ester and carboxyl groups to form imide rings and the volatiles, water and methanol. The average chain length of the molecules formed is determined primarily by the relative amount of nadic ester (NE) present. At higher temperatures addition-type reactions occur at the nadic end groups by a complex set of reactions involving chain extension and an unknown degree of cross linking (ref. 7).

The changes in DF and C of unstaged PMR-15 material when heated at 9°C per minute to 317°C, held at 317°C for a time, and cooled to room temperature and reheated according to the same program are shown in fig. 2. A detailed understanding of the dielectric changes would require extensive chemical analysis of specimens withdrawn at various points during the heating cycle and correlation of the dielectrometry

Figure 16. - PMR polyimide reaction sequence

results with those obtained by other techniques such as DTA and viscosity measurements. Although this was not attempted because the main purpose of this report is to show the effects of processing variables on the changes in dielectric properties, several observations can be made on the nature of the peaks for PMR-15 in fig. 2. These are as follows: 1) Comparing the behavior of PMR-15 to that of a thermoplastic, polysulfone, shown in fig. 6, indicates that a permanent chemical change has occurred in PMR-15 after the first cycle and essentially no change in the polysulfone. 2) Heating PMR-15 through the first major peak in the DF curve (at 93° C) at 9° C/min to 115° C, cooling, and heating to 115° C again (see fig. 3) shows essentially no change in behavior and thus, no chemical reaction appears to have taken place - for example, to form amide-acid. Also, comparison of this PMR-15 peak to the changes occurring in the DF of MDA on melting (fig. 4) shows that the peak apparently is not due to melting alone. 3) Raising the temperature of PMR-15 to 195° C through the second peak in the DF curve at 157° C causes permanent change as evidenced by the absence of both the 93° C and 157° C

peaks upon recycle (fig. 5). This second peak corresponds to imidization as demonstrated by infrared spectroscopic studies (see ref. 6). The implication is strong that both steps of the condensation reaction occur practically simultaneously in this 157° C region. This is the so-called "staging" region. 4) The broad peak in the dissipation factor peaking at about 303° C (fig. 2) corresponds to the temperature region where crosslinking is thought to occur (ref. 7). On recycle, this peak no longer appears so it does represent some permanent chemical change in the resin. Some of the factors which affect this peak will be touched on later in this discussion. At a constant temperature of 317° C, after this peak is passed, the DF and C curves appear to slowly approach a constant value.

As previously mentioned, the staging of PMR resin is carried out to bring about imidization. This is intended to eliminate as much as possible of the volatile H₂O and CH₂OH to prevent void formation in the composites at later stages in the process. On the other hand, if staging temperatures and/or times are too great, cross-linking or unwanted side reactions might occur resulting in too little flow and formability upon pressure application and an undesirable end product. Figure 7 shows the effect of varying staging temperature for a fixed staging time on the behavior of the DF upon heating the staged material at the rate of 9° C/min from RT to 317° C (only the portions of the curves above 150° C are shown). The 204° C/ 1 hour curve represents the reference conditions. The peaks at 225°. 222°, and 229° C on the 121°, 149°, and 177° C staging temperature curves, respectively, possibly indicate incomplete imidization of the material. The peak in the 300° C region (believed to be related to the cross-linking reaction) is substantially decreased by the 232° C/1 hour staging conditions and suggests that staging at temperatures this high should be avoided or the staging time reduced. The temperatures at which the first increase in DF occurs differ significantly and increase with staging temperature. This potentially could be used as a criterion for quality control. Since it also indicates the temperature of the first decrease in viscosity it might be of interest in selecting processing conditions.

The effect of staging time at a constant temperature of 204° C on DF is shown in fig. 8. An additional peak is apparent at 233° C for the 5 minute staging time and at 255° C for the 15 minute staging time. This again may indicate incompleteness of imidization under these conditions. Compared to staging temperature, staging time appears to have only a small effect on the temperature of the initial increase in DF.

The behavior of the reference material, PMR-15, staged at the reference conditions of 204° C for 1 hour is plotted on fig. 9. In future

studies it would be of interest to analyze the behavior of the C and DF curves after the 298° C peak to obtain information on post-curing effects.

On figs. 10 and 11 the effects of chemical composition of PMRpolyimides on dissipation factor of cured specimens during a 90 C/min heat to 3170 C are summarized. Figure 10 shows the effect of formulated molecular weight (FMW) ranging from 1000 to 2000. The temperature of the first break in DF increases significantly with increasing FMW and the height of the maximum in the "cross-linking region" decreases with increasing FMW. But the temperature at which the maximum of this peak occurs does not vary significantly with FMW. The shape of this peak probably is determined by several complex factors including viscosity changes with temperature and rates and mechanisms of chain extension and cross-linking. Figure 11 shows similar information for 2NE/MDA and BTDE/MDA compared to PMR-15. The 2NE/MDA represents a special member of the FMW series (without BTDE) with the smallest FMW (i.e., 490) and with the greatest number of potential cross-links per unit volume. The first break in the DF curve of the 2NE/MDA does not fall in line with those of the 1000-2000 FMW series. The reason for this has not been determined. But the position of the high temperature peak is about the same and this peak follows the trend of increasing height with decreasing FMW. The BTDE/MDA has no end-group cross-linking capability and should form linear polymer chains. There is no maximum in the 300° C range for this material.

In practice, the change in behavior of the DF curve with FMW might be useful in quality control. And the shape of the peak in the 300° C temperature region might aid in the selection of processing conditions for forming polyimide materials. It is of special interest that the high temperature peak always appears very close to 300° C independent of FMW for the constant test conditions selected and is probably characteristic where NE is used as the end cap. Therefore this technique might be useful in evaluating other cross-linking systems with potential for lower curing temperatures. However, the potential applications of this method were not investigated in the present study.

The effect of the test conditions: 1) temperature gradient, 2) maximum cure temperature, 3) pressure, and 4) frequency were briefly examined and the results are shown on figs. 12, 13, 14, and 15, respectively. One obvious point is that if the electrical behavior during polymerization is to be compared it must be compared under the same controlled conditions.

Of the temperature gradients used (see fig. 12) 3° C/min was unnecessarily time consuming. Otherwise comparisons could probably be made at any constant gradient. The difference in positions of the DF maxima is probably due to the complicated kinetics of the reaction.

Increasing the final cure temperature causes a shift of the maximum in the DF to higher temperatures (fig. 13). This is probably because of a prolonged decrease in viscosity due to the higher temperature. Further work has to be done to see if electrical property measurements are useful to obtain a measure of the relative degree of cure at the different maximum temperatures. Perhaps comparison of recycle curves of these specimens to 345° C would be informative. Or dielectric relaxation measurements of the materials prepared at the different cure temperatures might give useful comparative information.

The range of pressures used did not noticeably affect the temperature or height of the DF maximum (fig. 14) so if there are differences in the reaction in this region due to pressure, this method showed no evidence for them. The effect of pressure on the temperature of the initial change in DF is surprising - unless the material undergoes a volume decrease in softening, or if some species which decreases the softening temperature was retained more effectively at higher pressures.

Finally, a test of the effect of measurement frequency is shown in fig. 15. This shows the expected sensitivity of the measurements to frequency. It is interesting that the sensitivity at the maximum is greater at 0.1 kHz but on the plateau of the curve just after the initial increase in DF the reverse is true. No explanation is offered for this.

It probably should be emphasized that the effects of the conditions as presented in this report must be clearly recognized before applying dielectric measurements to reacting systems - for example, for monitoring curing of polyimide composites in a press or autoclave.

CONCLUSIONS

A preliminary study of the influence of the reactions occurring during the PMR process on the dielectric properties of glass fiber reinforced composites as a function of materials composition, processing, and test condition variables leads to the following major conclusions:

1. Dielectrometry appears to be particularly useful for following addition polymerization reactions. For example, it is a good method for monitoring reactions occurring during the PMR process for fabrication of fiber reinforced polyimides and could be used for quality control and for monitoring the effects of processing conditions.

- 2. Repeated heating of air dried unstaged monomer mixtures to about 115° C causes no change and, therefore, the unstaged material appears to have sufficient chemical stability to be stored at ambient temperatures.
- 3. The staging conditions of one hour at 204° C appear to be a good compromise between incomplete imidization and undesirable premature crosslinking or decomposition resulting in potentially inferior processability.

REFERENCES

- Serafini, Tito T.: Processable High Temperature Resistant Polymer Matrix Materials. NASA TM X-71682, 1975.
- Yalof, S.; and Wrasidlo, W.: Cross-Checking Between Dielectric Measurements, DTA, and Other Methods of Thermal Analysis in Research and Production. J. Appl. Poly. Sci., vol. 16, no. 8, Aug. 1972, pp. 2159-2173.
- Pike, R. A.; Douglas, F. C.; and Wisner, G. R.: Electrical Dissipation Factor: Guide to Molding Quality Graphite/Resin Composites. Poly. Eng. Sci., vol. 11, no. 6, June 1971, pp. 502-506.
- Delvigs, Peter; Serafini, Tito T.; and Lightsey, George R.: Addition-Type Polyimides From Solutions of Monomeric Reactants. NASA TN D-6877, 1972.
- Yalof, S. and Brisbin, D.: The Dielectric Probe: A Useful Tool for Research and Process Central. Am. Lab., vol. 5, no. 1, Jan. 1973, pp. 65-74.
- Lauver, R. W.: The Effect of Ester Impurities in PMR-Polyimide Resin. NASA TM X-73444, 1976.
- Burns, E. A.; et al.: Thermally Stable Laminating Resins. (TRW-11926-6013-RO-00, TRW Systems Group; NAS3-12412), NASA CR-72633, 1970.

SESSION V: MOISTURE CHARACTERIZATION

Chairman: L. Krichew National Defence, Canada

THE SURFACE COMPOSITION AND ENERGETICS OF GRAPHITE REINFORCING FIBERS L. T. Drzal, University of Dayton Research Institute

TRANSPORT BEHAVIOR OF WATER IN POLYMERIC MATERIALS J. L. Illinger and N. S. Schneider, AMMRC

AD-A036 082

ARMY MATERIALS AND MECHANICS RESEARCH CENTER WATERTO--ETC F/G 11/9

PROCEEDINGS OF THE TTCP-3 CRITICAL REVIEW: TECHNIQUES FOR THE C--ETC(U)

AND THE TTCP-3 CRITICAL REVIEW: TECHNIQUES FOR THE C--ETC(U)

AND THE TTCP-3 CRITICAL REVIEW: TECHNIQUES FOR THE C--ETC(U)

NL

AGENTICAL REVIEW: TECHNIQUES FOR THE C--ETC(U)

NL

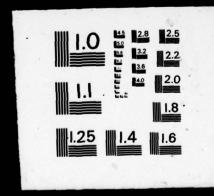
AGENTICAL REVIEW: TECHNIQUES FOR THE C--ETC(U)

NL

AGENTICAL REVIEW: TECHNIQUES FOR THE C--ETC(U)

AND THE C--ETC(U

4 OF 4 ADA036082



THE SURFACE COMPOSITION AND ENERGETICS OF GRAPHITE REINFORCING FIBERS*

by

Lawrence T. Drzal

University of Dayton Research Institute

Dayton, Ohio 45469

Graphite-fiber reinforced epoxy matrix composites are receiving increasing attention as possible structural components in aircraft. Although composite technology has advanced dramatically in the last decade, little is understood about the interactions that occur between graphite fiber and matrix at the interface. Recent work has shown that interfacial properties can have pronounced effects on composite durability, fatigue resistance and energy absorption. The work described here is an initial attempt to determine on a molecular level both the surface chemical composition as well as the surface energetics of some graphite reinforcing fibers used in composites and to relate these parameters to the engineering parameters of composite materials.

A combination of techniques has been used here to characterize these surfaces. Mass spectrometric analysis of thermal desorption products (to 300°C) has been combined with sub-monolayer krypton adsorption measurements for surface thermodynamic information, and with ion scattering spectrometry (ISS) and positive secondary ion mass spectroscopy (+SIMS) to provide atomic information about the surface. This combination has provided information about the initial surface composition, changes due to thermal treatment, surface energetic changes due to environmental exposure and identification of surface species contributing to loss of interfacial durability. The advantages and disadvantages of these techniques are summarized in Table 1.

Table 1.

Advantages and Disadvantages of Adsorption and Ion Scattering Techniques for Surface Analysis

Adsorption Thermodynamics

- ADVANTAGE o Does not perturb the surface
 - Measures energy of attraction of an inert gas molecule for the surface as a function of coverage
 - o Can characterize the surface from 0.1% to 100%
 - Operating technique and data reduction is readily amendable to computerization
- DISADVANTAGES o Expensive ~ \$55K including mass spectrometer
 - o Research tool confined to the

laboratory

- o Requires a large amount of time to determine the adsorption thermodynamics
- o Must be used with surface spectroscopy for maximum utility

Ion Scattering Spectroscopy with Positive and Negative Secondary Ion Mass Spectroscopy

- ADVANTAGE o Samples only outermost layer
 - o Sensitive to all atomic species
 - o Can detect both scattering atom and scattered species

- DISADVANTAGES o Expensive ~ \$60K
 - Research tool confined to laboratory
 - o Gives no molecular information
 - o Semi-quantitative at best

Fibers used in this study were polyacrylonitrile based fibers of low modulus supplied with and without the manufacturer's surface treatment.

The results of this study have shown that initially the surface treated fiber has five times as much material (4 monolayers) that volatilizes at temperatures up to 300°C as the untreated fiber. However, the surface areas of both treated and untreated fibers are approximately identical.

Energetically, the untreated surface adsorbs krypton similarly to adsorption by a carbon. The isosteric heats are uniform to about 80% coverage and exhibit a lack of lateral mobility. The treated fiber exhibits a pronounced increase in the isosteric heat, for the first 30% of a monolayer, over the untreated surface. Exposure of these fiber surfaces to air results in a slight change in the isosteric heat for the untreated surface. However, the treated fiber surface retains high values of the isosteric heat on the 30% portion of the surface but exhibits a pronounced decrease on the remainder. Repetition of the thermal treatment restores both surfaces energetically to their unexposed states.

ISS and +SIMS spectra from these surfaces indicate that a significant portion of each surface contains sodium and other cations which may be responsible for the energetic losses due to environmental exposure. Bulk analysis of these fibers indicate their presence in only trace amounts and that in adhesive applications, characterization of the polymer itself is not sufficient information for understanding adhesion.

* The complete text of this presentation will be available in the ("Treatise on Adhesion") Series Volume 5, R. Patrick, editor, Marcel Dekker.

TRANSPORT BEHAVIOR OF WATER IN POLYMERIC MATERIALS

J. L. Illinger and N. S. Schneider

Organic Materials Laboratory
Army Materials and Mechanics Research Center
Watertown, Massachusetts 02172

ABSTRACT

Water is taken up by organic materials in varying degree depending upon polymer structure. Structure affects both solubility and diffusion coefficients which determine overall permeability of the systems to water. Concentration dependence of diffusion coefficients run the gamut from D increasing with increasing concentration through concentration-independent D to D decreasing with increasing concentration. Temperature also affects both diffusion and solubility coefficients.

Techniques for measuring permeability, solubility and diffusion coefficients both dynamically and in the steady state are discussed. Temperature and concentration effects are considered in terms of Fickian diffusion, clustering phenomena, condensation theory, and plasticization. Results from supplementary calorimetric measurements are also included.

INTRODUCTION

Moisture is ubiquitous and affects all materials to varying degrees. Both chemical structure and morphology of polymeric materials influences solubility and diffusion coefficients which determine the overall permeability of these materials to water.

Diffusion behavior was first quantified by Fick (1) drawing analogy to equations for heat flow and stated for one dimension as:

$$J = -D \frac{\partial C}{\partial x} \tag{1}$$

and
$$\frac{\partial C}{\partial t} = \frac{\partial}{\partial x} \left(D \frac{\partial C}{\partial x} \right)$$
 (2)

where J is the flux

D is the diffusion coefficient

C is concentration

x is the direction of flow

t is time

Solutions for these equations for different geometries and boundary conditions are discussed in detail by Crank (2). The use of appropriate solutions allows calculation of D from experimental measurements and examination of the concentration dependence of D.

Figure 1 illustrates schematically several relationships of D with C (3) all of which have been found when water is the penetrant molecule.

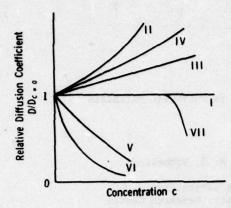


Figure 1. Concentration dependence of diffusion coefficient.

.

Curve I is the simplest where D is independent of concentration. This is usually the situation for inert gases diffusing through polymers but has also been found for water diffusing through polyethylene and polypropylene. Curve II shows an increasing exponential dependence of D with C which is typical of a system where the penetrant interacts with and swells, plasticizes, or dissolves the polymer. This behavior has been seen in steady state measurements of the water-poly(vinylalcohol) system. Curve III shows a linear increase of D with C and may be considered as a limiting case of II and generally occurs in systems with greater crosslinking so that swelling and plasticization are decreased. Curve IV is an intermediate case and has been attributed to two different mechanisms. One is that the degree of crosslinking and amount of plasticization are intermediate. The other, in polar materials such as wool, cellulose and nylons, is attributed to initial immobilization of water on polar sites. Then with additional sorption and higher concentration there are more mobile molecules which contribute to plasticization and increased diffusion. Curves V and VI, decreasing D with increasing C, are seen in systems where penetrant-penetrant interactions may predominate over polymer-penetrant interactions. In these systems one postulates the formation of "clusters" of water as concentration increases. As size or number of "clusters" increases, the proportion of monomeric water which represents the diffusing species decreases, hence D decreases. Curve V behavior has been seen with water in a number of poly(alkyl acrylates) and VI in ethyl cellulose and the polyurethanes to be discussed later.

An interesting variation has been found by Barrie (4); curve VII for water in a synthetic 1,4 cis polyisoprene and also silicone rubbers shows D is initially constant and then decreases at higher concentration. This implies a critical concentration before "clustering" sets in.

Even more complex relationships of D with C can be seen when two or more mechanisms of sorption and diffusion interact.

EXPERIMENTAL TECHNIQUES

Immersion Uptake

Equilibrium water sorption measurements can be performed by immersing a preweighed sample of polymer in distilled water maintained at desired temperature. Samples are allowed to come to equilibrium (up to 16 hours for most polymer thin films), then removed from the water, blotted with two sets of filter paper and immediately placed in a tared weighing bottle. Weight gain is measured and samples returned to immersion for repeat determinations.

Transmission Measurements

Steady state bulk permeabilities with liquid up-stream can be simply measured in inverted cup cells, the top being sealed by the polymer film of interest. The cells are

placed in an Aminco Aire cabinet controlled at 15° , 30° or 50° ± 0.5° C and $50 \pm 1^{\circ}$ RH. Periodic weighings are made to determine weight loss. Evaporation rate of water should be measured at the same positions and conditions to obtain limiting values required by the flux equation when the films have high water flux values (5).

 $J^{-1} = mL + b$

where $J = flux (gm/cm^2 sec)$

m = reciprocal of bulk permeability (gm-mil/cm² sec)⁻¹

L = the film thickness (mil)

b = reciprocal of water evaporation rate (gm/cm² sec)⁻¹

Weight loss can then be converted to flux from which the bulk permeability can be calculated. In conjunction with the solubility, S, from immersion data and the relation

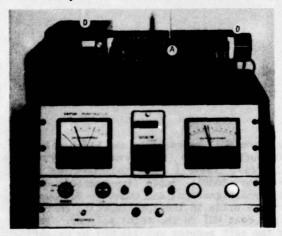
D = P/S

diffusion coefficients may be calculated.

Figure 2 shows a Modern Controls IRD Diffusometer. Different upstream humidities are produced by use of sponges (B) saturated with salt solutions inside thermostatted chambers which clamp a film against the block (C) which forms the chamber. This instrument detects the build up of water concentration in the dry down stream chamber by means of an infrared beam and a detector (D) of narrow band width centered at the water infrared sorption. The time necessary to build up a small concentration (less than one percent) of water is measured, the chamber is then swept dry and the measurement automatically repeated until a constant interval is reached. This indicates that steady state permeation has been attained.

Sorption Isotherms

We currently measure sorption isotherms with the vacuum system shown in Figure 3. The cabinet temperature is controlled to 5°C above the sample temperature by means of a heater which cycles in response to the sensor shown at F. The source (B) contains water which is outgassed through five freeze-thaw cycles. The ballast volume (C) is incorporated to limit pressure changes as sorption occurs. The recording balance (Perkin-Elmer AR-1) is recalibrated at each cabinet temperature. Isotherms are measured stepwise by admitting a small amount of vapor to the system and monitoring weight gain until equilibrium is established.



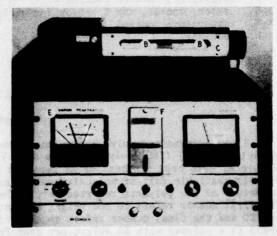


Figure 2. IRD Diffusometer Top: with chambers closed; bottom: front chamber removed.

- A. Thermostatted chamber for sponges. B. Sponges with saturated salt solution.
- Block-film is barrier between A & C. D. IR source & detector. E. Current meter.
- C. Block-F. Timer.

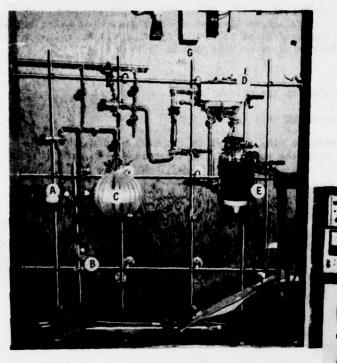


Figure 3. Sorption Apparatus

- A. Pressure Sensor and Electronics (a)
- B. Source of H20
- C. Ballast Volume
- D. Recording Microbalance and Electronics (d)
- E. Thermostatted bath around sample chamber
- F. Circulating bath to control E
- G. Heater, cooler, fan & sensor for cabinet temperature control
- H. Recorder

APPLICATION OF TECHNIQUES TO POLYURETHANES

Polymers

Several segmented polyether polyurethanes based on MDI, butanediol, and block poly(ethylene oxide) (PEO)/poly(propylene oxide) (PPO) soft segments (of general structure as in
Figure 4) have been synthesized as reported earlier (6). Table I shows the structure of
glycols available (all of molecular weight approximately 2000). Table II summarizes the
structure of the polymers reported here. The polymer designations are coded as follows.
The first number refers to the weight percent ethylene oxide in the soft segment, PE refers
to PEO and the final number refers to the weight per cent MDI in the total polymer. Thus
SPE33 is a polymer with 50 weight per cent PEO in the soft segment and 33% MDI by weight
in the total polymer.

TABLE I

Glycol Composition and Structure

Glyco1	Composition	<u>a</u>	b
C1540	100% PEO	36	0
L35	50/50 PPO/PEO	11	17
L43	70/30 PPO/PEO	7	23
L61	90/10 PPO/PEO	2.5	33
P2010	100% PPO	0	35

TABLE II

Sample Characterization

Sample			position Polyol	M _n ×10 ⁻³	Tg°K
10PE33	4.20	3	1C1540	22.1	242
5PE33	4.20	. 3	1L35	38.2	236
3PE33	4.20	3	L43	24.3	230
1PE33	4.20	3	1161	21.1	
OPE33	4.20	3	1P2010	23.1	232

M[~ (MB) xM] y~ M

M is MDI

0=C-N (C) CH2 (C) N=C=0

B is Butanediol

HO CH2CH2CH2CH2OH

is a macroglycol

 $HO(CH_2CH_2O)_a(CH_2CHO)_b(CH_2CH_2O)_a$ H CH_3

Figure 4. Polyurethane Structure

RESULTS AND DISCUSSION

Immersion Data: Figure 5 and Table III summarize the swelling behavior from liquid water at various temperatures. Values in Figure 5 are per cent water on total polymer, and those in Table III are per cent on PEO portion. It is apparent that under immersion conditions there are much larger differences in sorption with variations in composition than are seen in terms of the sorption isotherms.

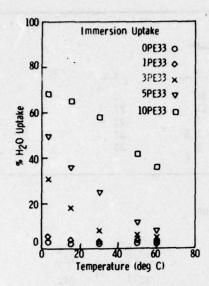


		TABLE	III		
	IMME	RSION	UPTAKE		
Polymer			T(°K)		
	276	288	303	323	333
10PE33	126	120	107	81	67
5PE33	167	127	83	27	20
3PE33	158	86	35	20	17
1PE33_	55	29	20	18	18
OPE33	4.9	4.1	3.3	4.6	4.6
*g/100g PPC	in po	lymer			

Figure 5. Water uptake under immersion conditions.

Figure 6 is a plot of the natural logarithm of water concentration (based on PEO) versus reciprocal temperature. The heats of sorption ΔH_S are represented by the negative slope of these curves. These values of ΔH_S are negative over the entire temperature range although the details of the variation with temperature are complex. In the polymer with pure PEO soft segment (10PE33) ΔH_S is slightly negative and becomes more so with increasing temperature. For the sample with pure PPO soft segment (0PE33) ΔH_S appears to change from somewhat exothermic to slightly endothermic with increase in temperature although this variation may fall within the experimental error due to the relatively small amounts of water taken up. The various polymers with block copolymer soft segments show abrupt changes in ΔH_S between the low and high temperature intervals. The change in ΔH_S is suggestive of a transition related to structural organization within soft segment phase, perhaps due to a change in miscibility of the PPO and PEO blocks of these moderately swollen polymers as a function of temperature. It is interesting to note that the slope of the set of curves at higher temperatures beyond the transition region again approaches that observed at lower temperatures. Because of the various complexities illustrated in Figure 6 no values of ΔH_S have been tabulated.

Sorption Isotherms: Figure 7 shows the isotherms for 10PE33, 5PE33, and 0PE33 at different temperatures. These sorption isotherms appear to be surprisingly simple, showing a linear region at low water vapor activity with rapidly increasing sorption at high activity. In the two PEO-containing polymers, sorption levels increase with decreasing temperature, the changes being most marked at p/p_0 above 0.8. The polymer with the pure PPO soft segment (0PE33) differs in that the isotherms are superposable at all temperatures. The changes in sorption behavior with composition are illustrated by Figure 8 where sorption is plotted as molecules of H_2 0 per EO unit. Figure 8 compares isotherms at 30°C for polymers varying over the full range of relative PPO/PEO composition at fixed hard segment content. The isotherms for the three samples with block copolymer soft segments are virtually superimposable to p/p_0 of 0.8 while 10PE33 shows progressively higher sorption levels starting at p/p_0 of 0.5. These isotherms as well as those at 50°C, which are not shown, display increasing sorption with increasing PEO in the soft segment. However, when considered on the basis of molecules of water per ethylene oxide unit, the increase is not proportional to the PEO content and the deviations are greatest at high activity.

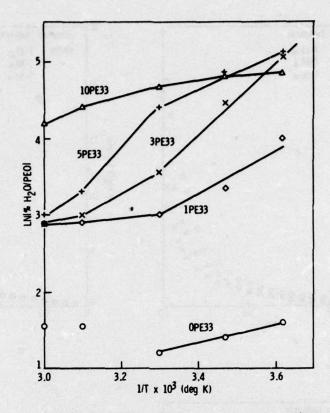


Figure 6. Water uptake - log S versus 1/T.

<u>Diffusion Behavior</u>: Diffusion coefficients, D, were calculated from the transients at each step of the determination of the isotherm. The approximation involving the time to reach sorption, which is one-half that at equilibrium, was used as

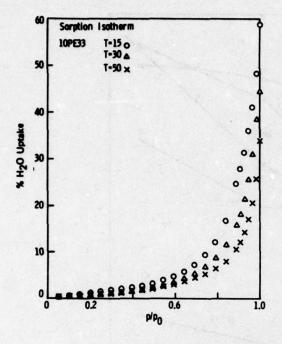
$$(t/\ell)1/2 = -\frac{\ln \left[(\pi^2/16) - 1/9 (\pi^2/16)^9 \right]}{\pi^2/D_{t_{1/2}}}$$

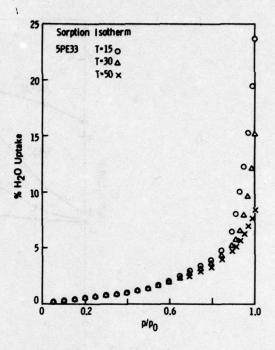
which upon rearrangement gives

$$D_{t_{1/2}} = \frac{0.04939 \ \ell^2}{t_{1/2}}$$

This approach assumes constant diffusion coefficient and an initial concentration, c=0. Because these coefficients are calculated from small p/p_0 intervals where c_{i-1} has a finite value, a correction was applied from

$$D_{i_{corr}} = \frac{(D_{i-1}_{corr}) (c_{i-1}) + D_{t_{1/2}} (c_{i} - c_{i-1})}{c_{i}}$$





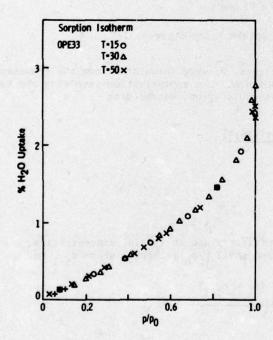


Figure 7. Sorption isotherms as a function of T for 10PE33, 5PE33, and OPE33.

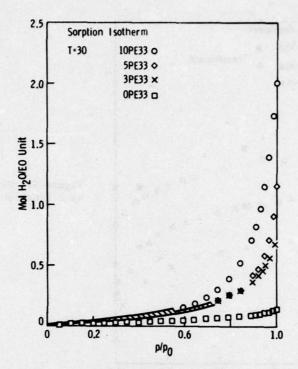


Figure 8. Sorption isotherms as a function of soft segment composition.

Figure 9 shows the change of the diffusion coefficients so calculated with both temperature and concentration. We have chosen to use activity rather than concentration as the abscissa to spread out the data. The diffusion coefficients increase by an order of magnitude with increasing temperature over the range studied. We also note that the decrease in the diffusion coefficient with concentration is greatest at high activity. The squares and diamonds are values of D calculated from steady state transmission assuming that D = P/S. P is the steady state permeability from the Mocon instrument or the cup cell measurements, and S is taken from the isotherms and immersion data. Agreement at low activity is good, but the values at saturation deviate markedly from D calculated from kinetics of sorption. Since the conditions of measurements are so different this is not unexpected.

Table IV presents the values of the diffusion coeficients from the various methods of measurement as a function of activity and variation in polymer structure. As the soft segment is varied the coefficients decrease with increasing PEO concentration at constant activity. Figure 10 compares this diffusion behavior across variation in soft segment as a function of concentration. The continuous decrease in D from very lowest concentration is in marked contrast to that reported by Barrie (4) who found that there was an initial region of low concentration where the diffusion coefficient is constant. He concluded that this showed that a critical concentration of water was required for clustering. Our results imply that in these urethane systems this does not occur. Rather there are probably two competing effects which decrease D even at the lowest sorption levels. At low activity and water content specific polymer-water interactions immobilize some of the water and then at higher concentrations clustering contributes more heavily to the decrease in D.

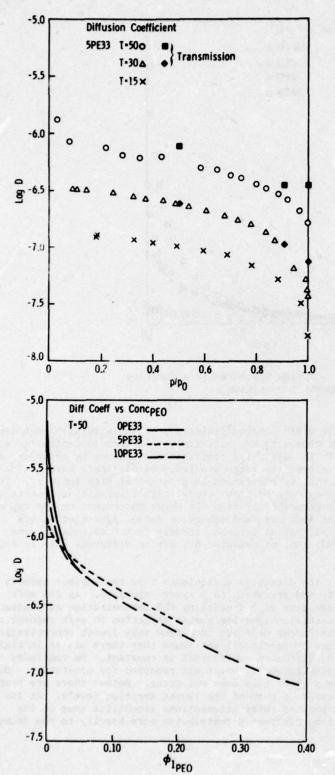


Figure 9. Diffusion coefficients as a function of T.

Figure 10. Diffusion coefficients versus ϕ_1 , variation in polymer composition.

1

TABLE IV

DIFFUSION COEFFICIENTS $(cm²/sec) \times 10⁸$

Polymers		Activity								
	0.	5	0.8	0.8 0.			1.0			
	*	+		•			+	+		
10PE33										
50°C	55.9	45.8	29	19	19.6	7.6	19.8			
30°C	-	16.7	12	7	6.6	4.3	6.9	14.9		
26°C	13.0	-	11	-		-				
15°C	7.9		5.4	3.3	•	1.7		-		
5PE33										
50°C	80	72.6	51	40	35.6	25	33.8	-		
30°C	25	22.1	18	12	10.7	5.9	7.6	7.8		
15°C	8.7	-	6.8	4.9		1.8		-		
OPE33										
50°C	90	72.6	67	60	60.4	45	56.3	-		
30°C	20	22.0	17	16	18.0	11	17.5	24.1		
15°C	4.3	-	3.7	3.4		3.0	-	-		

- * from isotherms
- + from Mocon transmission
- t from cup cell transmission

Cluster Analysis: A more general thermodynamic approach to examining the sorption behavior is by means of cluster function of Zimm and Lundberg (7):

$$G_{11}/V_1 = -\phi_2(d\gamma_1/da_1) - 1$$

where

G11 is the cluster integral

V₁ is the molar volume of the solvent

is the volume fraction of polymer

φ₁ is the volume fraction of solvent

is the activity coefficient a_1/ϕ_1

is the activity of solvent

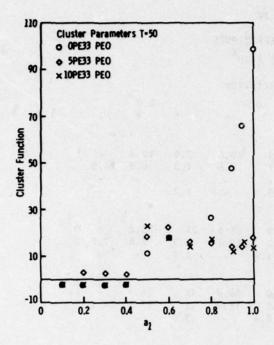
and mean cluster size:

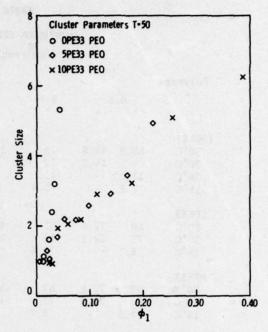
$$1 + (G_{11} \phi_1/V_1).$$

In addition Starkweather's (8) approach to calculation of a cluster number was applied using $w/[1 + (G_{11}\phi_1/V_1)]$, with w = g/100g polymer.

These polyurethanes contain phase-segregated hard segment structures. It has been found that no measurable sorption occurs on copolymers of the same composition as the hard segment. Therefore, it seems appropriate to carry out the clustering analysis assuming that all sorption occurs in the soft segment phase.

Figure 11 compares cluster functions, size and number across variation in soft segment composition at T = 50°C. In the hydrophobic PPO polymer the cluster function increases continuously, particularly steeply after activity 0.8, while the PEO-containing polymers reach a maximum value and then decrease. This would indicate that there is a greater tendency for water to cluster rather than interact with the PPO polymer. Just the reverse





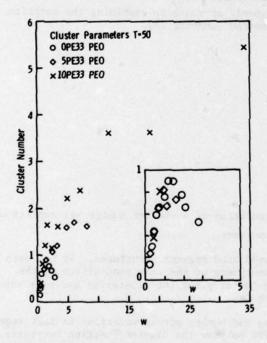


Figure 11. Cluster Parameters at T = 50 for 10PE33, 5PE33, and OPE33.

is observed for the PEO polymers even though much higher sorption levels are achieved. Cluster size in all three polymers of different soft segment composition continues to increase with increasing sorption. However, maximum size is about the same in all three, regardless of final concentration at an activity of 1.0. The change in cluster number with concentration reveals marked sensitivity to the soft segment composition. The pure PPO polymer goes through a maximum then decreases with a slope of 0.25 which, according to Starkweather's formalism, would indicate bridging of two or more clusters by incoming water molecules. The 50/50 PPO/PEO soft segment polymer reaches a maximum number and levels off, indicating that near saturation incoming molecules add to already formed clusters increasing their size. The pure PEO polymer cluster numbers continue to increase throughout the concentration range, which implies continued nucleation of clusters with the cluster size increasing to moderate levels.

This tendency to cluster in all of these polymers is consistent with the decrease in D, particularly at high activities.

Calorimetric Measurements: With the high degree of clustering found we hoped to further elucidate interaction between water and these polymers using scanning calorimetry on the wet polymers. Figure 12 shows preliminary scans of 5PE33 at different added water content. Note that well below immersion water uptake values an endotherm is visible. For further work the amounts of water added to the polymer were determined from previous immersion data measured as a function of temperature as shown. We chose to use those amounts sorbed at 293° and 323°K. Early runs on samples which had remained at room temperature until scanning showed endotherms (even on low water content polymers). Further, the Tg and the area under the endotherms changed from run to run depending upon the temperature history and conditions. This suggested that the water in the polymer is redistributed depending upon the temperature and time allowed at temperature. Accordingly samples were equilibrated at temperatures from 273° K to 323° K at 10-degree intervals. As T_{eq} was decreased the effect on T_g became greater and the "melting" endotherm decreased. It would seem reasonable to assum that the area under this endotherm is a valid measure of water behaving as "bulk" water with the heat of fusion of pure water. Subtraction of the amount of water so calculated from the amount of water added is a measure of the water "bound" to the polymer. Figure 13 plots and Table V shows the percent water "bound" in the polymer versus ΔT_g [T_g (wet) - T_g (dry)] for these polymers. The water content is calculated assuming constant small sorption by the PPO block which is subtracted before normalizing to the PEO content. The line through the points from 5PE33 continues through those from 0PE33 while those points from 10PE33 show much more displacement in Tg for a given amount of water on the PEO. The pure PPO polymer shows a small increase in Tg with water content. This would suggest that the presence of central PPO blocks in the soft segment of 5PE33 may lead to incomplete miscibility among the blocks of the soft segments, constraining the mobility of the PEO portion. In 10PE33 there is no such constraint, thus the effect of water on the segmental motion and therefore the glass transition is more marked.

Except for 10PE33 where the data does not allow extrapolation to T_g = 0, we note that the intercept shows a finite amount of water in the polymer. This would indicate that some of the nonfreezing water is not interacting with the polymer and may be present as monomeric or dimeric species which are too small to "melt".

Diluent depression of T_g is often rationalized in terms of free volume theory. Following Meares (9) the depressed T_g may be calculated by

$$T_{g} = \frac{v_{p} T_{gp} (\alpha_{\ell} - \alpha_{g}) + v_{d} T_{gd}^{g} \alpha_{d}}{v_{p} (\alpha_{\ell} - \alpha_{g}) + v_{d} \alpha_{d}}$$

where

 T_{σ} is the depressed glass transition temperature,

 T_{gp} , T_{gd} are glass transition temperatures of polymer and diluent,

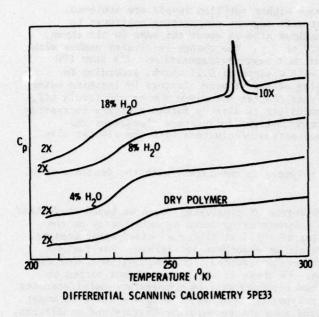


Figure 12. Preliminary DSC scans.

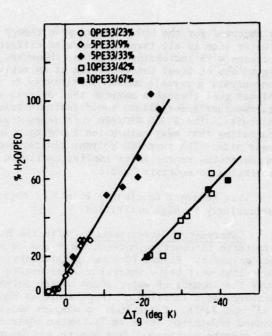


Figure 13. Water in PEO portion of polymers versus $\Delta T_{\mbox{\scriptsize g}}$.

						TABLE \	I					
					T AND	H20 WATE	ER ON PE)				
						T _{eq} (°1	()					
SAMPLE	2	73	28	33	2	93	30	03	31	3	32	23
	Tg		Tg	%H ₂ O	Tg	%II ₂ 0	Tg	%H20	Tg	\$H20	T _g	%H20
OPE33	+1.3	3.5	+1.2	3.4	+2.4	2.6	+2.3	2.8	+2.8	2.8	+3.8	2.4
5PE 33								185 465			100	
9%	-6.4	29	-4.8	29	-4.0	29	-4.2	26	-0.6	11	+2.6	10
5PE33 33%	-24	104	-25	97	-19	65	-18	70	-2.0	19	-0.7	16
10PE33												
42%	-49	55	-46	46	-48	51	-50	50	-48 (-28)	48 (30)	-34 (-26)	(22)
10PE33												
67%	-38	62	-38	52	-36	54	-38	57	-38	50	-20	19

 v_p , v_d are volume fractions of polymer and diluent, $({}^a\ell^{-\alpha}{}_g)$ is the difference in expansion coefficients of polymer in glass and liquid, ${}^\alpha{}_d$ is the expansion coefficient of diluent.

Table VI gives values of calculated and measured T_g at several volume fractions of water for these polymers. These values were calculated assuming $(\alpha_{\ell} - \alpha_g)$ is 4.8×10^{-4} (see Reference 10), $\alpha_d = 2.07 \times 10^{-4}$ (see Reference 11), and T_g equals $137^\circ K$ (12). Figure 14 is a plot of ΔT_g measured versus ΔT_g calculated. The line is that which obtains if theory holds. The measured values for the PEO/PPO block copolymer soft segment polymers fall near the theoretical line around another line of the same slope but showing smaller T_g than that calculated. This substantiates the earlier implications that not all of the "bound" water is tied to the polymer and that some is probably present as monomeric and dimeric species. In the PPO polymer the antiplasticizing effects are not in agreement with theory and must be attributed to specific local immobilizing interactions rather than free volume effects. The opposite deviation for 10PE33 implies that interactions in addition to free volume effects are operative when no PPO block is present.

CONCLUSION

Techniques for measuring water sorption and diffusion into polymers have been applied to polyurethanes with variation in soft segment composition. The results of these measurements in conjunction with calorimetric studies have shown that the compositional variables affect the amount of water sorbed and the rate of diffusion through the system. Clustering phenomena occur in all compositions contributing to a concentration dependence of D which decreases with increasing water concentration.

						TABLE VI						
			T _g MF	ASURED A	ND T _g CA	T _{eq} (°)		LUENT DE	EPRESSION	1		
SAMPLE	27	73	28	13	29	3	30)3	31	13	323	,
	T _g calc	T g meas	T _g calc	T _g meas	T _g calc	T _g meas	T _g calc		T _g calc	T g meas	T _g calc	T _g meas
OPE33												
2.3%	231.7	234.5	231.8	234.4	232.1	235.6	232.0	235.4	232.0	236.0	232.2	237.0
5PE33	221.7	226.1	221.7	227.7	221.8	228.5	222.8	228.8	228.3	231.9	228.6	235.1
5PE33 33%*	202.5	210.3	203.8	207.5	211.2	213.0	209.9	214.1	225.2	230.5	226.3	231.8
10PE33 42%*	221.8	193.8	224.7	196.5	223.2	194.4	223.5	191.6	224.2	194.7	226.9	208.2
10PE33												
67%	219.8	204.6	222.8	204.5	221.1	206.0	221.2	204.1	223.3	203.9	234.2	222.0
* Amount	of add	led water										

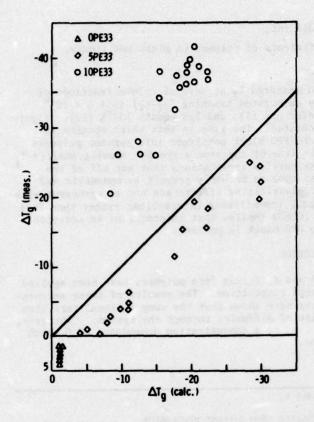


Figure 14. Glass transition change: measured versus calculated.

REFERENCES

- 1. Fick, A., Ann. Phys. Lpz. 170, 59 (1855).
- 2. Crank, J., "The Mathematics of Diffusion," Oxford University Press, London (1956).
- Rogers, C. E., and Machin, D., "The Concentration Dependence of Diffusion Coefficients in Polymer Penetrant Systems," CRC Critical Reviews in Macromolecular Science, 245-313, (1972).
- Barrie, J. A., Machin, D., and Nunn, A., "Transport of Water in Synthetic Cis-1,4-polyisoprenes and Natural Rubber," Polymer, 16, 811 (1975).
- Schneider, N. S., Allen, A. L., and Dusablon, L. V., "Water Vapor Permeability of Ultrathin Polyurethane Films," J. Macromol. Sci-Phys. <u>B3</u>, 767 (1969).
- 6. Illinger, J. L., Schneider, N. S., and Karasz, F. E., "Water Vapor Transport in Hydrophilic Polyurethanes," Hopfenberg, H. B. ed., Plenum Press, New York (1975) p. 183.
- 7. Zimm, B., and Lundberg, J. L., "Sorption of Vapors By High Polymers," J. Phys. Chem 60, 425 (1969) and Lundberg, J. L., J. Macromol. Sci-Phys, B3, 693 (1969).
- Starkweather, H. J., Jr., "Some Aspects of Water Clusters in Polymers," Macromolecules 8, 476 (1970).
- 9. See development and references from Meares, "Polymer Structure and Bulk Properties," Van Nostrand Co. (1965) Chap 10.
- Williams, M. L., Landel, R. F., and Ferry, J. D., J. Amer. Chem. Soc. 77, 3701 (1955).
- 11. CRC Handbook of Chemistry and Physics.
- 12. Rasmussen, D. H., and MacKenzie, A. P., J. Phys, Chem., 75, 967 (1971).

SESSION VI: APPLICATIONS

Chairman: D. Pinkerton
Materials Research Laboratories, Australia

NOVEL TECHNIQUES FOR MEASURING FIELD SERVICE DETERIORATION OF COMPOSITE MATERIALS R. E. Sacher, AMMRC

APPLICATION OF THE DIELECTRIC ANALYSIS TO POLYMERIC MATERIALS CONTROL D. H. Kim, The Boeing Commercial Airplane Co.

DYNAMIC MECHANICAL PROPERTIES IN FIBER REINFORCED EPOXY RESIN BASED NETWORKS J. G. Williams, Materials Research Laboratories, Maribyrnong, Victoria 3032, Australia

ELECTRON SPIN RESONANCE STUDIES OF THE DEGRADATION OF POLYMERIC MATERIALS D. K. C. Hodgeman, Materials Research Laboratories, Maribyrnong, Victoria 3032, Australia

POLYMER CHARACTERISATION BY PYROLYSIS GAS CHROMATOGRAPHY J. R. Brown and D. J. Hall, Materials Research Laboratories, Maribyrnong, Victoria 3032, Australia

VAPOUR PRESSURE OSMOMETRY - ITS LIMITATIONS AS A METHOD FOR MOLECULAR WEIGHT DETERMINATIONS

C. E. M. Morris, Materials Research Laboratories, Maribyrnong, Victoria 3032, Australia

di

NOVEL TECHNIQUES FOR MEASURING FIELD SERVICE DETERIORATION OF COMPOSITE MATERIALS

Robert E. Sacher

Organic Materials Laboratory Army Materials and Mechanics Research Center Watertown, Massachusetts 02172

INTRODUCTION

Composite materials have outstanding properties of strength and low weight and represent important present and potential applications to Army material. Previous studies of the environmental susceptibility of these materials have been of an engineering and quality control nature and has resulted in a study of the effect of outdoor exposure on mechanical properties (1,2). The deterioration observed in an unprotected composite system due to weathering can be separated into two distinct processes:

 (a) Rapid degradation of the surface layer of resin leading to fiber blooming;
 (b) Deterioration of the bulk of the composite by a number of processes - for example, loss of interlaminar shear strength due to fiber-resin debonding or a loss in resin mechanical strength.

The role that the respective environmental parameters of sunlight, temperature, humidity and rainfall play in these processes can be studied by exposing samples at a wide range of exposure sites and conditions as well as by laboratory experiments. This approach has had only limited success with mechanical measurements in particular (1). Fundamental studies of the weathering process have been hampered by:

(a) The uncertainty in epoxy resin composition due to both the proprietary nature of many materials and uncertain quality control;

(b) The wide variability in composite structure due to hand lay-up procedures followed by an often uncontrolled cure cycle;

(c) The intractable nature of the cured composite that prevents the use of conventional techniques of polymer analysis.

As part of a U. S. Army unified program for the prevention of deterioration of organic materials an indepth study has been made of the weathering of one commercial sevenply composite that can be well characterized. This has been exposed at a number of sites and the critical mechanical properties and concurrent chemical changes in the system measured.

In practice a surface coating, either as a gel coat or a separate paint system, is applied to a fabricated composite before it is used outdoors. This frequently provides only partial protection as the gel coat - up to 0.025 mm thick - is often unstable and fiber blooming ultimately occurs. It has also been suggested that surface protection by painting could lead to accelerated deterioration of bulk mechanical properties by moisture (3). In addition, the deterioration problem of the paint is substituted for that of the composite and the fundamental problem of environmental degradation of the surface is not addressed. This study has aimed at determining the mechanism and rate of deterioration and identifying the initiation process for resin degradation. To accomplish this, a number of analytical techniques have been applied to overcome the intractable nature of a cured epoxy resin.

RESULTS AND DISCUSSION

1. Materials: The fiberglass epoxy resin system, Scotchply 1009-26, is a seven-ply laminate (alternating 0° and 90°) of 73% Owens Corning 801 E-glass and 27% of a mixed epoxy resin. The resin composition is 67% of a tri-functional epoxy Novolac (DEN 438) and 33% of a diglycidyl ether of bisphenol A (Epon 828) with 3% by weight of BF3:Monoethanol amine complex curing agent. The chemical composition is summarized in Figure 1. The laminates were cured at 344 Pa and 164°C for 45 minutes, cooled and post cured for 4 hours at 177°C. No surface treatment was given prior to exposure trials.

DEN 438

EPON 828

BF₃ • MEA COMPLEX
OWENS CORNING 801-E GLASS FIBER

Figure 1. Chemical Composition of 1009-26 Laminate

2. Exposure Trials: Panels have been exposed for periods up to 2 years at sites covering a wide range of environments as summarized in Tables 1 and 2. In addition, accelerated exposure was performed in a carbon arc fadeometer, Atlas xenon arc weatherometer and at EMMA and EMMAQUA mounts at Desert Sunshine Tests Incorporated, Arizona. These simulated hot dry and hot wet exposure conditions but with maximum solar radiation dose rates of typically 5900 Langleys/day for EMMA and 4500 Langleys/day for EMMAQUA.

TABLE 1

U. S. TEST SITES FOR EXPOSURE OF COMPOSITES

Site	Zone	Met. Data-Yearly Averages						
	Temperature Max Min		Precipitation	R.H. Max Min		Solar Radiation		
Market State 198				cm		4	Langleys	
Panama Canal Lat: 9° 20'N	Tropical Open	27.8	23.9	330	98	73	146,000	
	Rainforest	26.6	24.1		95	82		
Yuma, Arizona Lat: 32° 50'N	Desert	29.5	14.3	6.8	48	16	172,000	
Maynard, Mass Lat: 42° 25'N	Temperate	14.1	3	.122	89	54	110,000	

TABLE 2

TEST SITES

SITE		TYPE OF	ENVIRO	MENT	
Fort Sherman, Sunshine (Atlantic) (Open Site)	Panama	Sun	Hot	Humid	
Fort Sherman, Coastal (Atlantic) (Breakwater)	Panama	Sun	Hot	Humid	Salt
Fort Sherman, Jungle (Rain Forest)	Panama	Hot	Humid	Microbi	ological
Chiva Chiva, Sunshine (Pacific)	Panama	Sun	Hot	Humid	
Maynard, Sunshine	Massachusetts	Temper	rate		
Yuma, Sunshine	Arizona	Sun	Hot	Dry	
Caribbean, Sunshine	Puerto Rico	Sun	Hot	Humid	
Innisfai	Australia	Sun	Hot	Humid	
Cloncurry	Australia	Sun	Hot	Dry	
Maribyrnong	Australia	Temper	rate		
North Sea	Germany	Temper	rate		
Weatherometer					
EMMAQUA		Accele	erated of	outdoor Humid	
EMMA		Accele Sun	erated of	outdoor Humid	
Soil Buried					

^{3.} Deterioration Measurements: Ion Probe Microanalysis (Secondary Ion Mass Spectrometry) (SIMS)). This technique was utilized to determine the finish thickness of the epoxy resin system on the surface of the composite material. Measured amounts of the finish were sputtered off and introduced into the mass spectrometer for analysis. The depth at which silicon-containing peaks were identified on the mass spectrometer was interpreted as the thickness of the outer resin.

Three different materials were analyzed:

SAMPLE	DESCRIPTION OF MATERIAL
e in 1 % on the sea the larger of each activity	Lot I - stored in laboratory light for 2 years
2	Lot I - stored in desk (no light) for 2 years
3	Lot II - new

The samples were found to contain severe inhomogenities in the film thickness. Sample 1 has a mean thickness of 1.1 micrometers; sample 2, 0.7 micrometer and sample 3, 0.4 micrometer. The thinnest areas on sample 1 were about 0.6 micrometer while the thickest were about 1.3 micrometers. On sample 2 the thinnest areas were about 0.4 micrometer with the thickest being about 0.8 micrometer. On sample 3 the thinnest areas were about 0.3 micrometer and the thickest about 0.7 micrometer.

3.1 ESCA (Electron Spectroscopy for Chemical Analysis): With this technique we were able to follow the production of carbonyl in the surface of the composite as a function of depth. The carbonyl content increases from negligible amounts in the 6-month samples to over 20% carbonyl concentration in the 18-month on the uppermost 50 angstroms of the exposed surfaces (Figure 2). In argon ion etching experiments the surface of the composite was sputtered off at 50-angstrom intervals. The carbonyl content was found to decrease about half after the first etch, and after the second etch of an additional 50-angstrom elimination, no carbonyl band was detected even after 24 months' exposure. We assume that carbonyl development is an indicator of photo-oxidation. Based on this assumption, the depth of UV penetration is about 50 angstroms deep.

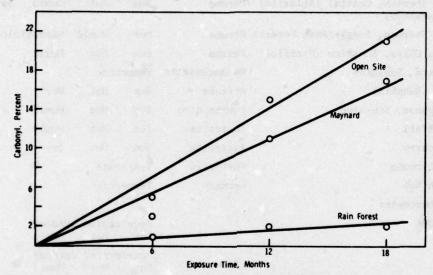


Figure 2. ESCA analysis of surface layer of composite after exposure at sites indicated (Table 1)

3.2 Fourier Transform Infrared Spectroscopy: The loss of surface resin can be directly monitored nondestructively by ATR-IR spectroscopy, in this case using a Fourier transform IR spectrometer (Digilab FTS-10M). The FTS system, being based on an interferometer, has the advantage of high energy throughput and a rapid scan rate enabling signal averaging of a large number of scans to enhance the weak surface absorption spectra (4). The inset of Figure 3 shows three typical ATR spectra of a composite panel before exposure and after 6 and 12 months at Yuma. The detailed information from the ATR of the unexposed resin is discussed later. Resin absorption is very weak after even short exposure and the spectrum is dominated by the Si-0 stretch at 893 cm⁻¹ and a band at 1400 cm⁻¹ probably due to B-0 stretch. This can be used to give an index of fiber blooming from sample to sample and the growth of glass absorption in samples at Yuma and Panama are shown in Figure 3. After 6 months in Panama the ATR spectrum is indistinguishable from that of E-glass so that blooming is almost complete and the surface can be classified as totally degraded. A TGA of fiber taken from the surface showed no residual organic material.

The penetration depth of the IR radiation in the ATR experiment (using a KRS-5 crystal at 45°) is 1.2 μ m at 1400 cm⁻¹ and 2 μ m at 850 cm⁻¹. The surface layer of resin in the unexposed composite has been determined by ion microprobe analysis using secondary ion mass spectrometry.

The surface resin was stripped at a known rate with an ion beam until silicon was detected. This gave a thickness estimate of from 0.7 to 1.1 μ m, i.e., on the order of the penetration depth of the radiation in the ATR experiment. This explains the sensitivity of the spectra in Figure 3 to small changes in the resin thickness at the onset of degradation.

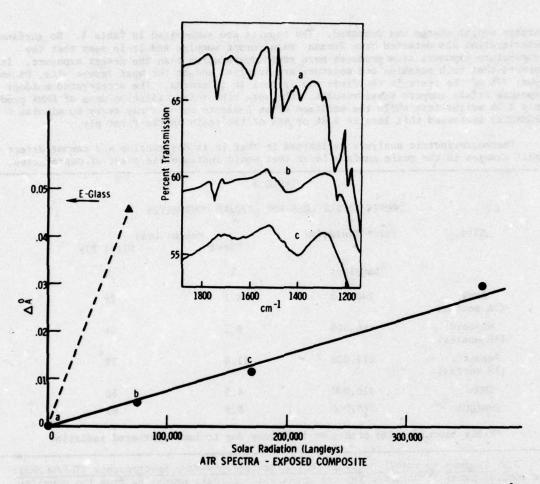


Figure 3. ATR-IR study of composite surface on weathering. Change in absorbance (ΔÅ) of 1400 cm⁻¹ band at Panama open site (Δ) and Yuma (•). The absorbance value for pure E-glass is also shown.

- 3.3 <u>Laser Pyrolysis GC-MS</u>: The use of a defocussed ruby laser pulse to pyrolyze a sample for on-line GC-MS analysis has two advantages in the study of the system:
 - (a) the surface is specifically analyzed;

0

(b) secondary radical reactions and rearrangements are minimized, so that pyrolysis products can be directly related to the materials structure.

Full details of this analysis have been published by Merritt et al. (6). Two principal oxidation products detected were acetone and acetophenone and the relative concentration of these increased on outdoor exposure as shown in Figure 4. Other pyrolysis products such as toluene, benzene and 2-phenyl propane also increased with sample exposure time. This, together with the observation that no volatile organics could be detected from the unexposed material, suggests that outdoor exposure is lowering the total cross-link density, so enhancing the pyrolysis yield. This result is substantiated by dynamic mechanical measurements.

3.4 TGA Analysis: Resin burnoff from 50 to 100 mg samples cut from the exposed panels was measured. The smaple was programmed to 600°C in nitrogen and held in air until no

further weight change was detected. The results are summarized in Table 3. No surface deterioration was detected from Panama rain forest samples and it is seen that the temperature exposure site produces more resin degradation than the desert exposure. It appears that both sunshine and moisture are involved and at the most severe site, Panama open, 77% of the resin in the first ply is lost in 18 months. The accelerated outdoor exposure trials support these results. The very high solar radiation dose of EMMA produced only 4.3% weight loss while the addition of an 8-minute water spray every 60 minutes (EMMAQUA) increased this loss to 9.8% or 69% of the resin in the first ply.

Thermogravimetric analysis is limited in that it is destructive and cannot detect very small changes in the resin surface layer that would indicate the onset of degradation.

TABLE 3
RESIN WEIGHT LOSS FOR EXPOSED COMPOSITES

Site	Solar Radiation	Weigh	nt Loss
		Total	First Ply
	Langleys	•	
Yuma (18 months)	248,000	4.2	29
Maynard (18 months)	166,000	9.2	64
Panama (18 months)	211,000	11.0	77*
EMMA	420,000	4.3	30
EMMAQUA	318,000	9.8	69

^{*}Fiber blooming also occurs on back face due to back-scattered radiation

When the sample was heated, it was found that water diglycidyl ether of bisphenol A (unreacted epoxy) and hydrogen fluoride were evolved. The hydrogen fluoride is believed to be a product of the low temperature reaction of trapped water and the BF_3 complex used for crosslinking the epoxy. These reaction products were detected without stressing the material.

When the composite specimen is subjected to a torsional stress while simultaneously experiencing a tensile stress at room temperature, both water and higher molecular weight compounds are evolved. These higher molecular weight compounds are oligomers of both the EPON 828 and DEN 438 resin systems.

Studies of stress on the epoxy resin system by itself should reveal whether these

^{3.5} Thermogravimetric Analysis-Gas Chromatography-Mass Spectroscopy (TGA/GC/MS): The control panel illustrated typical organosilicon peaks emanating from the coupling agent. After 6 months higher molecular weight organosiloxanes were detected with a minor amount of the virgin coupling agent. After 12 months of exposure, no silicon-containing masses were detected. Either the silicon coupling agent has further polymerized to more stable polysiloxanes, converted to inorganic silicon derivative, or has been broken down and volatized into the atmosphere. Clearly, the concepts of how a coupling agent contributes to the properties of a composite must be revaluated in light of these findings.

^{3.6} Stress Mass Spectrometric Analysis (SMSA): This technique was applied to determine the amount of volatiles trapped in the composite material, and the products evolved when a physical stress was induced upon the composite.

evolved materials are inherent in the epoxy matrix or induced by the fiber at the interface. Also, information to determine whether these materials are absorbed or trapped species or formed as stress-induced degradation products will be sought from further studies using this technique.

3.7 Changes in T_g on Exposure: A torsional pendulum study has been carried out on the samples exposed at Panama open site for up to 18 months (7). The seven-ply laminate was split to study three-ply sections taken from the exposed surface, the center and the unexposed side. It was found that the glass transition temperature, T_g , defined as the peak in the damping curve, decreased with outdoor exposure. This is shown in Table 4 for the top, center and lower plies. The effective molecular weight between cross-links, M_c , was calculated from the T_g data and the drop in M_c with exposure was linearly related to the total concentration of volatiles released from the sample by the laser pyrolysis. A study of a rainforest 18-month sample showed a T_g of 180°C for both top and center plies.

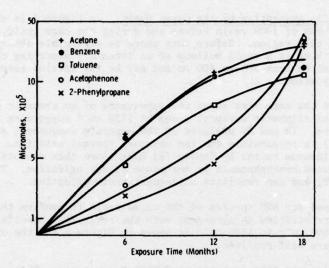


Figure 4. Growth of laser pyrolysis products with exposure at open site, Panama

TABLE 4 GLASS TRANSITION TEMPERATURE (Tg) OF THREE-PLY SECTIONS FROM PANELS EXPOSED AT OPEN SITE, PANAMA

Exposure Time	Solar Radiation		Tg	
		Тор	Center	Bottom
Months	Langleys		°C	
0	0	180	180	180
12	146,000	175	180	177
18	211,000	165	179	169
24	318,000	145	177	150

CONCLUSIONS

- 4. Surface Analysis Studies: There are two general conclusions that can be drawn from the exposure trial: (1) The surface loss of resin leading to fiber blooming is most severe in hot, wet climates with high total solar radiation doses. Those accelerated tests such as EMMA and carbon arc Fadeometer produced only surface resin darkening, whereas addition of water spray to the exposure cycle (i.e., EMMAQUA and Atlas weatherometer) produced fiber blooming. (2) The resin in the surface ply degrades by photo-oxidation to produce low molecular weight segments. These may be directly washed from the surface or, if remaining plasticized the resin, so lowering Tg.
- 5. Epoxy Resin Photo-Oxidation: In order to obtain insight into the photo-oxidation process of the resin and, in particular, how the degradation is initiated and may be inhibited, experiments have been performed on sections of resin of the same thickness as the surface layer of the composite, i.e., approximately 1 µm.
- 5.1 Solar Radiation Absorption by the Cured Resin: In Figure 5 is shown the electronic absorption spectrum of 1009 resin before and during the cure cycle. Also shown is the solar band edge in this region. Before cure there is negligible absorption of radiation, but during cure there is a rapid buildup of an intensely absorbing chromophore. This is unstable to UV radiation from 300 to 400 nm and may be the species responsible for the initiation of photo-oxidation.

The IR spectrum at the same time shows the appearance of an aromatic carbonyl absorption at 1650 cm⁻¹ and an aliphatic carbonyl group at 1735 cm⁻¹ suggesting thermal oxidation of the resin during cure. IR and UV analysis of the separate components show that the epoxy Novolac resin (DEN 438) is responsible for the observed thermal oxidation. Studies on analogous phenol formaldehyde resins by Conley (8) have shown that oxidation at 150° to 200°C produces substituted benzophenones by methylene bridge oxidation. These groups absorb strongly in the near UV, and can sensitize subsequent photo-oxidation.

FTS-IR has been used for ATR spectra of the cured resin to confirm that the surface of the composite panels are oxidized in agreement with the resin film results. The portion of the IR spectrum from 1800 cm⁻¹ to 1400 cm⁻¹ is shown in Figure 6 and the oxidation bands on the composite surface are well resolved.

5.2 Photo-Oxidation and Photoprotection of 1009 Epoxy Resin: Thin cured films of 1009 resin and the separate components were exposed to UV radiation from 300 to 400 nm and the oxidation followed by IR (Figure 7). The oxidation rate measured from the aliphatic carbonyl band growth for DEN 438 is eight times that for Epon 828 and dominates the photo-oxidation of the 1009 system. This agrees with the conclusion of the above section concerning the photo sensitivity of the epoxy Novolac oxidation products formed in air.

Improvement of the stability of this resin system to outdoor exposure should be possible by suppressing the oxidation during cure. This has been studied by either curing and postcuring in a vacuum oven or using a compatible antioxidant that will suppress oxidation without affecting the cure.

The results are summarized in Figure 7. The improvement factor of less than two for vacuum oven cure and the limited protective efficiency of the antioxidant even at high concentration suggest that other initiation processes are also occurring.

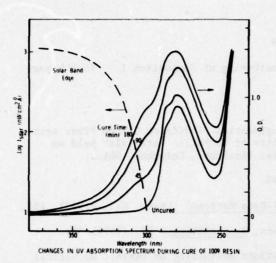


Figure 5. Change in UV absorption spectrum of 1009 resin on cure, and the solar spectrum in this region.

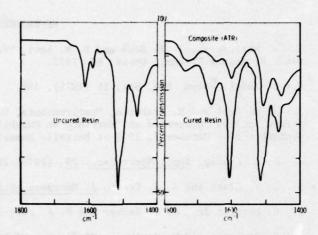


Figure 6. Transmission IR spectrum of 1009 resin before and after cure and ATR-IR spectrum of composite surface.

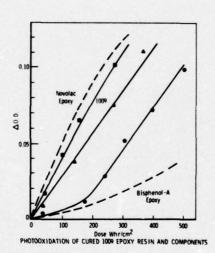


Figure 7. Change in absorbance at 1735 cm⁻¹ (ΔO.D.) with UV dose (290 to 350) for:

(i) 1009 resin (m) and

- components (--)
- Novolac epoxy cured in vacuum (A) and with 1% Irganox 1010 as antioxidant ().

REFERENCES

- 1. J. Maciejczyk, R. B. Bonk and D. W. Levi, 'Weathering of Composites I." Tech Report 4467, Picatinny Arsenal, Dover, NJ 1973.
- 2. O. Ishai, Polym. Eng. Sci, 15 (1975), 486.
- 3. J. M. Augl and R. Trabocco, "Environmental Degradation Studies on Carbon Fiber Reinforced Epoxies" presented at "Workshop on Durability of Composite Materials" held on September 30 October 2, 1975 at Battelle Memorial Institute, Columbus, Ohio.
- 4. J. L. Koenig, Appl. Spectrosc., 29, (1975) 293.
- 5. D. T. Clark and W. J. Feast, J. Macromol. Sci-Revs Macromol. Chem., C12, (1975), 191.
- 6. C. Merritt Jr., R. E. Sacher and B. A. Petersen, J. Chromatog., 99, (1974) 301.
- 7. D. Roylance and M. Roylance, "Influence of Outdoor Weathering on Dynamic Mechanical Properties of Glass/Epoxy Laminate" in ASTM Special Technical Publication "Environmental Effects on Advanced Composite Materials", 1976, in press.
- 8. R. T. Conley, J. Appl. Polym. Sci., 9, (1965) 1117.

APPLICATION OF THE DIELECTRIC ANALYSIS
TO
POLYMERIC MATERIALS CONTROL

DUK H. KIM
The Boeing Commercial Airplane Company
Seattle, Washington

This paper describes specific applications to the dielectric and the DC conductance technique to control polymeric materials. The proposed dielectric method can provide an objective test for gel time measurement in place of the conventional method which is rather subjective. Simultaneous operation of the dielectric and the DC conductance can determine when the cure cycle is complete and when pressure should be applied during the cure cycle to have a dense and void-free laminate. The dielectric and the DC conductance were also found feasible to determine quantitatively flow characteristics of "aged" materials ("B"-stage advancement).

1. INTRODUCTION

Due to large batch-to-batch variations in polymeric materials, their usage in aerospace industry will be significantly reduced even though their properties are attractive to the designer. Better quality assurance methods for these materials become even more necessary with current shortages in primary resins and other chemicals.

Quality assurance must provide an adequate control for incoming materials to meet service requirements as well as proper processability during production. More than often the processability has been a problem rather than meeting and receiving inspection requirement for short-term mechanical and physical properties. A typical example of a failure during production is shown in Figure 1 where the core was moved and crushed during fabrication, this was due partially to excessive material flow. Finally, quality assurance should also provide an adequate control for cure, a nondestructive inspection for integrity of final product and an in-service monitoring technique for its structural integrity.

This paper described the application of instrumental techniques to material control and cure cycle monitoring for polymeric materials and discusses the limitations of these techniques. Recently significant progress has been made in the characterization of polymeric materials using modern instrumental techniques. An on-site control technique is required to be operated outside of the test cells, translating its results from the laboratory to the production parts. Only a few techniques meet an on-site requirement and provide a significant role in the characterization. They are the dielectric analysis and the DC conductance technique (ion graphing) which are main instrumental tools used in this study to develop specific applications to quality assurance activity. However, it should be clarified that dielectric, heat capacities, coefficients of linear thermal expansion, dynamic modulus and glass transition temperatures of polymer materials can not always be treated like materials constants. These properties are variable, depending among other things upon sample environments and thermal histories. Thus it is important to establish a range of heating rates in which reproducible results can be obtained and avoid side effects such as thermal and oxidative crosslinking or degradation during measurements.

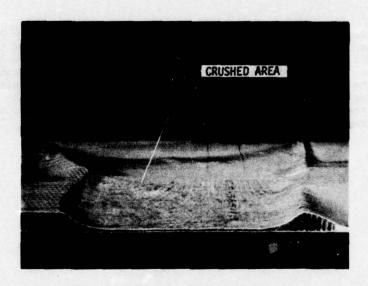


FIGURE 1. CORE CRUSHED DURING FABRICATION

2. BACKGROUND OF THE DISSIPATION AND THE CONDUCTANCE

When a sinusoidal voltage, V, is applied, the current for capacitor I_C,

$$I_C = J\omega CV$$

where ω is the frequency of a sinusoidal voltage applied and C is the capacitance of a material.

In addition to the charging current, the current for capacitor, there may appear a loss current due to the conductance of the dielectric material,

in phase with the voltage. G represents the conductance of the dielectric.

The ratio of loss current to charging current, commonly referred to as the dissipation factor D or loss tangent tan δ , where

$$D = \tan \delta = \frac{I}{I_C} = \frac{GV}{\omega CV} = \frac{1}{\omega CR}$$

and R is the resistance of the dielectric material. So-called "ion graphing" (2) which uses a system based on monitoring the change in electrical resistance in polymeric material is proportional to the resistance of materials,

at zero frequency.

Thus, assuming that the resistance does not vary much within the range of the frequency used, the relationship between the dissipation and ion-graphing is Figure 2

$$D \propto \frac{1}{\omega} \cdot \frac{1}{C} \cdot \frac{1}{\text{Ion graphing}}$$

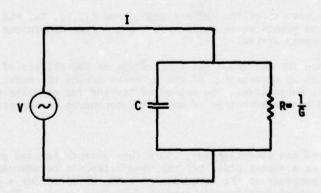


FIGURE 2. EQUIVALENT PARALLEL CIRCUIT FOR CAPACITOR AND CONDUCTANCE

Ion-graphing, the conductance, is caused by a migration of a charge carrier in a polymeric material. The DC conductance requires both the presence of ions and sufficient mobility for them to migrate through the material. Dissipation can occur, in addition to the conductance, by resonance absorption of charges, bound elastically to an equilibrium and relaxation of charge or a dipole. However, it has been difficult to accurately relate the result of the dissipation and the conductance to flow characteristics, gel time and cure completion of the polymeric material (1).

3. EXPERIMENT

3.1 Gel Time

The materials used in this study are glass fabric preimpregnated epoxy resins, low temperature curing systems (250 F), manufactured by Fiberite, Hexcell, Narmco and DuPont. The current method for gel time uses the heated platen of a press regulated at a temperature of 275 - 5 F (Figure 3). Upon inserting the specimen, sufficient pressure is then applied to create a bead of resin around the edge of the sample. A stop watch is started as soon as pressure is applied and the resin bead is probed with a wood glass rod until the specimen has gelled. Gelling will be preceded by the appearance of stringiness, i.e., long strands of resin drawn out from the bead when probed, followed by the disappearance of these strands upon gelation. Gelation is the point where no stringing of the resin is noticed and the probed material has a rubbery feel.

The proposed method using a dielectrometer to determine gel time requires a simple monitoring of the dissipation after inserting the specimen into the heated platen regulated at a temperature of 275 - 5 F and a reading of gel time on the curve of the dissipation.

A typical result with the dielectrometer at the frequency of 1 KH, is shown in Figure 4. As the test starts, the dissipation becomes immediately near zero, since the dipoles in the matrix resin are still readily movable. As the test progresses, the dissipation starts increasing until it reaches a peak. The increase in the dissipation may be caused by an initiation of cross linking of the matrix resin which allows the dipoles to move only with great difficulty. When the resin is hard or cured, the dipoles are locked in place and will not attempt to follow an alternating electrical field. This gives a peak in the dissipation curve. Thus the time span measured from the beginning of the test either is an initial increase in the dissipation (t_1) or the inflection point (t_2) , or to the formation of a peak (t_3) , which can be interpreted as the gel time of the matrix resin at a fixed temperature.

Table 1 compares results of the current method and t_1 , t_2 , t_3 , and shows that the time for the inflection points agrees well with the gel time determined using the current method for the glass/epoxy system.

The current method for measuring gel time relies on the ability of the operator to determine the gel point by observation of the material during the test. This method tends to make the test subjective. The method of testing for gel time using a dielectrometer is objective and has an advantage of not being dependent on appearance.

3.2 Cure Completion

For the purpose of the investigation, 250 F cure glass/epoxy and graphite/epoxy materials were cured in a platen press per the manufacturer's recommendation. Figure 5 shows the dielectric response at the frequency of 1 KH, obtained for a single sample which was heated and cooled continuously through four cure cycles. The glass transition temperatures after the first cure cycle and the fourth cure cycle were measured using the differential scanning calorimeter and are also shown in Figure 5.

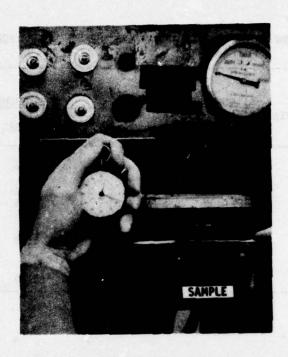


FIGURE 3 THE CURRENT METHOD FOR GEL TIME MEASUREMENT

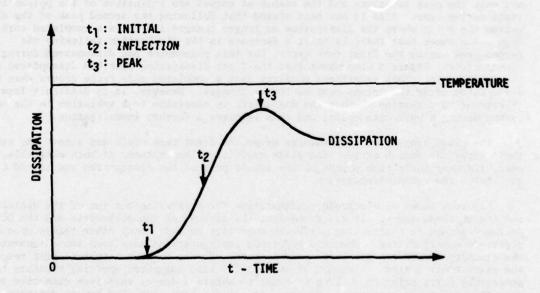


FIGURE 4 A TYPICAL CURVE OF THE NEW METHOD FOR GEL TIME

TABLE (1) COMPARISON OF THE CURRENT AND THE NEW METHOD FOR GEL TIME

MATERIAL - Glass/Epoxy Source	CURRENT METHOD MIN:SEC	DIELECTROMETER		
		MIN:SEC	t ₂ MIN:SEC	MIN:SEC
FIBERITE	4:30	3:00	4:15	6:30
HEXCELL	4:30	4:30	3:38	6.38
DuPONT	4:45	2:50	3:48	10:08
NARMCO	3:45	2:00	3:30	8:16

It has been reported that the absolute values of the dissipation are not important and only the peak locations and the shapes of curves are indicative of the polymeric state during cure. Also it has been stated that following the second peak of the dissipation the point where the dissipation no longer changes indicates a completed cure. Figure 5.b shows that there is still a decrease in the dissipation following the second peak during the first cure cycle, but this phenomenon had disappeared during the second cycle. Figure 5 also shows that the first dissipation peak had disappeared after the first cycle. This experiment confirms that a completed cure cycle occurs when the dissipation after the second peak no longer changes. However, it is difficult from this experiment to determine whether the dielectric is sensitive to a variation in the matrix system during a post cure cycle, and thus requires a further investigation.

The glass transition temperatures after the first cure cycle are almost the same as those after the fourth cycle. The glass transition temperatures of both materials, however, lie near inflection points on the second peak of the dissipation and are 20 C to 30 C below the curing temperature.

Figure 6 shows an electrode configuration for a simultaneous run of the dielectometer and the DC conductance. It was found that the success of the dielectric and the DC conductance method in controlling polymeric materials depends among other things upon a proper electrode configuration. Specific electrode configurations have been found separately for the glass/epoxy and the graphite/epoxy systems. Figure 7 shows a typical test result for the glass/epoxy system. A number of authors (3) have suggested applying pressure to the processing parts prior to gelling in order to obtain a dense, void-free composite structure with the proper resin content. However, it has not been clarified how to determine using a dielectrometer at a specific point when pressure should be applied to consolidate the lay-up. Figure 7 indicates that the peak of the DC conductance occurs always at the valley between the two peaks of the dissipation.

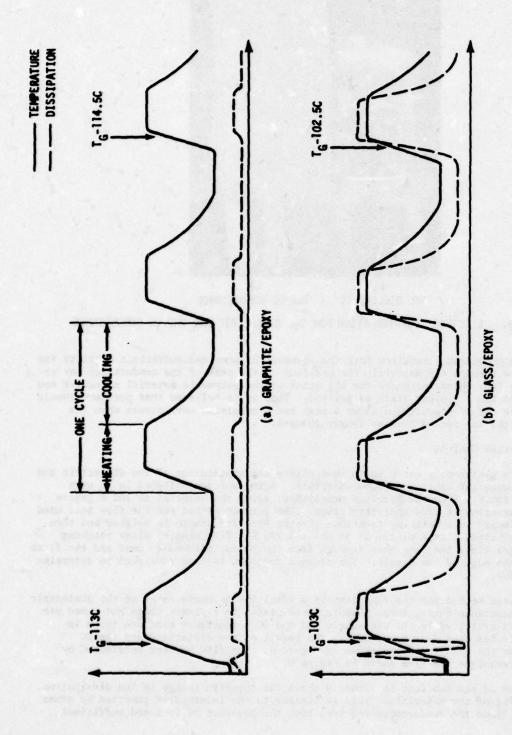
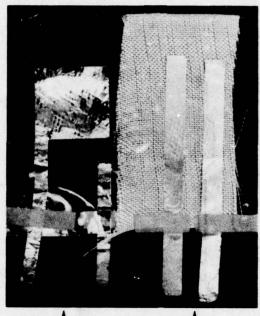


FIGURE 5 DIELECTRIC RESPONSE OBTAINED FOR A SINGLE SAMPLE SUBJECTED TO FOUR CONTINUOUS CURE CYCLES



THE DIELECTRIC THE DC CONDUCTANCE

FIGURE 6. ELECTRODE CONFIGURATION FOR THE DIELECTRIC AND THE DC CONDUCTANCE

Since the conductance requires both the presence of ions and sufficient mobility for them to migrate through the material, the position of the peak of the conductance may be related to the flow characteristics for all sizes of the polymeric material molecules and particularly to the incipient state of gelling. Thus it is believed that pressure should be applied when the DC conductance shows a peak and a completed cure occurs when the dissipation after the second peak no longer changes.

3.3 Aged Material Control

250 F cure glass/epoxy was used to investigate the application of the dielectric and the DC conductance for control of aged materials. Aging was accomplished in an oven maintained at 100 F. From our previous experience, aging the material at 100 F gave a significant variation in flow characteristics. The current method for the flow test used for the glass/epoxy is a weighing technique (Figure 8). The sample is weighed and then placed between heated platen plates at 50 psi and 275 F. Five minutes after reaching the measured gel time, the sample is removed from the press, allowed to cool and the flash scraped from the edge of the sample. The cleaned specimen is then reweighed to determine the percent flow.

The proposed method for the flow test is a simultaneous measurement of the dielectric and the DC conductance during cure. Samples were placed in a platen press and cured per the recommended cycle, while the dielectric and the DC conductance were monitored to determine their response during the cure. The result of the dielectric and the DC conductance for the glass/epoxy is shown in Figure 9. The flow percent determined by the weighing technique are also shown in Figure 9.

Comparison of the two data in Figure 9 shows the specific change in the dissipation, indicating aging of the materials. This is similar to the information reported by other authors (3). Since the conductance requires both the presence of ions and sufficient

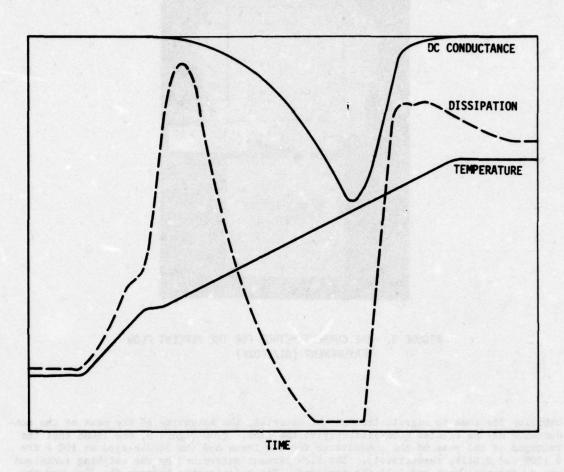


FIGURE 7 A SIMULTANEOUS RUN OF THE DIELECTROMETER AND THE CONDUCTANCE METHOD - GLASS/EPOXY

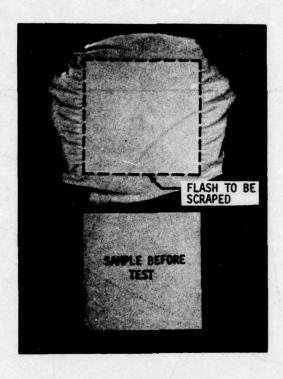
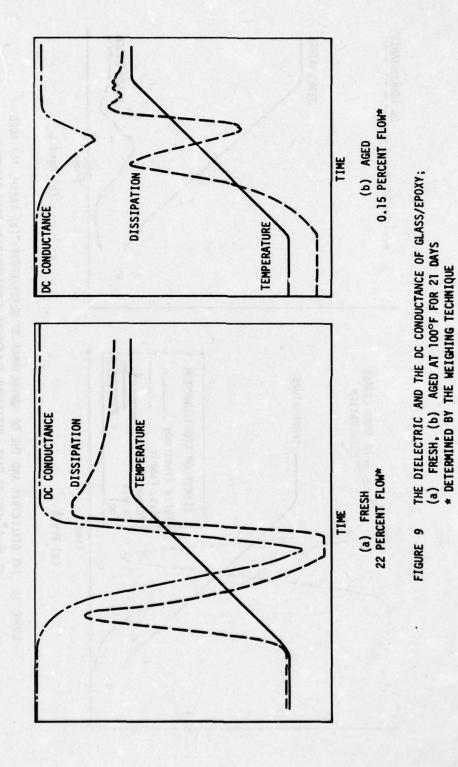


FIGURE 8. THE CURRENT METHOD FOR THE PERCENT FLOW MEASUREMENT (G1/EPOXY)

mobility for them to migrate through the material, the intensity of the peak of the conductance may be related quantitatively to the flow. From Figure 9, one found that the voltages of the peak of the conductance for the fresh and the 21-day-aged at 100 F are 0.170V and 0.013V, respectively. The flow percent determined by the weighing technique are 22 for the fresh and 0.15 for the aged. The relationship between the flow and the conductance is still under investigation. However, from the preliminary test results, it is feasible to determine the percent flow rather objectively with the method described above, while the current method is subjective and extensively depends upon an individual operator.

Figure 10 shows the result of the dissipation and the DC conductance using the same material as one used in Figure 9, except a different electrode configuration from Figure 6 was incorporated. The specific electrode configuration used in shown in Figure 10. The voltages of the peak of the conductance for the fresh and for 21-day-aged at 100 F are 0.140V and 0.0V, respectively. which are close to those shown in Figure 9. However, the shape and the location of the dissipation are significantly altered, due to the change in electrode configuration. This may be due to the time-dependent flow property of the prepreg material. Thus it is important to establish a range of heating rates as well as a specific electrode configuration in which reproducible results can be obtained to control polymeric materials.



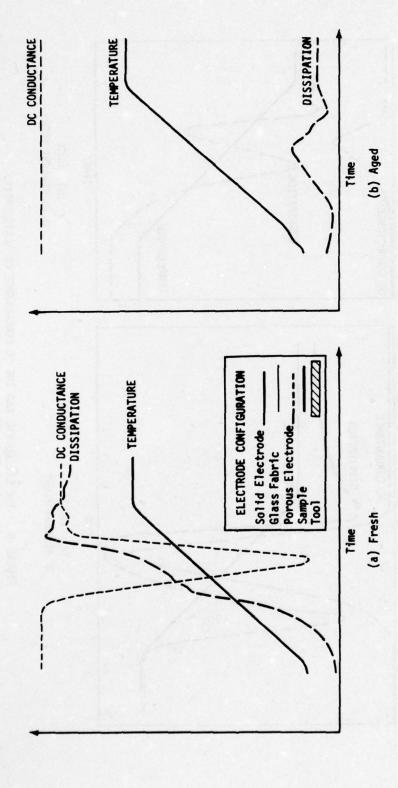


FIGURE 10 THE DIELECTRIC AND THE DC CONDUCTANCE OF GLASS/EPOXY: (a) FRESH, (b) AGED AT. 100°F FOR 21 DAYS. DIFFERENT ELECTRODE CONFIGURATION FROM FIGURE 6

4. CONCLUSIONS

The results presented in this paper show that the dielectric and the DC conductance technique can provide useful tools for quality assurance activity. Specifically the dielectric method can provide an objective test for the gel time measurement while the current method is rather subjective. Simultaneous operation of the dielectric and the DC conductance can determine when the cure cycle is complete, when pressure should be applied to obtain dense, void-free laminates, and will fingerprint flow characteristics of "aged" materials (B-stage advancement).

REFERENCES

- J. F. Carpenter, "Instrumental Techniques for Developing Epoxy Cure Cycles," 21st National SAMPE Symposium Vol 21, 783, 1976.
- D. J. Crabtree and G. H. Bischoff, "The Electrical Analysis of Adhesive Cure," SAMPE Tech. Conf. 1973.
- C. A. May, "Dielectric Measurements for Composite Cure Control Two Case Studies," 20th National SAMPE Symposium Vol 20, 108, 1975.

DYNAMIC MECHANICAL PROPERTIES IN FIBER REINFORCED EPOXY RESIN BASED NETWORKS

John G. Williams

Materials Research Laboratories

Maribyrnong, Victoria 3032, Australia

SYNOPSIS

The dynamic mechanical properties of an amine-cured epoxy resin filled with a range of fillers including glass, carbon and aramid fibers, and glass beads have been determined on a torsion pendulum. The effects of fiber content, orientation and surface treatment on the beta-relaxation near -50°C at 1 Hz have been studied. For carbon and aramid fiber filled systems, the loss maximum appears to be proportional to the volume fraction of resin present, but for glass-filled systems the observed loss is larger than expected. It is not dependent on fiber orientation or on surface treatment.

Composite samples were exposed to boiling water and the dynamic properties determined after periods up to 500 h immersion. It is suggested that the results may be interpreted as the effects of two processes, both leading to the formation of a peak between -20° C and -30° C. One is slow and may be related to the absorption of water, and occurs in all systems. The other is initially slow but occurs at an increasing rate but is only observed on systems containing cleaned glass or aramid fibers. This process may be associated with deterioration at the interface.

INTRODUCTION

Phase transitions are well known to occur in all polymers. The principle transitions are the glass-rubber transition for amorphous materials and the melting transition for crystalline materials, but many polymers show other transitions. A common nomenclature refers to the highest significant transition as the alpha transition and letters transitions in order of decreasing temperature with greek letters. Relatively minor transitions, which may not be detected in all samples or by all techniques are given the closest major transition letter with a superscript.

The temperatures at which the transitions occur depend on the time-scale of the experimental technique. Quasi-static methods such as creep and stress-relaxation studies give higher temperatures for the transition than methods using dynamic techniques at high frequencies as, for example, studies of absorption of ultrasonic waves. A complete description of the transition should include both temperature and time-scale information.

A convenient method for minor transitions uses a free oscillation torsion pendulum to detect relaxation processes in a sample as a function of temperature and, to a limited extent, frequency. Typical equipment has been described (1,2) and sources of error have been studied (3). From the period of vibration of a torsional oscillation initiated in the sample and the geometry and moment of inertia of the system, the real shear modulus of the material may be calculated. From the rate of decay of the oscillations, the loss factor may be found and conveniently expressed by the loss tangent $(\tan \delta)$, a dimensionless

constant independent of geometry of the sample and calculated from the ratio of amplitudes of successive vibrations (An, An+1) using the equation :

$$\tan \delta = \frac{1}{\pi} \ln \left(\frac{An + 1}{An} \right)$$

Results are usually given as plots of loss tangent as a function of temperature at a fixed frequency. (Termed loss spectra). The temperature of a transition can be defined as the temperature at which the loss tangent is a maximum. The maximum value of the loss tangent is an estimate of the strength of the relaxation.

The results of such studies on polymers have been reviewed (1). For metals and other crystalline materials, the mechanisms of many relaxations have been proposed (2), but for polymers the mechanisms are generally unknown or subject to controversy. Semi-crystalline polymers show relaxations due to both amorphous and crystalline regions and are particularly complex. For amorphous materials, the major relaxation (almost always the alpha relaxation) occurs at the temperature at which the polymer network changes, between the rigid glassy state, in which large molecular segments have no long-range translational movement, and the rubbery state where such movement is possible and molecular segments are free to move between many equivalent configurations. It has been suggested (4) that the mechanisms of minor relaxations may be related to a similar onset of mobility in small, isolated segments of the polymer chain. The size of the moving segment may be 50-100 atoms, 3-4 atoms or possibly single atoms.

Loss spectra may be used to characterise polymers in three ways, depending on the background information available. Even if no knowledge of the mechanisms is available, the spectrum can be used as a non-destructive test to "fingerprint" the sample. In some instances, relaxations may be associated with the presence of foreign material such as water in polymides (5), or with particular phases in multiphase systems such as thermoplastic rubbers (6) or semi-crystalline polymers (7). In these cases, the spectra can be used to characterise the material quantitatively. In a few cases, relaxations have been associated with particular molecular segments of the polymer and these relaxations can be used to study in detail subtle changes in molecular structure.

Such a well-defined relaxation is observed in amine-cured epoxy resins near -50°C at 1 Hz and is known as the beta-relaxation for these materials. It was first reported by Kaelble (8) and has been extensively studied since the structure of the polymer can be readily modified chemically by alterations to the resin and curing agent. It has been suggested that the beta-relaxation is related to the presence of the glyceryl unit formed by reaction of the glycidyl unit of the resin with amine (9):

$$R-OCH_{2}CH-CH_{2} + HNR_{2} \longrightarrow R-\begin{pmatrix}OH\\OCH_{2}CH-CH_{2}-\\glyceryl unit\end{pmatrix}NR_{2}$$

Several factors affect the height of this loss peak, e.g. the presence of fillers, the degree of cure and variation of the resin/amine mixing ratio affect the concentration of glyceryl units in the sample and a decrease in concentration leads to a decrease in peak height. It has been suggested that peak height is proportional to glyceryl concentration (10,11). Other factors which affect the peak height and position include absorption of water (12,13), mechanical fatigue (14) and thermal degradation (15). Studies on the absorption of water by resins and derived composites (16,17) have shown that as water is absorbed, the relaxation increases in magnitude and the transition temperature increases. For systems containing clean glass beads, a new relaxation appears near -8°C which has

been suggested to be associated with free water in the system (17). Systems containing silane treated glass beads do not show the appearance of this relaxation. This paper extends these results to fiber-filled systems.

EXPERIMENTAL

The resin used in this study was the purified diglycidyl ether of 2,2-bis(4'-hydroxy-phenyl-)-propane supplied as 'Epon' X22 by Shell Chemical(Aust) Pty.Ltd.. The curing agent, 1,3-diaminopropane, was laboratory grade material supplied by Koch-Light Laboratories Ltd and was redistilled before use (bp 138-140°C).

The glass fiber used was continuous E-glass roving (K filament, 20 end) supplied by Australian Fibre Glass Pty.Ltd., and was coated with a proprietary, epoxy-compatible, silane size. This is referred to as treated glass. Some fiber was washed repeatedly with chromic acid solution in concentrated sulphuric acid to remove all size and subsequently washed with water and acetone and dried at 150°C and stored over silica gel. This is referred to as cleaned glass.

Carbon fiber used was supplied by Morganite Modmor Ltd. as Type II, treated fiber and aramid fiber was supplied as PRD 49 Type III, 20 end continuous roving by E.I. du Pont de Nemours & Co.Inc.. Soda-glass beads were supplied by Catasphere Bead Co. and were sieved to a size range of 105-210 μ and cleaned with the chromic acid solution as described for the glass fiber.

Some samples were prepared from unfilled matrix, and from matrix containing liquid water or glass beads. Fiber reinforced samples were prepared from cleaned and treated glass in axial and circumferential orientations and from carbon and aramid fibers in axial orientation only.

All samples except the water filled matrix were prepared by premelting the resin and adding a stoichiometric quantity of amine (9.8 wt %). Unfilled and bead-filled systems were cast vertically in teflon-lined copper tubes. Beads were allowed to settle during cure and the test specimens were cut from the bottom of the cured rod, where the glass content was highest. Samples with axially-oriented fiber were prepared by looping an appropriate weight of fiber over a wire, wetting thoroughly in a premixed matrix bath and pulling the doubled fiber hank into a teflon-lined copper tube. For circumferentially aligned fiber-filled samples, a filament winding technique was used. Continuous fiber was passed through a resin bath and wound onto a teflon-coated rod. A total of two layers of glass were applied at a helix angle of ± 70°.

All systems except the water filled matrix were cured for 20h at 60°C and postcured for 200 min at 150°C. Filament-wound samples, which were not protected externally by a layer of teflon, were postcured under nitrogen to prevent oxidative degradation.

The water filled sample contained 0.81 pt wt resin, 0.11 pt wt amine and 0.08 pt wt liquid water. The resultant creamy emulsion was cast normally and cured for 20h at 60°C, but was not postcured. It contained a 25% excess of amine.

Specimens as tested were approximately 120 mm long and rods were 5 mm in diameter; tubes were 5 mm in internal diameter and approximately 7 mm in outside diameter. All samples for dynamic testing were fitted with aluminium end pieces.

Dynamic mechanical properties were determined using an inverted, free-oscillation torsion pendulum. The accuracy of this instrument has been described (3). The frequency of oscillation was adjusted to remain in the range 0.8 to 1.2 Hz and the temperature range studied from -150° C to the glass transition temperature of dry samples, or to room temperature for samples exposed to water.

Specimens with fitted end pieces were exposed to water by immersion in distilled water maintained at a temperature just below boiling (98-100°C). Samples were removed periodically, the end pieces cleaned of corrosion products, the samples dried with tissue and the dynamic properties determined. They were then returned to the same water bath.

Fiber contents of the axially-aligned, fiber-filled systems were calculated from the weight per unit length of the fiber hank used to prepare the sample, and the calculated volume of the specimen, assuming the density values of the fibers reported in the supplier's literature. The fiber contents of glass-filled systems were checked by ignition and found to be in agreement with the calculated value. Glass contents of bead-filled and filament-wound samples were also determined by ignition.

To determine the rate of absorption of water, rods of 10-30 mm length were dried for 2 h at 150° C and weighed. After immersion for a known period in boiling water, superficial water was removed using absorbent paper and the samples were reweighed.

RESULTS

The effect of the fibers on the beta relaxation is shown in Figure 1 as plots of loss tangent against temperature. The peak is depressed in height by the presence of fiber. Figure 2 shows the dependence of peak height on the volume fraction of resin present (V_p) .

The beta peak for the waterfilled sample occurred at -55° C at a height of 0.0805. No sign of any peak near -30° C or -8° C could be detected.

Exposure of unfilled matrix to boiling water for prolonged periods has little observable effect on the loss tangent peak. The height decreases from a value of 0.0725 to 0.070 after exposure for 3500 hours.

Results of exposure of composite samples are depicted in Figures 3-6 as a series of curves showing the beta relaxation after successive exposures to water and after drying under dry nitrogen at 150° C for 2 hours.

For samples filled with glass treated with a silane finish, exposure to boiling water leads to an increase in height and a shift to higher temperatures as illustrated in Figure 3. For cleaned glass, this change occurs much more rapidly and to a greater extent, and a peak appears near -20°C as shown in Figure 4. The results from exposure of filament wound glass systems are not significantly different from those with axially aligned glass fibers; both cleaned and treated cases. The filament wound specimens, however, become very fragile, especially those based on cleaned glass, and sample failure occurs during dynamic testing after 30-100 hours exposure. Exposure of axially aligned carbon fiber composites results in peak changes similar to those for treated glass reinforced specimens whereas axially aligned aramid based samples are similar to cleaned glass based samples. Figure 5 illustrated the effect of water on these systems.

As exposure of composites based on cleaned glass beads has been reported to give a peak near -8°C after exposure to boiling water for 20 h (17) and this peak could not be detected in fiber reinforced systems, prolonged exposure of bead-filled systems was carried out and the results are shown in Figure 6. Further testing was not possible due to failure of the sample.

Water absorption rates are very similar in all systems when calculated on the basis of per cent change in weight of the matrix as has been reported for systems filled with glass beads (17). After 100h exposure, a weight increase of 3-4% is observed. The absorption rate slowly decreases and at 300 h exposure a total weight increase of 5-6% is observed.

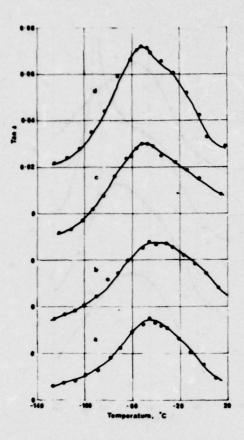


FIG. 1 - The effect of fiber content on the beta relaxation of an amine cured epoxy resin filled with axially aligned fibers.

- a) filled with carbon fiber; V = 0.54
- b) filled with aramid fiber; $V_R = 0.64$
- c) filled with cleaned glass fiber; $V_R = 0.66$
- d) unfilled matrix

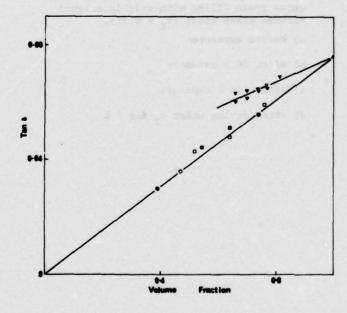


FIG. 2 - The effect of resin content by volume (\mathbf{V}_R) on the height of the beta relaxation.

- V axial glass treated fiber
- ▼ axial glass cleaned fiber
- o circumferential glass treated fiber
- circumferential glass cleaned fiber
- axial carbon fiber
- · axial aramid fiber

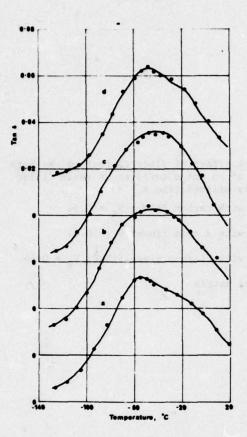


FIG. 3 - The effect of exposure to boiling water on the beta relaxation for an amine cured resin filled with axially aligned treated glass fiber ($V_R = 0.74$).

- a) before exposure
- b) after 150 h exposure
- c) after 494 h exposure
- d) after drying under N_2 for 2 h

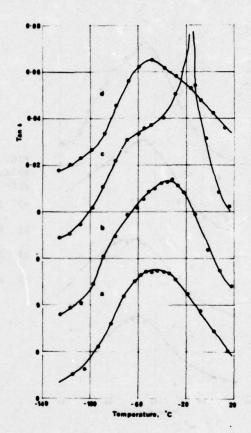


FIG. 4 - The effect of exposure to boiling water on the beta relaxation for an amine cured resin filled with axially aligned cleaned glass fiber ($V_R = 0.74$).

- a) before exposure
- b) after 96 h exposure
- c) after 494 h exposure
- d) after drying under N2 for 2 h

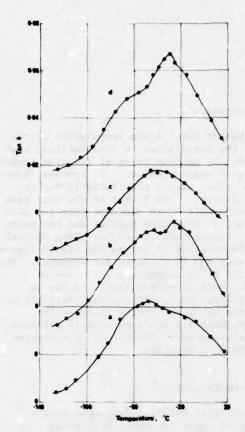


FIG. 5 - The effect of exposure to boiling water on the beta relaxation for an amine cured resin filled with axially aligned fiber.

- a) carbon fiber ($V_R = 0.64$) before exposure
- b) after exposure for 294 h
- c) aramid fiber (Vp = 0.64) before exposure
- d) after exposure for 297 h

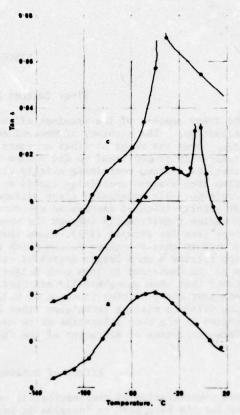


FIG. 6 - The effect of exposure to boiling water on the beta relaxation for an amine cured resin filled with cleaned glass beads ($V_R = 0.65$).

- a) before exposure
- b) after 27 h exposure
- c) after 96 h exposure

DISCUSSION

Fiber Content and Orientation

The fiber content of the specimen affects the height but not the temperature of the beta relaxation. The accuracy of determination of the temperature is somewhat low, however (3). Over the range of fiber contents studied, the maximum value of the loss tangent is approximately proportional to the volume fraction of resin present. It appears, however, that the systems containing axially orientated glass show a significantly higher absorption than systems containing carbon or aramid fibers. The height of the beta peak of circumferentially orientated glass (filament wound samples) are somewhat less reliable than for axially-oriented samples as the outer surface is much less regular and the resin content varies significantly through the specimen. Examination of samples using optical microscopy (see for example (18)), shows that the distribution of carbon and aramid fibers is more uniform than for glass fibers which are stiffer due to their larger diameter. The glass tow retains a much larger degree of order in the axial composites which may be related to the deviation in loss peak height for the axial glass samples. It may be significant that when using axially oriented glass fibers, the glass content could not be increased past about a fiber fraction of 0.35, whereas using the softer fibers or by utilising filament winding techniques fiber fractions near 0.6 could be readily obtained. No variation in the beta relaxation which could be attributed to the effect of variation in surface properties or alignment of the fibers, could be detected.

The Effect of Boiling Water on Composites

From consideration of the results, it can be seen that all filled systems show a tendency for the beta peak to increase in height and to shift to higher temperatures on exposure to boiling water. This effect is very small in the unfilled system even after very long exposures. In the case of treated glass and carbon fiber filled systems, prolonged exposure results in a shift of the peak to between -20°C and -30°C but the rate of increase of height decreases. This may be associated with the decrease in the rate of absorption of water described above. For systems based on aramid or cleaned glass fibers, the peak moves rapidly to -30°C and increases in height dramatically although water absorption rates are very similar to other fiber systems. Bead filled samples showed the formation of the peak near -8°C as earlier reported but on prolonged exposure also showed the formation of a peak at -30°C . All samples recovered their original properties on drying by heating to 120°C for 1-2 hours.

It is possible to describe these occurrences by the formation of a peak between -20° and -30° C by two processes. The first, which may be associated with absorption of water, occurs at a decreasing rate as water absorption rate decreases. The second process appears to be slow to start but occurs more rapidly as exposure increases.

Water has been reported to show two relaxation processes in this region. The principle occurrence is the melting process near 0° C depending on purity and the second occurs from -20° to -30° C (19). It has been suggested (17) that the relaxation at -8° C in bead-filled samples could be due to molecular water. As fiber-filled samples do not show this relaxation, this interpretation appears unlikely. When molecular water is mixed with uncured resin-amine mixture, a relatively stable emulsion is formed and the water becomes basic due to the extraction of part of the amine. If an excess of amine is present, cure at 60° C occurs normally to give a white tough solid which contains droplets of encapsulated water. A sample containing about 10% by weight of water cured in the presence of 25% excess amine showed a normal beta peak with increased height near -55° C and this effect is probably due to the presence of excess amine (20). No peak could be detected near

either -30° C or -8° C and consequently the presence of molecular water cannot explain the occurrence of these peaks.

It is suggested that the slow change observed in all cases as exposure time increases, is caused by the slow absorption of water. For the untreated fibers, including the cleaned glass and the aramid systems, a further degradative process occurs probably associated with interfacial region as it is dependent on the presence of fiber.

CONCLUSIONS

The beta relaxation by amine cured epoxy systems is depressed by the presence of fibrous fillers and an approximately linear relationship exists between volume fraction of resin and the maximum volume of the loss tangent.

The effect of boiling water on the beta relaxation of amine-epoxy fiber composites may be explained in terms of two concurrent processes, both leading to a peak between -20° and -30°C. The first, observed in all systems, may be associated with the slow absorption of water by the matrix. The second, observed for systems containing cleaned glass or aramid fibers may be associated with deterioration of the interface. Both processes appear to be reversible.

REFERENCES

- N.G. McCrum, B.E. Read and G. Williams, "Anelastic and Dielectric Effects in Polymeric Solids", Wiley and Sons, London (1967).
- A.S. Norwick and B.S. Berry, "Anelastic Relaxation in Crystalline Solids", Academic Press, New York (1972).
- J.G. Williams, "The Sources of Error in a Free Oscillation Torsion Pendulum", MRL Report 647 (1976).
- R.F. Boyer, "Introductory Remarks for Symposium on Transitions and Relaxations in Polymers", J. Polym. Sci:Pt C, 14, 3-14 (1966).
- K.H. Illers, "Der Einfluss von Wasser auf die Molekularen Beweglichkeiten von Polyamiden", Makromol. Chem. 38, 168-188 (1960).
- S.L. Samuels and G.L. Wilkes, "Effects of Gamma Radiation and Swelling Behaviour of Styrene Butadiene Block and Random Copolymers", Polym. Eng. Sci. 13, 280-286 (1973).
- H.A. Flocke, "Ein Berkag Zum Mechanischen Relaxationsverhalten von Polyathylen, Polypropylen, Gemischen aus diesen und Mischpolymerisaten aus Propylen und Athylen", Kolloid Z. 180, 118-126 (1962).
- D.H. Kaelble, "The Dynamic Mechanical Properties of Epoxy Resins", S.P.E.J. 15, 1071-1077 (1959).
- F.R. Dammont and T.K. Kwei, "Dynamic Mechanical Properties of Aromatic, Aliphatic and Partly Fluorinated Epoxy Resins", J. Polym. Sci. 5, 761-769 (1967).
- O. Delatycki, J.C. Shaw and J.G. Williams, "Viscoelastic Properties of Epoxy-Diamine Networks", J. Polym. Sci:Pt A-2, 7, 753-762 (1969).
- 11. E.F. Cuddihy and J. Moacanin, "Superposition of Dynamic Mechanical Properties in the Glassy State", J. Polym. Sci:Pt A-2, 8, 1627 (1970).

- D.E. Kline and J.A. Sauer, "Radiation and Moisture Effects in Polymerised Epoxy Resins", SPE Trans. 21-24 (1962).
- 13. G.A. Pogany, "Gamma Relaxation in Epoxy Resins", Poly. 11, 66-78 (1970).
- M. Schrager, "Fatigue as Monitored by the Torsion Pendulum", J. Polym. Sci:Pt A-2, 8, 1999-2014 (1970).
- J.C. Patterson-Jones and D.A. Smith, "The Thermal Degradation of an Amine-Cured Epoxide Resin at Temperatures between 200°C and 310°C", J. Appl. Polym. Sci. 12, 1601-1620 (1968).
- J.A. Manson and E.H. Chiu, "Effects of Water on the Mechanical, Dielectric, and Swelling Behaviour of Glass-Sphere-Filled Epoxy Resin", A.C.S. Polym. Preprints 14, 469-474 (1973).
- M.P. Ebdon, O. Delatycki, and J.G. Williams, "Dynamic Mechanical Properties of Glass-Filled Epoxy Resin", J. Polym. Sci., Polym. Phys. Ed. <u>12</u>, 1555-1564 (1974).
- C.W. Weaver and J.G. Williams, "Deformation of a Carbon-Epoxy Composite under Hydrostatic Pressure", J. Mat. Sci. 10, 1323-1333 (1975).
- P. Schiller, "Die Mechanische Relation in Reinen Eiseinkristallen", Z. fur Physik 153, 1-15 (1958).
- R.P. Kreahling and D.E. Kline, "Thermal Conductivity, Specific Heat, and Dynamic Mechanical Behaviour of Diglycidyl Ether Bisphenol A Cured with m-Phenylenediamine", J. Appl. Polym. Sci. 13, 2411-2425 (1969).

ELECTRON SPIN RESONANCE STUDIES OF THE DEGRADATION OF POLYMERIC MATERIALS

D.K.C. Hodgeman

Materials Research Laboratories,

Maribyrnong, Victoria 3032, Australia

INTRODUCTION

A wide variety of physical and chemical methods has been applied to the characterisation of polymeric materials and many of them have found use in the study of polymer degradation. Electron spin resonance (ESR) is a spectroscopic technique used for the characterisation and study of chemical species containing unpaired electrons, species such as free radicals and transition metal ions. This technique has been successfully applied to the study of free radicals produced in polymeric materials undergoing different types of degradation and has provided valuable information on the mechanism of the degradation reaction.

Free radicals are produced in organic materials on homolytic fission of chemical bonds. These reactions may be initiated by the action of heat, ultraviolet light, and ionising radiation or by the rupture of chemical bonds by mechanical forces. Reactions of the initially formed radicals with the polymer or with oxygen lead to secondary radicals and recombination between radicals can lead to crosslinking and the formation of abnormal groups in the polymer.

In this paper we will outline the theory of ESR spectroscopy, restricting the discussion only to those parts necessary to show the origin of the ESR spectrum and those parts relevant to free radicals in polymeric materials (greater detail will be found in references (1) and (2)). We will then briefly describe the main features of the ESR spectrometer and the experimental methods used in the study of polymeric materials, and then illustrate, by selected examples from the literature, the application of ESR spectroscopy to the study of polymer degradation.

THEORETICAL ASPECTS

An unpaired electron in a free radical has an associated magnetic moment which can interact with an external magnetic field resulting in a splitting of electron energy levels. Transitions between these levels are observed in ESR spectroscopy. The magnetic moment of the unpaired electron is due to orbital and spin motion of the electron both of which are quantised. The allowed values of spin angular momentum and its components are

$$\sqrt{S(S+1)}^h/_{2\pi}$$
 and $M_S^h/_{2\pi}$ (S = $\frac{1}{2}$, M_S = $\frac{1}{2}$ for one electron)

This results in two allowed values of spin angular momentum shown in Fig. 1. The quantised electron magnetic moment is

$$\mu_z = -g\beta M_S$$

where β is a constant and g is a factor dependent on the system under study. The energy of the allowed values in an external magnetic field (H) is

For one unpaired electron this results in two energy levels \pm $^1\!\!\!/_2$ g ß H (Fig. 2) and the separation between the energy levels and the condition for resonance is

$$\Delta W = hv = g \beta H_r$$

Further splitting of the energy levels is caused by adjacent magnetic nuclei (such as H-1 and N-14) and is due to modification of the external magnetic field ($H_{\rm eff}=H+H_{\rm local}$). The effects of a single proton on the energy levels are shown in Fig. 3 where the splitting due to the proton is the hyperfine splitting constant, a. For a radical with several nearby magnetic nuclei a multi-line spectrum will be observed from which a great deal of information about the structure around the free radical centre may be obtained.

The important parameters which can be obtained from the ESR spectrum are the g-factor and the various hyperfine splitting constants. These parameters may be either isotropic (independent of orientation of the free radical relative to the magnetic field) or anisotropic. In the latter case the g-factor and the hyperfine splitting constants are dependent on orientation of the free radical with respect to the magnetic field. This has important consequences on the appearance of the ESR spectra of polymers.

In a crystalline solid where all free radicals are aligned in the crystal lattice, sharp ESR lines are observed and the anisotropic behaviour of g and a may be studied by rotating the crystal. However, in an amorphous or polycrystalline solid such as a polymer all orientations of the free radical are present, i.e. all values of g and a are represented so that the ESR lines are considerably broadened. This results in loss of definition and resolution in the ESR spectrum so that g and a cannot be measured with high accuracy and some information relating to the structure of the free radical is lost. Line broadening can also result from restricted motion of the radical centre in the polymer chain and can be used to study movement in the polymer system.

EXPERIMENTAL ASPECTS

The resonance condition, $h\nu = g \ B$ H, can be achieved by varying either H or ν . Since electromagnetic radiation in the microwave region is used to induce transitions between the energy levels it is technically easier to maintain the frequency constant and to vary the strength of the external magnetic field. The bulk of work on organic free radicals is performed at a frequency of about 9.5 GHz (X-band) in which case the spectra are centred at a field of about 3400 G and cover a range of up to about 200 G.

A block diagram of a typical ESR spectrometer is shown in Fig. 4. The sample is contained in a resonant microwave cavity placed between the poles of an electromagnet. Absorption of energy from the microwave field at electron resonance in the sample is detected and displayed.

The sensitivity of an ESR spectrometer is very high and radicals can be detected in concentrations as low as about 10^{-10} M. However, since free radicals are in general very reactive their concentration in the sample may be very low. In many cases it is necessary to take steps to maintain a sufficiently high concentration of radicals for detection either by continuous generation of the radicals or by cooling of the sample to slow reactions of the radicals. In polymeric materials, due to the restricted movement of the radicals, some of the more stable radicals can be studied at room temperature.

The formation of free radicals in polymers by heat, ultraviolet light, ionising radiation and mechanical forces can all be studied by ESR spectroscopy. The reaction may be

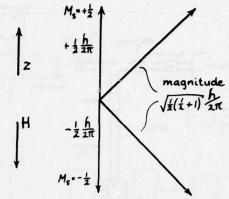


FIG. 1 - Allowed values of spin angular momentum and components in a fixed direction (for $S = \frac{1}{2}$).

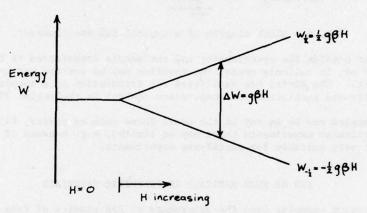


FIG. 2 - Energy level scheme for a single electron in an external magnetic field.

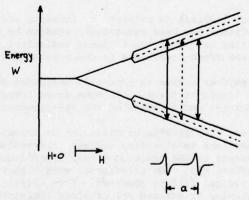


FIG. 3 - Energy level scheme showing nuclear hyperfine splitting for a single nucleus of I = ½ (e.g. 'H).

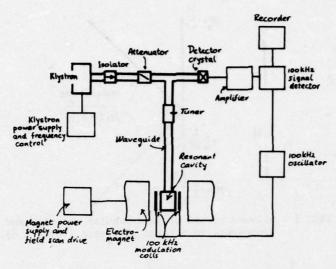


FIG. 4 - Block diagram of a typical ESR spectrometer.

performed either outside the spectrometer and the sample transferred to the spectrometer for measurement or, in suitable cases, the reaction may be carried out in the cavity of the spectrometer. The cavity has facilities for irradiation of a sample with UV light within the cavity and facilities for temperature control in the region 77K to about 500K.

Polymer samples may be in any of the usual forms such as powder, film, fibre or rod although in particular experiments these may be limited, e.g. because of light scattering, powders are not very suitable for photolysis experiments.

ESR OF FREE RADICALS IN POLYMERIC MATERIALS

In this section examples from the literature of ESR studies of free radicals formed in polymers on interaction with heat, UV light, ionising radiation and mechanical forces are presented. The reactions of the radicals and information gained on the mechanisms of the degradation reactions are discussed.

Ionising Radiation

The formation of free radicals in polymers by ionising radiation such as X-rays, \u03c4-rays and accelerated electrons has been extensively studied by ESR spectroscopy. Due to the particularly penetrating nature of the ionising radiations, free radicals are formed in substantial amounts and are often stabilised in the crystalline regions of the polymer.

Irradiation of the polymer sample is generally performed outside the cavity with cooling of the sample in liquid nitrogen. In some cases irradiation can be carried out in the cavity but considerable modification of the spectrometer is required.

Polyethylene undergoes crosslinking or oxidation on irradiation with ionising radiation. Both of these reactions involve free radical intermediates. On γ -irradiation of polyethylene at 77K in vacuum an ESR spectrum of six broad lines is observed (3) and is assigned to the chain radical (I). On irradiation with higher doses the more complex spectrum of the allylic radical (II) is observed. This allylic radical is stable even at room temperature. On allowing irradiated polyethylene containing the chain radical to warm to near room temperature the spectrum of the allylic radical is also observed (4).

$$\sim CH_2 - \dot{C}H - CH_2 \sim$$
 (I)

$$^{\sim}$$
 CH₂ - CH - (CH = CH)_n - CH₂ $^{\sim}$ (II)

Irradiation of polyethylene with ionising radiation initially forms radical ions and excited species (Scheme 1) which undergo further reactions forming the radicals observed. On warming the sample, these radicals undergo migration by a series of hydrogen abstraction reactions finally forming crosslinks and the more stable allylic radicals. On irradiation of the polymer in air radicals formed in the amorphous regions of the polymer can react with oxygen to give peroxy radicals and, ultimately, hydroperoxides.

$$RH \xrightarrow{RH^{+}} + e^{-} \xrightarrow{R} (RH)^{*}$$

$$RH^{+} + RH \xrightarrow{R} R + RH_{2}^{+}$$

Scheme 1

Campbell and Turner (5) have examined the free radicals formed on γ -irradiation of crystalline and amorphous samples of poly(ethylene terephthalate) and have found different radicals in the two samples. In the crystalline material, which contained all crystal orientations, a complex spectrum was observed and was assigned to the chain radical (III). Much less detail was observed in the spectrum from the amorphous material. Some components of this spectrum were assigned to the radical (IV) whilst the other components could not be assigned. Although no chain scission radicals were observed, which would lead to a reduction in molecular weight, recombination reactions between the radicals formed would lead to crosslinking and a change in the physical properties of the polymer.

$$\sim$$
 CO - O - CH₂ - CH - O - CO \sim (III)

$$\sim 0 - \infty \longrightarrow_{H} \longrightarrow_{H} \infty - 0 \sim (IV)$$

Ultraviolet Light

The photodegradation and photo-oxidation of polymeric materials is a field presently undergoing active study and in which ESR spectroscopy can provide valuable information on reaction pathways involving free radical intermediates. To obtain sufficiently high concentrations of free radicals for detection with the ESR spectrometer intense sources of light are required. At MRL there is a 900 W xenon arc fitted with a 10 cm quartz focussing lens for concentration of the point arc on the sample. Various filters and additional lenses may be included and the lamp can be conveniently used for photolysis of samples either within the cavity of the ESR spectrometer or on the bench with subsequent transfer of the irradiated sample to the spectrometer. The arrangement for photolysis of a sample at 77K within the cavity is illustrated in Fig. 5.

Tsuji and co-workers (6,7) have made an extensive study of the photodegradation of polyethylene by ESR spectroscopy. Photolysis of polyethylene at 77K gave a broad eight-line spectrum which differs from that observed with ionising radiation (4) and is assigned to the radical (V). This radical is formed on photolysis of carbonyl group impurities

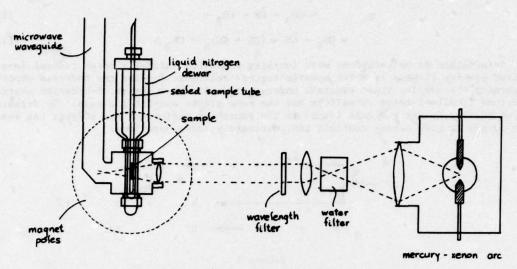


FIG. 5 - Experimental arrangement for photolysis within the cavity.

(from oxidation or from carbon monoxide impurities present in the polymerisation) by a Norrish I process followed by rearrangement of the excited radicals (Scheme 2). On warming the irradiated sample to about 150K the eight line spectrum is replaced by a sharp singlet (g \simeq 2.001) assigned to an acyl radical (VI) resulting from reaction of the carbon monoxide (from the photolysis) with carbon radicals. UV irradiation of polyethylene in air (6) at 77K gives the same eight-line spectrum but on warming the sample the asymmetric spectrum characteristic of peroxy radicals (VII) is observed. These peroxy radicals are very important intermediates in the photo-oxidation of polyethylene.

√СН₂ - СН - СН₃

Scheme 2

$$\sim CH_2 - \dot{C}H - CH_2R \xrightarrow{CO} \sim CH_2 - \dot{C}H - CH_2R$$
 (VI)

$$\sim CH_2 - \dot{C}H - CH_2R \xrightarrow{O_2} \sim CH_2 - \dot{C}H - CH_2R$$
 (VII)

Tsuji and co-workers have also examined the effects of some photo-sensitisers on radical production during photolysis of polyethylene. Photo-sensitisers such as ferric stearate (8) and aromatic compounds such as phenanthrene (9) were shown to increase the rate of radical production on photolysis. With ferric stearate free radicals were still observed when light of wavelengths greater than 360 nm was used, conditions under which no radicals were observed in the absence of the photo-sensitiser. Both metal compounds and aromatic compounds can be present as impurities in commercial polyethylene and will affect the lifetime of the polymer in sunlight.

Osawa et al. (10) have recently examined the photodegradation of polyurethanes by ESR spectroscopy. These authors found that polyurethane derived from a polyester diol - p,p' diphenylmethane diisocyanate gave a broad singlet spectrum (width ca. 23 G) on photolysis at 77K with a high pressure mercury lamp. On raising the temperature to 252K for a short period the signal intensity was reduced and some fine structure consistent with a quartet signal observed. On raising the temperature further the signal decayed to a broad The model compound, ethyl phenylcarbamate (VIII) behaved in a similar manner singlet. giving a better resolved quartet. The authors interpret the initial singlet spectrum as due to the free radicals produced on cleavage of the C - N and C - O bonds of the carbamate linkage (Scheme 3). They also suggest that the quartet signal observed on warming is due to the alkyl radical (X) formed on loss of carbon dioxide from the primary radical (IX) and that the final singlet is due to the aminyl radical (XI). These photolytic reactions result in cleavage of the polymer chain and reduction in the molecular weight. Reaction of the free radicals produced with oxygen would lead to the formation of further chromophores and further degradation of the polymer.

$$\begin{array}{c}
0 \\
Ph - NH - C - O - CH_2CH_3
\end{array}$$
(VIII)

$$Ar - NH + C + O - CH_2 - R$$

$$\downarrow hv$$

$$Ar - NH + C - O - CH_2R + Ar - NH - C + OCH_2R$$

$$\downarrow -CO_2 \qquad \downarrow -CO$$

$$CH_2R \qquad Ar - NH$$

$$(X) \qquad (XI)$$

Thermal Degradation

Scheme 3

Free radicals are important intermediates in the thermal degradation of polymers but, due to their high reactivity at elevated temperatures, only the more stable radical intermediates can be observed by ESR spectroscopy. Some free radicals produced during thermal oxidation fall into this category.

The autoxidation of polypropylene has been studied in the temperature range 110-140C by Chien and Boss (11,12,13) using ESR combined with other techniques. The only radical observed during this autoxidation is the intermediate peroxy radical (XII). At the lower temperatures of this study the ESR spectrum of the peroxy radical showed marked g-factor anisotropy indicating hindered rotation of the peroxy group. Using the ESR results combined with other analytical techniques the kinetics of the autoxidation was followed. Inhibited autoxidation of polypropylene in the presence of the antioxidant 2,6-di-tert-butyl-p-cresol was examined and, in the early stages of the reaction, the phenoxy radical (XIII) was observed.

$$(CH_3)_3C$$
 CH_3 $C(CH_3)_3$ (XIII)

Chiang and Sibilia (14) have shown the formation of relatively stable nitroxyl radicals during the thermal oxidation of nylon-6. This radical was observed during the oxidation of unterminated and amine terminated nylon-6 but not during the oxidation of the acid terminated polymer. From the splitting pattern of the spectrum the nitroxyl radical was identified as having the partial structure (XIV) and the authors suggest it results from autoxidation of the secondary amine (XV).

$$^{\sim}$$
 NH - CO - (CH₂)₅ - NH - (CH₂)₅ - CO - NH $^{\sim}$ (XV)

It is suggested that this secondary amine is formed during polymerisation by the deamination reaction

$$2 \sim \text{NHCO(CH}_2)_5 \text{NH}_2 \longrightarrow (\text{XV}) + \text{NH}_3$$

In addition to the nitroxyl radical a singlet spectrum was observed and became the major signal at higher temperatures. The radical giving this singlet was not identified.

Mechanical Degradation

Polymeric materials are subject to mechanical forces both in processing and in use and in many cases these forces are strong enough to rupture chemical bonds with the formation of free radicals. Rupture of the chemical bonds results in reduction of molecular

weight of the polymer and, after reaction of the free radicals with oxygen, the formation of thermally and photochemically labile groups.

Free radicals produced on mechanical degradation of polymers can be studied by stretching, milling, drilling, or sawing etc. of the polymer, usually at liquid nitrogen temperature and in the absence of oxygen to prevent reaction of the radicals.

Sohma et al. (15) have examined the free radicals produced in polyethylene by sawing at 77K. The ESR spectrum of these radicals differed from those obtained by irradiation with ionising radiation and ultraviolet light and were identified as the chain scission radicals (XVI). On warming to 152K the spectrum changed to that of the radicals (XVII) which are those observed on photolysis. Further warming in the presence of oxygen gave the peroxy radicals (XVIII). The radicals produced during this mechanical degradation were very reactive to oxygen which is consistent with their being trapped in amorphous regions of the polymer near the surface.

$$\sim CH_2 - CH_2 - \dot{C}H_2$$

$$\sim CH_2 - \dot{C}H - CH_3$$

$$\sim CH_2 - \dot{C}H - CH_3$$

$$(XVIII)$$

$$(XVIII)$$

Tino, Placek and Szocs (16) have examined the free radicals produced in nylon-6 by drilling at 77K and have followed the changes in these radicals on raising the temperature to 323K (50C). The initially formed radicals are the chain radical (XIX) and the chainend radicals (XX) and (XXI). On raising the temperature the concentration of these radicals decayed rapidly in the region of 273K and a smaller concentration of two new radicals was produced. One of the new radicals was suggested to be the allylic radical (XXII) whilst the other radical was not identified. During the warm-up procedure the overall radical concentration decreased due to radical combination reactions and the new radicals were produced as a result of these migration and combination reactions. The spectra observed were complicated by the presence of several radicals and computer analysis was necessary to separate the individual spectra.

SUMMARY

As can be seen from the above discussion ESR spectroscopy can provide direct information on the presence and nature of free radicals in polymeric materials. The technique can be used to examine the kinetics of radical formation and decay and the conversion of radicals to secondary radicals of different structure. The method is highly specific detecting only those species with unpaired electrons. Interpretation of the ESR spectra of polymers can be complicated by the broad lines generally observed with polymers which, particularly in the case of overlapping spectra, can lead to inaccurate assignments of radical structure. The information provided by ESR spectroscopy cannot be provided directly by any other physical technique.

Although ESR spectroscopy can provide valuable information on free radicals present in polymers during degradation it provides only part of the information required to establish the degradation mechanism of a polymer and the results must be considered in conjunction with those obtained by other techniques. Due to the short-lived nature of most free radical intermediates the technique finds application mainly as a research tool and is largely restricted to studying degradation mechanisms rather than the extent of degradation of a polymer sample. Sample size places no restriction on the technique as samples from a few milligrams to a few grams may be conveniently studied. However, the instrumentation is expensive and has few routine applications.

Many studies on the nature of free radicals in polymers have been carried out and reported in the literature. However, there remains a great deal of scope for further work particularly in relating the free radicals and free radical reactions to the degradation mechanisms of the polymer. There is also further scope for studying the effects of polymer additives and their oxidation products on the rates of radical formation and on the nature of the radicals produced.

REFERENCES

- 1. N.M. Atherton, "Electron Spin Resonance", Ellis Horwood, Chichester (1973).
- 2. D. Campbell, "Electron Spin Resonance of Polymers", J. Polym. Sci., D, 4, 91 (1970).
- N. Grassie, "Polymer Degradation and Electron Spin Resonance Spectroscopy", Pure Appl. Chem., 16, 389 (1967).
- K. Tsuji, "Comparison of Photo- and Radiation-Induced Radical Formation in Polyethylene by ESR Spectroscopy", J. Polym. Sci., Polym. Chem. Ed., 11, 1407 (1973).
- D. Campbell and D.T. Turner, "ESR Study of Radicals Trapped in Amorphous and Crystalline Samples of Poly(ethylene terephthalate) After γ-Irradiation", J. Polym. Sci., A-1, 5, 2199 (1967).
- K. Tsuji and T. Seiki, "Electron Spin Resonance Study of Polyethylene Irradiated with Ultraviolet Light", Polymer J., 2, 606 (1971).
- K. Tsuji and S. Okamura, "ESR Study of Polyethylene Irradiated with Ultraviolet Light and Electron Beams", in P-O. Kinel, B. Ranby and V. Runnstrom-Reio, Editors, ESR Applications to Polymer Research, Nobel Symposium No. 22, p. 187, Almqvist and Wiksell, Stockholm (1973).
- K. Tsuji, "Electron Spin Resonance Study of Polyethylene Irradiated with Ultraviolet Light: Effect of Addition of Ferric Stearate", J. Polym. Sci., Polym. Lett. Ed., 11, 351 (1973).

- T. Takeshita, K. Tsuji and T. Seiki, "ESR Study on the Photosensitized Decomposition of Polyethylene", J. Polym. Sci., A-1, 10, 2315 (1972).
- Z. Osawa, E-L. Cheu and Y. Ogiwara, "Study on the Degradation of Polyurethanes. II. ESR Study on the Photodecomposition of Polyurethanes and Ethylphenylcarbamate", J. Polym. Sci., Polym. Lett. Ed., 13, 535 (1975).
- 11. J.C.W. Chien and C.R. Boss, "Electron Spin Resonance Spectra of Low Molecular Weight and High Molecular Weight Peroxy Radicals", J. Amer. Chem. Soc., 89, 571 (1967).
- J.C.W. Chien and C.R. Boss, "Polymer Reactions. VI. Inhibited Autoxidation of Polypropylene", J. Polym. Sci., A-1, 5, 1683 (1967).
- J.C.W. Chien and C.R. Boss, "Polymer Reactions. V. Kinetics of Autoxidation of Polypropylene", J. Polym. Sci., A-1, 5, 3091 (1967).
- T.C. Chiang and J.P. Sibilia, "Electron Paramagnetic Study of Thermal-Oxidative Degradation of Nylon-6", J. Polym. Sci., A-1, 10, 605 (1972).
- 15. J. Sohma, T. Kawashima, S. Shimada, H. Kashiwabara and M. Sakaguchi, "ESR Studies on the Polymer Radicals Produced by Mechanical Fracture", in P-O. Kinel, B. Ranby and V. Runnstrom-Reio, Editors, ESR Applications to Polymer Research, Nobel Symposium No. 22, p. 225, Almqvist and Wiksell, Stockholm (1973).
- J. Tino, J. Placek and F. Szocs, "Free Radicals in Mechanically Destructed Polyamide-6 as Studied by the ESR Method", Europ. Polym. J., 11, 609 (1975).

POLYMER CHARACTERISATION BY PYROLYSIS GAS CHROMATOGRAPHY

J.R. Brown and D.J. Hall

Materials Research Laboratories

Maribyrnong, Victoria 3032, Australia

SYNOPSIS

The characterisation of polymers by pyrolysis gas chromatography has been briefly reviewed. Different types of pyrolysers have been discussed and some recent applications given to illustrate the scope of the technique.

INTRODUCTION

Pyrolysis gas chromatography (PGC) has recently been recognised as an effective tool in the field of polymer characterisation, particularly in the elucidation of detailed structure, thermal stability and degradation kinetics of polymers. An essential part of most pyrolysis studies is the analysis of the products formed. This previously depended on fraction collection and subsequent tedious analysis, but now can be performed more rapidly and conveniently by gas chromatography or combined gas chromatography and mass spectrometry.

PGC can be used for polymer characterisation in two ways; (a) to establish characteristic "fingerprint" pyrograms of materials and subsequent identifications by comparison with standard pyrograms and (b) to determine the composition and structure of polymers from analysis of pyrogram components, from which the mechanism of thermal degradation can often be deduced.

The inter-laboratory usefulness of PGC is limited by difficulties encountered in standardising the pyrolysis process. The requirements for reproducible and quantitative PGC are (a) rapid and complete pyrolysis to minimise secondary reactions by use of small samples pyrolysed for an effective time interval; (b) minimum dispersion by diffusion of gaseous pyrolysis products, which is achieved by pyrolysis in the immediate vicinity of the column of the gas chromatograph in a streamline gas flow; (c) the presence of a heated zone between the pyrolyser and the column to avoid condensation of products and possible consequent side reactions so that the pyrogram can be related to structure and (d) careful control of carrier gas flow rate and column temperature to minimise chromatographic variables.

TYPES OF PYROLYSER

The main cause of variance in the comparison of inter-laboratory pyrolysis results has been due to the use of different types of pyrolyser units. There are other factors which can affect pyrograms, e.g., pyrolysis temperature, sample size, residual entrapped solvent and heating techniques. Farre-Rius and Guiochon (1) suggested that a critical factor in

polymer pyrolysis studies is the rate of heat transfer to the sample. They showed in the pyrolysis of polytetrafluoroethylene, using a Curie-point pyrolyser with a temperature rise time (TRT) to 600°C of 30 ms, that about half of the sample had pyrolysed after 26 ms at a temperature below the equilibrium temperature of the pyrolyser. The requirement, therefore, is for rapid TRT's to ensure pyrolysis occurs at or near the equilibrium temperature.

. 1

Levy (2) has shown that the choice of materials used in pyrolysis units is important. Materials used in their construction should be carefully chosen to avoid catalytic effects during the pyrolysis process. This problem is accentuated by the high temperatures encountered in PGC. Quartz, stainless steel (3) and nichrome (4) have all been reported as having catalytic effects, while gold and platinum have reduced catalytic effects (5).

The types of pyrolyser currently in use are :

- 1. Electrically heated filaments.
- 2. Ferromagnetic materials heated to their Curie-points (6).
- 3. Tubular furnaces.
- 4. Lasers.

Filament pyrolysers (usually platinum) are heated by a constant voltage to the required pyrolysis temperature. Their main advantages are that they are relatively inexpensive and can be controlled over a wide temperature range. Pyrolysis samples are either coated onto the filament wire from solution or are simply located on the filament coil. application on a filament can result in a number of difficulties with respect to uniform sample size (7) which reduces the prospects of using filament pyrolysers for quantitative analysis. Solid samples placed on the filament are also likely to encounter appreciable temperature gradients (8). Other disadvantages of the filament pyrolyser are its short service life and a build up of carbon on the filament which alters the filament current and There are also several variations of the filament wire the pyrolysis temperature (7). The use of platinum grids (4) and "ribbon" pyrolysers (3) has been reported. These have the advantage of greater surface area allowing more even heating of a solid sample thereby reducing thermal gradients within the sample. TRT's for filament pyrolysers are relatively slow, which results in many cases in poor repeatability. Faster TRT's have been achieved by the use of capacitive-boosted filaments (9).

The Curie-point pyrolyser is an adaption of the filament pyrolyser. The sample to be pyrolysed is located on a ferromagnetic wire and is heated by induction in a radio-frequency electromagnetic field to a temperature which is dependent on the composition of the alloy wire. A large range of Curie-point temperatures can be obtained from alloys of iron, cobalt and nickel (10). The maximum temperature (the Curie-point) is attained when the ferromagnetic wire becomes paramagnetic and is incapable of absorbing any more energy from the high frequency induction source. Initial heating takes place on the surface and is conducted to the bulk of the wire (7). Problems have arisen with Curie-point pyrolysers due to inadequate quality control of alloy composition (9) which has resulted in differing TRT's and equilibrium temperatures for a specified alloy. Disadvantages of the Curie-point pyrolyser are that solid samples are difficult to apply and it is not possible to carry out multiple temperature or step-wise pyrolyses on one sample due to the fixed Curie-point temperature of a given alloy. Advantages include good pyrolysis temperature repeatability, short TRT's, the small unit size and reduced possibilities of secondary reactions.

In a tubular furnace pyrolysis unit, a sample is inserted into a pre-heated furnace by some mechanical means. Disadvantages of the tubular furnace include the relatively long residence time of the sample and products in the heated zone, increasing the possibility of secondary reactions, and the relatively large "dead volume" which can nullify the use of high resolution columns. The TRT is dependent on the mass and size of the carrier vessel used for sample introduction. Ettre and Varadi (11) have shown that variations in sample

size and carrier vessel size can affect the distribution of pyrolysis products. Advantages of the furnace unit are (a) many sample types and sizes can be analysed; (b) pyrolysis can be carried out under set conditions at an accurately maintained temperature if the temperature profile of the furnace is known (to ensure correct sample placement within the heated zone (7)); (c) the use of a pre-heating zone at 75°C - 150°C reduces pyrogram contamination by solvent, water etc; (d) the thermal stability of materials can be investigated by stepwise pyrolyses at several temperatures.

A more recent technique that shows considerable promise is laser pyrolysis. Pyrolysis by a laser beam produces specific but usually simple pyrograms (12) due to the high temperatures obtained (13). It has been reported that energy absorption and subsequent cooling occur in a time span much shorter than that achieved by other pyrolysis units such as Curie-point pyrolysers and capacitive-boosted filaments (14). Fanter et al (13) estimated TRT's of $\sim 10~\mu s$ to equilibrium temperatures of 927°C to 1227°C. An inherent problem in laser pyrolysis is the transparency of many materials to the lasing frequency. This has been overcome by "colouring" materials with absorbing centres to effect energy transfer (15,16). Walker (3) and Levy et al (9) have used blue glass sample holders to accept the energy and subsequently heat pyrolysis samples. Both these methods have drawbacks (17), e.g. carbon additives can alter the pyrolysis product distribution and heating the sample holder lowers the maximum pyrolysis temperature. Vanderborgh and Ristau (17) reported that in the laser pyrolysis of polystyrene and polyethylene, the amount of material pyrolysed is not reproducible but the fragmentation pattern is constant and re-Disadvantages of laser pyrolysis include the use of relatively large samples, higher equilibrium temperatures than in other pyrolyser types and difficulties with lasertransparent materials. Advantages are very rapid TRT's and simple, specific and reproducible pyrograms.

APPLICATIONS

Polymer Identification and Compositional Analysis

Pyrolytic degradation of organic materials is not a random phenomenon but can be statistically predicted because, for a selected thermal energy input, the fracture of specific molecular bonds is favoured. At high temperatures, organic materials fragment mainly into simple molecules, e.g. hydrogen, carbon monoxide, carbon dioxide, methane, water etc. At lower temperatures, short-chain organic fragments are obtained which reflect to a large extent the elemental and structural character of the parent material.

The "fingerprint" method of comparing the pyrogram of an unknown material with that of a polymer of known structure pyrolysed under the same conditions has been used successfully for some years as a means of identification of polymeric materials, without the need for identification of pyrogram components (18,19,20). Identifications of major pyrogram components have provided indications of classes to which polymers belong, e.g. polyolefins can be identified by sequences of olefinic and saturated hydrocarbon components in their pyrograms, with the particular monomer usually being the most abundant product (12,21,22). Similarly, materials containing aromatic segments, e.g. polystyrene, epoxy resins, phenolics, aromatic polyamides and polyesters, give characteristic pyrograms containing benzene, toluene, ethyl benzene and styrene (12,17).

Structural Analysis

Complete identification of pyrograms (which in many cases has recently been greatly facilitated by combined gas chromatography-mass spectrometry (23-27)), has provided not only material identification but also detailed structural information. Macleod (28) used a Curie-point pyrolyser to quantitatively determine the components of thermosetting acrylic resins. Alkyd paints have also been analysed by PGC for forensic purposes (29). In

these laboratories, PGC studies of high performance fibers have provided details of their composition before and after outdoor durability testing, from which some conclusions can be drawn on possible degradation processes (30).

PGC has also been a useful technique in structural analysis of copolymers. Tanaka et al (31) have investigated the relationships between pyrolytic products and microstructures of vinyl chloride-methyl methacrylate and vinyl chloride-acrylonitrile copolymers. Krishen (32) has determined quantitatively the constituent composition of styrene-butadiene and ethylene-propylene rubbers. Wallisch (33) showed that PGC can distinguish between random and block copolymers of ethyl acrylate and methyl methacrylate. The distribution of chlorine atoms in chlorinated polymers, which have been synthesised in the search for improved performance and flame resistance, has been studied. Analysis of pyrolysis products such as benzene, toluene and chlorobenzenes has been related to various structures of chlorinated polystyrenes (34).

Wall (35) developed a theory to relate the monomer yield from the thermal degradation of vinyl-type copolymers to the arrangement of monomer units and introduced the concept of a boundary effect caused by the neighbouring monomer units. Shibasaki (36) modified Wall's concept and suggested that the boundary effect is mainly due to the influence of penultimate units on the stability of depropagating copolymer chain radicals. PGC has been employed with the Wall-Shibasaki theory to determine triad distributions in vinylidene chloride-vinyl chloride copolymers (37), the microstructures of chlorinated polyethylene (38) and ethylene-propylene polymers (39), and characterisation of sequence distributions in methyl acrylate-styrene copolymers (40). A method for determining the distribution of dyads in styrene-meta and para chlorostyrene copolymers using PGC has been described (41) and is applicable for characterising the microstructures of copolymers in which the comonomers undergo similar thermal depolymerisation processes.

Degradation Kinetics and Thermal Stability

PGC has also been an effective method for studying degradation kinetics and thermal stability of polymeric materials. Thermal degradation kinetic results of poly(2-hydroxy-ethyl methacrylate) by PGC showed that in the initial stages of degradation, depolymerisation to monomer occurred in a similar manner to the degradation of poly(n-alkyl methacrylates), but that the polymer is also crosslinked during pyrolysis as indicated by the other main pyrolysis product, ethylene dimethacrylate, which is a direct product of cleavage of the crosslinked polymer (42). PGC has also been used to investigate the thermal behaviours of untreated and flame retarded wool. Ingham (43) showed that phosphorus containing flame retardants in wool result in no new pyrolysis products but cause an appreciable increase in evolved water and a simultaneous decrease in the yield of flammable volatile organic products.

The thermal and oxidative stability of the high performance fibers Kevlar 49, Nomex and PBI are being investigated at Materials Research Laboratories (44,45). PGC combined with mass spectrometry has been used to determine the temperature at which rapid thermal degradation and thermal oxidation of each fiber occurs and analysis of the pyrolysis products has revealed the chemical bonds which are preferentially fractured or oxidised.

The current literature shows that polymer characterisation by PGC is an area of active research, and it is the purpose of this brief review to outline the capabilities of the various types of pyrolysers and to show, by a limited number of examples, some of the ways in which this technique has been usefully employed in the characterisation of polymeric materials.

REFERENCES

 F. Farre-Rius and G. Guiochon, "On the Conditions of Flash Pyrolysis of Polymers as used in Pyrolysis-Gas Chromatography," Anal. Chem. 40, 998-1000 (1968).

- R.L. Levy, "Pyrolysis Gas Chromatography. A Review of the Technique", Chromatographic Reviews 8, 48-89 (1966).
- J.Q. Walker, "A Comparison of Pyrolysers for Polymer Characterization", Chromatographia 5, 547-552 (1972).
- V.R. Alishoev, V.G. Berezkin and A.I. Malyshev, "Pyrolysis Gas Chromatography of Polymers", J. Anal. Chem. USSR 27, 929-943 (1972).
- C.A.M.G. Cramers and A.I.M. Keulemans, "Pyrolysis of Volatile Substances (Kinetics and Products Studies)", J. Gas Chromatogr. 5, 58-64 (1967).
- B.R. Northmore, "The Characterisation of Polyolefins using a Curie-point Pyrolyser and Gas Chromatography", Br. Polym. J. 4, 511-525 (1972).
- J.K. Haken, "Gas Chromatography of Coating Materials", p. 249-297, Marcel Dekker Inc. New York (1974).
- J.C. Daniel and J.M. Miekel, "Pyrolysis of Copolymers of Vinyl Acetate with other Esters", J. Chromatogr. Sci. 5, 437-446 (1967).
- 9. R.L. Levy, D.L. Fanter and C.J. Wolf, "Temperature Rise Time and True Pyrolysis Temperature in Pulse Mode Pyrolysis Gas Chromatography", Anal. Chem. 44, 38-42 (1972).
- K.V. Alexeeva and L.P. Khramova, "Comparison of Various Pyrolysers in the Study of Polymer Compositions", J. Chromatogr. 69, 65-70 (1972).
- K. Ettre and P.F. Varadi, "Pyrolysis-Gas Chromatographic Technique. Effect of Temperature on Thermal Degradation of Polymers", Anal. Chem. 35, 69-73 (1963).
- N. Iglauer and F.F. Bentley, "Pyrolysis GLC for the Rapid Identification of Organic Polymers", J. Chromatogr. Sci. <u>12</u>, 23-33 (1974).
- 13. D.L. Fanter, R.L. Levy and C.J. Wolf, "Laser Pyrolysis of Polymers", Anal. Chem. $\underline{44}$, 43-48 (1972).
- W.T. Ristau and N.E. Vanderborgh, "Laser-Induced Degradation of Hydrocarbon Compounds Analysed Using Gas-Liquid Chromatography", Anal. Chem. 43, 702-707 (1971).
- B.T. Guran, R.J. O'Brien and D.H. Anderson, "Design, Construction and Use of a Laser Fragmentation Source for Gas Chromatography", Anal. Chem. 42, 115-117 (1970).
- W.T. Ristau and N.E. Vanderborgh, "Effect of Carbon-Loading upon Product Distribution of Laser-Induced Degradations", Anal. Chem. 44, 359-363 (1972).
- N.E. Vanderborgh and W.T. Ristau, "Reproducibility of Laser Induced Pyrolysis", J. Chromatogr. Sci. 11, 535-537 (1973).
- B. Groten, "Application of Pyrolysis-Gas Chromatography to Polymer Characterization", Anal. Chem. 36, 1206-1212 (1964).
- 19. H. McCormick, "Quantitative Aspects of Pyrolysis/Gas-Liquid Chromatography of Vinyl Polymers", J. Chromatogr. 40, 1-15 (1969).
- N.B. Coupe, C.E.R. Jones and S.G. Perry, "Precision of Pyrolysis-Gas Chromatography of Polymers. A Progress Report", J. Chromatogr. 47, 291-296 (1970).
- D. Deur-Siftar, "Application of Pyrolysis-Gas Chromatography for Characterization of Polyolefins", J. Gas Chromatogr. 5, 72-76 (1967).

- F.W. Willmott, "Pyrolysis-Gas Chromatography of Polyolefins", J. Chromatogr. Sci. 7, 101-108 (1969).
- R.L. Foltz, M.B. Neher and E.R. Hinnenkamp, "Applications of Mass Spectrometry and Gas Chromatography to the Analysis of Polymer Systems", J. Appl. Polym. Sci. Appl. Polym. Symp. 10, 195-204 (1969).
- M.M. O'Mara, "High-Temperature Pyrolysis of Poly(vinyl chloride): Gas Chromatographic-Mass Spectrometric Analysis of the Pyrolysis Products from PVC Resins and Plastisols", J. Polym. Sci. A-1, 8, 1887-1899 (1970).
- M.T. Jackson, Jr., and J.Q. Walker, "Pyrolysis Gas Chromatography of Phenyl Polymers and Phenyl Ether", Anal. Chem. 43, 74-78 (1971).
- C. Merritt, Jr., R.E. Sacher and B.A. Petersen, "Laser Pyrolysis-Gas Chromatographic-Mass Spectrometric Analysis of Polymeric Materials", J. Chromatogr. 99, 301-308 (1974).
- N. Sellier, C.E.R. Jones and G. Guiochon, "The Examination of Some Vinyl Acetate/Olefin Copolymers by Pyrolysis Gas Chromatography Mass Spectrometry", J. Chromatogr. Sci. 13, 383-385 (1975).
- 28. N. Macleod, "Quantitative Analysis by Pyrolysis Gas Chromatography of Thermosetting Acrylic Resins Used in Automotive Enamels", Chromatographia 5, 516-520 (1972).
- B.B. Wheals and W. Noble, "Forensic Applications of Pyrolysis Gas Chromatography", Chromatographia 5, 553-557 (1972).
- J.R. Brown, P.J. Burchill, G.A. George and A.J. Power, "The Photodegradation of Poly 2,2'-(m-Phenylene)-5,5'-Bibenzimidazole", J. Polym. Sci. Polym. Symp. 49, 239-247 (1975).
- M. Tanaka, F. Nishimura and T. Shono, "Pyrolysis-Gas Chromatography of Vinyl Chloride-Methyl Methacrylate and Vinyl Chloride-Acrylonitrile Copolymers", Anal. Chim. Acta 74, 119-124 (1975).
- A. Krishen, "Quantitative Determination of Natural Rubber, Styrene-Butadiene Rubber and Ethylene-Propylene-Terpolymer Rubber in Compounded Cured Stocks by Pyrolysis-Gas Chromatography", Anal. Chem. 44, 494-497 (1972).
- K.L. Wallisch, "Pyrolysis of Random and Block Copolymers of Ethyl Acrylate and Methyl Methacrylate", J. Appl. Polym. Sci. 18, 203-222 (1974).
- S. Tsuge, H. Ito and T. Takeuchi, "Pyrolysis Gas Chromatographic Investigation of Chlorinated Polystyrenes", Bull. Chem. Soc. Japan 43, 3341-3344 (1970).
- 35. L.A. Wall, "Analytical Chemistry of Polymers", Part II, Interscience, New York (1962).
- 36. Y. Shibasaki, "Boundary Effect on the Thermal Degradation of Copolymers", J. Polym. Sci. A-1, 5, 21-34 (1967).
- S. Tsuge, T. Okumoto and T. Takeuchi, "Pyrolysis-Gas Chromatographic Studies on Sequence Distribution of Vinylidene Chloride-Vinyl Chloride Copolymers", Makromol. Chem. <u>123</u>, 123-129 (1969).
- S. Tsuge, T. Okumoto and T. Takeuchi, "Structural Investigation of Chlorinated Polyethylenes by Pyrolysis - Gas Chromatography", Macromolecules 2, 200-202 (1969).
- H. Seno, S. Tsuge and T. Takeuchi, "Pyrolysis-Gas Chromatographic Studies on the Structure of Ethylene/Propylene Copolymers", Makromol. Chem. 161, 195-205 (1972).

- S. Tsuge, S. Hiramitsu, T. Horibe, M. Yamaoka and T. Takeuchi, "Characterization of Sequence Distributions in Methyl Acrylate-Styrene Copolymers to High Conversion by Pyrolysis Gas Chromatography", Macromolecules 8, 721-725 (1975).
- T. Okumoto, T. Takeuchi and S. Tsuge, "Pyrolysis Gas Chromatographic Study on Sequence Distribution of Dyads in Styrene-m-Chlorostyrene and Styrene-p-Chlorostyrene Copolymers", Macromolecules 6, 922-924 (1973).
- 42. J. Razga and J. Petranek, "Thermal Degradation of Poly-2-Hydroxyethyl Methacrylate by Pyrolysis Gas Chromatography", Europ. Polym. J. 11, 805-808 (1975).
- P.E. Ingham, "The Pyrolysis of Wool and the Action of Flame Retardants", J. Appl. Polym. Sci. 15, 3025-3041 (1971).
- 44. J.R. Brown, "Environmental Effects on Temperature Resistant Polymer Fibres", TTCP Critical Subject Review, The Prevention of the Deterioration of Organic Materials in Operational Environments", Report TTCP/AUS/P3/15, Materials Research Laboratories, Maribyrnong, Victoria (1975).
- 45. J.R. Brown and A.J. Power, unpublished data.

VAPOUR PRESSURE OSMOMETRY - ITS LIMITATIONS AS A METHOD FOR MOLECULAR WEIGHT DETERMINATIONS

C.E.M. Morris

Materials Research Laboratories

Maribyrnong, Victoria 3032, Australia

SYNOPSIS

Some of the factors which affect the accuracy of number-average molecular weight determinations by vapour pressure osmometry are discussed. It is shown that care is required in the choice of the size of the drops used and in the selection of compounds for calibration purposes to ensure that drop size and solute volatility effects do not lead to erroneous results. It is also demonstrated that, in certain systems at least, the calibration factor has a small but important dependence on the solute molecular weight over the molecular weight range examined. Failure to recognise this effect introduces significant errors into the determination of molecular weight by this method.

INTRODUCTION

The use of vapour pressure osmometry for the determination of number-average molecular weight of polymeric compounds, up to molecular weights of about 20,000, has been widely accepted for some time. Indeed, this is virtually the only generally applicable, absolute method available for such determinations within the molecular weight range 1,000 to 20,000.

The basic design of commercial instruments available for this purpose is the following: Two thermistor beads are suspended in a thermostatted chamber, which also contains a reservoir of solvent, and in which the atmosphere is saturated with solvent vapour (Figure 1). By means of guided syringes, drops of solution and solvent can be placed on the

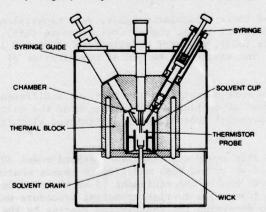


FIG. 1 - Schematic diagram of thermal chamber.

thermistor beads, which form two arms of a bridge circuit. With solvent on both beads the zero (baseline) reading is established. The liquid on one bead is then replaced with a drop of solution of the compound to be measured. Considered in simplistic terms, because of the difference in vapour pressure between solution and solvent, solvent condenses on the solution drop thereby warming that bead. It is this difference in temperature between the two beads which is detected as a bridge imbalance. Actually, other factors also affect the temperature difference. These include heat conduction from the solution drop surface to the ambient vapour and from the solution drop to the thermistor lead wires, the thermodynamic efficiencies of the heat transfer processes and diffusion controlled processes with the solution drop (1).

By taking measurements with a number of solutions, usually four, of different concentration, the number-average molecular weight can be calculated from the relation

$$\overline{M}_n = \frac{k}{(\Delta V/C)} c = 0$$

where ΔV is a measure of the bridge imbalance with solution of concentration C. k, the calibration factor, regarded as a kind of cell constant, is determined for each thermistor pair/solvent/temperature combination by measurements with a substance of known, usually low, molecular weight.

In earlier model instruments the bridge imbalance was given as a resistance (ΔR) but in more recent models the imbalance is measured as a voltage. This can cause problems with sensitivity in certain circumstances because of the magnitude of the signal (down to perhaps $10~\mu V$). Care is then required to ensure that thermal emfs and junction potentials make an insignificant contribution to the signal. The use of more concentrated solutions to give a larger signal is not, in general, an acceptable course of action because the departure from ideality of polymer solutions dictates the use of solutions as dilute as possible, but the judicious choice of a solvent can, to a certain extent, alleviate this problem. Having the imbalance in the form of a voltage does permit the use of a recorder to give a continuous readout of the signal, which is a considerable advantage in the recognition of (all to common) spurious results.

This paper describes the results of a study of the various factors which affect the accuracy of this method for the determination of number-average molecular weight.

EXPERIMENTAL

The compounds used, and their molecular weights, were naphthalene (128), benzil (210), methyl stearate (298), cholesterol (386), cholesteryl caproate (485), cholesteryl stearate (653), dicholesteryl adipate (883), glyceryl tripalmitate (807) and 1,2-dichlorobenzene (147) and squalane (423). The source and method of purification of these compounds is described elsewhere (1).

Purification procedures were repeated until there was a difference of less than 0.5° C between the extrapolated onset of melting and the maximum of the melting peak as measured on a du Pont model 900 Differential Thermal Analyzer equipped with its DSC cell and using a heating rate of 5° C/min.

The instrument used in this study was a Hewlett-Packard model 302 B Vapor Pressure Osmometer, the electronics of which had been modified to reduce sources of thermal emfs and junction potentials and to enable the equipment to be operated in the recorder and null method modes simultaneously (2). The routine operating procedure was to record the bridge imbalance-time curve, but to determine the equilibrium reading by the null method, three readings being taken at each concentration. In most cases, the solution concentrations were in the range 2-10 g/kg.

RESULTS AND DISCUSSION

Drop Size Effects

Some workers have claimed there is an effect on the measured bridge imbalance caused by the size of the solution drop (3,5) whereas contrary results have been reported by other workers (6,7). This matter has been investigated and it is apparent that there is a drop size effect which is related to the concentration of the solution. The effect is shown partly by the shape of the imbalance vs time curve and partly by the actual magnitude of the reading. Drop sizes, assessed by measurement of the length of the thermistor bead and solution drop with a travelling microscope, ranged from about 1.4 mm to about 3.0 mm in length. For these studies solutions of squalane in toluene and an operating temperature of 50°C were used.

For dilute solutions (less than about 6 g/kg or 1.5 x 10^{-2} M) the shape of the bridge imbalance-time curve was the same for all drop sizes. More concentrated solutions (6-12 g/kg) showed a downwards curvature in the ΔV -t curve with small drops ($\sim 1.4 - 1.5$ mm in length) but not with larger drops, while with solutions of greater than 12 g/kg concentration a downwards slant was apparent with drops up to about 1.8 mm in length. slope of this trace for a given drop size increased with increasing concentration. Representative curves are shown in Figures 2 and 3.

Thus, care is required in the selection of the drop size used to minimise these effects.

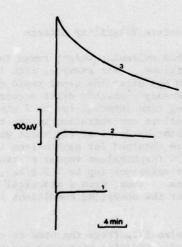


FIG. 2 - Effect of concentration on AV-time curves for small drops.

- Drop length 1.36 mm, concentration 1.78 g/kg;
- 2. Drop length 1.37 mm, concentration 6.77 g/kg;
- Drop length 1.41 mm, concentration 14.61 g/kg.
 All solutions squalane in toluene at 50°C.

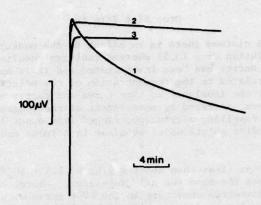


FIG. 3 - Effect of drop size on ΔV -time curves. Drop lengths: 1. 1.41 mm; 2. 1.76 mm; 3. 2.61 mm. Solution 14.61 g/kg squalane in toluene at $50^{\circ}C$.

Solute Volatility Effects

The lower limit of the usable molecular weight range is set by the volatility of the solute under the operating conditions. For example, with 1,2-dichlorobenzene in toluene at 40°C, (vapour pressure 3.5 mm Hg) after the usual rapid changes of bridge imbalance on replacing the solution drop, a steady downwards drift occurred and no equilibrium value was reached in the normal reading time interval (up to 7 min). Furthermore the drift rate increased with increasing solute concentration in the range examined (0.4 - 2.1 g/kg). With the solvent on both thermistor beads, a steady value was reached in about one minute (Figure 4). Similar traces were obtained for naphthalene in toluene at 60°C (vapour pressure 1.8 mm Hg) while at 40°C (naphthalene vapour pressure 0.3 mm Hg) equilibrium was reached within 2 min with dilute solutions (up to 1.3 g/kg), but a downwards drift was apparent at higher concentrations. Thus, from a practical standpoint, the use of a compound whose vapour pressure under the operating conditions is more than about 0.2 mm Hg should be avoided.

The traces in Figures 2-4 also illustrate the need to continuously monitor the bridge imbalance. Use of the recommended practice of taking readings after a fixed time interval, without waiting for the attainment of equilibrium (8), or of extrapolating the readings to zero time (4), would both give erroneous results in this situation.

Constancy of the Calibration Factor

Recently, it has been suggested that the calibration factor, k, may not be a constant (5,9,10). A number of attempts have been made to calculate the value of k, for a given set of circumstances, but these have not been very successful (4,7,11,12).

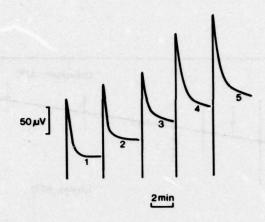


FIG. 4 - Effect of solute volatility. Representative ΔV-time traces for the system 1,2-dichlorobenzene/toluene/40°C. Solution concentrations: 1. 0; 2. 0.44 g/kg; 3. 1.1 g/kg; 4. 1.77 g/kg; 5. 2.11 g/kg.

To investigate whether the calibration factor depends on the nature of the solute, especially its molecular weight, k was determined with a number of solutes in the molecular weight range 128-883 under a variety of solvent/temperature conditions. The values of k were calculated from the slope of the line of best fit of the plot bridge imbalance vs concentration and these values are plotted against the solute molecular weight (Figure 5), the error bars denoting the 95% confidence limits. All lines were calculated by unweighted linear regression analysis.

Thus, there is a small but real dependence of the value of k on the molecular weight of the calibrating compound, but the form, magnitude and even the sign of the variation is less certain.

The compounds used as calibration standards include a wide variety of chemical classes as well as a set of related compounds. It appears that molecular size rather than chemical composition determines the variation in the calibration factor.

Bersted suggested (5,10) that certain diffusion controlled reactions at the drop surface and thermistor self-heating effects, which were previously considered to be insignificant, do contribute to the total effect measured. He proposed that the calibration factor is a constant only under certain combinations of circumstances; otherwise such factors as the magnitude of the heat losses from the thermistor supporting wires and the tendency for evaporation or condensation of solvent vapour at the drop surface to predominate, depending on the magnitude of the thermistor self-heating effect, determine the extent to which k varies with solute molecular weight.

As the determination of k is normally made at a considerable distance, in molecular weight terms, from the range of interest for polymers, this small dependence of k on molecular weight becomes important because of the length of the extrapolation required for polymers. The usual assumption that the calibration factor is a constant independent of molecular weight can then lead to significant errors in the determination of the number-average molecular weight of polymers by this method.

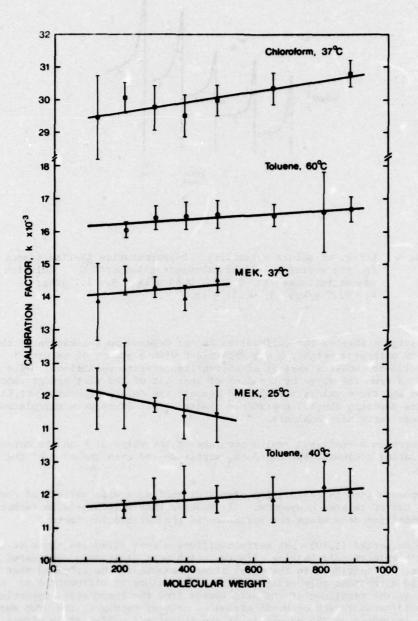


FIG. 5 - Dependence of the calibration factor, k, on solute molecular weight for various systems. Error bars denote the 95% confidence limits.

CONCLUSIONS

For accurate molecular weight determinations the dependence of the calibration factor on molecular weight under the particular operating conditions and over the appropriate molecular weight range should be determined using compounds of the highest obtainable purity. The use of a recorder to show the shape of the bridge imbalance-time trace is most desirable as an aid to the rapid recognition of non-steady state conditions arising from such factors as solute volatility or drop size effects. Readings should be taken when the system has reached a steady state, rather than after some fixed time interval.

ACKNOWLEDGEMENTS

I am indebted to Dr. B.C. Ennis for the preparation of some of the cholesterol derivatives and for the thermal analyses.

REFERENCES

- 1. C.E.M. Morris, "Aspects of Vapor Pressure Osmometry", J. Appl. Polym. Sci., in press.
- C.E.M. Morris and R.A. Humphreys, "Modification of a Vapour Pressure Osmometer", Report 616, Materials Research Laboratories, Melbourne (1974).
- W. Simon, J.T. Clerc and R.E. Dohner, "Thermoelectric (Vapormetric) Determination of Molecular Weight on 0.001 Molar Solutions: A New Detector for Liquid Chromatography", Microchem. J. 10, 495-508 (1966).
- A.C. Meeks and I.J. Goldfarb, "Time Dependence and Drop Size Effects in Determination of Number Average Molecular Weight by Vapor Pressure Osmometry", Anal. Chem. 39, 908-911 (1967).
- B.H. Bersted, "Molecular Weight Determination of High Polymers by Means of Vapor Pressure Osmometry and the Solute Dependence of the Constant of Calibration", J. Appl. Polym. Sci. 17, 1415-1430 (1973).
- W. Simon and C. Tomlinson, "Thermoelektrische Mikrobestimmung von Molekulargewichten", Chimia 14, 301-308 (1960).
- A. Adicoff and W.J. Murbach, "Some Aspects of Thermoelectric Vapor Pressure Osmometry", Anal. Chem. 39, 302-308 (1967).
- 8. Hewlett-Packard Vapor Pressure Osmometer, Model 302B, Operating Manual.
- J. Brzezinski, H. Glowla and A. Kornas-Calka, "Note on the Molecular Weight Dependence
 of the Calibration Constant in Vapour Pressure Osmometry", Eur. Polym. J. 9, 1251-1253
 (1973).
- B.H. Bersted, "Vapor Pressure Osmometry: A Model Accounting for the Solute Dependence of the Calibration Constant", J. Appl. Polym. Sci. 18, 2399-2406 (1974).
- C. Tomlinson, Ch. Chylewski and W. Simon, "The Thermoelectric Micro-determination of Molecular Weight III", Tetrahedron 19, 949-960 (1963).
- K. Kamide, K. Sugamiya and C. Nakayama, "Theory of Vapor Pressure Osmometry when Ambient Solvent Vapor is Unsaturated", Makromol. Chem. <u>133</u>, 101-109 (1970).

CLOSING REMARKS

Dr. George R. Thomas Army Materials and Mechanics Research Center Watertown, Massachusetts 02172

First, I want to thank our speakers and chairmen for having put on an outstanding conference.

I think we are all convinced that if material A and material B give the same results from all of the tests we've heard here they are indeed the same. If the values differ, then the materials must be in some way different. The fact that some of the methods can only be interpreted empirically does not bother me at all. I leave this review with the feeling that we have a large number of tools at our disposal.

(Now I would like to deliver that keynote address which I avoided at the outset of this conference by limiting myself to Introductory Remarks. It's really too late for that so let's just call this an Epilogue. Heed me not and you might call it an Epitaph!!)

I also leave here with the knowledge that these methods have not been used to characterize or predict the life of composite materials. Differences in chemical characteristics have not been correlated with differences in performance characteristics. This must be done if we are going to get anywhere in the prediction of deterioration. I am a little uneasy on this point because of my personal bias that, as scientists, we love to do basic research and abhor engineering research, particularly when it is obvious that it is a data collection and analysis process and we are going to have to do it. I am uneasy because we, as administrators, would rather not present and defend the long-term engineering data collection essential to the utilization of composites. Such programs have been, are currently, and in the future will continue to be held in bureaucratic disrepute. Although we can develop methods, collect data, administer programs, because we would rather not propose unpopular programs, no matter how essential, we probably won't. That worries me.

I often hear that a particular method is too expensive to use or it can't be done in Joe's barn by a third-grade dropout. Therefore, don't develop it or don't use it. This also concerns me greatly. We must recognize that at this point in time we don't know what we can afford to do without. Let me borrow an example from another field. We were told that chemiluminescence could be used to follow deterioration in foods. Suppose that it can be used to follow the freshness of fish. As a practical matter, if I catch a fish, clean it, and cook it immediately, I've operationally eliminated the need for chemiluminescence. If I'm willing to eat fish which have been out of the water longer and I can characterize it as edible or inedible by odor or taste, I still don't need chemiluminescence. That's the way we do it now. But - if, on the other hand, I'm a distributor with a large inventory, I would like to know how long the fish has been out of the water and how much time remains before the buyer will reject it. The requirements of the fish merchant for freshness tests for fish can no longer be met by the old nasal test done by an experienced operator with a modest technical or trade background,

particularly if the fish merchant needs to predict when the fish will fail the nasal test. It is in this situation that chemiluminescence (or another technique) has value. In short, the utility value of a technique may range from zero, i.e., we don't need to do it - to infinite, i.e., we cannot stay in business without doing it. I full well recognize at some point in time each method must be put into perspective or rationalized but we must resist rationalizing until we know the significance of the results. If chemiluminescence had been suggested as a way to control inventory before it had been explored it would have been rejected out of hand because it would be too complicated and too expensive. This happened in the past to methods presented at this review, and it will continue to happen if we don't challenge and change traditions with advancing technology.

Let me express another concern...that there are number of observations which may or may not be related to the methodologies present at this review. Let me illustrate with two examples.

First, in Figure 1 we see residual strains in the several layers of a filament-wound tube. Clearly, when separated the inner two wraps appear to have been under tension whereas the outer wrap was under compression.

Second, in Figure 2 we see differences in fracture in identical samples. One sample was stored in the laboratory, the other was exposed at a desert test site. Note how in one case there is good adhesion between the fiber and the resin and in the other poor adhesion.





Demonstration of Residual Internal Stresses in a Filament Wound Hybrid Composite Tube

Figure 1



Control - Laboratory Stored



Exposed at Yuma - Hot-Sunny-Dry

Electron Microscope Photographs (3500X) of Fractured 1009-26 System Samples After 18 Months on Location Figure 2

At this review, I did not hear any methods presented which would relate to either of these two phenomena even though the performance of composites must relate in some way to residual stresses and fracture mechanisms. To the degree that these and similar times were not treated, this Critical Review was incomplete. This might be called "Monday morning quarterbacking" but I feel it must be said lest the record of this review becomes the Bible for what is known and what needs to be done.

Finally, there is need for a cooperative program for the measurement and prediction of deterioration in composite materials.

To do a total job on one fiber-reinforced plastic system cured under three combinations of time and temperature, exposed at five sites (including one laboratory and one accelerated), stressed under three conditions (no load, static, and dynamic) would require about 2500 tests over a period of five years just to establish base line data. To get a rough estimate of how large the program can theoretically get, multiply 2500 by the number of curing agents and the number of coupling agents which might be used, the variations possible in the orientation in laminates, the several thicknesses necessary for reliable engineering extrapolation and interpolation, etc. You can stop multiplying when the last number you get gives you a feeling of complete futility, or you feel the need for a cooperative program.

The fact that no one organization has the fiscal resources, personnel, and equipment to do the whole job further compounds the problem. Furthermore, at the risk of offending some, no one organization in any country appears to have the genius to do the whole job. I include countries (and organizations) represented in TTCP, their universities, and their industries.

Clearly we've got to change to get anywhere at all.

I submit for your consideration the following suggestion: Borrow from the metallurgist, the ceramist, and the analytical chemist and adopt standard reference materials for cooperative effort. Speaking for my own Laboratory, we will be exploring the feasibility of such a concept in our own program and would be pleased to share our samples and data with any group which would like to cooperate.

To sum up, at this review we have heard how a wide variety of characterization techniques can be applied to a wide variety of materials. We are one step closer to our goal, which is to be able to predict and/or prevent deterioration of organic materials -but there remains much to be done.

In closing I again thank you all for coming and hope that you have gotten as much out of this review as I have.